

Stratigraphy and volcanology of a submarine apron from an offshore stratovolcano, Waitakere Group, Muriwai, New Zealand

Emma Mathews (BSc)

A research thesis submitted in partial fulfilment of the requirements of the
Degree of Bachelor of Science with Honours



University of Tasmania



Centre for Ore Deposit Research
(CODES)

School of Earth Sciences

November 2003



Abstract

A mid to late Miocene volcanic sequence is well exposed along the west coast of the Northland Peninsula, New Zealand. The Waitakere Group are uplifted submarine apron deposits from offshore arc stratovolcanoes, and outcrop from Kaipara in the north, to Manukau Harbour in the south. The submarine coherent and clastic succession at Muriwai (the Muriwai volcanic succession) is well preserved and records the medial depositional environment of a volcanoclastic apron from one or more submarine to emergent stratovolcanoes. Several major Miocene volcanic centres have been identified offshore from Northland. The present location of Muriwai is closest to the Manukau (WSW) and Kaipara (NE) centres. The stratigraphy is dominated by resedimented volcanoclastics, thinly bedded fine sandstone, coherent lava and pyroclastic fallout.

Six lithofacies groups were identified in the Muriwai volcanic succession, and each represents various transport and deposition process. Basal thinly bedded fine sandstone represents slow background sedimentation, prior to the onset of extensive eruptive activity. Scoriaceous and pumiceous facies, volcanic conglomerate facies and coarse granule sandstone facies record resedimentation of more proximal volcanoclastic deposits. Thin pumice and crystal rich facies record water-settled fallout from explosive eruptions. Coherent facies probably represent satellite vent eruptions on the volcano flanks. In general, the facies document rapid submarine deposition in the closing stages of the eruptive history of the source volcano(es).

Transport and deposition of the pumice and scoria, conglomerates and granule sands was dominated by water-supported sediment gravity flows. Rounded to subangular volcanic clasts are a significant component of these deposits, which suggests they were sourced from existing deposits that became remobilised on the upper flanks of a volcanic edifice. Uncommon allochthonous pebbles suggest this depositional environment also incorporated a component of non-volcanic sediments, derived from the Northland Allochthon to the north.

Pumice and scoria clasts record significant explosive eruptions, whereas coherent bodies and lava clasts record effusive eruptive activity. Bulk rock geochemistry defines the volcanic succession as a medium-K, calc-alkaline suite, a characteristic product of arc volcanism. Lavas and volcanic clasts have a compositional range from basalt to andesite. Representative

sampling suggests each clast type corresponds to a distinct bulk rock composition. Lavas are basalt to basaltic andesite, pumice are basaltic andesite, and scoria and hyaloclastite are andesitic. The chemical variations suggest multiple eruptive events and varying degrees of fractionation. Many pumice clasts are compositionally banded, suggesting magma mingling and complexities in the magma chambers of the source stratovolcanoes.

Stratigraphic relationships, facies types and comparison with other arc stratovolcanoes suggests that the bathymetry surrounding the source volcanoes once consisted of a series of radial erosional submarine canyons, separated by depositional highs. Towards the final stages of volcanism, mass wasting and edifice degradation disrupted background sedimentation in the marine basin. Resedimentation processes lead to the extension of a volcanoclastic apron, which in-filled submarine canyons at medial distances from the source volcano. The facies within the Muriwai volcanic succession form a thick canyon filling sequence and represents part of a clastic apron that formed in the basin adjacent to one or several volcanic centres.

Acknowledgements

The production of this thesis would not have been achieved without the support of many, and I am grateful for their advice, assistance and encouragement.

Thankyou to my supervisor, Dr. Sharon Allen, for the regular advice and direction given throughout this year, it has been great working with you. Also, for patience and understanding for those first days in the field. Thanks also to my secondary supervisors Dr. Catherine Reid and Dr. Cathryn Gifkins, for the proof readings and support.

Much thanks to Dr. Bruce Hayward, whose expertise on the rocks at Muriwai proved invaluable. Thankyou for the guidance and information provided while in the field, and for the many insightful articles that you have produced.

Thankyou very much to Assoc. Prof. Jocelyn McPhie, for advice, and for initially suggesting this project to me, which has been a terrific opportunity.

This research was funded by an ARC fellowship to S. Allen with additional support for analyses from the School of Earth Sciences. Greatest thanks.

Thanks to Fernando Della Pasqua, Greg Ebsworth and Wally Hermann for advice. I appreciate the work of Simon Stephens, for preserving my crumbly rocks in thin sections, Katie McGoldrick and Phil Robinson, for analyses, and June Pongratz and Alistair Chilcot for resolving computer issues. In addition, I would like to acknowledge Russell and Don for the use of their tracks to the southern parts of the field area.

Thankyou my darling David, for the support, encouragement, and understanding that you have given me all the way through. I appreciate you urging me to pursue my passions, and especially for the cuddles. You are wonderful.

Lastly, to the honours group, what a year it has been. Now we have made it! All the very best for the future.

Contents

| | |
|-------------------------|-------------|
| <i>Abstract</i> | <i>i</i> |
| <i>Acknowledgements</i> | <i>iii</i> |
| <i>Contents</i> | <i>iv</i> |
| <i>List of Figures</i> | <i>vii</i> |
| <i>List of Tables</i> | <i>viii</i> |

| | |
|--|---------------|
| | <i>pages</i> |
| Chapter 1: Introduction | 1 |
| 1.1 Preface | 1 |
| 1.2 Aims and significance | 2 |
| 1.3 Thesis organisation | 5 |
| 1.4 Project Location | 5 |
| 1.5 Methods | 6 |
| 1.6 Previous work | 6 |
| Chapter 2: Regional Geology and Setting | 7 |
| 2.1 Introduction | 7 |
| 2.2 Tectonic Framework | 7 |
| 2.3 Regional Geology | 10 |
| 2.4 Age | 15 |
| 2.5 Volcanic History of Northland from the Miocene | 16 |
| 2.6 Depositional Environment | 18 |
| Chapter 3: Stratigraphy | 19 |
| 3.1 Introduction | 19 |
| 3.2 Stratigraphic Framework | 22 |
| 3.2.1 Site 1 (Otakamiro Point) | 24 |
| 3.2.2 Site 2 (Maori Bay) | 26 |
| 3.2.3 Site 3 (Collins Bay) | 29 |
| 3.2.4 Site 4 (Pillow Lava Bay) | 32 |
| 3.2.5 Site 5 (Powell Bay) | 36 |
| 3.2.6 Site 6 (Bartrum Bay) | 38 |
| 3.3 Unit Correlation Between Sites | 41 |
| 3.4 Discussion | 42 |

Chapter 4: Lithofacies of the Muriwai volcanic succession 44

| | |
|---|----|
| 4.1 Introduction | 44 |
| 4.2 Pumiceous and scoriaceous lithofacies group | 46 |
| 4.3 Thin pumice and crystal rich lithofacies group..... | 55 |
| 4.4 Volcanic conglomerate lithofacies group | 57 |
| 4.5 Thickly bedded granule sandstone lithofacies group..... | 62 |
| 4.6 Thinly bedded fine sandstone lithofacies group | 67 |
| 4.7 Bioturbated pebbly sandstone facies..... | 71 |
| 4.8 Polymictic breccia facies | 74 |
| 4.9 Coherent lithofacies group | 76 |
| 4.10 Discussion..... | 80 |

Chapter 5: The physical properties of coherent and clastic volcanic components 82

| | |
|---|----|
| 5.1 Introduction | 82 |
| 5.2 Lava | 82 |
| 5.3 Hyaloclastite..... | 84 |
| 5.4 Pumice | 84 |
| 5.5 Scoria | 85 |
| 5.6 Free Crystals..... | 85 |
| 5.7 Comparison of vesicular clasts..... | 85 |
| 5.8 Diagenesis | 86 |
| 5.9 Discussion..... | 86 |

Chapter 6: Discussion 88

| | |
|---|----|
| 6.1 Introduction | 88 |
| 6.2 The Muriwai volcanic succession | 88 |
| 6.3 Regional Setting..... | 89 |
| 6.4 Depositional Environment | 90 |
| 6.5 Source..... | 91 |
| 6.6 Eruption Processes | 92 |
| 6.7 Petrogenesis | 92 |
| 6.8 Transport and deposition..... | 93 |
| 6.9 Facies architecture | 95 |

Chapter 7: Summary 97

| | |
|--|----|
| 7.1 Conclusions..... | 97 |
| 7.2 Recommendations for further work | 99 |

References 100

APPENDIX 1 Literature Review

APPENDIX 2 Nomenclature

APPENDIX 3 Stratigraphic details of study sites

APPENDIX 4 Thin section data

APPENDIX 5 Point counting data and thin section descriptions of lava and volcanic clasts

APPENDIX 6 Bulk rock geochemistry

APPENDIX 7 Vesicularity data

APPENDIX 8 PIMA data

List of Figures

| | <i>pages</i> |
|--|--------------|
| Figure 1.1. Location of the study area in the Northland region..... | 2 |
| Figure 2.1. Location of the Waitakere Group subgroups..... | 8 |
| Figure 2.2. Present orientation of subduction zone, east of N.Z..... | 8 |
| Figure 2.3. Waitakere Group stratigraphy | 11 |
| Figure 2.4. Regional geology map | 12 |
| Figure 2.5. Chronology of volcanic activity in Northland, with biostratigraphic ages | 14 |
| Figure 2.6. Early Miocene reconstruction of Northland | 16 |
| Figure 2.7. Original Miocene volcanic centres around Northland..... | 17 |
| Figure 2.8. The eruptive stages of arc volcanism around Northland | 17 |
| Figure 3.1. The study area, and study site details..... | 20 |
| Figure 3.2. North-south cross section through the six study sites | 22 |
| Figure 3.3. Stratigraphic log of site 1B | 24 |
| Figure 3.4. Stratigraphic logs of site 2..... | 27 |
| Figure 3.5. Stratigraphic logs of site 3..... | 29 |
| Figure 3.6. Stratigraphic logs of site 4..... | 33 |
| Figure 3.7. Stratigraphic logs of site 5..... | 36 |
| Figure 3.8. Stratigraphic log of site 6..... | 38 |
| Figure 3.9. Correlation diagram of stratigraphic logs..... | 42 |
| Figure 4.1. Planar to low-angle cross stratified facies | 47 |
| Figure 4.2. Normally graded and diffusely bedded facies | 48 |
| Figure 4.3. Scour and infill facies | 50 |
| Figure 4.4. Thinly bedded and convoluted facies | 51 |
| Figure 4.5. Detailed log of Pumiceous and scoriaceous lithofacies group | 52 |
| Figure 4.6. Massive pebble facies..... | 53 |

| | |
|--|----|
| Figure 4.7. Thin pumice and crystal rich lithofacies group | 56 |
| Figure 4.8. Tabular pebble-cobble facies | 59 |
| Figure 4.9. Lensing pebble-cobble facies..... | 60 |
| Figure 4.10. Weakly stratified pebbly sandstone facies | 61 |
| Figure 4.11. Very thick, poorly sorted cobble-boulder facies..... | 63 |
| Figure 4.12. Massive normally graded facies..... | 65 |
| Figure 4.13. Cross-stratified facies..... | 66 |
| Figure 4.14. Thinly bedded and normally graded facies..... | 68 |
| Figure 4.15. Thinly bedded calcareous facies..... | 70 |
| Figure 4.16. Bioturbated pebbly sandstone facies | 72 |
| Figure 4.17. Detailed log of bioturbated pebbly sandstone facies..... | 73 |
| Figure 4.18. Polymictic breccia facies | 75 |
| Figure 4.19. Pillow lava and sheet flow facies..... | 78 |
| Figure 4.20. Feeder dyke and mega-pillow facies..... | 79 |
| Figure 6.1: Miocene setting of the Manukau and Kaipara volcanic centres, and sediment transport directions | 89 |
| Figure 6.2. Volcaniclastic apron flanking the Lesser Antilles volcanic arc..... | 94 |
| Figure 6.3. Modern location of Manukau and Kaipara in relation to Muriwai.... | 96 |

List of Tables

| | |
|---|----|
| Table 1. Characteristics of the Waipoua subgroup | 13 |
| Table 2. Characteristics of the Hukatere subgroup..... | 13 |
| Table 3. Characteristics of the Manukau subgroup | 13 |
| Table 4. Lithofacies groups and constituent facies | 45 |
| Table 5. Physical properties of four major volcanic clasts | 83 |

Chapter 1: Introduction

1.1 Preface

The aim of this thesis is to investigate the stratigraphy and volcanology of a Miocene, submarine volcanic succession within the Waitakere Group at Muriwai, New Zealand. The Waitakere Group outcrops on the North Island, from Kaipara in the north, to the south head of Manukau Harbour (**Figure 1.1**) and comprise a sequence of submarine volcanic sediments derived from a Miocene arc. The Muriwai volcanic succession is well exposed and preserved, and provides a good opportunity to improve understanding of a volcanoclastic apron and medial depositional environment that once formed the eastern parts of one or more, submarine to emergent stratovolcanoes. The succession includes sedimentary, volcanoclastic and coherent volcanic facies. The clastic deposits in this succession provide information on the occurrence and interaction of volcanic and sedimentary processes in the submarine environment. The coherent facies provide direct evidence of volcanism and constrain the proximity to vents. A combination of volcanic and sedimentary processes contributes to the complex submarine environment surrounding the stratovolcano. Pyroclastic eruptions associated with stratovolcanoes can contribute more than 95% of all the products erupted at island arcs (McBirney, 1973) and form thick volcanoclastic aprons that extend from the stratovolcano. The large volumes of volcanoclastic detritus and unusual hydrodynamic properties of volcanic particles are an important consideration in understanding submarine transport and depositional processes from stratovolcanoes located in marine environments. There are very few well-documented examples of submarine volcanoclastic aprons of stratovolcanoes. Hence, this study contributes to the understanding of volcanoclastic aprons. This detailed work on the Muriwai volcanic succession adds to current knowledge of Miocene volcanic activity on Northland. It also has implications for the understanding of island or emergent arc environments and their deposits worldwide.

1.2 Aims and significance

This study of the stratigraphy, facies types, and physical properties of the coherent and clastic components that comprise the Muriwai volcanic succession, will enhance knowledge of the characteristics of submarine aprons associated with stratovolcanoes. This study involved mapping and detailed stratigraphic analysis of an exposure of the Waitakere Group at Muriwai. These exposures have been termed the Muriwai volcanic succession.

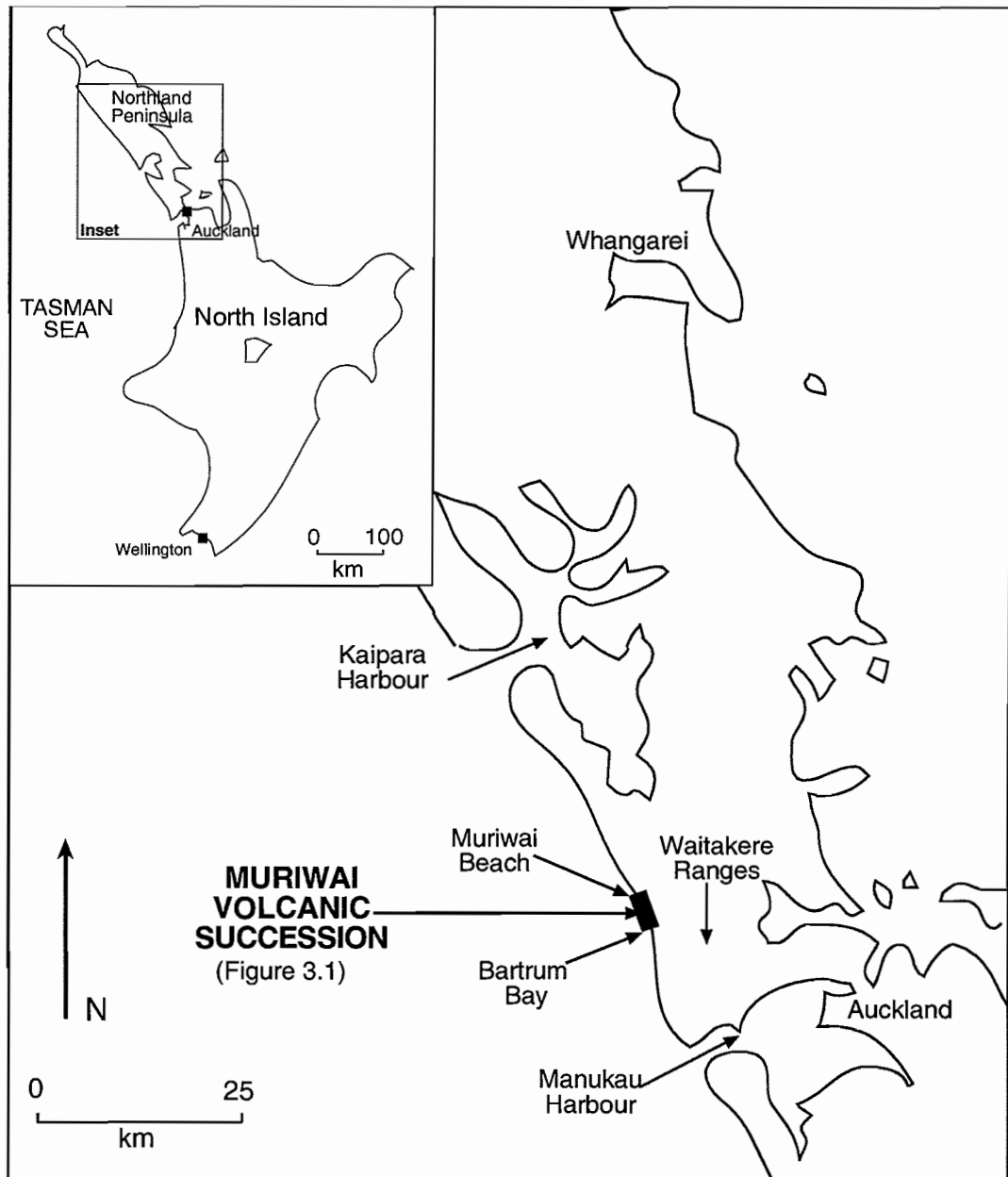


Figure 1.1. *Location of the study area, and the Muriwai Volcanic Succession, in the Northland region of New Zealand.*

The Muriwai volcanic succession extends from Muriwai Beach in the north, southwards to Bartrum Bay. Near continuous coastal exposures offered the opportunity to study the features of a medial, submarine volcanoclastic apron, derived from one or more stratovolcanoes. The succession includes sedimentary deposits, and primary and reworked volcanic deposits that include mud, crystal- rich sand, pumice- and scoria- rich units, volcanic conglomerates and pillow lavas. The primary objective of this study is to characterise the facies and their origin, and to interpret the transport and depositional mechanisms involved in the construction of a medial, submarine volcanoclastic apron of a stratovolcano.

The abundance of vesicular pumice and scoria in the pumiceous and scoriaceous facies suggests significant pyroclastic eruptions occurred during the eruptive history of the stratovolcano. In contrast, the coherent volcanic facies and dense rounded lava clasts within the volcanic conglomerate facies, suggest a history of effusive activity and erosion from the contributing volcanic centre. These conglomerates, along with the sedimentary units provide constraints on the setting for the pyroclastic and coherent units. Lithofacies characteristics of the pumiceous and scoriaceous deposits, are used to help interpret the submarine transport and depositional processes of the pyroclasts.

The regional setting and depositional environment of the Waitakere Group have been well established by previous workers (Hayward, 1976a, Hayward, 1976b, Hayward, 1979, Hayward et al, 2001, Chapter 2), and provide good constraints for this detailed volcanological study.

This study aims to;

1. Map the Muriwai volcanic succession between south Muriwai Beach and Bartrum Bay, identify lithological units and determine the stratigraphy using stratigraphic logs and cross sections.
2. Undertake detailed lithofacies, compositional and textural studies of the volcanoclastic units.
3. Identify and characterise the volcanic components and determine their origin.
4. Interpret the (i) eruption styles, transport and deposition mechanisms of the lithological units, and to (ii) determine the depositional environment.

5. Reconstruct the volcanic setting and determine the likely relationship to the Miocene source volcanoes.

1.3 Thesis Organisation

This thesis comprises six chapters. Chapter 1 introduces the project aims, location of the study area, field and analytical methods, previous work and background to the study area. Chapter 2 introduces the regional geology and previous research on the volcanic evolution of Northland, the Waitakere Group, and the depositional environment of Muriwai.

Chapters 3 to 5, include new data from this research project on the geology of the Muriwai volcanic succession. Chapter 3 details the stratigraphy of the succession, by using stratigraphic logs and cross sections. The stratigraphic relationships between six field sites (1-6) are highlighted in a fence diagram and the major features of each site are described. Chapter 4 describes in detail characteristics of the major lithofacies, with interpretations of the submarine transport and deposition mechanisms involved in their formation. Petrographic, textural and compositional features, and the vertical and lateral variations of each unit are described. Chapter 5 uses geochemical, density and petrographic analysis to characterise the physical properties of the major volcanic clasts, and to determine clast composition(s). The volcanic clasts and enclosing clastic matrix is characterised by Short Wave Infra-Red (SWIR) analysis.

Chapters 6 and 7 synthesise and discuss the data. The discussion includes interpretations on the origins of the clastic rocks, through a review of the main deposit characteristics. Chapter 6 discusses the results of this research project and interprets the origins of the succession. In particular, the characteristics of the volcanic source are discussed, including depositional environment, eruption styles, petrogenesis and facies architecture. Reconstructions of the volcanic setting and the relationship of this deposit to the source volcanoes are established, in comparison with the relevant literature. Chapter 7 provides a summary of the thesis. The significance of these results to studies of submarine successions are highlighted, and recommendations are made for further study.

1.4 Project Location

The Muriwai volcanic succession includes a 2.6 km stretch of coastline. It is located 32 km northwest of Auckland, in the northern the Waitakere Ranges on the Northland Peninsula. The study area covers the western-most outcrops of the Waitakere Group, known as the Manukau subgroup. The study area falls in the 1:50 000 geological Waitakere map Sheet (Hayward, 1983).

The coastal terrain is rugged and steep, with sheer cliffs and tidal rock platforms. Six rocky headlands separate a series of small bays. Well-exposed cliff sections define six major outcrop sites. Each site contains a 30-40 m high cliff section (each of <100 m width). Along the coast, outcrop accessibility is subject to the tides. At low tide, Maori Bay was the primary access route to northern parts of the study area. Permission was granted to use tracks on private property, which were valuable at high tide, and for the southern part of the study area.

1.5 Methods

A concentrated period of field mapping and sampling of the major units, was conducted between 16th March to 9th April, 2003. The six sites were mapped using stratigraphic logs and cross sections, with detailed stratigraphic logs of accessible beds. Lithological, compositional, and textural features of the major units were documented. Fallen boulders of the upper units enabled further investigations of inaccessible units. Binoculars were also employed where outcrop height restricted close inspection.

Photographs were taken to document both small and large-scale features in the field. The lithological relationships, unit distributions, sedimentary structures, rock components and textures were recorded in the field and photographed. Rock samples of the major volcanoclastic and sedimentary units, and pillow lavas were collected for petrographic and geochemical analysis. A total of eight XRF analysis of the lavas and volcanic clasts were undertaken. The altered matrix of the lavas and volcanic clasts of the major units were analysed using SWIR techniques in the Portable Infra-red Mineral Analyser (PIMA) instrument. Density testing and point counting of the volcanic components, including vesicle content, permitted a more detailed assessment of their physical properties (Appendix 5).

1.6 Previous Work

Initial work on the Waitakere Group began with the geological investigations of the Auckland region by Hochsletter (1864), and the geology of North Head, Manukau Harbour by Hutton (1870). This was followed by further geological investigations on the Waitakere Ranges by Taylor (1927), Searle (1944) and Brothers (1954). Other early studies concentrated on the coastal features of Northland, including coastal changes (Smith, 1881), and on the Tertiary Mollusca of the west coast and Maori Bay (Powell, 1935).

Geological work at Muriwai began in the 1930's, with a study on the Maori Bay pillow lavas (Bartrum, 1930). Since this time palaeontology, stratigraphy, structure, and age relationships of the Waitakere Group, and the Miocene arc have been the focus of many research projects by Auckland geologists. In particular, Bruce Hayward recorded and described the Waitakere Group geology in the Waitakere Ranges (Hayward, 1975), and the presence of Lower Miocene Polychaetes (Hayward, 1977a) and corals (Hayward, 1977b), along with the micropalaeontology and palaeoecology of the Waitakere Group (Hayward 1976c). Less is known on the geochemistry of the Waitakere Group. Wright and Black (1981), and Smith et al (1986) constrained the petrology and geochemistry of the Waitakere Group lavas. In addition, Yamagishi (1985) examined pillow lava morphologies from Muriwai and Te Henga, to determine pillow lobe growth.

Hayward's work formed the basis for the 1:50 000 Waitakere, Sheet Q11 Geological Map (Hayward, 1983). Hayward (1976b) defined the broad structure of the Lower Miocene Waitakere Group and introduced new stratigraphic subdivisions. Three new subgroups (the Waipoua, Hukatere and Manukau subgroups), excluded the outdated Manukau Breccia from stratigraphic terminology. Sediments of the Muriwai volcanic succession and further south to Te Waharoa were part of this change, and were mapped by Hayward (1976a).

Palaeontological work has been carried out on biostratigraphy at Muriwai (Bandy et al, 1970), submarine trace fossil assemblages (Hayward, 1976d) and fossil fauna in the eastern Waitakere Ranges (Hayward, 1979d). This work includes the taxonomy of benthic foraminifera of Northland and the Tasman Sea (Hayward and Buzas, 1979).

Miocene arc evolution and tectonic plate orientation of Northland are topics of past and current contention. Regional arc studies have been used to reconstruct the tectonic evolution of the arc (Ballance, 1976), and the development of Northland (Ballance et al, 1982). The issue of the direction of subduction and migration of volcanic activity on North Island is also contentious (Brothers, 1984). Cole (1986) gives an account of the relationship of Northland to Cenozoic volcanism in New Zealand. The Miocene Volcanic Centres of the Waitakere Ranges and the eruptive history of the Miocene arc have been described and discussed by Hayward (1977; 1979) and supplemented by K-Ar dating (Hayward et al, 2001). Current knowledge of the development of Northland, the arc, its volcanic history and related deposits have been clarified and summarised by Hayward et al (1993). Davey (1974) used geophysical methods to identify numerous volcanic centres offshore from Northland.

Chapter 2: Regional Geology and Setting

2.1 Introduction

On the Northland peninsula, the rocks of the Waitakere Group record arc-related volcanism and largely submarine volcanoclastic deposition. The Miocene Waitakere Group cover a significant proportion of Northland, from Auckland to Hokianga Harbour (Hayward, 1976c). The Waitakere Group is comprised of three geographically separate subgroups; the Waipoua Subgroup in the Hokianga-Kaihu area, the Hukatere Subgroup in the Tokatoka-Okahukura Peninsula area and the Manukau Subgroup, which occurs in the Waitakere Ranges and on the west coast of the Auckland region, and at Waiuku south of Manukau harbour (Hayward, 1976b) (**Figure 2.1**). This group is inferred to continue west of Northland (Hayward, 1983) and is related to distinct centres of Miocene volcanism, mainly situated to the west. This chapter will review the regional geology and depositional environment of the Waitakere Group, and the volcanic history and the tectonic origin of the Northland Peninsula.

2.2 Tectonic Framework

The volcanic history and geological development of the North Island is controlled by plate convergence at the Indian-Pacific plate boundary (**Figure 2.2**). The Indian-Pacific plate boundary is thought to have propagated through New Zealand in the Early Miocene, marked by normal and transcurrent faulting (Ballance, 1976). The intensity of volcanism increased at the beginning of the Miocene (Cole, 1986) at the Western Northland / Three Kings rise arc, and the Tonga-Lau / Kermadec-Colville arc (Ballance et al, 1982). Magmatic arc volcanism occurred on and offshore from Northland, while intra-plate activity occurred at the Banks Peninsula and Dunedin (Cole, 1986). Miocene volcanism preceded modern volcanic activity at the Tonga-Kermadec-New Zealand Arc that is responsible for the current Taupo Volcanic Zone (Hayward, 2001). In New Zealand, volcanism on the North Island appears to have steadily migrated eastward from the Northland arc in the Miocene, to its present position in the Taupo Volcanic Zone.

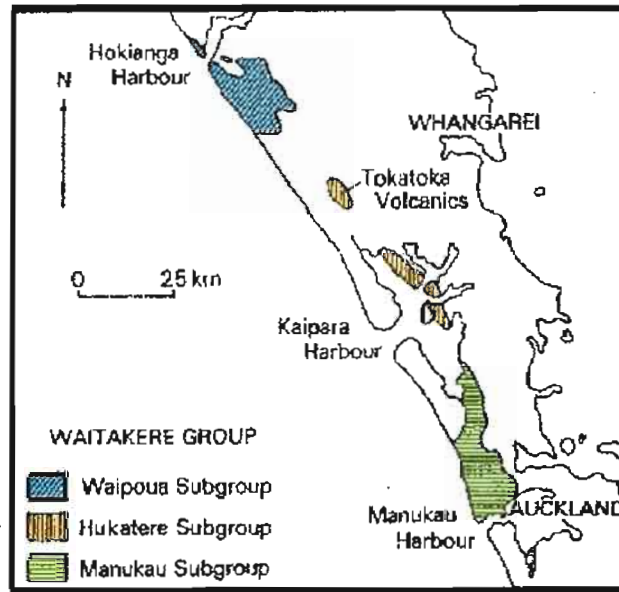


Figure 2.1. Location of Waitakere Group in central Northland, with each of the subgroups highlighted (modified from Hayward, 1976b).

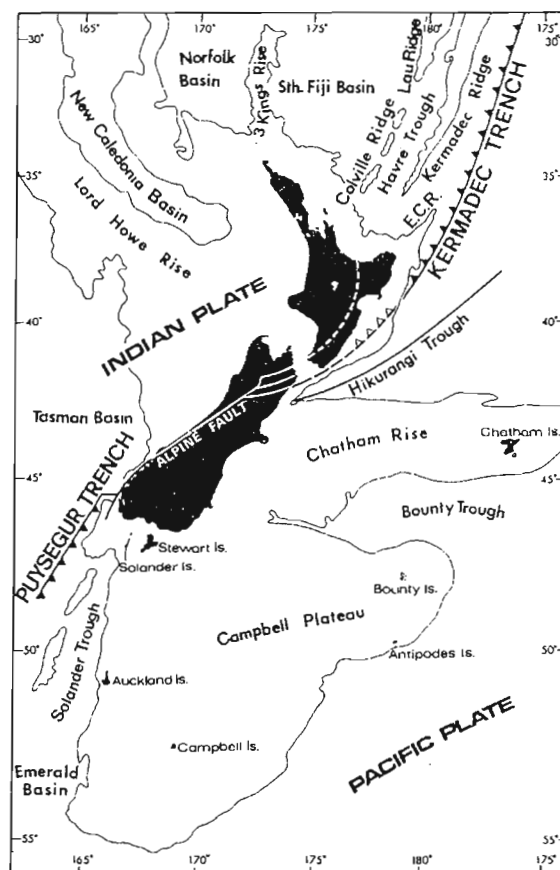


Figure 2.2. Tectonic structure of the south-west Pacific, showing the present location and orientation of the subduction zone east of the North Island (from Cole, 1986).

Miocene volcanism in Northland is represented by two belts of volcanoes, one to the east (eastern belt), and one to the west (western belt). The Waitakere Group is part of the western belt. The broad volcanic and tectonic evolution of the North Island remains the subject of debate (Ballance, 1976; Brothers, 1984; Kamp, 1984; Ballance et al, 1982; Ballance et al, 1985; Kear, 1994). Issues of contention relate to the degree and direction of subduction, the tectonic controls, and the sequence of eruptive events.

Miocene volcanism in Northern New Zealand began at approximately 25 Ma, and was active until 15 Ma (Hayward et al, 2001). Based on a small suite of K-Ar ages, Brothers (1984) and Kamp (1984) have suggested that a short, northeast-southwest volcanic arc extended through northern New Zealand in the Early Miocene. This line of evidence suggests that a northeast-southwest oriented subduction zone was in operation. The parallel orientation of the western and eastern volcanic belts, on either side of the Northland region is now interpreted as one broad volcanic arc (Hayward et al, 2001). K-Ar ages presented by Hayward et al. (2001), points towards effectively contemporaneous volcanic activity from the two belts. Evidence presented by Hayward et al. (2001) suggests the subduction zone was trending NNW-SSE, and the eastward migration of volcanic activity is not supported by Hayward et al. (2001). Kear (1994) simplifies the volcanic history by proposing a “least complex” model for the development of two volcanic belts that relate past, to present day activity.

2.3 Regional Geology

Permian and Jurassic igneous and sedimentary rocks dominate the Northland basement (Hayward, 1993). These rocks comprise the eastern Waipapa Terrane and the western Murihuku Terrane that form two north-west trending belts separated by a zone of serpentised ultra-mafic rocks (the Junction Magnetic Anomaly). Cretaceous basement of volcanic and sedimentary rocks of the Te Kuiti Group and Houhora complex have a limited extent, possibly related to tectonic erosion and decollement in the Early Miocene (Hayward, 1993).

The Waitakere Group replaces a group of similar rocks previously known as the Manukau Breccia. The Manukau Breccia was regarded as a part of the Waitemata Group as similar, but poorly defined rocks from Kaipara Harbour, Tokatoka, Hokianga and North Cape were grouped together (Hayward, 1976b). The Waitakere Group is comprised of coherent and clastic volcanic rocks that were produced during Early to Mid Miocene volcanism from the western Northland Arc belt (Hayward, 1976b). The Waitakere Group preserves island arc lithologies, with coarse volcanoclastic sediments grading away from the volcanic centres to finer sediments in the east.

The Waitakere Group is closely related to the Lower Waitemata Group sediments further east. The Waitakere Group conformably overlies the Waitemata Group in the Waitakere Ranges, and has an inter-fingering relationship in the east (Hayward, 1983) (**Figure 2.3**). The Waitemata Group is comprised of mixed flysch facies of submarine fan and proximal turbidites that were deposited in an inter-arc basin (Hayward, 1983). In the west, the Waitemata Group is overlain by lava flows, eruptive centres and intrusions of the Waitakere Group (Hayward, 1976b). Andesitic and basaltic volcanoclastic debris flow deposits (Parnell Grits) are interbedded with the Waitemata Basin flysch (Hayward, 1993). They are concentrated south Kaipara and occur infrequently around Auckland. The unstable subaerial and shallow submarine slopes of the western arc centres are believed to be the source of these grits.

The three subgroups of the Waitakere Group (Waipoua, Hukatere and Manukau) correspond to offshore magnetic anomalies that mark the Miocene volcanic centres and may be genetically related. The Waipoua Subgroup consists of coherent and clastic basalts and volcanogenic sediments (Hayward, 1976b) (**Table 1**). It has a variable unconformable relationship in contact with the underlying Otatau Group (**Figure 2.3**). The Hukatere Subgroup consists of intrusive and extrusive andesite, basalt and Dacite, and related proximal volcanogenic sediments (Hayward, 1976b) (**Table 2**). It has an unconformable relationship with the Timber Bay Formation of the Waitemata Group, (**Figure 2.3**). The Manukau Subgroup consists of coherent and clastic andesites and dacites, with volcanogenic sediments (Hayward, 1976b) (**Table 3**). Beds in the Waitakere Ranges thin towards the west, and have gradational contact relationships with adjacent units. Recurring sediments, lack of significant marker horizons and high amounts of faulting, have made stratigraphic correlations problematic in this area (Hayward, 1976b) (**Figure 2.4**).

Several constituent members and formations of the Manukau Subgroup are present along the Muriwai coastline. Hayward (1976b) defined the Nihotupu and Tirikohua formations at Muriwai. The Nihotupu formation broadly contains muddy volcarenites and large pillow lava piles (Maori Bay Member), and thinly laminated volcarenites (Wairere Member). The Tirikohua Formation broadly consists of high amounts of coarse volcorudite, and pumice and scoria lapilli of the Maori Bay Conglomerate, Bartrum Member, Te Waharoa Conglomerate and Otakamiro Member (Hayward, 1976a). The Muriwai rocks have been shown by Hayward (1976b) to interfinger with the Piha Formation of the Manukau subgroup, which outcrops on the coast further south. The Piha Formation is generally comprised of stratified cobble, pebble volcorudites (Hayward, 1976a). In general, the Manukau Subgroup consists of coarse- and fine-grained volcanic sediments.

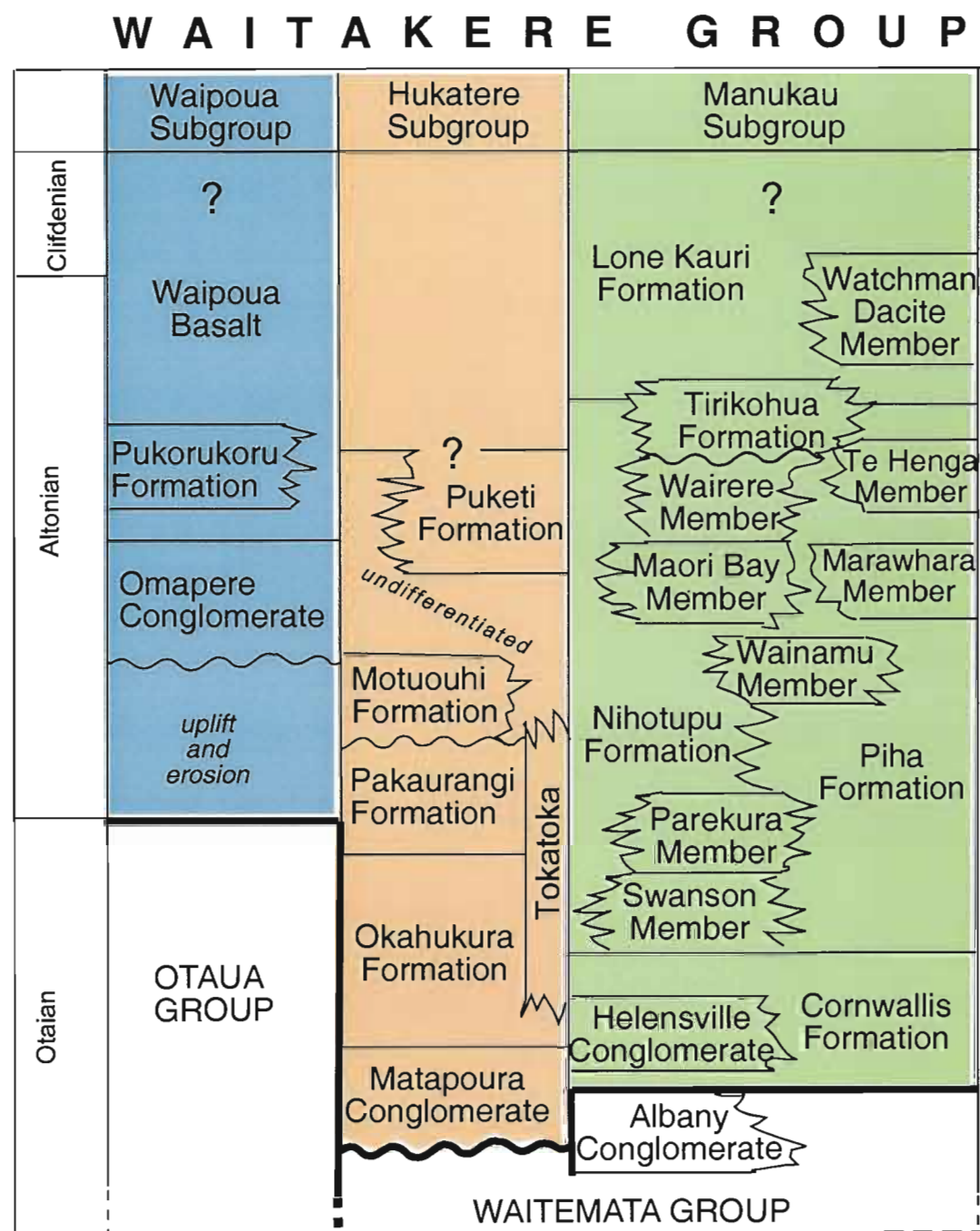


Figure 2.3. The stratigraphy of the Waitakere Group rocks, showing the age relationship of each of the constituent formations within the subgroups (modified from Hayward, 1976b).

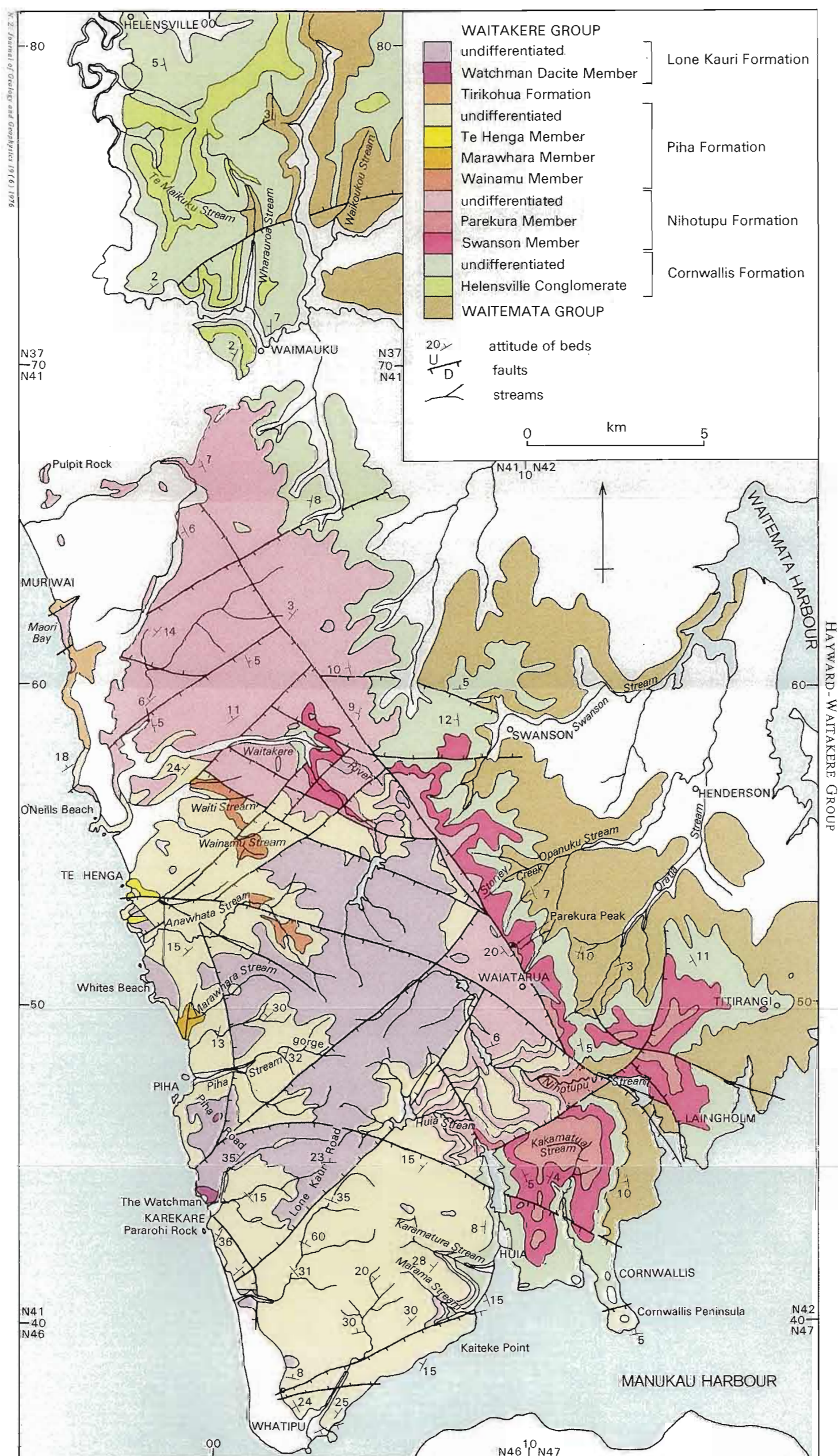


Figure2.4. *The Waitakere Group in the Waitakere Ranges, from Helensville in the north, to Manukau Harbour in the south (from Hayward, 1976b).*

| WAIPOUA SUBGROUP | |
|-------------------------|---|
| Formation | Description |
| Waipou Basalt | Basalt flows, dykes, pyroclastics |
| Pukorukoru Formation | Well-rounded cobble-pebble rudites, arenites, lignites, loc insitu tree stumps |
| Omapere Conglomerate | Well-rounded cobble-pebble rudites, interbedded arenites |

Table 1. *Characteristics of the Waipoua Subgroup of the Waitakere Group (modified from Hayward, 1976b).*

| HUKATERE SUBGROUP | |
|-----------------------------------|--|
| Formation | Description |
| Puketi Formation | Andesitic tuff breccias, tuffs, pumiceous tuffs, lignite, basalt |
| Motuouhi Formation | Dark brown vitric tuffs |
| Pakaurangi Formation | Fossiliferous, sandy lutites, andesitic arenites, hyaloclastites |
| Unnamed Tokatoka | Basalt, andesite, Dacite sills, dykes and breccia pipes |
| Okahukura Formation | Argillaceous limestone, andesite, interbedded volcarenites and volclutites. |
| Undifferentiated Hukatere Pen. | Pillow lavas, pumice lapilli tuffs, lignites, arenites, limestone |

Table 2. *Characteristics of the Hukatere Subgroup of the Waitakere Group (modified from Hayward, 1976b).*

| MANUKAU SUBGROUP | |
|-------------------------|--|
| Formation | Description |
| Lone Kauri Formation | Predominantly andesitic extrusives, pyroclastics, basaltic andesite and minor dacite intrusives |
| Tirikohua Formation | Coarse cobble rudites and fine arenites with pumice lapilli and scoriaceous clasts |
| Piha Formation | Stratified, coarse subangular to subrounded volcaniclastics, andesi pillow lavas and hyaloclastites |
| Nihotupu Formation | Massive and well bedded fine volcaniclastics, volcarenites volclutites and andesite pillow lavas |
| Cornwallis Formation | Sandy volcorudite with andesitic scoriaceous and pumiceous clast Contains thin, laminated volcarenite interbeds |

Table 3. *Characteristics of the Manukau Subgroup of the Waitakere Group (modified from Hayward, 1976b).*

Petrographic and geochemical features of the Waitakere Group rocks are typical of calc-alkaline magmatism, and volcanic activity at a convergent plate margin (Wright and Black, 1981). Trace element and bulk rock analysis of representative samples from the Waipoua, Hukatere and Manukau Subgroups revealed high-Al₂O₃ contents and low Rb/Sr, Ni and Cr (Wright and Black, 1981). The Manukau Subgroup has lower K₂O contents than Waipoua and Hukatere, which may relate to the dip of the Benioff zone at the site of magma generation (Wright and Black, 1981).

2.4 Age

K-Ar dates and biostratigraphic ages provide a well-constrained time frame for the Miocene sediments and volcanics. The New Zealand stages from the Late Oligocene to Late Miocene are well characterised by planktonic foraminifera zones (**Figure 2.5**). K-Ar ages have constrained the sequence of volcanic events in Northland (Hayward, 1993), and have been compared with biostratigraphy, structures and volcanic stratigraphy (Hayward et al, 2001). Foraminifera at Muriwai contain the youngest known biostratigraphic age for the entire Waitakere Ranges, which is mid Altonian (Hayward, 1979d).

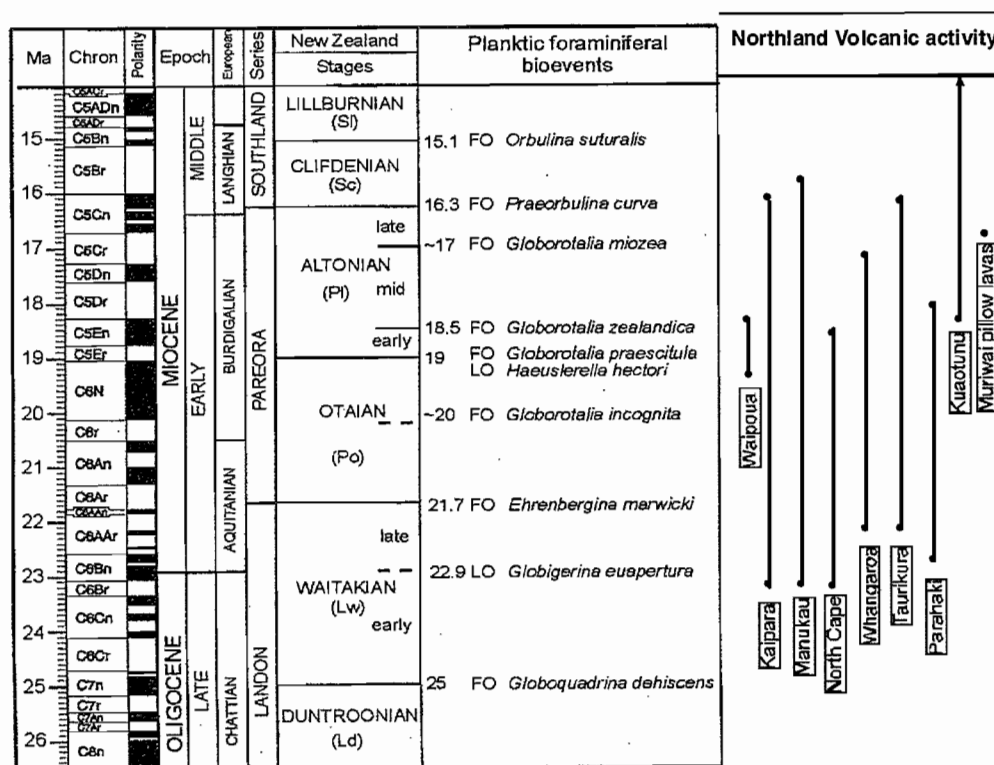


Figure 2.5. Chronology of Northland volcanic activity as determined by K-Ar ages, in relation to the New Zealand stages constrained by biostratigraphic ages (modified from Hayward et al, 2001)

2.5 Volcanic History of Northland from the Miocene

Plate convergence at the Indian-Pacific plate boundary triggered a series of tectonic and volcanic events in the Early Miocene. Subduction of the Pacific plate beneath the North Island is thought to have begun in the Late Oligocene – Early Miocene, between 30-35 Ma. During the Late Cretaceous or Palaeocene, subsidence of the north and west parts of Northland produced a south and eastward transgression that resulted in the formation of a broad sedimentary basin, the Northland Basin (Hayward, 1993) (**Figure 2.6**). The Northland Basin was a part of the arc-trench gap that existed between an eastern trench and parallel volcanic arc (Hayward and Buzas, 1979). The basin persisted through the Eocene to Oligocene, covering Auckland and south Auckland, an area known as the Waitemata Basin. At approximately 25 Ma, obduction of the south propagating Northland allochthon and regional thrusting was followed closely by magmatic arc activity (Ballance et al, 1982).

Volcanism commenced on the North Island at Northland, 5-10 Ma after subduction began (Hayward, 1993). A series of magmatic arcs have been the source of volcanic activity from Miocene times, and include the Northland arc, the Coromandel Arc, the Whitianga Arc, the Tauranga Arc and the Taupo Arc (Ballance, 1976). Volcanic activity at the Northland arc continued for 10 Ma, and once activity ceased volcanism migrated east to the Coromandel Peninsula (Hayward et al, 2001).

Throughout the evolution of island arc activity, calc-alkaline products typical of continental margin volcanism have changed, from basic to more silicic compositions. Present day volcanism on the North Island is characterised by dacites, voluminous rhyolite and ignimbrite at the TVZ and andesitic compositions at Mt Egmont / Taranaki. Basaltic volcanic activity has occurred from numerous small, monogenetic volcanoes in Auckland, south Auckland (Auckland Volcanic Field), and Northland (Bay of Islands, Whangarei). The latest volcanism has been during the last 150 000 years, when lava fields, scoria cones and tuff rings formed, and 600 years ago Rangitoto erupted (Kermode, 1992).

From 25 to 15 Ma, magmatic arc volcanism occurred in Northland through two 300 km long, parallel arc belts either side of the peninsula. The western and eastern belts were separated by a 30-60 km wide non-volcanic region (Hayward et al, 2001) (**Figure 2.7**). Hayward et al (2001) show that eruptions from the western and eastern belts were coeval, with no significant difference in age of the two belts (**Figure 2.8**). The western belt was active from 25-15 Ma, and the eastern belt from 20-17 Ma (Hayward et al, 2001). Activity on the western belt was initiated 5 Ma prior

to eruptions commencing on the eastern belt. The Manukau centre records some of the first and last eruptions from the Northland arc (Hayward et al, 2001).

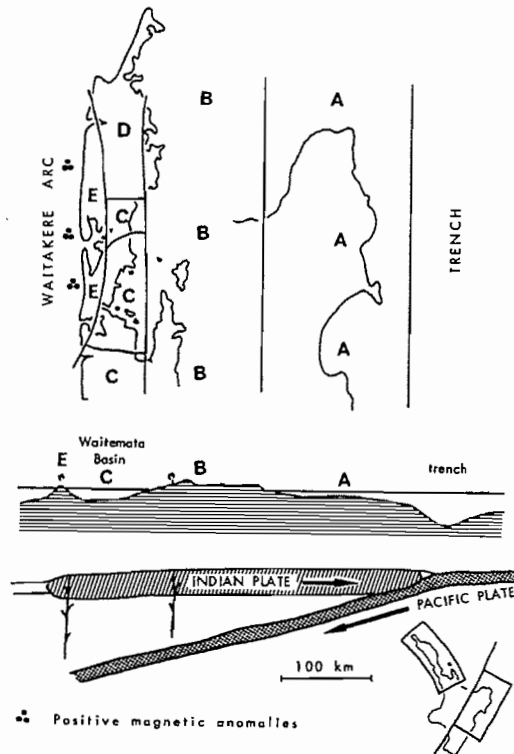


Figure 2.6. *Reconstruction of Northland during the Early Miocene, showing the eastern slope and marine shelf (A), the central basement high (B), the elongate marine basin (C), a northern landmass (D), and the western Northland arc belt (E) (from Hayward and Buzas, 1979).*

The original centres of the Miocene arc volcanoes are marked today by a small number of major, and numerous smaller, terrestrial and offshore magnetic anomalies in the Northland region (Davey, 1974) (**Figure 2.7**). The major anomalies define a basalt shield volcano (Waipoua) and two stratovolcanoes (Kaipara and Manukau). Other large anomalies are inferred to be stratovolcanoes (Hayward, 1993). Three major stratovolcano complexes (Whangaroa, Taurikura and Kuaotunu) and dacite domes comprise the eastern belt (Hayward, 1993). The Manukau complex, west of the Waitakere Ranges is inferred to have been a 2-3 km high and 60x40 km across submarine stratovolcano (Hayward et al, 2001).

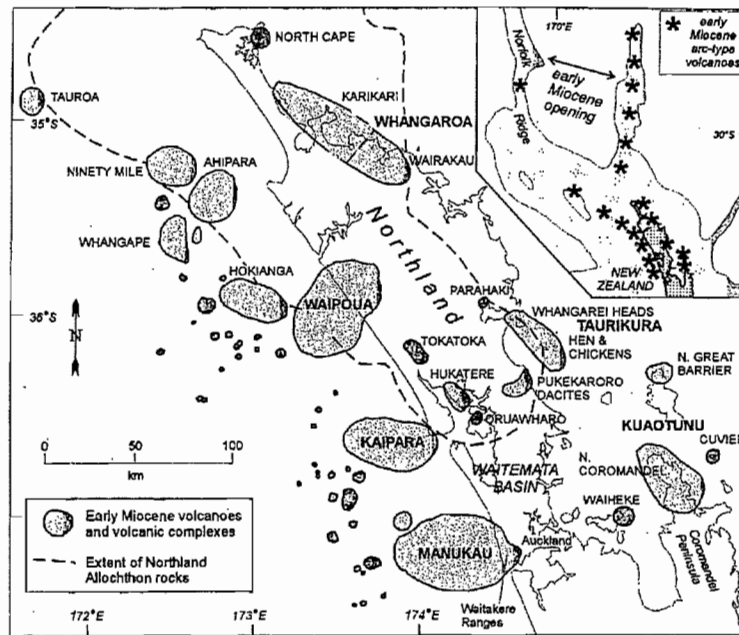


Figure 2.7. The original centres of Miocene volcanism, located on and offshore from Northland (from Hayward et al, 2001).

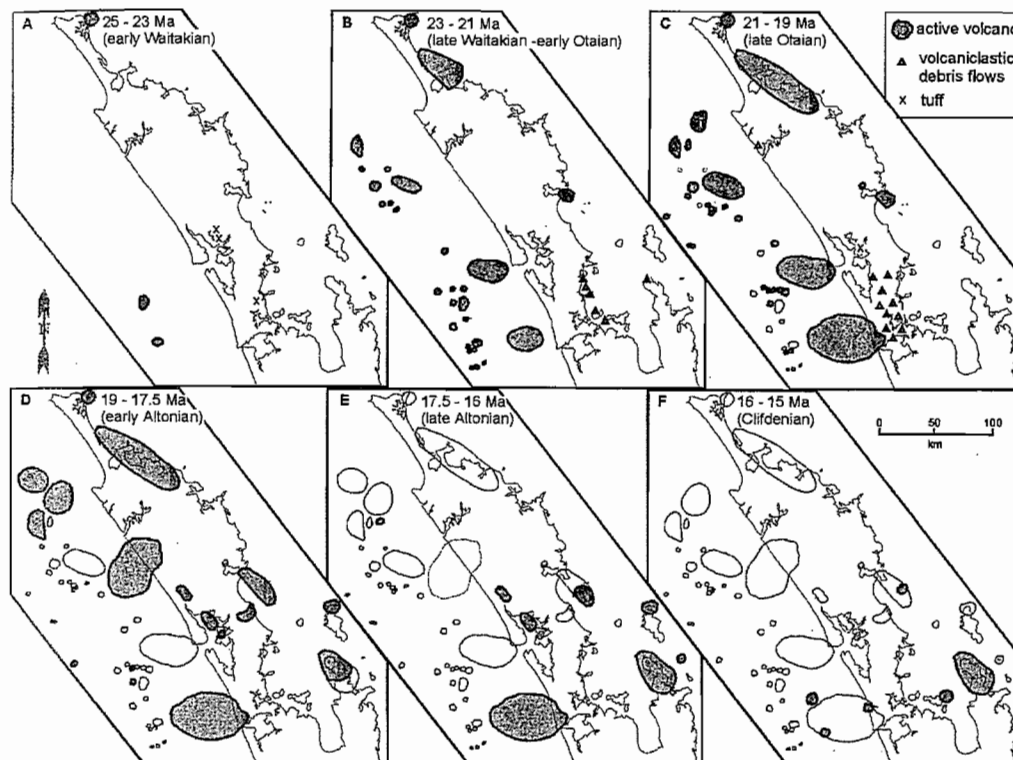


Figure 2.8. Arc volcanism on Northland, between 25 and 15 Ma (from Hayward et al, 2001).

The exposed eastern flank in the Waitakere Ranges is composed of lava flows, pillow lavas, breccias, coarse and fine-grained volcanoclastics (Piha Formation) and marine sediments. Subaerial craters, diatremes and intrusions are overlain by subaerial andesite flows.

2.6 Depositional Environment

In the Early Miocene, Northland was characterised by two volcanic chains separated by an inter-arc basin. An elongate marine basin formed south of the allochthon (Hayward, 1993), between a basement high and the volcanic edifices (Hayward, 1976c) (**Figure 2.6**). Volcanoclastic detritus generated largely during explosive activity transformed the quiet Northland Basin into a major depocentre, surrounded by widespread volcanism (Hayward, 1993). Coarse and fine-grained volcanoclastics and sediments of the Waitakere Group accumulated in the western parts of the basin. Marine macrofossils, microfossils and trace fossils in the Waitakere and Waitemata Groups provide information on the Early Miocene submarine depositional environment.

The palaeoenvironment and palaeobathymetry is constrained by marine organisms including bivalves, gastropods, polychaetes, echinoids, shrimps, scaphopods, serpulids, sponges, benthic foraminifera, ostracods (Hayward, 1976d), hermatypic and ahermatypic corals. In-situ, undisplaced biocoenoses from Muriwai and the eastern Waitakere Ranges suggest mid to lower bathyal water depths (1000-3000 m) occurred in submarine canyons on the eastern flank(s) of the western arc centres (Hayward, 1976c). Deep-waters occurred in the Waitemata Basin in the Mid Altonian (Hayward, 1979d). The presence of macrofossils and corals in displaced thanatocoenoses indicates that intertidal, shallow gravel banks and upper to mid neritic environments existed on the upper submarine volcano flanks (Hayward, 1976c). Shallow water corals imply a north and westwards shallowing of the Waitemata Basin to neritic depths (20-100 m) (Hayward, 1977b). These displaced thanatocoenoses also reflect sediment redeposition by mass flows from shallow to bathyal water depths and suggests that instability produced by explosive eruptions and seismic events on the volcano edifice was a major control on the submarine palaeoenvironment. The presence of corals suggests that shallow and stable water conditions necessary for coral colonization may have been intermittently produced on the volcano edifice(s) (Hayward, 1977b). However continuous coral establishment was not favoured by the repeated construction and destruction of volcanoes in the Early Altonian. The occurrence of reef corals suggests that a warm palaeoclimate existed during the Otaian and Lower Altonian (Hayward, 1977b).

Chapter 3: Stratigraphy

3.1 Introduction

The coherent and clastic rocks comprising the Muriwai volcanic succession form a series of distinct, interrelated submarine volcano-sedimentary rock sequences. The succession is horizontally bedded, with local occurrences of shallowly dipping beds, post-depositional faults and sedimentary structures. The Muriwai volcanic succession is divided into six study sites, the location of which is based on the natural separation of cliff and headland exposures by bays (**Figure 3.1**). Details of individual facies types at the six study sites provide a framework in which lithostratigraphic features can be established. Each site has been separated into one or up to four different sections depending on the level of stratigraphic variability, so that all major changes in stratigraphy were recorded. The Muriwai volcanic succession comprises a total of fifteen sections. Each section is distinguished by variations in sedimentary, volcanic and stratigraphic features. However in many cases the sections show lateral gradational contacts. Due to coastal embayments, variations on the north and south side of each headland could be identified.

This chapter provides the stratigraphic framework for the Muriwai volcanic succession. The stratigraphic framework of the Muriwai volcanic succession used herein provides a basis for presentation of the main facies types in chapter 4, with detail of their volcanic components provided in chapter 5. Stratigraphic data at each section was recorded in stratigraphic logs and cross sections. Stratigraphic logs record lithological information including bedding style and thickness, components, grainsize, sorting, fossils and internal sedimentary structures such as grading and bedding. Photos were taken of small-scale features to record examples of individual units and the field layout of each section. The reference line for the base of the stratigraphic logs was the level of beach sand. Changes to the sand level over time will alter the proportion of basal beds that are exposed. Where possible, rock samples were collected of each distinct lithological interval. The final outcome of this chapter is to provide a correlation diagram that connects the major units identified at each section.

The units are described in terms of their lithology, and lithofacies information including bedding thickness and bed-forms, components, grainsize and composition. Bed thickness followed the

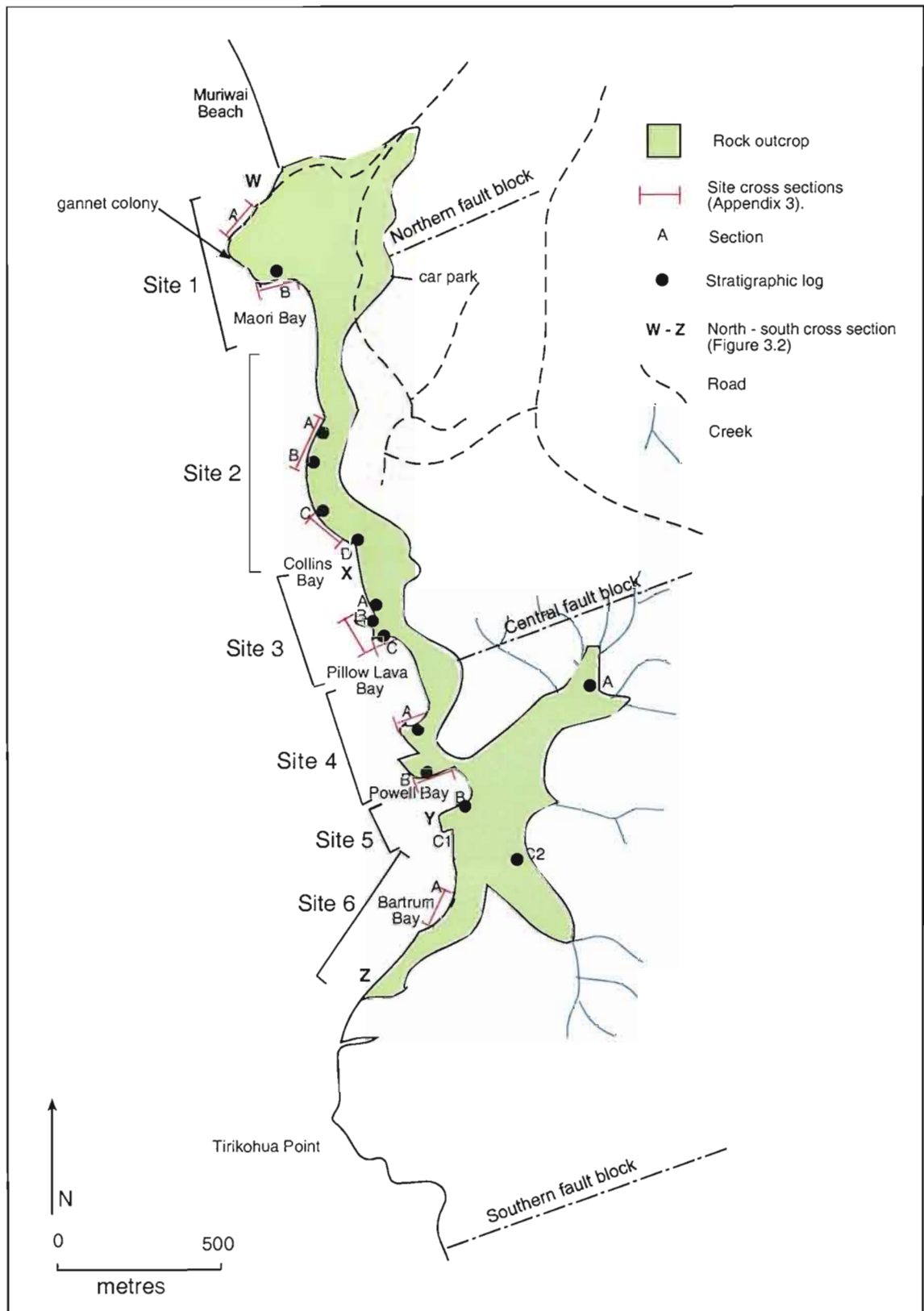


Figure 3.1. Study area, with site details including location of sites and sections. Location of site cross sections, stratigraphic logs and the N-S cross section are shown. Fault blocks follow Hayward (1976a).

scheme of McPhie et al. (1993). Grainsizes were estimated in the field, and in thin sections. Grainsize classification uses the sedimentary scheme for sedimentary and volcanic clast types. Classification schemes are shown in Appendix 2.

Hayward (1976a) divided the Muriwai volcanic succession into 3 major fault blocks (**Figure 3.1**). The fault blocks are part of a regional block-faulted sequence that have been progressively downthrown south in a stepwise manner (Hayward, 1976a). This structure is related to large scale block faulting of the Waitakere Ranges, produced by regional tectonic, and local volcanic activity during the Miocene (Hayward, 1976b). Site 1 occurs within the northern block, sites 2 and 3 in the central block and sites 4-6 in the southern block. The northern and southern blocks were thought to have been downthrown relative to the central block (Hayward, 1976a). The northern and central blocks have gentle dips and anticlinal folds.

3.2 Stratigraphic Framework

The field characteristics of each section are shown in sketches and photos, in Appendix 3. The lithological units of each site are described in chronostratigraphic order, from the base to the top, with field data displayed in stratigraphic columns. A schematic north-south oriented cross section shows the contact relationship of the six sites and cross sections (**Figure 3.2**).

The sections from cliffs that have a north westerly or south easterly aspect, although parts of the headland at site 2 and 3 face west. Each site has been separated into units based on lithological features. Coherent and clastic units dominate the Muriwai volcanic succession. The division of each site into broad lithological units provides a basis for correlation of the succession and a framework from which the major lithofacies types can be determined.

Bedded sandstone forms the basal part of the stratigraphy and is found at all sites (2, 3, 4, 5 and 6), except site 1. These sandstone beds have an eroded, u-shaped upper relief and an undetermined lower extent. Coherent units occur in the lower and upper parts of the stratigraphy at sites 2, 3, 4 and 5. The coherent units form broadly conformable mounds and cross cutting structures. Conglomerate inter-bedded with sandstone comprise a large proportion of the upper clastic sequence at site 3. Beds of pumice and scoria dominate the succession at sites 1 and 4, and form the uppermost unit at site 5 and 6. Beds of pumice and scoria, and conglomerate occur in different parts of the stratigraphy, except for a thin conglomerate layer within the pumiceous and scoriaceous beds at site 4, 5 and 6.

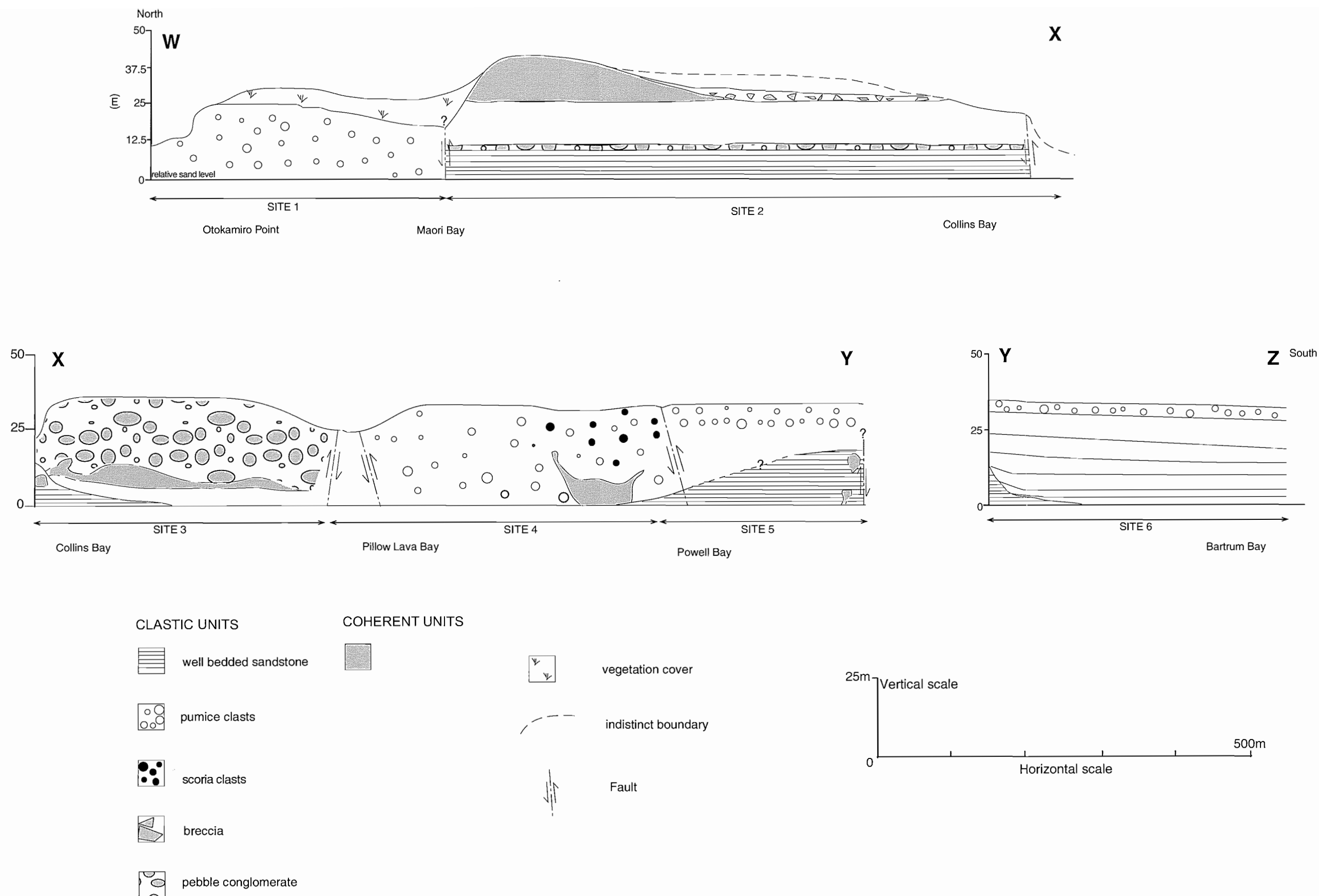


Figure 3.2. North-south cross sections, from Otokamior Point (W), to Collins Bay (X), and from Collins Bay to Powell Bay (Y), and from north Bartrum Bay (Y) to before Tirikohua Point (Z).

3.2.1 Site 1 (Otakamiro Point)

The northernmost site, site 1 is <100 m long (E-W) and 18-20 metres high, and separated into two sections (A and B) (**Figure 3.1**) (**Appendix 3A, 3B**). Site 1 is heterogenous in bedding style and bedding thickness. The site is dominated by a single unit comprising pumice and scoria in moderately developed, laminated to thick, laterally discontinuous beds. Grain-sizes range from pebble, to coarse sand and granule. Fine-grained rip-up clasts occur throughout the succession and are often associated with scours. The best exposure is in the headland cliffs, with some exposure also in the rock platform and coastal stack. Section B at the north end of Maori Bay forms the basis for description of site 1 as it provides the most complete exposure in height and width.

Sections A and B are dominated by pumice, with areas of scoria and dense porphyritic clasts (gravel), pebble-sized or metre long sand rip-up clasts. Individual beds are massive to diffusely bedded, with internal and basal erosional scours. Beds vary laterally, with low angle cross-beds, localised trough cross beds and convoluted fine sand beds. Some beds include flame structures.

Section B comprises three lithostratigraphic units (**Figure 3.3**). Subunit 1: a basal subunit, 5 m thick of thin and diffusely bedded pumice-rich, subunit 2: a middle subunit, 7 m thick of weakly bedded and pumiceous with pinch and swell bedding, and subunit 3: an upper 6 m thick subunit, low angle cross-bedded with erosional scours and discontinuous beds. In addition, a 10-15cm thick, fine-grained indurated layer occurs at 5 m, at the top of subunit 1. Each subunit shows vertical and lateral variability including prolific diffuse beds, scours and variable bed thicknesses.

Subunit 1 contains weakly developed diffuse and planar stratified beds of pumice, in a coarse sand and granule matrix. Bed thickness ranges from cm to 10's of cm in scale, and includes single pumice pebble bedss, and clast-supported beds of pumice and scoria granules and fine pebbles. Individual beds are laterally discontinuous and undulating, they can be traced for 5-15 m. Low angle cross beds truncate planar beds and also occur in-filling scours. The lowest part of subunit 1 (0-1 m) comprises weakly bedded, undulating, cm-thick, fine pumice pebble beds. These pumice beds are separated by a discontinuous fine sand interval and coarse sand to granule beds, of variable thickness, with scattered fine pumice pebbles. Weakly diffuse planar stratification, and cross beds of scoria and pumice pebbles, characterise the upper part of this basal subunit (2-5 m). Individual beds in the upper part are normally graded, and contain thinly stratified sand and fine pumice pebbles.

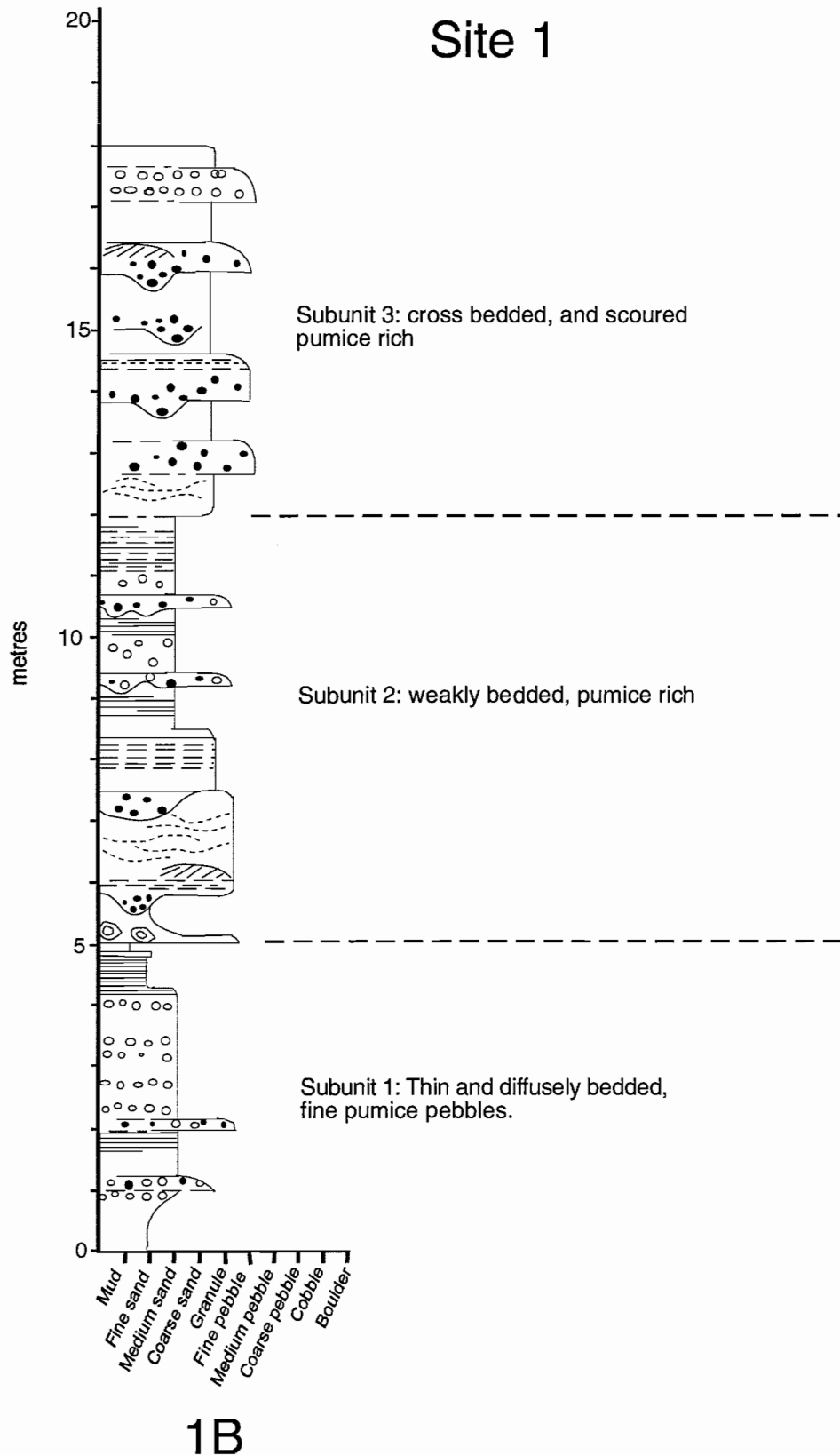


Figure 3.3. *Stratigraphic log of site 1B, with subunits marked.*

Subunit 2 contains diffusely stratified pumice pebbles in pinch and swell beds. This subunit is dominated by fine to coarse sand with thin beds of fine pumice and scoria pebbles but includes undulating pinch and swell beds of pumice pebbles. An indurated interval occurs at 5 m. The indurated interval consists of two fine sand-silt layers, a lower 10-15 cm layer and an upper discontinuous, 1-5cm thick layer. Above the indurated layers (~2 m) are, undulating coarse and fine sand beds, with diffusely and weakly bedded clusters of fine sand intraclasts (5-10 cm long). Between 6-12 m is massive sand with weakly developed diffuse, planar scoria and pumice pebbles beds. The fine pumice pebble beds are truncated by erosional scours and in-filled with sand and granules. A discontinuous layer of convolute fine sand beds occurs at 11 m.

Subunit 3 contains cross beds and weakly developed planar and pinch and swell stratification, with numerous erosional scour domains. Diffuse, thick beds dominated by fine and medium scoria pebbles occur between 12 and 14 m, between thin beds of massive coarse sand and granules. Stratification consists of weakly developed pumice pebble beds. Erosional scours are 2-10 m long and in-filled with weakly developed low angle cross beds. A major erosion surface truncates planar and cross-stratified bed-forms at 16-13 m. This scour is 2 m deep and is in-filled with diffusely bedded pumice and scoria pebbles and intraclasts. The upper part (16-18 m) is dominated by scours that are in-filled with massive domains and crude bedding, with low angle cross beds at the tops of the infill.

3.2.2 Site 2 (Maori Bay)

Site 2 is the most extensive in outcrop area being 500 m long (N-S) and 35-40 m high and comprises 4 sections (**Figure 3.1**) (**Appendix 3C, 3D**). Site 2 is exposed along the headland and cliffs and in an old quarry in the Maori Bay car park. Large, irregularly shaped porphyritic, conglomerate and breccia boulders eroded from the cliff, are scattered on the beach. Bedded clastic units dominate this site, although a coherent unit dominates the upper 10-15 m of section A. Beds are horizontal to subhorizontal and dip 10° towards the east at section D.

The lower 4-5 clastic units are laterally continuous and gradually change in thickness from section A to D, with individual beds either increasing or decreasing in thickness southward. The upper lava and breccia units are discontinuous. Where the coherent unit ends in section B, the breccia unit begins. The breccia has a chaotic thickness distribution. Overlying the breccia at section C, a resistant coarse sandstone unit protrudes from the section.

The main stratigraphic features of site 2 are described at section A, with differences noted between sections A to D. Site 2 comprises 6 lithostratigraphic units (**Figure 3.4**). These include unit 1: a basal well bedded, calcareous sandstone unit up to 10 m thick, unit 2: a massive fine to coarse pebble conglomerate, 2 m thick, unit 3: a fine grey sand, unit 4: a thickly bedded coarse sand, 1.5 to 12 m thick, unit 5: a pillow lava pile, of 2 to 15 m thickness, and unit 6: a breccia, 2 to 3.5 m thick.

Unit 1, the basal unit is laterally continuous, and dominated by planar, fine calcareous sandstone beds, with regular coarse sand beds at 30 to 80 cm intervals. Bed thicknesses range from 5-10 cm, with a maximum thickness of 60 cm. The fine sand beds are massive and often normally graded, with coarse sand at the base and mud at the top. The fine sandstone contains scattered foraminifera tests (*lenticulata*), and several beds contain thin (1-5 mm), weak and diffuse, planar or undulating beds of white granule-sized pumice-like clasts. The coarse sand beds are 2-30 cm thick. They are either laterally continuous with planar stratification, or occur as thin, discontinuous beds due to bioturbation. Bioturbation occurs throughout this unit.

Unit 2, the conglomerate, is a very thick, single tabular bed of medium to coarse pebbles. It is massive or weakly normally graded, clast-supported at the base of section A and B, and matrix supported towards the top. This unit is laterally continuous and reduces in thickness (<1 m) at section D to the south. It has an irregular, erosional basal contact.

Unit 3, the fine grey sandstone occurs above unit 2, as an interval within unit 4 and above unit 6. It is massive to weakly bedded in thin, medium planar beds. Where this unit occurs above the conglomerate, it thickens southward from section A to D. It is discontinuous below the pillow lava at section A and above the breccia at sections B and C. The unit ranges from 1 m to 4 m thick.

Unit 4, the medium to coarse granule sandstone unit is medium to thickly bedded, with a grey interval similar in character to unit 3. Individual beds are massive to normally graded. It contains occasional discontinuous thin beds of mud or fine grey sand. This unit increases in thickness from 6 m at section A to 13 m at section C. At section D it is 16 m thick and contains a lower 40-50 cm-thick massively bedded interval, overlain by 10-20 cm-thick, normally graded beds. At sections A and B, bedding is truncated by unit 5.

Unit 5, the lava unit occurs at section A and B. Section A has the most extensive and thickest occurrence of lava in the Muriwai volcanic succession, at ~150m long and 15 m thick. The lava unit tapers abruptly from section A to B, giving the appearance of a toe as it abuts unit 6. It has a

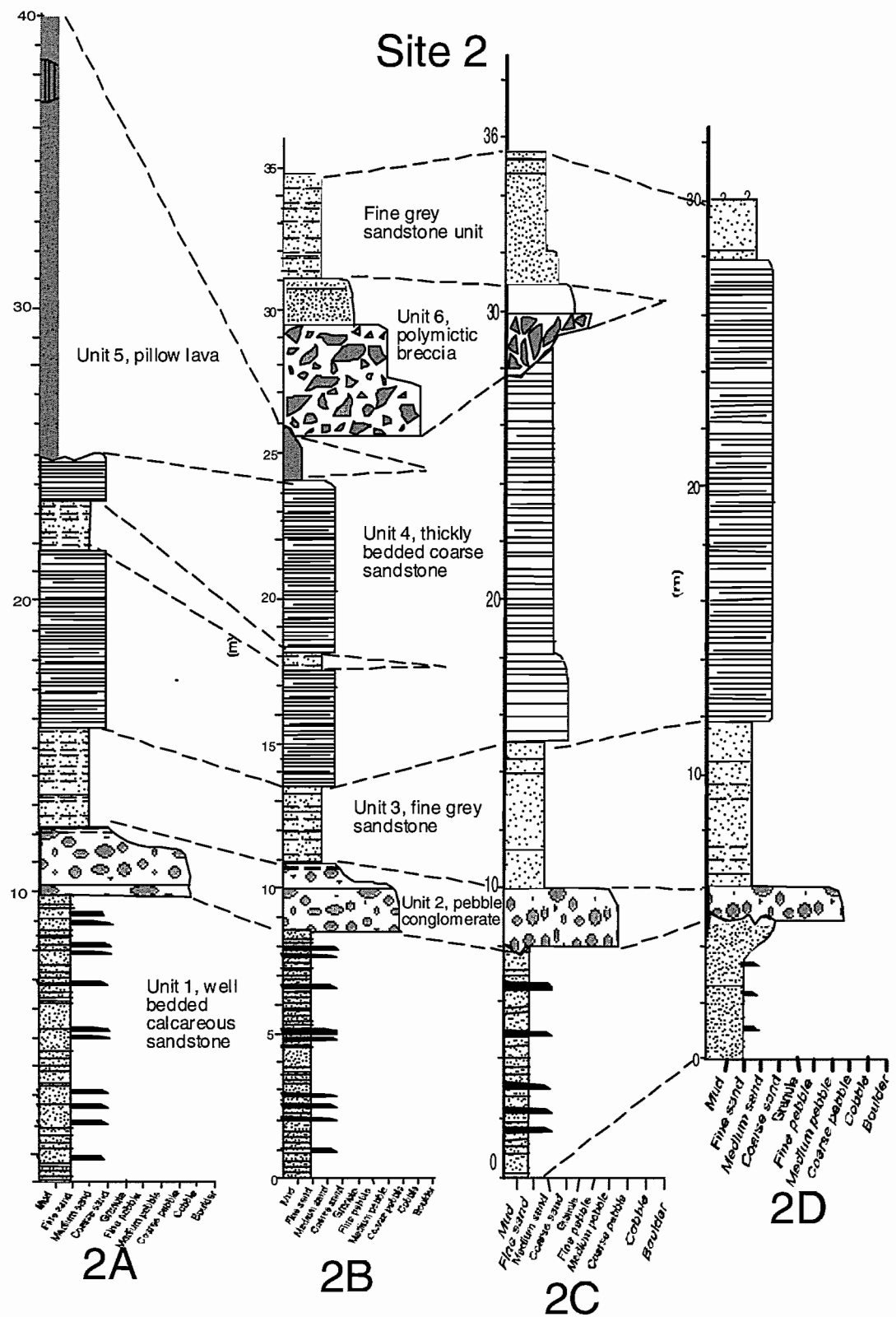


Figure 3.4 Stratigraphic logs of site 2, with units marked.

broadly undulating, mound-like relief, with a planar to slightly irregular, erosional base. This lava unit is characterised by pillow forms, each of which have radial jointing patterns that form a pillow

lava pile. The pillow lava pile can be broadly divided into mega-pillows, 10-15 m across, surrounded by smaller pillows, 1-10 m in diameter. A domain of thick vertical jointing occurs towards the base of the mega-pillow. The pillow lobes are larger in diameter towards the base but progressively decrease in size with stratigraphic height. Pillow forms are ovoid in cross section. Sheet lava flows occur at the base and top of the lava pile and are 1-1.5 m thick, of limited extent, and are characterised by closely spaced, vertical parallel jointing.

Unit 6, the breccia unit is thickest at section B (3.5 m) where it overlies the 2 m thick toe of the pillow lava pile and also occurs at section C (2 m). It is not present at section A where the lava pile is thickest, nor seen at section D where the lava is absent. This is a single normally graded unit that broadly comprises three parts; a breccia part of pillow lava clasts, a middle part rich in intra-clasts and an upper coarse sand to granule part. The lower breccia contains angular to irregularly-shaped lava clasts that have at least one glassy rind that range from curvy-planar pillow fragments and angular glassy clasts, 5 to 40 cm in size. The intra-clast breccia contains elongate and wispy sandstone clasts (<1 m long). Both lava breccia and sandstone clasts occur in an angular granule to fine pebble matrix. The upper parts is a resistant metre-thick, coarse sand and granule layer with rare metre-sized sandstone clasts. Clasts have a jumbled and chaotic arrangement or are weakly inclined.

3.2.3 Site 3 (Collins Bay)

The volcanic succession at site 3 extends for 80-100 m (E-W) and 30-35 m high, and is separated into 3 sections (**Figure 3.1**) (**Appendix 3E, 3F**). Rocks are predominantly exposed in a cliff headland and to a lesser extent on a rock platform. The headland is susceptible to erosion, with large fallen boulders of conglomerate and sandstone scattered at the cliff base. A 2-3m deep gut, incised into the platform separates section B from C.

The main stratigraphic features of site 3 are described by integrating sections B and C, with additional information from site A. Sections B and C comprise 5 lithostratigraphic units (**Figure 3.5**). From the base to the top these are, unit 1: a thin to medium bedded sandstone (2.5 m thick sections A and B), unit 2, a pebbly- granule sandstone (1.5-3.5 m thick section B and C), unit 3: a 5-6 m thick lava unit; and unit 4, a ~6 m thick volcanoclastic sand enclosing the lava (section C).

Site 3

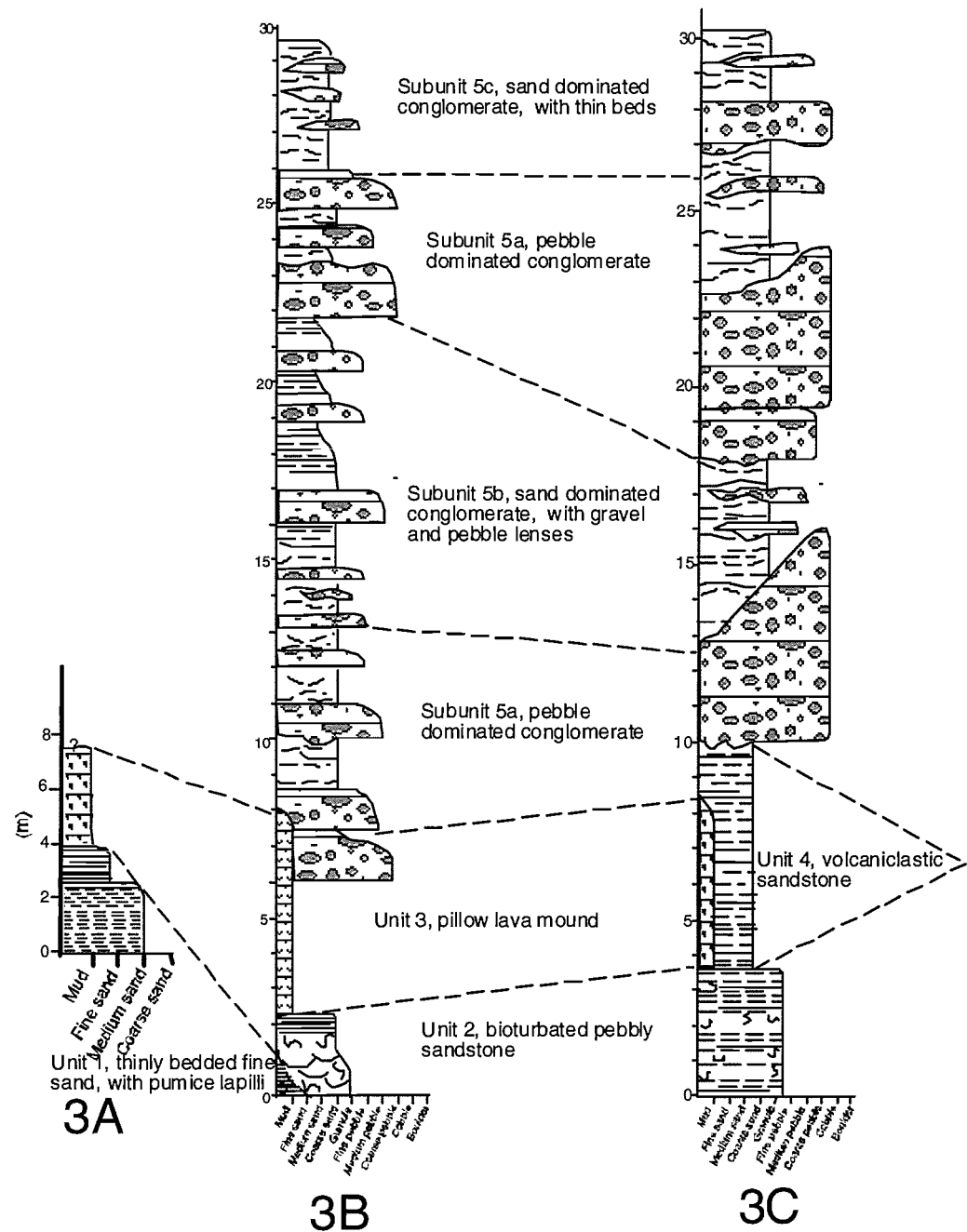


Figure 3.5. Stratigraphic logs of site 3, with units marked

The conglomerate, unit 5 is subdivided according to dominant lithology, grainsize and bedding style, into subunit 5a: a pebble dominated conglomerate (sections B and C), subunit 5b: sand dominated with gravel and pebble lenses (sections B and C) and subunit 5c: thinly bedded sand-dominated (sections B and C).

Section A contains a small occurrence of unit 1 and lava (unit 3). Sections B and C are dominated in its upper parts by conglomerate (unit 5), with the basal part comprised of pillow lava (unit 3) and sand (unit 1). The lavas display a mound-like morphology in contact with the conglomerate.

Unit 1, the basal fine and medium grained sandstone is well-sorted, and medium to thick beds, with diffusely stratified thin pumice pebbles. This unit has a concave-up relief, but is absent from section C. It contains weakly developed beds of pumice sand and pebbles. The 10-30 cm thick medium sand beds are laterally continuous and graded, with fine sand and pumice pebble tops. Stratification is poorly developed, with planar stratification highlighted by different grainsizes. Bedding is truncated by unit 3 and by unit 2 between sections B and C. Coarse and fine pumice pebbles define 5 mm to 2 cm thick beds, which are weakly developed and diffuse.

Unit 2 is a very weakly bedded to massive, bioturbated, pebbly granule- sandstone. This unit overlies and truncates unit 1. Irregular pebbly sand / gravel beds predominate at section B and C, beneath the lava. It contains erosional scours, scattered wood and fine pebbles of dense porphyritic rock fragments. It contains 5 separate layers, which have diffuse to irregular boundaries, or sharp, erosional boundaries that truncate bedding. Beds are massive, with very weak and diffuse, wood, pumice and fine pebble stratification. Locally, some areas are rich in woody material. Vertical and horizontal bioturbation disturbs bedding. A weak bed of single pumice cobbles (10-30 cm size) occurs at section C, where unit 2 has a gradational contact with unit 4. The base of the lava unit slightly intrude the upper parts.

Unit 3, the lava unit has a mound-like relief and dominantly contains closely packed pillow lobes, with a localised sheet flow occurring at the base. Large, metre-sized pillows occur at the base of the pillow mound and decrease in size towards the top. The pillow lobes are radially jointed and are exposed in longitudinal form at section C. The sheet flow is 10-80 cm thick and columnar jointed. The basal contact of the pillow lava and units 1 and 2 is conformable, to unconformable. It becomes discontinuous at section C, where it is characterised by separate pillows that are less closely packed and separated by fine sediments, which are likely to be unit 4.

Unit 4, the volcanoclastic sand unit is weakly and diffusely bedded. It has a gradational lower boundary with unit 2 at the termination of the pillow lavas, although this relationship is poorly defined. The upper contact with the conglomerate sequence is diffuse. Unit 4 is massive with intervals of weakly developed, diffuse and undulating beds of sand and pebbles of pumice, vitric clasts, scoria and crystals. Beds are either heterolithological domains, or comprise diffusely bedded intervals of volcanic clasts and / or pumice pebbles.

The conglomerate unit 5 is heterogenous, with discontinuous lenses and layers of boulders, cobbles, pebbles and gravel or sand, of variable thickness and length. Sandstone beds occur between the conglomerate lenses and at the top of unit 5 where they become regularly bedded. Beds within the conglomerate unit are discontinuous in the north-south direction, and thick and thin in an east-west direction.

The pebble-dominated subunit 5a comprises medium to coarse pebbles, cobbles and scattered boulders. At section B the conglomerate beds in this subunit pinch and swell in beds 10 cm-2 m, in lenses that are continuous for 10-20 m. At section C the conglomerate beds are continuous in an easterly direction. A 1-5 m thick pinch and swell bed of medium to coarse pebbles gradually thickens towards the east over 40 m. Fine to coarse pebble lenses are interbedded with 20 cm-thick sand beds. Boundaries between the pebble lenses and sand beds are irregular and diffuse. The upper pebble dominated subunit, above the sand dominated subunit contains 2-5 m thick conglomerate lenses.

The sand and gravel dominated subunit 5b comprises scattered, discontinuous thin pebble and gravel lenses between medium to coarse sand. The sand is thinly or thickly bedded, with scattered pebbles and diffusely stratified wood rich layers. The conglomerate lenses are undulating to planar and 10-20 cm thick and weakly bedded pebble layers delineate wavy bedding. Gravel and fine pebble lenses, 5-10 m long occur at section B and C.

The upper sand dominated subunit is comprised of medium to thickly bedded sand, with rare gravel or coarse sand lenses and erosional scours. Beds are planar or shallowly inclined, laterally continuous to diffuse. Thin, weakly developed beds of wood particles also occur within the sand.

3.2.4 Site 4 (Pillow Lava Bay)

The volcanic succession at site 4 extends for 100-120 m in length and is 25-30 m high and has been divided into two sections (**Figure 3.1**) (**Appendix 3G, 3H**). Rocks are exposed in cliffs on the

headland that separates Pillow Lava Bay and Powell Bay and on a rock platform. Observations are obscured in some areas of section A by vegetation cover. Scattered boulders encircle the cliff base and a waterfall flows over the southern end of the cliff.

The main stratigraphic features of site 4 will be described in terms of both sections A and B. Site 4 contains 7 separate lithostratigraphic units (**Figure 3.6**). The basal part is comprised of unit 1: thin to medium bedded fine sandstone, unit 2: bioturbated pebbly sandstone, unit 3: a cross-cutting coherent unit, unit 4: weakly bedded pumiceous pebbles and sandstone, unit 5: in section B, a normally graded pebble conglomerate, unit 6: a variable, thickly bedded pumiceous unit (section A and B), in the upper part, unit 7 contains subunit 7a: conglomerate and gravel, and subunit 7b: weakly bedded scoria lapilli with gravel lenses.

Sections A and B are divided into a basal sand sequence (units 1 and 2), a central conglomerate and pumiceous sequence (units 4, 5 and 6) and an upper conglomerate, gravel, pumice and scoria sequence (unit 7). The central and upper parts of sections A and B are variable. The lower part of the section is cross cut by a pillow lobe atop a dyke (unit 3). In both sections pumiceous beds are interbedded with, and occur above and below gravel and conglomerate.

The basal unit 1 is a thin to medium bedded fine sandstone with mud-rich layers that is laterally continuous except for an irregular scoured upper contact with unit 2. Wood particles define a weak stratification towards the top of beds at section A. In general beds are normally graded, with fine sand or muddy tops and coarse sand-granule (section A) or a fine to medium sand base (section B). Scattered fine pebbles occur at section A. Load casts occur at the base of beds and bioturbation disturbs bedding. Beds strike 260° and dip 8-10° northwest at section B.

Unit 2 is a massive to weakly stratified bioturbated pebbly sandstone with poorly defined bedding at section A. This unit has an irregular and erosional contact with unit 1. It is overall normally graded, from a coarse sand to granule base, up to a thinly bedded medium to coarse sand. Erosional scours with a sharp base and a diffuse top occur throughout and define coarser grained intervals comprised of coarse sand to granule, with a fine pebble base. Scours at section B are shallowly inclined and taper east into poorly defined planar stratification.

Unit 3, comprises a pillow lava structure atop a feeder dyke that intrudes the lower parts of the succession and has an unknown western lateral extent where it continues beneath the sea. This unit changes thickness from section A to B, and is 8 (section B)-18.5 m (section A) high, and elongate (<100m long) in the north south direction. The pillow lobe at section A displays a radially jointed

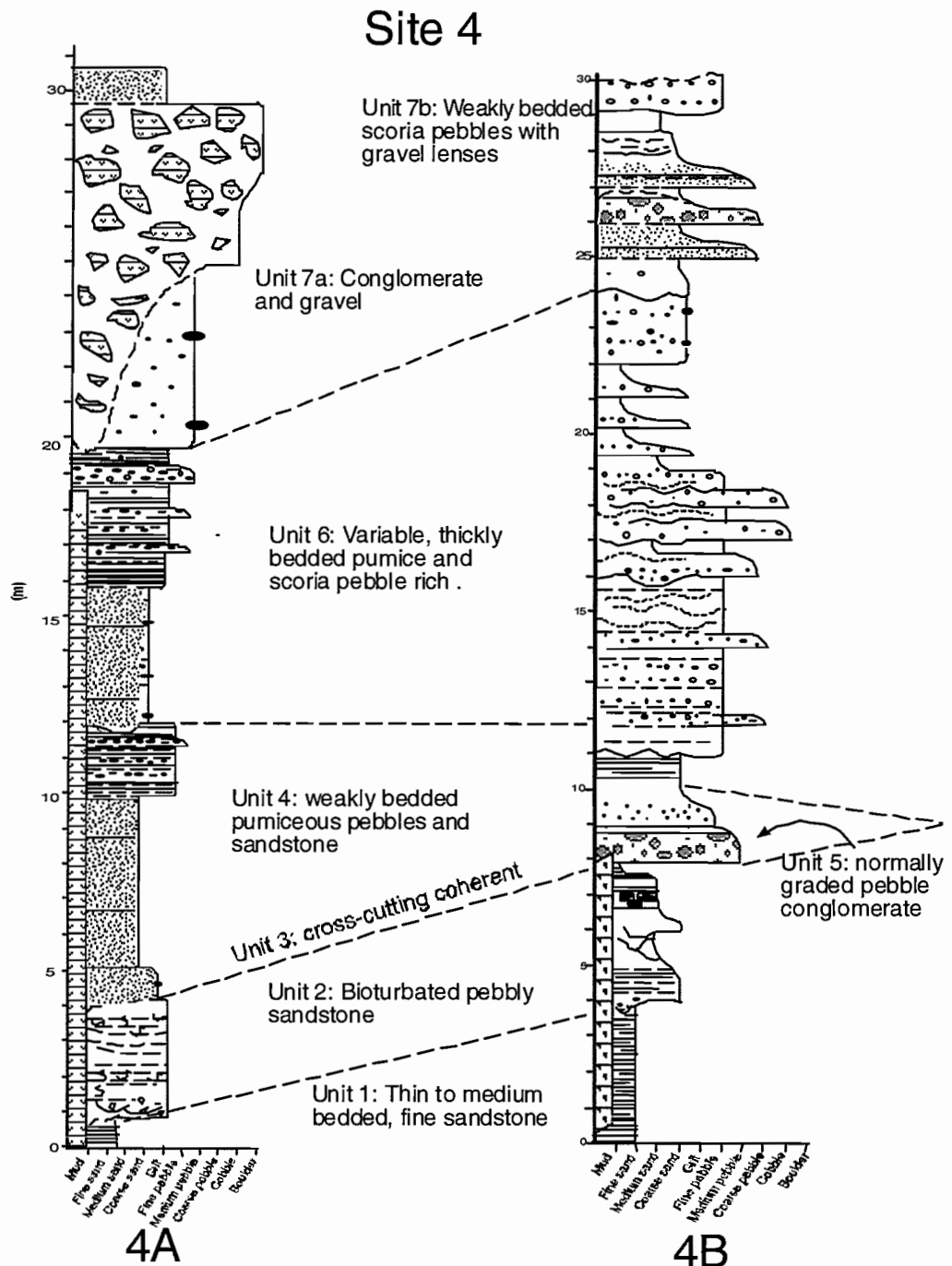


Figure 3.6. Stratigraphic logs of site 4, with units marked.

character. Its upper and lower margins and interior are brecciated, with a regularly spaced, blocky fracture system, which extends the length of the dyke at section A, and occurs in a cross-hatching style at section B. Regularly spaced breccia blocks, are four or five-sided and separated by a cm wide, sediment-filled gap at section B. These blocks occur in the surrounding sediments.

Unit 4 comprises weakly bedded, pumice pebbles and sandstone (section A), and is not recognised at section B. 1-2m thick beds, are continuous for ~10-20 m, and comprise diffuse beds of pumice granules and pebbles. Individual beds are either well stratified or weakly defined. Weakly bedded pumice pebbles and sandy intervals define some beds.

Unit 5, the fine to medium pebble conglomerate (section B) is normally graded and contains weakly stratified, subrounded pebbles of dense porphyritic clasts, pumice and scoria. This unit is discontinuous in the east and cross cut by unit 3, and vertically grades into a pebbly sandstone. In addition, this unit grades laterally into medium bedded fine pebbles. It has an irregular, erosional base in contact with 2.

Unit 6, a variable and thickly bedded pumice and scoria pebble rich unit contains weakly developed <1 m thick, diffuse beds of pumice and scoria pebbles. This unit has an irregular upper boundary, and may have a gradational lower contact at both sections. Discontinuous pumice beds comprise layers and beds of varying thickness, and are inter-bedded with diffusely bedded scoria pebble layers. Numerous erosional scours comprised of coarse scoria pebbles and pumice in-fills are found within the thicker beds. Weakly bedded scoria pebbles or medium dense porphyritic pebbles define 1-5 m long, large-scale low angle cross beds at section B. Individual beds are comprised of medium to coarse sand with diffusely bedded scoria lapilli. A 6-7 m deep erosion surface can be recognised in this unit at section B.

Subunit 7a (section A) a conglomerate and gravel has a diffuse lower boundary with unit 6. It has a faulted eastern contact and an indistinct lateral extent. The basal 1-4 m thick gravel layer is deeply scoured by the conglomerate at several locations. The overlying conglomerate comprises two parts, a clast-supported base (4.5 m), and a matrix-supported top (5-6m), which is normally graded. The conglomerate comprises rounded to sub-angular dense black fine-grained clasts, scoria and pumice, in a granule to clay matrix.

Subunit 7b (section B) weakly bedded scoria pebbles with sand and gravel lenses occurs at the same stratigraphic interval as subunit 7a. This subunit is continuous on to the upper parts of sites 4 and 5. Large scoria pebbles, thin, discontinuous gravel and conglomerate lenses, and medium to

coarse sand with pumice lapilli dominate this unit. The large scoria pebbles and small pumice lapilli occur within weakly developed and diffuse beds, which have variable forms, such as low angle cross beds and layers. Well-stratified fine to medium sands beds, of 10-60 cm thickness and thin, pumiceous lapilli-rich layers occur in the upper 1-3 m and thin towards site 5. Discontinuous, 30 cm to 1 m thick pebble conglomerate lenses, gravel, and poorly bedded sandstone intra-clast layers, also occur. This subunit contains numerous erosional scours.

3.2.5 Site 5 (Powell Bay)

The volcanic succession at site 5 is ~60-70m long and 25-30 m high and is divided into three sections (**Figure 3.1**) (**Appendix 3I, 3J, 3K**). Rocks are exposed in cliff section at the southern end of Powell Bay and on a wide rock platform that extends from Powell Bay to the north of Bartrum Bay. This platform slightly increases in height towards the south, where sections A and B are separated from section C by a gut and rock face. Behind Powell Bay a vegetated zone obscures parts of the outcrop. Waterfalls mark the cliffs at section A and C2.

Site 5 consists of the three major lithostratigraphic units (**Figure 3.7**). Unit 1: a basal cross-cutting coherent unit, unit 2: a thinly-bedded sandstone, and an uppermost unit 3: pumice pebble sandstone unit.

The upper parts of the stratigraphy are shown in section A, which comprises pumice pebble sandstone and conglomerate. Thinly bedded sandstone dominates the lower parts of section B and C. A dyke and mega-pillow occur in section C, which is overlain by pumice pebble sandstone.

Unit 1, a feeder dyke with two distinct pillow lava lobes possesses two parts, a basal thin dyke and mega-pillow, and an upper, mega-pillow. The dyke cross-cuts the well bedded sands at section C1 and intrudes the pumiceous sandstones at section C2. The dyke is ~16 m long (E-W) and is 30-80 cm thick in the west where it tapers to an end point. It varies in height from 4-10 m, and has an undulating vertical contact with bedded sand. A brecciated zone occurs at the eastern extent of the dyke and adjoins a basal mega-pillow. The breccia is comprised of closely-fitting joint blocks. The upper mega-pillow is ~10m in diameter and has brecciated margins, with a ~2m wide zone on the lower margin. The mega-pillow is characterised by radial jointing patterns and has an undefined relationship to the lower body.

Unit 2, thinly-bedded sandstone dominates site 5 and is overlain by, and has an indistinct contact with, unit 3. This unit consists of horizontally and monotonously bedded fine sand, with intervals

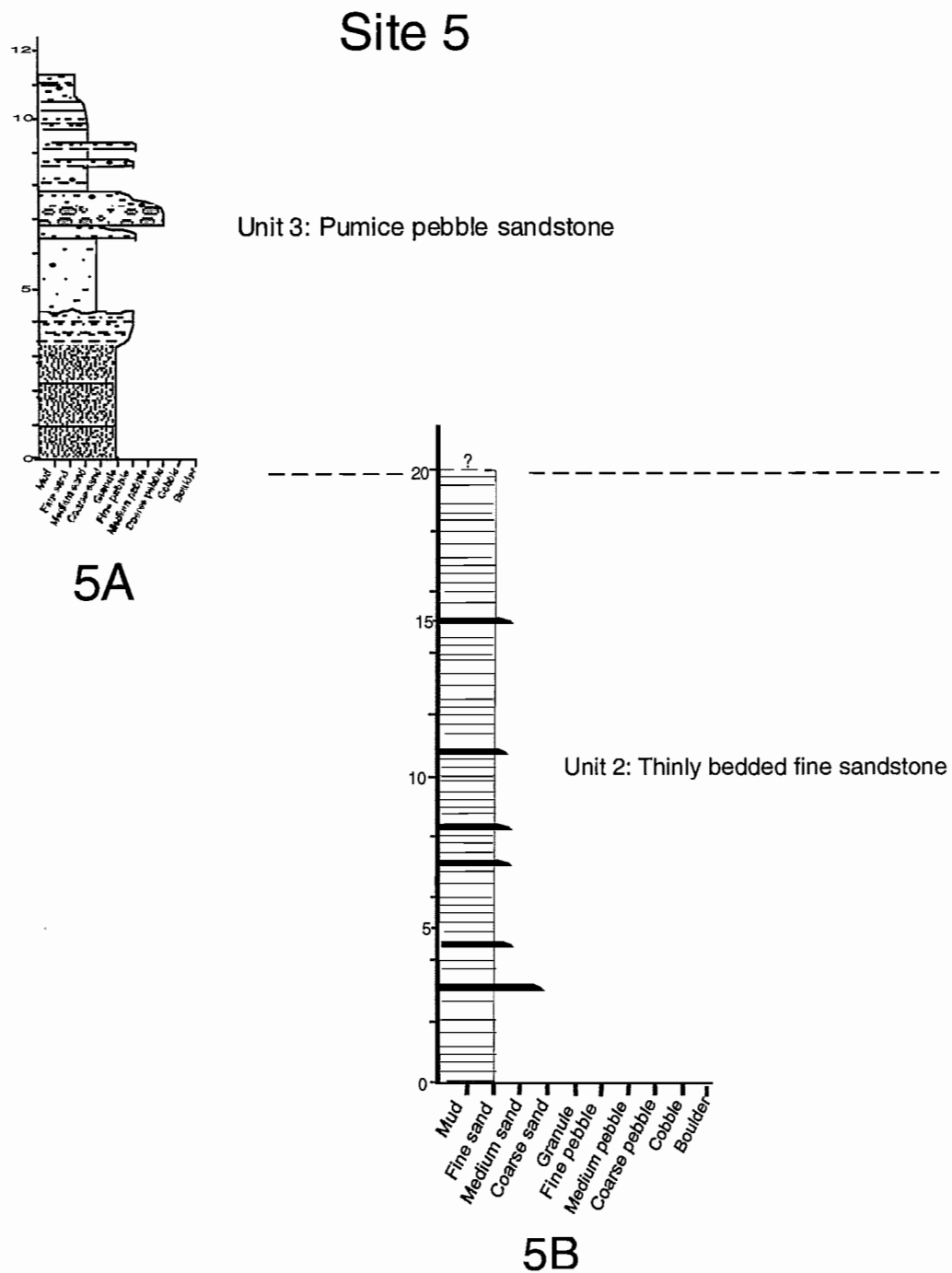


Figure 3.7. Stratigraphic logs from site 5, with units marked.

of medium sand, and coarse, crystal-rich sand. Beds are 1-35 cm thick and laterally continuous for ~50m, with shallow dips (8°) southward. Beds are laminated, cross-bedded or diffusely stratified,

and massive or normally graded. Beds of 30-40 cm thickness have a medium to coarse sand base and fine sand or mud tops. The thin coarse crystal rich sand intervals are a subunit of unit 2, and have irregular, erosional bases and may be normally graded. Selected fine to medium sand beds contain various thin broken and contorted layers. Small-scale reverse faults dissect unit 2.

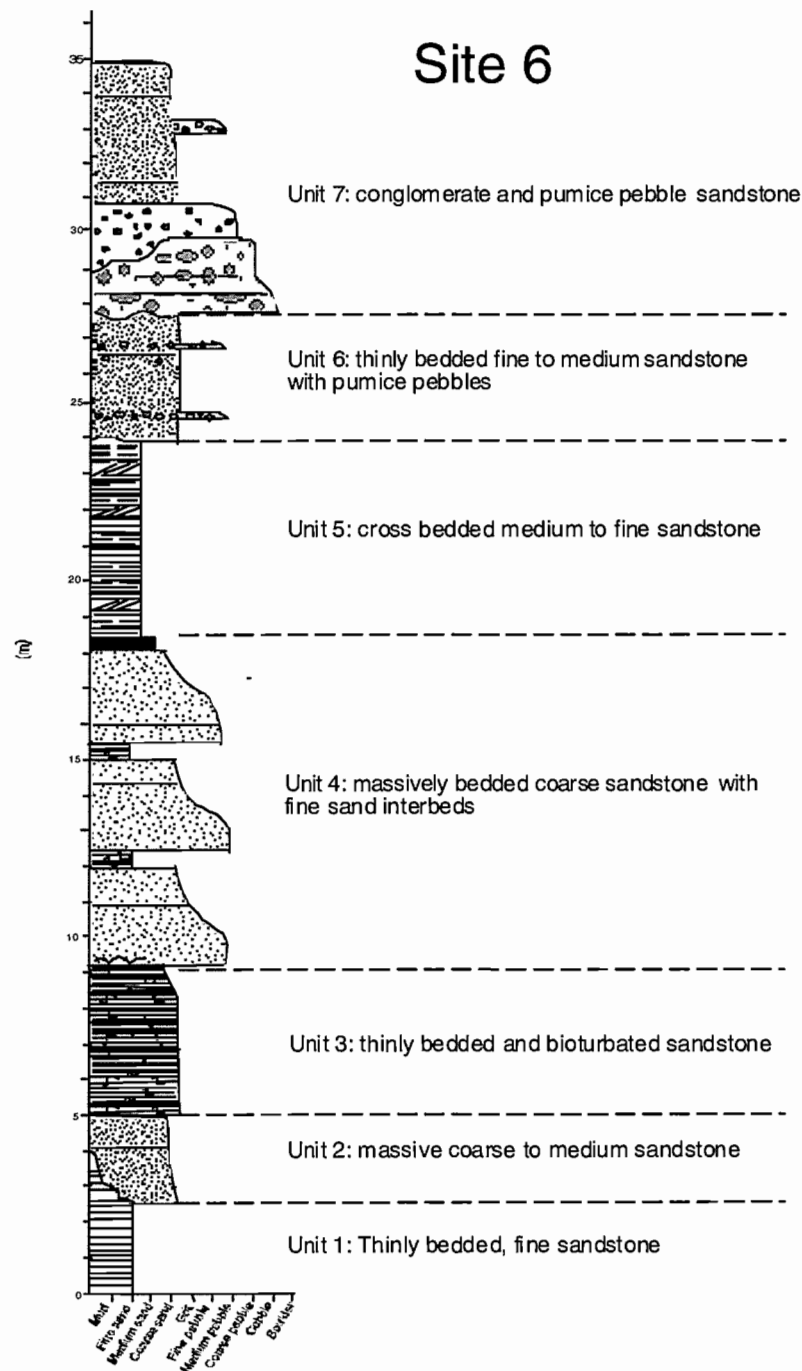
Unit 3, pumice pebble sandstone contains variable pumice sand, fine sand and silt, and a lithic conglomerate and gravel layer. Beds are thin and laterally continuous for 10-20 m but gradually thin towards the north and south, and inter-finger with sand and pumice lapilli beds from site 4 and pumiceous sands at site 6. At section A, the basal 4 m contains metre thick beds of volcanic sandstone, overlain by massive and poorly sorted pumice lapilli sand, weakly bedded pumice and a 1.5 m thick pebble conglomerate bed. The conglomerate is normally graded with gravel and pumice lapilli occurring at the top. Thin and weakly stratified pumice and scoria beds, convoluted coarse sand, and fine sand and silt comprise the uppermost part. This unit have been up-thrown relative to site 4, where a fault marks the boundary between site 4 and 5.

3.2.6 Site 6 (Bartrum Bay)

The southern most site, site 6 is ~300 m long and 35 m high, and has been assigned one section (**Figure 3.1**) (**Appendix 3L**). Rocks are exposed in a northwest facing cliff section and tidal rock platform that juts into the southern end of Bartrum Bay. The cliff base and rock platform are exposed at low tide. Many small ephemeral watercourses mark the rock face. A major fault and incursion into the rock platform marks the end of the study area and boundary between another cliff-forming volcanic succession further south. Section A displays the main stratigraphic features of the clastic units of site 6. Bedding is laterally continuous over 30-50m, however the basal lithostratigraphic units are onlapping in the northeast and shallowly inclined towards the southwest.

The site is comprised of 7 lithostratigraphic units (**Figure 3.8**). Unit 1: basal thinly bedded sandstone, unit 2: coarse to medium sandstone, unit 3: thinly bedded, bioturbated sandstone, unit 4: massively bedded coarse sandstone with fine sand inter-beds, unit 5: cross bedded medium to fine sandstone, unit 6: thinly bedded, fine to medium sandstone and pumice pebbles, and unit 7: conglomerate and pumice pebble sandstone.

Unit 1, a basal thinly bedded sandstone is fine grained and contains thin to medium sized beds.



6A

Figure 3.8. Stratigraphic log from site 6.

Beds are horizontal to shallowly dipping, with the upper surface eroded and inclined towards the south-west. Fine sand beds are 10-35 cm thick and slightly normally graded, with a medium sand base and a silt top. It contains thin intervals of cross-bedded medium sand, bioturbated and carbonaceous intervals, and rare mud beds of millimetre-thickness. The upper 10-15 cm and unit interior are heavily bioturbated, which is in some cases restricted to carbonaceous intervals.

Unit 2, a massive to normally graded, medium to coarse sand bed, which onlaps the basal sand in the north east and dips shallowly to the south west. This unit is normally graded at the base, with the lower 10-15 cm of coarse sand to granules, with sparse, irregular to elongate (10-20 cm long) and bioturbated intra-clasts of bedded sand. The upper part of this unit is massive, medium to coarse sand, with an irregular to gradational upper contact with unit 3.

Unit 3, a thinly bedded and heavily bioturbated medium sand comprises planar, well-stratified beds 10-60 cm thick. The unit thickens towards the northeast as it onlaps onto the basal unit 1 and has an uneven to diffuse lower contact. It varies laterally, with pinch and swell and cross beds, with an overall mega-ripple structure. Fine sand beds with gradational boundaries and heavily bioturbated, woody intervals occur.

Unit 4, a massively-bedded coarse sandstone, comprises three 2-3 m thick beds that contain thin, bioturbated and medium to coarse sand intervals. Beds are planar to gently inclined and laterally continuous, thickening in the north-east and slightly thinning towards the south west. The upper bed of this unit becomes discontinuous over 100 m. Each bed is planar, except for the bioturbated interval, which has a weakly undulating character. The thick beds are moderately normally graded at the top, and have massive coarse sand bases. The bioturbated and medium to coarse sand intervals reduce in thickness and some become discontinuous in the southwest.

Unit 5, a bedded fine to medium sandstone has a gradational lower contact with unit 4. It contains medium to fine sand beds 4-10 cm thick and is overall normally graded with fine sand towards the top. Thin to medium beds are diffusely stratified and cross-bedded. The upper contact with the pumiceous units is planar and dips towards the southwest.

Unit 6, a thinly bedded fine to medium sandstone with pumice pebbles, is thickly bedded with thin internal layers. It has a variable, sharp to diffuse lower contact that is shallowly inclined towards the southwest. Beds increase in thickness towards the southwest, with the sand-dominated beds thinning to cm scale in the north east, where they abut unit 5. This unit contains sand-dominated, pumice sand-dominated and discontinuous gravel beds, with thin planar stratification that is locally

weakly developed. Thin pumice and gravel beds are diffuse and have a slightly wavy appearance. The upper contact is irregular and scoured by unit 7.

Unit 7, an upper-most conglomerate and pumice pebble sandstone, is normally graded with conglomerate at the base, and gravel and fine-grained, pumiceous sand at the top. This unit is of variable thickness and laterally continuous from site 5. It has a shallowly inclined upper limit, and thickens towards the south west where it is progressively overlain by another sedimentary succession. The basal conglomerate bed has a discontinuous to pinch and swell form and varies from 40 cm to 1.5 m thick. It has a planar to undulating lower contact and may continue from site 5. The conglomerate bed comprises a fine to medium pebble base and coarse sand and gravel top. It is in irregular contact with the overlying pumice pebble sandstone. The pumice pebble sands are variable and contain numerous erosional scours, with fine pumice pebble bases. Stratification is weakly developed, with low angle cross bedding, and pumice pebble beds of medium thickness.

3.3 Unit Correlation Between Sites

The stratigraphic columns of the Muriwai volcanic succession contain a range of coherent and clastic units with distinctive and diagnostic lithological features. Lithostratigraphic units are placed in a conventional stratigraphic sequence. Most sites (except 5 and 6) are separated by faults (**Figure 3.9**). Several units can be correlated across the succession. The distribution, organisation and extent of the lithological units has implications for the morphology and facies architecture of the volcanoclastic apron (**Chapter 6**). The Muriwai volcanic succession is broadly comprised of a series of laterally discontinuous, horizontal to subhorizontal lithological units.

Correlations are found in units at site 2, and between the units of site 4, 5 and 6. Several sites have similar lithofacies units, for example, site 1 and 4 and the upper parts of sites 5 and 6, are dominated by the pumiceous and scoriaceous units (pumiceous and scoriaceous facies group, Chapter 4). The upper part of site 3 and a narrow interval at sites 4, 5 and 6 comprise conglomerate units (conglomerate facies group, Chapter 4). The central part of sites 2 and 6 comprise thickly bedded medium to coarse sandstone units (thickly bedded medium to coarse granule sandstone facies group, Chapter 4). The upper parts of site 2 and the lower parts of sites 3, 4 and 5 contain lava units (coherent facies group, Chapter 4). The upper part of site 2 contains a polymictic breccia unit (polymictic breccia facies, Chapter 4). The base of sites 3 and 4 contain poorly bedded, pebbly sandstone units (bioturbated pebbly sandstone facies group, Chapter 4). The base of sites 2, 3, 4, 5 and 6 comprise thinly bedded fine sandstone (thinly bedded fine sandstone facies group, Chapter 4).

Sites are separated by faults and major erosion surfaces that often scour into basal thinly bedded sandstone units. The faulted contact relationship occurs in between site 1 and 2, and is shown on the surface as ground subsidence. Site 2 is separated from site 3 by a fault, but in addition the basal bedded sandstones of site 2 have a concave upper relief, perhaps evidence of erosion by the conglomerates. The contact between sites 3 and 4 is marked by two faults, with slumping of units within the faulted area. A fault separates site 4 from site 5. The upper units of site 5 have the appearance of continuing into the upper parts of site 6. However a fault in the basalt bedded sandstone, along with a coherent intrusive unit, separates the sites. Towards the end of site 6, clastic units steadily overly its upper parts, and continue to outcrop onwards past Tirikohua Point. Although an incursion into the rock platform marks a fault zone, before the point.

3.4 Discussion

The Muriwai volcanic succession outcrops in coastal cliffs and headlands in the study area, from which six sites are identified. Bedded fine and coarse clastic units with minor coherent units dominate the Muriwai volcanic succession. Pillow lavas comprise a small proportion of the Muriwai volcanic succession. Several coherent and clastic lithostratigraphic units make up each site. The units are separated by sedimentary (conformable, unconformable) and / or intrusive (concordant, discordant) contact relationships. The sites are separated by faults, which dominate contact relationships of the Muriwai volcanic succession. Bedded fine sandstones at sites 3, 4, 5 and 6 form the basal fine-grained sedimentary sequence. Coherent and coarse volcanoclastic units overlie the basal sandstones. The bedded sandstones are horizontal to sub-horizontally bedded. The bedded sandstones have an inclined erosional upper surface, which at many sites is bioturbated and represents a semi-consolidated surface. This surface marks a boundary between the overlying volcanoclastic and coherent units, and is likely to be a depositional hiatus. In comparison, individual unit contacts within the upper clastic sequence are horizontal, with localised erosional scours. Bioturbation is mainly scattered throughout the upper clastic sequence, which implies no major time breaks during deposition. A small number of thin bioturbated intervals appear locally, and are evidence that infrequent breaks in deposition did occur.

The main lithostratigraphic units are present at one or several of the study sites, and comprise pumiceous and scoriaceous units, conglomerate units, thickly bedded medium to coarse granule sandstone units, lava units, polymictic breccia unit, pebbly sandstone units, and thinly bedded fine sandstone units. The pumiceous units at sites 1, 4, 5 and 6 and the conglomerate units at sites

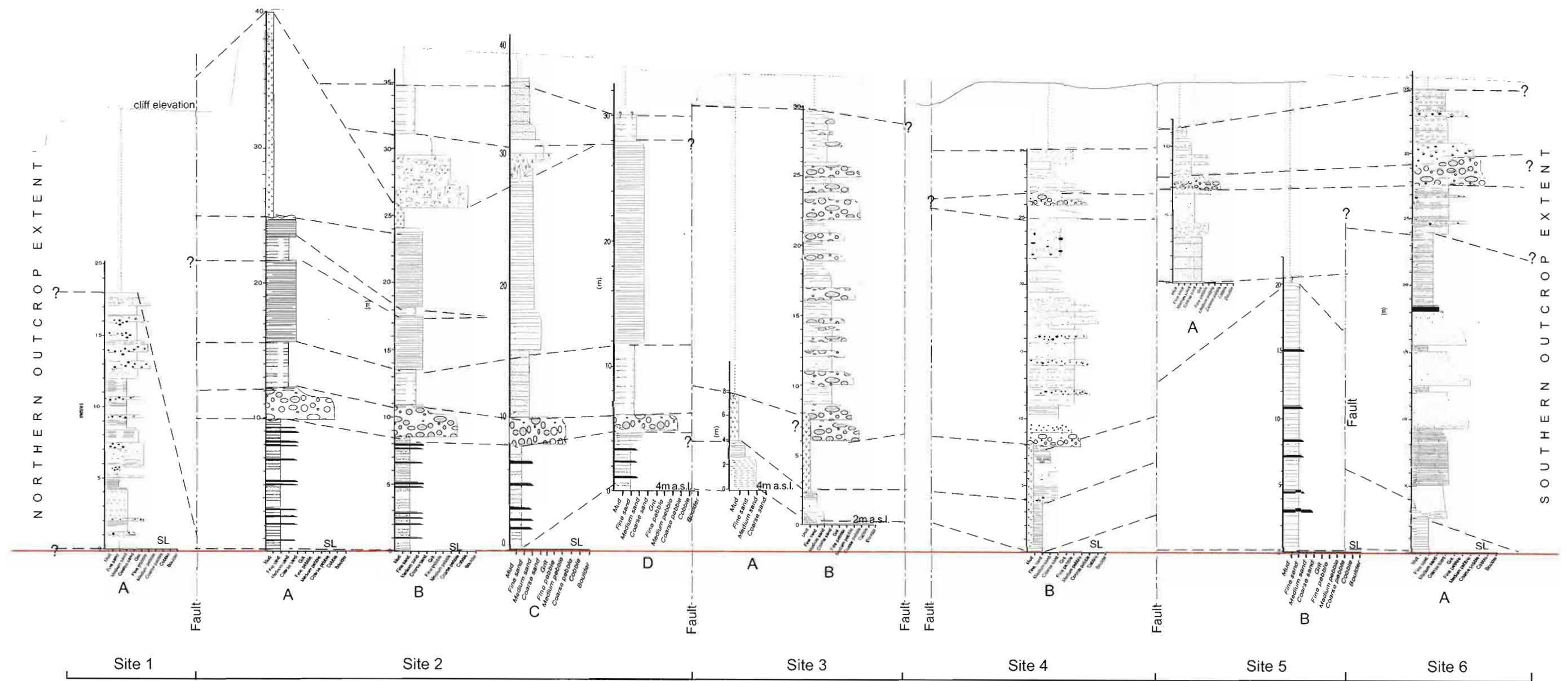


Figure 3.9. Correlation diagram from site 1 at the northern end of the study area, to site 6 at the southern end

2, 3, 4, 5 and 6 are highly variable. Together they form the upper units of the Muriwai volcanic succession. Conversely, lensing beds, rapid thickness changes and erosional contacts create vertical and lateral variability, which can make correlations problematic. In general, the recognition of marker horizons in the pumiceous and scoriaceous and conglomerate units is inhibited by the bedding variability. The pumiceous and scoriaceous unit at site 4 inter-finger with the same units at site 5. Pumiceous units at site 6 onlap onto those units at site 5. The medium to coarse granule sandstone units at sites 2 and 6, have similar characteristics and occur in the central to upper parts of the succession. The lava unit at site 2 forms in the upper most unit, whereas at sites 3, 4 and 5 they intrude the basal parts of the succession. The polymictic breccia unit at site 2 only occurs there at the same stratigraphic interval of the lava unit. The pebbly sandstone units at sites 3 and 4 are localised and overly the basal bedded sandstones.

This stratigraphic framework forms the basis for the lithofacies groups for the Muriwai volcanic succession (Chapter 4).

Chapter 4: Lithofacies of the Muriwai volcanic succession

4.1 Introduction

The Muriwai volcanic succession contains a series of related and recurring lithostratigraphic units that have been classified into several distinct lithofacies groups and facies types (Table 4). Separate facies have been identified on the basis of their textural and compositional features, and physical appearance; including bedforms, sedimentary structures and fossils. Each lithofacies is the product of set of conditions, such as erosion, transport and deposition, source area characteristics, depositional environment, and eruption processes in volcanic settings, which control facies variations. The lithofacies identified in the Muriwai volcanic succession are known to have formed in the submarine environment, from a combination of volcanic (eruptive) and non-volcanic (marine) products and processes. The Muriwai volcanic succession is dominantly comprised of six lithofacies groups.

The lithofacies comprise varying amounts of vesicular pumice and scoria, crystals, vesicular and porphyritic basaltic – andesitic rock fragments, sand and mud. Angular, unmodified juvenile pyroclasts are uncommon, whereas sub-angular to rounded volcanic clasts are ubiquitous, this modification is the result of sedimentary reworking. Although most of the pumice and scoria was presumably pyroclastic, due to the resedimented nature of the succession, sedimentary nomenclature has been applied. Lithofacies nomenclature follows the scheme of McPhie et al (1993) (**Appendix 2**).

In this chapter, the distinguishing features each facies are described. Facies are described in relation to table 4, followed by an interpretation and discussion on the transport and deposition mechanisms that were involved in their formation. Detailed stratigraphic logs and diagrams of grainsize, bedding styles, thickness and lateral variations supplemented with photographs, highlight the distinctive features of each facies. These facies descriptions along with interpretations of transport and deposition form the basis for later explanations of the origin of the Muriwai volcanic succession (Chapter 6).

TABLE 4: Chapter order of lithofacies groups, with constituent facies, and their occurrence, including type location, which forms the basis for descriptions.

| Lithofacies Group | Facies | Occurrence | Type Location |
|----------------------------------|--|--|--------------------------|
| Pumiceous and scoriaceous | Planar to low angle cross stratified | Site 1, section A | 11-14 m |
| | Normally graded and diffusely stratified | Site 1, section B | 0-5 m |
| | Scour and infill | Site 1, section A | ~ 10 m |
| | Thin to laminated facies | Site 1, section | Above scour and infill |
| | Massive pebble | Sites 1, 4, 5 and 6 | Sites 1 and 4 |
| Thin pumice- and crystal- rich | Crystal rich sand | Site 2 sections A-D, site 5, section B | Site 5 (~5 m) |
| | Pumice and crystal rich | Site 4, section A | Float |
| Volcanic conglomerate | Tabular pebble-cobble | Sites 2, 5 and 6 | Site 2 (10-12 m) |
| | Lensing pebble-cobble | Site 3 (8-14 m and 22-26 m) | Site 3 |
| | Weakly stratified pebbly sandstone | Site 3 (14-22 m) | Site 3 |
| | Very thick, poorly sorted cobble-boulder | Site 4, section A | 20-30 m |
| Thickly bedded granule sandstone | Massive normally graded facies | Site 2 section A-D (~ 15-26 m) | float |
| | Cross stratified facies | Site 6 (5-9 m, 19-24 m) | 5-9 m |
| Thinly bedded fine sandstone | Thinly bedded and normally graded | Sites 3, 4, 5 and 6 (< 5 m) | Site 5, section B. |
| | Thinly bedded calcareous | Site 2, section A-D (~0-10 m) | Section A |
| | Fine grey sandstone | Site 2, all sections | Site 2, section A |
| - | Bioturbated pebbly sandstone | Site 3 and 4 (~ 0-4 m) | Site 3, sections B and C |
| - | Polymictic breccia | Site 2, section B-C (~26-28 m) | Boulder float |
| Coherent | Pillow lava and sheet flow | Site 2 (25-40 m), 3 (2-8 m) | Site 2, section A |
| | Cross-cutting dyke and mega-pillow | Site 4 (0-20 m), 5 (0-25 m) | Site 4, section A |

4.2 Pumiceous and Scoriaceous Lithofacies Group

4.2.1 Occurrence

The pumiceous and scoriaceous lithofacies group is found at sites 1, 4, 5 and 6. Facies of this group are inter-bedded with the thin pumice- and crystal- rich lithofacies group (4.3) and the tabular pebble-cobble facies at sites 4, 5 and 6 (4.4.3).

4.2.2 General description

Facies within this lithofacies group are distinguished by distinct bed-forms and sedimentary structures, and vary in terms of the dominant clast size (sand and pebble) and type (pumice and scoria). Pumice and scoria pebbles, and rare boulders, are rounded to sub-angular and occur in a medium to coarse sand matrix. The matrix comprises crystals, basalt / andesite rock fragments, scoria and pumice. Non-volcanic clasts include minor sandstone pebbles and wood and fine sand intraclasts. Intraclasts are dominantly rounded pebbles or rare elongate (2-15 m long) and wispy clasts.

4.2.3 Planar to low-angle cross-stratified facies

The planar to cross-stratified facies include laterally continuous (~ 70 m), 1.3-2 m thick beds, which thicken and thin (**Figure 4.1**). The lower contact of this facies ranges from sharp and erosional at the thin end, to diffuse and depositional at the thick end. In some cases flame structures are present at the lower contact. Internal stratification is typically discontinuous over the length of the bed, from 5-30 cm at the thin end, which is planar stratified, to 30 cm-20 m at the thick end, which consists of large-scale low angle cross beds. Planar stratification comprises thin to very thin medium to coarse sand and fine pumice pebble beds, of shallow, trough cross-beds, that flatten into planar beds. Cross-stratification is delineated by weakly developed, diffuse beds of rounded fine pumice pebbles. This facies is commonly overlain with an erosional contact, with the thin to laminated facies.

4.2.4 Normally graded and diffusely stratified facies

The normally graded and diffusely stratified facies comprises single, laterally continuous (~ 100 m) relatively tabular beds, ~ 5 m thick (**Figure 4.2**). The basal to upper contacts are planar to undulating. This facies comprises weakly developed, diffuse internal stratification of subrounded to subangular cream and grey pumice pebbles, and basalt / andesite pebbles, in a matrix of coarse sand to granules. Normally graded beds comprise fine pumice pebbles and granules towards the base, with thinly stratified fine sand towards the top. This facies varies vertically. Stratification ranges from planar to low angle cross-stratified, defined by diffuse pumice and / or basalt /

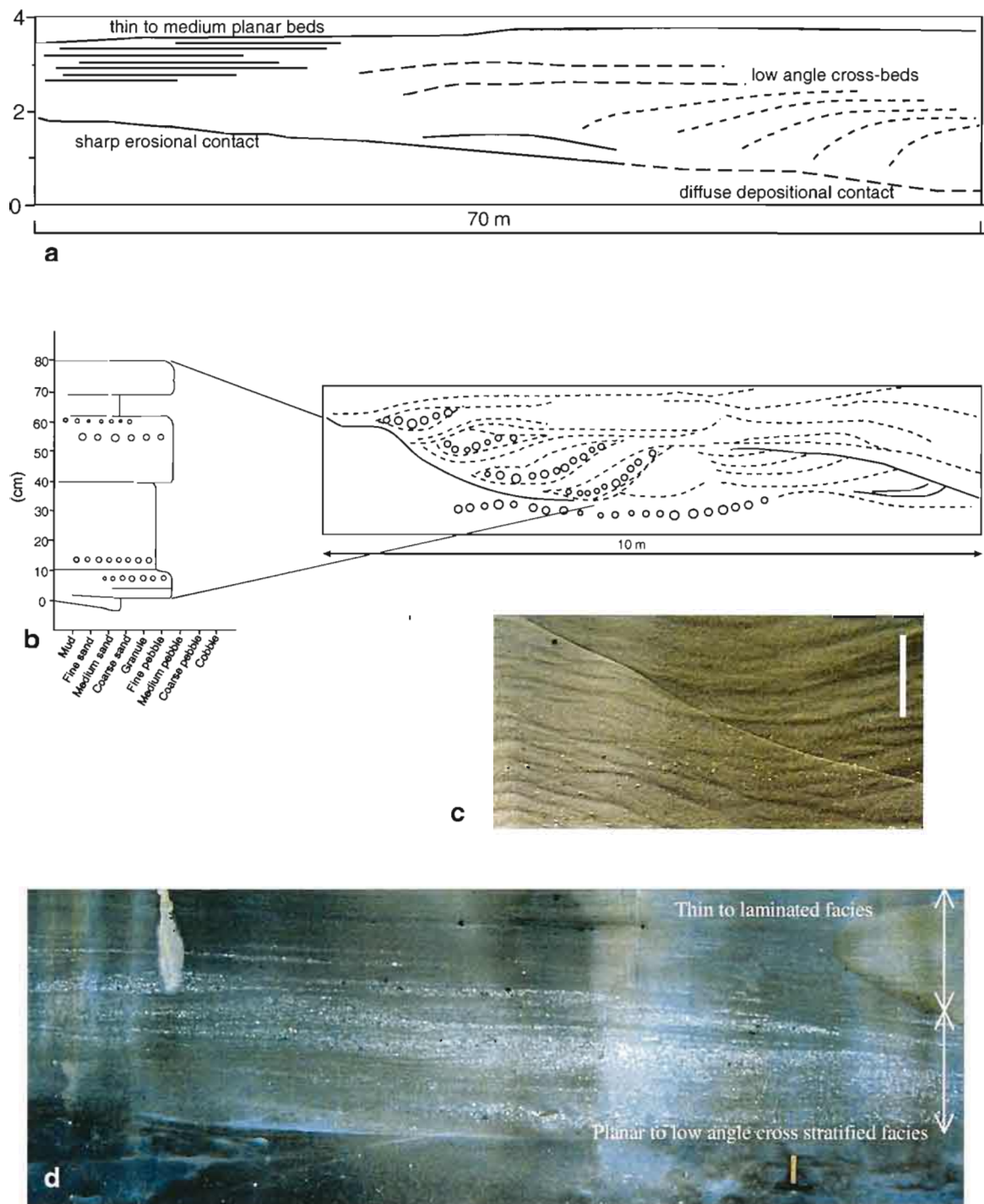


Figure 4.1. The planar to low-angle cross-stratified facies, (a) lateral variation from planar, to cross-stratified, (b) detailed log and diagram of the lateral variation in low angle cross bedded interval, (c) photo of localised trough beds (10 cm scale), (d) photo of fine pumice pebbles in a cross-bedded domain (see hammer for scale).

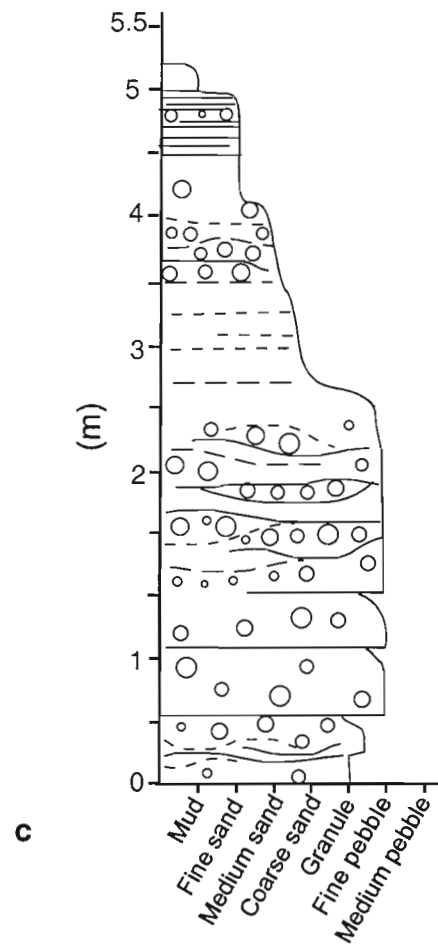


Figure 4.2. *The normally graded and diffusely bedded facies, (a) normal grading with typical weakly developed diffuse stratified pumice, scoria and lava pebbles, (b) detail of lateral variations in gravely intervals, with weak low angle pumice beds (hammer and hand lens for scale) (c) detailed stratigraphic log of bed.*

andesite pebbles. Low angle cross-stratified gravel and alternating planar fine and medium pumice pebbles with sand, delineate local vertical variations. Overall the stratification comprises diffuse (15-20 m), 2-10 cm thick, pumice pebble beds at the base, with thin, weak and diffuse pumice pebble beds in the middle, which decrease in thickness vertically to scattered pumice pebbles in sand at the top.

4.2.5 Scour and infill facies

The scour and infill facies is common in the pumiceous and scoriaceous lithofacies group, and range from single beds at the scale 1-2 m, to groups of beds, at 5 m thick (**Figure 4.3**). Bedding continuity is regularly disrupted by major and minor erosional scours that have sharp and planar or uneven bases, and are characterised by in-fills of medium to coarse sand, with rounded sand intraclasts, or fine and medium pebbles of pumice and basalt / andesite rock fragments. The in-fills are predominantly clast-supported, with weakly stratified intraclast pebbles and pumice pebbles in coarse sand in the lower part, which grades upwards to a finer-grained matrix-supported fabric, with localised thin beds. Thicker in-filled domains resemble the massive pebble facies. Scours are locally associated with flame structures and diffuse reworking structures of fine sand at the base, due to the disturbance of beds below. Scours have a gently concave morphology, and can be traced laterally into non-erosional, planar contacts. In some cases, scours delineate pinch and swell bed-forms that thicken and thin over short distances. This facies is commonly overlain by the thin to laminated facies.

4.2.6 Thin to laminated facies

The thin to laminated facies overlies the planar to low angle cross-stratified facies and the scour and infill facies. It typically includes thin to laminated, fine or coarse sand beds with localised pumice pebbles. This facies comprises 10-20 cm thick, planar beds of mud and sand, indurated horizons of silt-fine sand, and contorted fine sand beds. Occasional, thin to medium beds of silt and mud, or coarse sand to granule beds are also found (**Figure 4.4**). In general, this facies is laminated to thinly stratified, and convoluted beds show distorted bed-forms. Individual beds are typically fine grained, except for scattered coarse granules and rare outsized lava and pumice boulders. In general, the facies has a limited lateral extent due to local erosional scours, and localised disturbance of margins by bioturbation (**Figure 4.5**).

4.2.7 Massive pebble facies

The massive pebble facies is either dominated by fine to medium pumice pebbles or dominated by coarse scoria and basalt / andesite pebbles, or cobbles. Both types comprise a matrix of fine to

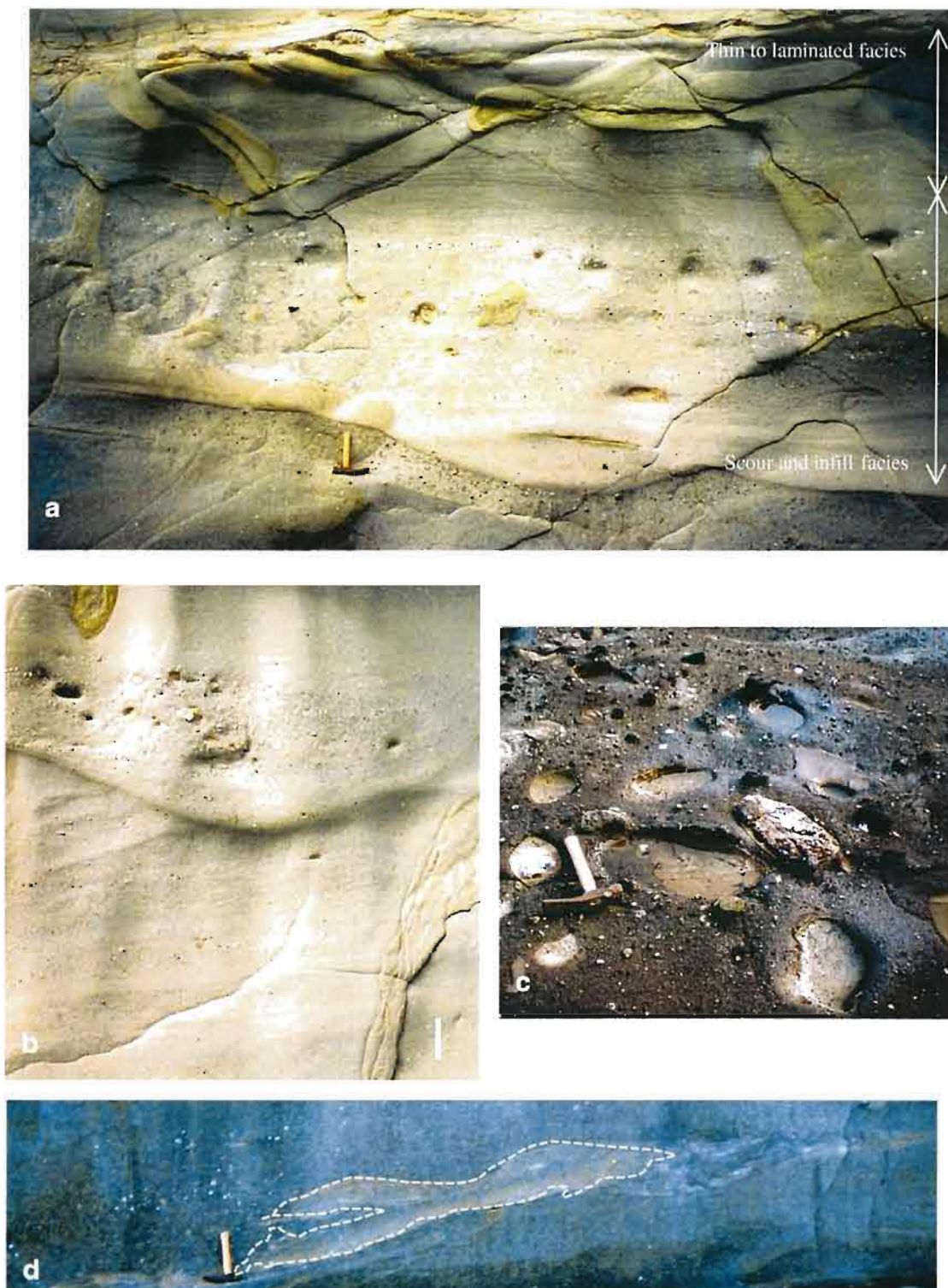


Figure 4.3. *Scour and infill facies, (a) erosional scour of gravel bed, with weakly stratified rounded intraclasts, in the lower part and an upper thinly bedded part, (b) scour into massive pebble facies (30 cm scale), (c) plan view of diffuse and weakly stratified domain in scour infill, of rounded medium to coarse intraclasts, (d) 5 m long wispy rip-up clast in basal part of scour infill (hammer for scale).*



Figure 4.4. *The thinly bedded and convoluted facies, (a) convoluted beds of fine and coarse sand interbeds (30 cm scale), (b) indurated layer at site 1 at top of the normally graded and diffusely bedded facies (30 cm scale).*

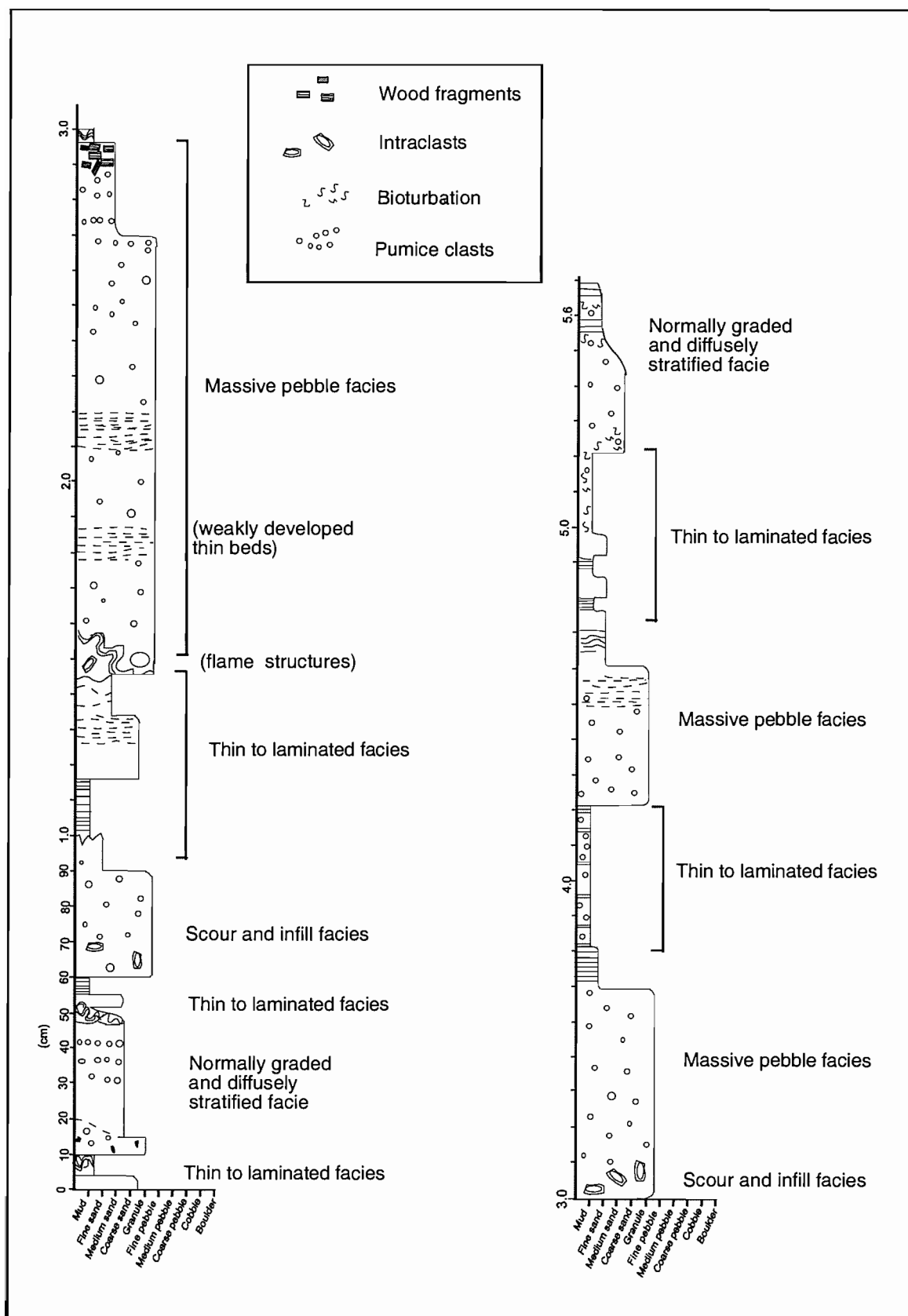


Figure 4.5. Detailed log of the pumiceous and scoriaceous lithofacies group at site 5.

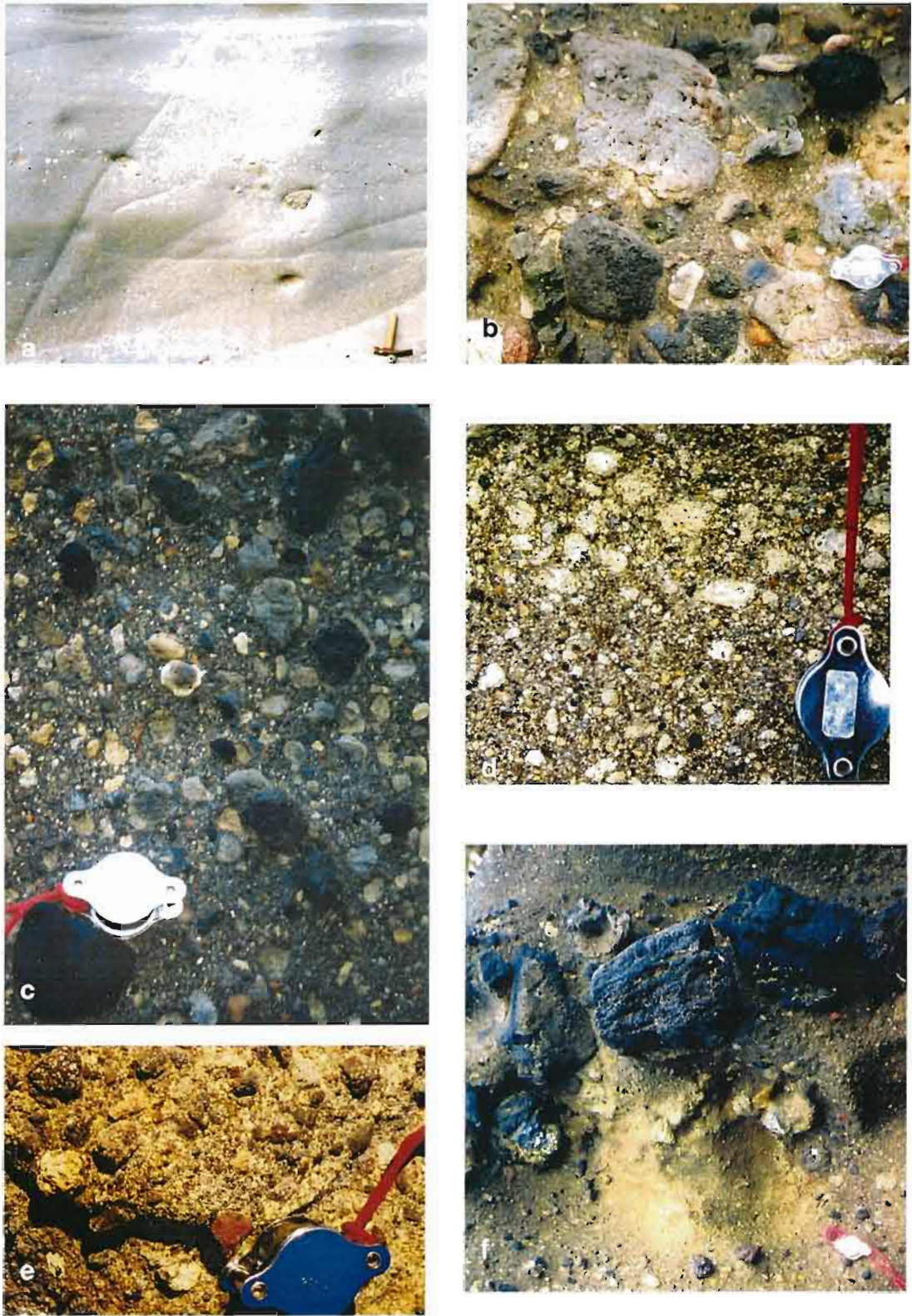


Figure 4.6. *Massive pebble facies (pumice and scoria types), (a) massive bed in pumice type, with sandstone intraclasts, (b) massive domain in scoria type, of grey and cream pumice, black and red scoria, and other volcanic clasts, (c) massive pumice and scoria pebbles, (d) detail of fine pebble pumice components, with black volcanic granules (e) gravel components of fine volcanic pebbles and granules, (f) single clast-thick bed of scoria cobbles, (see hand lens for scale).*

coarse sand, granules and in some cases fine pumice and / or basalt / andesite pebbles (**Figure 4.6**). Rare carbonaceous fragments are also found. The pumice dominant type is well sorted and mostly comprises pumice pebbles, with minor scoria and basalt / andesite rock fragments. The scoria dominant type is moderately sorted, and comprises medium to coarse scoria, basalt / andesite rock fragments and pumice pebbles. This facies ranges from 1-2 m thick, up to ~5-10 m thick. This facies is generally massive or weakly stratified, with a matrix-supported fabric. Local clast accumulations define crude beds and grading. Internal stratification is 30 cm to 5 m in lateral extent, weakly developed and diffuse. Stratification is of centimetre to 10's of cm in thickness, marked by scoria and pumice pebbles, or scoria and basalt / andesite pebbles, with scattered outsized lava boulders and sandstone intra-clasts. Stratification can be undulating, and is variably placed within massively bedded domains. The upper contacts of massive or weakly bedded domains are scoured.

4.2.4 Transport and deposition

The facies of this lithofacies group comprise a range of bed-forms, which rapidly vary in thickness and lateral extent. Scoured horizons, and stratified volcanic pebbles, supported by crystal-rich sands are ubiquitous. Lack of wave-generated bed-forms suggests deep marine deposition. In this environment mass flows, involving water-supported transport, comprise cold, subaqueous gravity flows, maintained by gravity-driven momentum (Stow, 1994). Together, the facies represent resedimentation of related material. Down slope sediment transport probably occurred in several connected flows, and as the flow energy waxed and waned with particle settling, a series of normally graded, vertically and laterally variable bed forms were produced. Various clast densities, and the presence of intraclasts suggests the transporting agents were of varying volume and capable of transporting clasts of varying size and density. Stratified and planar beds reflect the settling out of vesicular and dense clasts as the flow progressed. Cross-stratification and laminated beds are indicative of traction and suspension deposition of less dense particles (McPhie et al, 1993). Massive beds suggest rapid deposition. Turbidity current transport, in which particles are suspended by fluid turbulence in the upper parts of the flow, and traction in its lower parts, could form tractional bed-forms (Stow, 1994). Weak coarse pebble beds may have formed the bed load of a turbidity current (Stow, 1994). In sediment gravity flows, dense material is deposited closer to source, whereas smaller and low-density vesicular clasts would be deposited from upper and later, slower settling areas of the flow (Fiske and Matsuda, 1964). The erosive nature of the separate facies, with the occurrence of numerous erosional scours, suggests rapid sedimentation by a series of flows in close succession. The uppermost fine sand-mud intervals, suggests slow settling of fines arose once the high concentration part of the turbidity current had settled.

4.3 Thin pumice and crystal rich Lithofacies Group

4.3.1 Occurrence

The thin pumice and crystal rich lithofacies occur at site 2, 4 and 5. This lithofacies ranges from 2-20 cm thick and is interbedded the thinly bedded fine sandstone lithofacies group and the pumiceous and scoriaceous lithofacies group.

4.3.2 General Description

Two facies occur within the thin pumice and crystal rich lithofacies group and are distinguished by the thin bed thicknesses, limited clast types and well-sorted character. In general this lithofacies group is comprised of laterally continuous, thin isolated, planar beds with sharp to irregular bases and gradational tops. Beds are clast-supported and well-sorted coarse sand, granules and fine pebbles. Grains are subrounded to angular pumice, crystals, black porphyritic fragments, and scoria, with ragged pumice grains and euhedral or broken crystals. The crystal components comprise plagioclase, pyroxene, quartz and iron-titanium oxides, with lesser olivine, and calcite.

4.3.3 Crystal rich sand facies

The thin crystal rich sand facies (sites 2 and 5) comprise thin internal, well-sorted coarse sand beds (**Figure 4.7**). The sand layers are dominantly composed of crystals, and porphyritic and glassy fragments. The beds vary in thickness from < 1 cm to 5 cm, and can be very thin and diffuse or thicker and laterally continuous. The base of beds is undulatory, with load casts into the underlying beds. Individual beds can be normally graded, with a base of coarse sand to granules, and a fine sand top that grades into the fine to medium sand of the above bed. Internal, weakly developed and diffuse pumice beds and local bioturbation occurs.

4.3.4 Pumice and crystal rich facies

The pumice and crystal rich facies (site 4) comprise thin internal well sorted, granule to fine pebble layers interbedded with the pumiceous and scoriaceous lithofacies group (**Figure 4.7**). Individual beds are isolated and appear to be laterally continuous, < 30 cm thickness, and comprised of granule to pebble sized clasts. The layers have a planar to slightly undulating base. Pumice and crystal rich layers and pumice-dominant layers are recognised. Pumice and crystal rich layers are clast-supported, with grain-to grain contact, and dominantly composed of grey and cream pumice, plagioclase and pyroxene crystals, and minor black volcanic fragments (**Appendix 4**). The pumice clasts are pebble sized and the crystals are granule to coarse sand sized. Pumice-

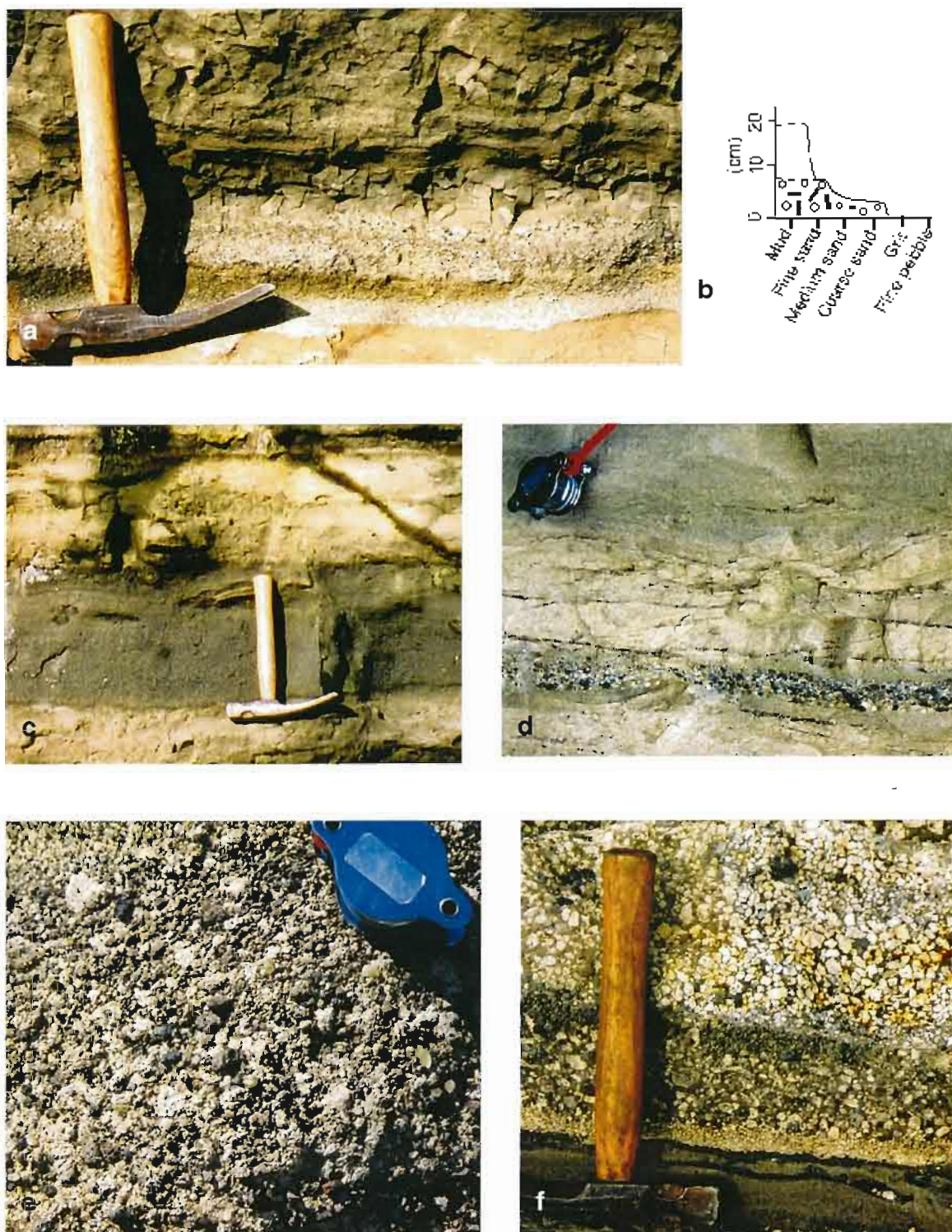


Figure 4.7. Thin pumice and crystal rich lithofacies group, (a) detail of crystal rich sand facies at site 5, with irregular base, (b) detailed log of crystal rich layer, (c) crystal rich sand facies at site 2, (d) cm-thick pumice and crystal layer, with fine black volcanic pebbles, (e) detail of pumice and crystal rich facies, (f) density stratified pumice dominant layer, of ragged cream pumice crystals in a fine sand-silt matrix (hand lens and hammer for scale).

dominant layers are clast-supported, with grain-to-matrix contact, and dominantly composed of angular cream pumice clasts in a grey, crystal-rich sand matrix. In these layers, the pumice clasts are crudely stratified and reverse graded, with a fine-grained, crystal-rich base and a fine-grained pumice rich top.

4.3.5 Transport and deposition

Facies of the thin pumice and crystal rich lithofacies group are fine-grained, but generally coarser than the enclosing facies (thinly bedded sandstone). Subaqueous transport of pumice and crystals is a function of their hydraulic properties, which is controlled by the differing size and density of pyroclasts (Smith and Smith, 1985). The occurrence of large pumice and small crystal clasts within a single bed is evidence of hydraulic sorting during transport (Cashman and Fiske, 1991). During direct suspension settling of vesicular and dense clasts in the water column, differing settling velocities create distinctive bimodal size distributions of pumice and crystals. The thinly bedded nature, and well-sorted volcanic clasts with euhedral and ragged shapes suggest a submarine pyroclastic fallout origin, with minimal secondary reworking (Cashman and Fiske, 1991). The normally graded, well-sorted crystal-rich facies and the pumice and crystal rich facies, suggest a fallout origin, however, density stratified pumice dominant layers, with a mud matrix implies sediment gravity flow transport of pyroclasts. The thin pumice and crystal rich facies may have formed as a result of water-settled fallout from an eruption plume, or suspension settling from a low-concentration volcanoclastic turbidity current.

4.4 Volcanic Conglomerate Lithofacies Group

4.4.1 Occurrence

The volcanic conglomerate lithofacies group occurs at sites 2, 3, 4, 5 and 6. This lithofacies group ranges from beds of single clast thickness (site 3), up to relatively tabular beds 2.5 m thick.

4.4.2 General Description

Four facies occur within the volcanic conglomerate lithofacies group and are distinguished by different bedding styles, grainsize and grain fabric. In general, this lithofacies group is comprised of tabular pebble, or lensing pebble or cobble beds that have uneven and erosional lower contacts, between weakly stratified intervals of gravel and sand. Pebbles and cobbles are subangular, blocky and elongate, or well rounded and spherical. The dominant clast types are fine and coarsely porphyritic basalt / andesite clasts with scattered fine-grained glassy clasts. Non-volcanic components include coral, oyster shells, and dark, well-rounded (allochthonous) pebbles. The pebbles and cobbles can be matrix or grain supported (grain-to-grain or grain-to-matrix

contact), in a matrix of medium to coarse sand, or coarse sand to granule, or pebbly granules. Beds are relatively well sorted and generally dominated by fine, medium or coarse pebbles and cobbles, but can consist of a range of clast sizes. Outsized clasts are uncommon. Coarse pebble beds comprise a matrix of fine to medium volcanic pebbles, granules, sand, clay, and feldspar crystals.

4.4.3 Tabular pebble-cobble facies

This facies comprises laterally continuous, tabular, thick beds of medium to coarse pebbles, with rare cobbles (**Figure 4.8**). The facies comprises a single bed 1 m to 2.5 m thick. The facies has an erosional lower contact and an irregular to locally gradational upper contact with the massive pebble facies (pumiceous and scoriaceous facies group). The tabular pebble-cobble facies is massive to weakly normally graded and dominantly clast supported with grain-to-grain and grain-to-matrix contact. However, matrix supported domains occur towards the top or mid part of some beds. Clasts of basalt / andesite and sandstone are subangular to angular, and moderately sorted, in a fine pebble, granule and sand matrix. At site 4, 5 and 6, the facies fine upwards to discontinuous fine pebble and gravel. Localised planar or inclined imbrication of elongate pebbles locally defines weakly developed internal stratification.

4.4.4 Lensing pebble and cobble facies

The lensing pebble and cobble facies comprises dominantly laterally discontinuous lenses of rounded basalt / andesite, with a thickening and thinning character that occur in between the weakly stratified pebbly sandstone facies. The lenses have a lateral extent of 10-20 m and vary in thickness from 30 cm-4.5 m. The basal contact comprises sharp, irregular basal scours that commonly scour into sand-dominated intervals. Domains of stacked thick lenses occur. This facies thin and pinch out to the weakly stratified pebbly sandstone facies. Lenses comprise fine to medium pebbles or coarse pebbles and cobbles (**Figure 4.9**), with scattered outsized boulders, and have matrix supported or clast supported fabrics. Fine to medium pebble lenses contain clast-supported fabrics with grain-to-grain contact, whereas the coarse pebble to cobble lenses contain grain-to-matrix contact. Matrix supported areas of coarse sand and granules with scattered fine pebbles define weakly developed and diffuse internal stratification.

4.4.5 Weakly stratified pebbly sandstone facies

The weakly stratified pebbly sandstone facies comprise thin internal pebble layers within thin to thickly bedded medium to coarse sandstone (**Figure 4.10**). The pebble layers are composed of clustered or scattered pebbles that are spaced at intervals of cm to 10's of cm. Uncommon coarse pebble clasts and woody layers occur. The pebble layers are of variable thickness, from the

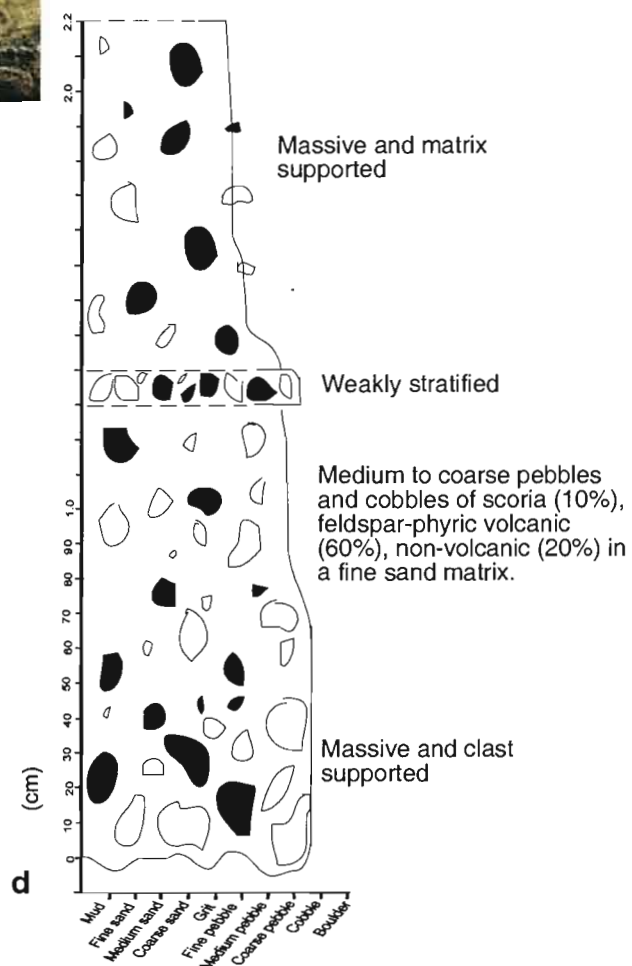
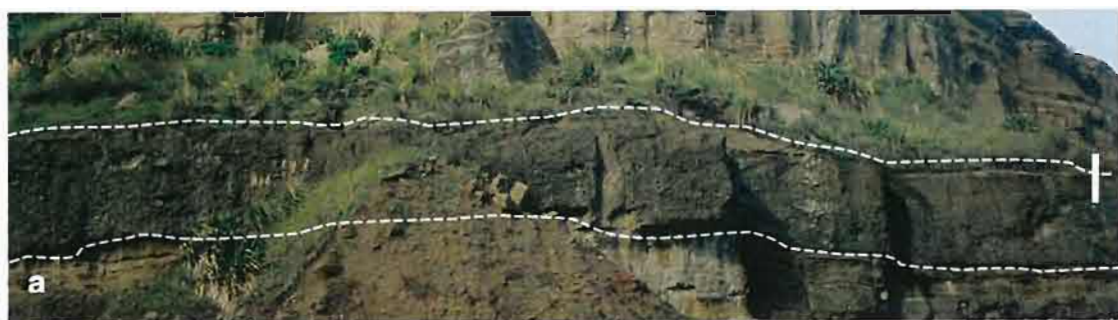


Figure 4.8. The tabular pebble-cobble facies, (a) 2-2.5 m thick tabular bed at site 2, (b) boulder of tabular bed, (c) detail of bed at site 6, with gradational gravel top, (d) detailed log of tabular bed at site 2.

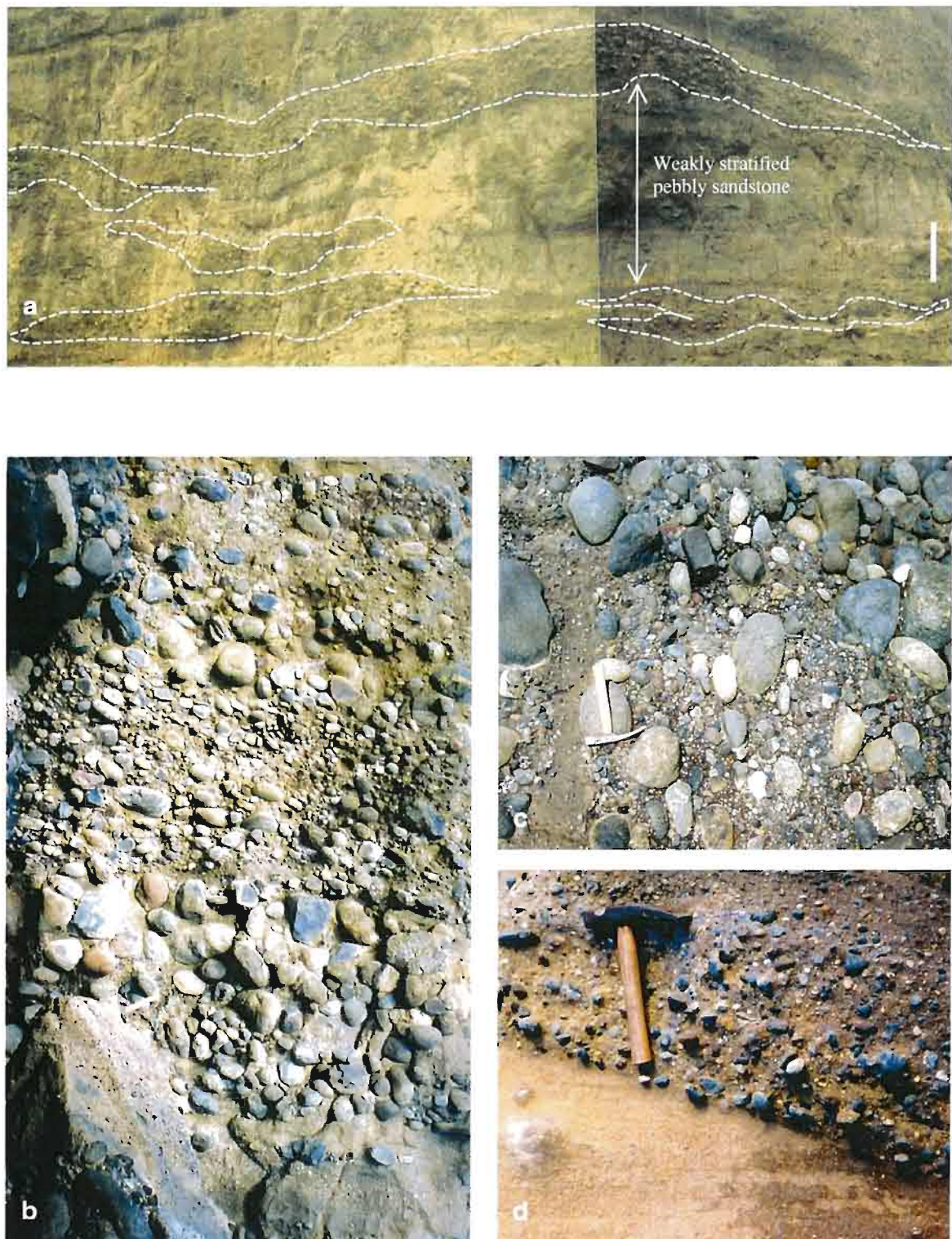


Figure 4.9. *The lensing pebble-cobble facies, (a) lensing and irregular bed-forms (dashed lines), occurring in between the weakly stratified pebbly sandstone (2.5 m scale), (b) clast and matrix supported pebble and cobble beds, (c) boulder of pebble components, (d) fine pebble scour into sandstone (see hammer for scale).*



Figure 4.10. *The weakly stratified pebbly sandstone facies; (a) undulating bed-forms (2.5 m scale), (b) diffusely stratified scattered pebbles in coarse sandstone (10 cm scale), (c) detail of weakly developed fine pebble layer, (d) coarse sand and granules, (e) diffuse and weakly developed stratification of wood (hammer and hand lens for scale).*

thickness of a single clast (1-2 cm), to coarse pebbles (6 cm) and define weakly developed stratification within the sandstone. They are weakly developed and diffuse, with an undulatory form, and can be traced for 5-20 m. Single layers are sparsely distributed, and are gradational with the surrounding fine to medium sandstone. The sandstone beds contain weakly stratified wood particles and rounded volcanic clasts.

4.4.6 Very thick poorly sorted cobble-boulder facies

The very thick poorly sorted, cobble-boulder facies (site 4) comprises a single localised bed of cobbles and boulders of glassy black volcanic clasts, and scoria. This facies is irregularly shaped, with a thick central part that tapers abruptly and becomes discontinuous over a distance of 20-30 m. It occurs as an irregular cluster of coarse pebble clasts that overlies the massive pebble facies (pumiceous and scoriaceous lithofacies group) (**Figure 4.11**). This facies is 10 m thick and consists of two parts, a clast-supported pebble-cobble base and a matrix supported cobble-boulder top. Clasts occur in a matrix of rounded to sub-angular fine pebbles, granules and coarse sand of glassy and porphyritic volcanic, scoria and non-volcanic material. It is well sorted, massive and lacks internal structure.

4.4.4 Transport and deposition

Pebble and cobble grains are transported down slope in sediment gravity flows. Coarse grain fractions are high density, and are transported as particle bed-load within grain-flows and high-density turbidity currents (Lowe, 1982). Coarse sediment transport is controlled by particle concentrations and grain-to-grain contact, where individual particles roll or bounce down slope. High-density turbidity currents move grains in turbulent form, supported by clast collisions and hindered settling (Lowe, 1982). The normal grading of the tabular pebble-cobble facies is consistent with deposition in the lower channelised slope of an inner submarine fan (Walker, 1975). The massive to disorganised nature of the lensing pebble and cobble facies is consistent with deposition in the upper parts of a submarine canyon or channel, with the weakly stratified pebbly sandstone deposited in the lower channelised zone of the fan (Walker, 1975).

4.5 Thickly-bedded granule Sandstone Lithofacies Group

4.5.1 Occurrence

This lithofacies group ranges from 1-12 m thick. It is associated with the fine grey sandstone facies at site 2, and grades up to bedded sandstone at site 6.



Figure 4.11. *The very thick, poorly sorted cobble-boulder facies, (a) outcrop expression at site 4 and relationship to beds below (10 m scale), (b) cobble and boulder sized lava clasts (5 m scale), (c) detail of matrix components (hammer for scale).*

4.5.2 General description

Three facies occur within the thickly bedded, medium to coarse granule sandstone lithofacies group and are distinguished by different bedding styles, thickness and sedimentary structures. In general, this lithofacies is dominantly comprised of planar, laterally continuous, 1-3 m thick, coarse granule sandstone beds, with less common 10-30 cm thick granule sandstone beds. Stratification is restricted to discrete intervals, with weakly bedded domains occurring locally within massive beds, cross-beds in large scale mega-ripples and planar stratification in thin, bioturbated beds. This facies is well sorted, and matrix-supported, with uncommon scattered fine pebbles and localised clast-supported pebble domains, within the coarse sand to granule matrix. The clastic components comprise sub-angular to angular crystals, basalt / andesite rock fragments, scoria, cream pumice and sandstone (**Appendix 4**).

4.5.3 Massive normally graded facies

The massive normally graded facies comprises laterally continuous medium to thick beds of medium and coarse sand, with coarser domains of granules and scattered fine to medium, sub-rounded pebbles, in the basal parts of beds (**Figure 4.12**). This facies ranges from 10 cm to 3 m thickness and are relatively homogenous, except for scattered, rare bioturbation burrows. Beds vary laterally the amount of bioturbation and development of the stratification, with many beds massive and unstratified. Individual beds show faint, diffuse normal grading, with a pebble and granule base, and rare occurrences of fine sandstone rip-up clasts. The tops of 10-30 cm of some thick beds comprise planar stratified fine sand or mud, which are bioturbated, and contain local diffusely stratified wood fragments. The crude internal stratification, is marked by rounded fine pebbles and granules, and occasionally comprises fine sub-rounded cream pumice, and angular scoria pebbles, and feldspar crystal sand (5 mm-2 cm size). Massively bedded domains occur above and below weakly bedded or normally graded beds.

4.5.4 Cross-stratified facies

The cross-stratified facies comprise single 3-4 m thick beds of both large and small-scale cross-bedding. At site 6, is medium to thickly bedded and continuous, and changes from planar to cross-bedded, over a distance of ~ 90 m. The cross beds are low angle, and have been defined as mega-ripples within a low amplitude pinch and swell bed (**Figure 4.13**). Pinch and swell beds have amplitudes of 80 cm-1.2 m, and wavelengths of 8-10 m and are asymmetrical. Individual foresets are planar, and gently curve towards horizontal at the base of the bed. Foresets are defined by coarse sand and granules, and oxidised wood fragments. The troughs separating foresets often contain accumulations of wood. Beds dip towards the northwest or



Figure 4.12. *The massively normally graded facies, (a) 10 m sequence at site 6, with arrows indicating stratified and bioturbated fine sand intervals (5 m scale bar), (b) massively bedded medium to coarse sandstone with weakly stratified granules and fine pebbles, dashed lines mark bioturbation, (c) crude grading of fine pebbles and granules, (d) fine sandstone rip-up clast in base of graded bed at site 6 (hammer and hand lens for scale).*

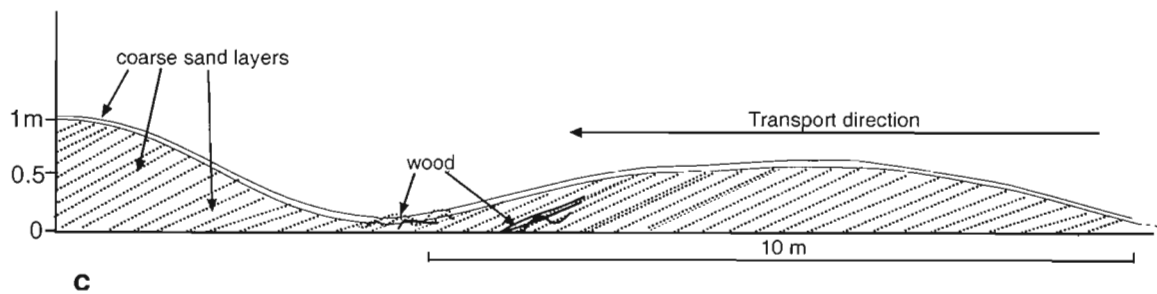
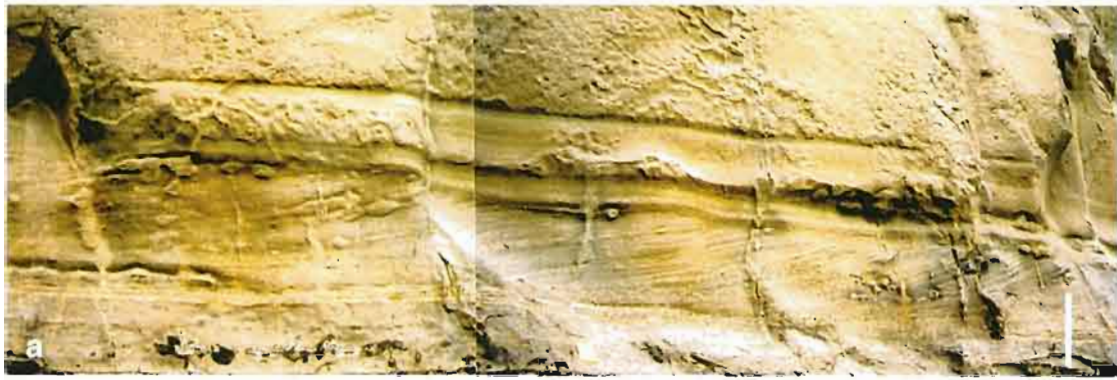


Figure 4.13. The cross-stratified facies, (a) the low angle cross-beds at site 6 (1 m scale bar), (b) change from planar to cross-bedded, outlines mark where low angle cross-beds pinch out (person for scale), (c) sketch of pinch and swell beds, with wood and coarse sand intervals in troughs.

northeast. A domain of herringbone and thinly cross-stratified intervals mark the point where planar stratification pinches out and cross-bedding commences. A further thickly bedded and cross-stratified interval, occurs in the upper parts of site 6, and comprises stratified planar beds at the base and top, with internal cross-bedded domains.

4.5.5 Transport and deposition

The different facies types suggest sediment gravity flow and bottom current transport processes. The thick massive facies suggest rapid deposition from gravity-driven high-density turbidity currents, supported by high particle concentrations (Lowe, 1982). However the thinly bedded and bioturbated facies indicate turbulence and suggest lower particle concentrations that could be associated with slow settling from the upper, or more distal parts of gravity currents (Stow, 1994). The cross-bedded facies records a change in sedimentation conditions, to protracted current-dominated transport. In deep water these facies may form from strong bottom currents, such as canyon currents and large scale eddies (Stow, 1994).

4.6 Thinly- bedded fine Sandstone Lithofacies Group

4.6.1 Occurrence

This lithofacies group occurs at sites 2, 3, 4, 5 and 6 and ranges from < 1 m thick at site 1, up to 20 m thick at site 5. Distinct thin beds of the thin pumice- and crystal- rich lithofacies group are locally interbedded with this lithofacies group (4.3).

4.6.2 General description

Fine sand and mud, planar, laterally continuous and regular bedding styles and normally graded beds distinguish the thinly bedded fine sandstone lithofacies group. Internal stratification occurs in the form of planar laminae, cross beds and diffuse planar or irregular beds. The thinly bedded fine sandstone lithofacies is dominantly composed of fine sand, with medium to coarse sand interbeds. It is well sorted and clast supported, comprised of angular to subangular sand grains of lava fragments, glass, lithics and crystals of quartz and iron-titanium oxide (**Appendix 4**), with marine fossils and uncommon wood and fine pumice particles. The thinly bedded fine sandstone lithofacies group is variably bioturbated.

4.6.3 Thinly bedded and normally graded facies

The thinly bedded and normally graded facies comprises fine sandstone beds, of 10-30 cm thick, with medium to coarse sand at the base, and mud occurring at the top (**Figure 4.14**). Individual

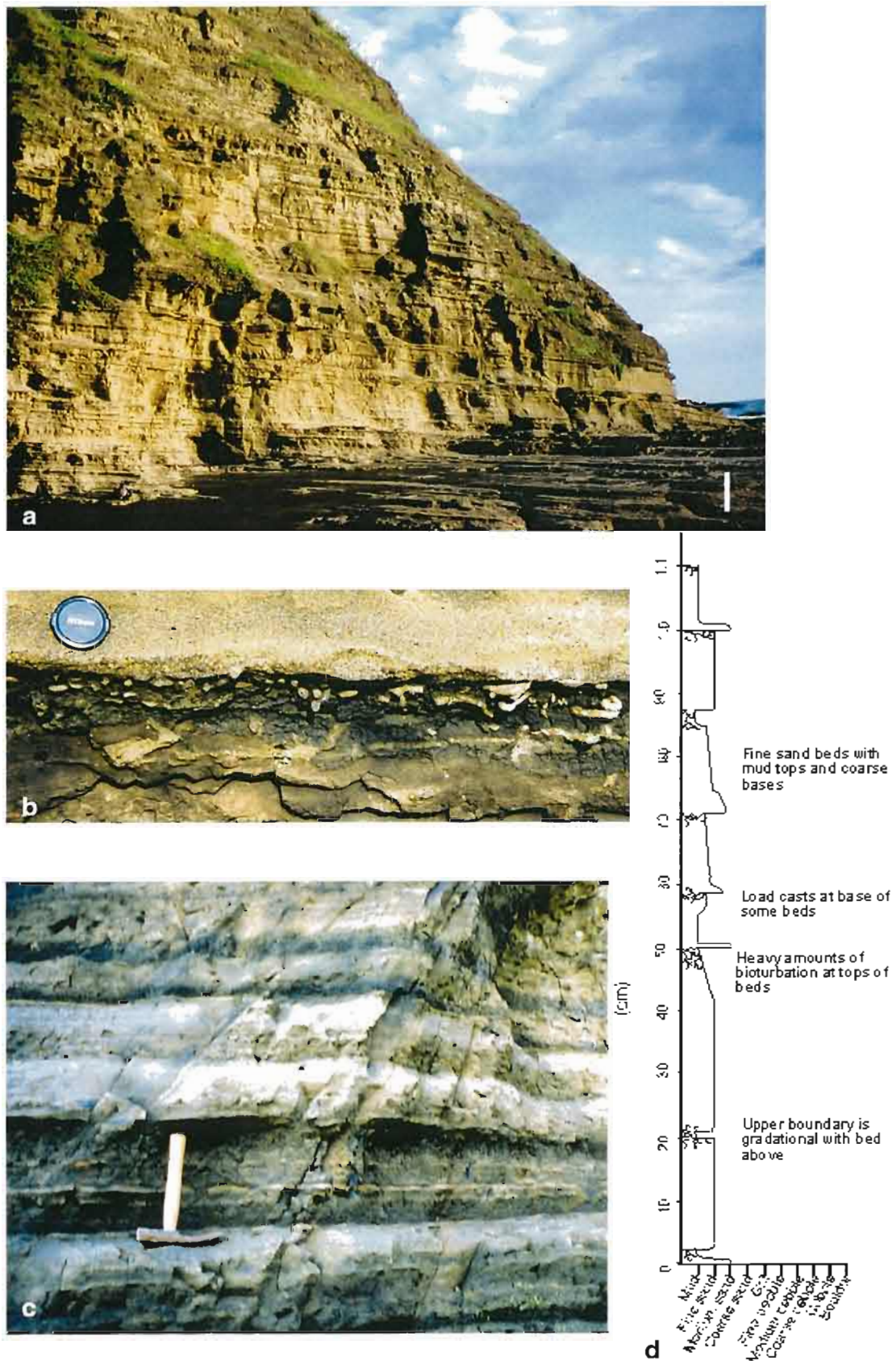


Figure 4.14. The thinly bedded and normally graded facies, (a) outcrop expression (1.5 m scale bar), (b) bioturbated mud top below the thickly bedded medium to coarse granule sand lithofacies at site 6, (c) detail of bed thicknesses, (d) detailed stratigraphic log.

beds can be massive or normally graded and have sharp or diffuse boundaries, with the upper boundary commonly gradational. A typical normally graded bed comprises 1-2 cm of medium sand at the base, then 20-30 cm of fine sand, followed by a 1-5 cm thick, discontinuous mud layer at the top. Bioturbation occurs at the base of medium to coarse sand beds, and in massive beds. The stratification of muddy intervals is disrupted by heavy amounts of bioturbation; trace fossil burrows are 5 mm and 1.5 cm wide (*Tigillites* ichnosp. and *Scalarituba*: Hayward, 1979d). Beds of thin crystal rich sand facies occur at repeated intervals throughout this facies (4.3.3), and at occasional intervals deformed beds comprising thin buckled and broken sandstone beds are also found.

4.6.4 Thinly bedded, calcareous facies

The thinly bedded, calcareous facies comprises fine sandstone beds of 5-65 cm thickness, with diffuse internal stratification and silt tops, and separate thin, bioturbated coarse sandstone beds (Figure 4.15). A typical calcareous sand bed comprises 20-60 cm of massive fine sand, with very weakly developed, diffuse stratification and a silt top. Beds are mostly massive, but contain localised diffuse, very thin pumice and scoria beds, with sharp, planar boundaries. Localised accumulations of carbonised fragments occur within massive intervals. 2-5 cm thick beds of crystal rich sand facies occur at repeated intervals (4.3.3), and are normally graded. In addition laminated mud intervals also occur. Scattered throughout are gastropod shells, coral fragments, scaplopod molluscs and *lenticulina foraminifera* tests.

4.6.5 Fine grey sandstone facies

This fine grey sandstone facies is grey and weakly bedded comprising planar fine grey sandstone beds 10-30 cm thick, and lack internal structure. Internal planar stratification is weakly developed and diffuse, with occurrences of mm to 1 cm sized, cream to white pumice clasts, in some cases defining thin beds. A small number of thin, fine to medium sandstone beds randomly occur. In general, this lithofacies is composed of fine sand to silt grains, which are well sorted, with rare fine pebbles and granules of pumice. It comprises euhedral crystals and fragments of feldspar, red scoria, dark glass or lithic particles, wood splinters and pumice, in a very fine-grained black / grey matrix.

4.6.6 Transport and deposition

Facies of the thinly bedded fine sandstone lithofacies group are dominated by fine, angular sand particles. In general, fine-grained sediments are transported and reworked by bottom currents, turbidity currents, flows and mass movements on the sea floor (Gorsline, 1984). The heavily bioturbated nature indicate slow sediment deposition between beds. The thin graded nature of the

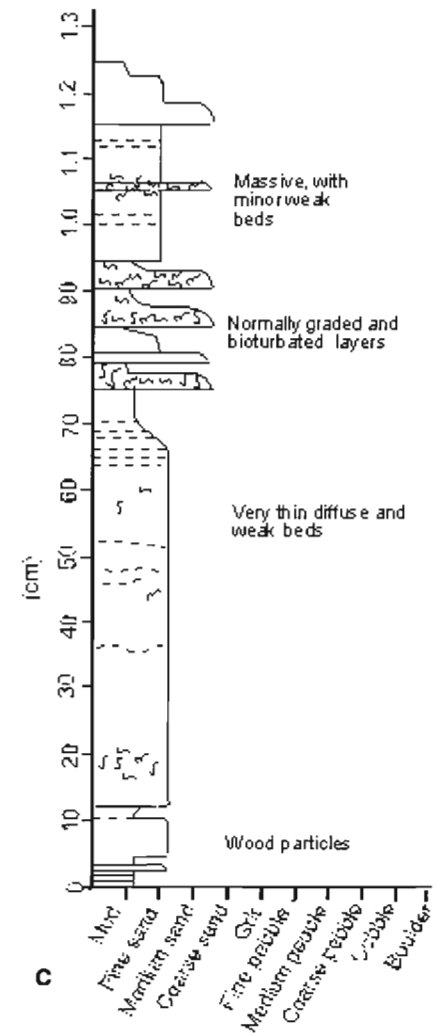


Figure 4.15. The thinly bedded calcareous facies, (a) outcrop expression, note dark layers of the crystal rich sand facies (b) detail of massive bed with diffuse wood particles, and (c) detailed log

beds resembles turbidity current deposition, and together with the dominance of fine grain-sizes suggests transport in low-density currents. Low-density turbidity currents contain dilute particle concentrations, which suggest that they are maintained by fluid turbulence and produce slow moving flows (Lowe, 1982). The comparable density of wood and pumice clasts, with fine sand grains, led to coincident transport and simultaneous deposition (Gorsline, 1984). The weak bedding of the fine grey sandstone suggests there was little variation in the particle concentration of separate flows, which can be mobilised by seasonal fluctuations that rework fine deposits on the sea-floor (Gorsline, 1984). The low density pumice clasts may have been remobilised by reworking or derived from contemporaneous distal pyroclastic fallout. The fine grain sizes in this lithofacies group suggests deposition on the mid to outer submarine-fan, from a distal source (Walker, 1975), and that deposition was part of background sedimentation, which occurred in intervals of the supply of coarse clastic sediment.

4.7 Bioturbated pebbly sandstone facies

4.7.1 Occurrence

The bioturbated pebbly sandstone lithofacies occurs at sites 3 and 4. This lithofacies is of variable thickness, and ranges from 1-2.5 m thick.

4.7.2 Description

In general, the bioturbated pebbly sandstone facies is disorganised, with indistinct intervals of localised and poorly defined, very diffuse planar to undulating stratification (**Figure 4.16**). Stratification is defined by woody layers, pumice clasts and erosional scours, which create abrupt grain-size changes and heavily bioturbated horizons (**Figure 4.17**). The scours include massive to crudely graded dish-structures, which have a few disseminated, coarse pebbles in the basal parts of the scour, and have irregular tops. This lithofacies contains granules and pebbles in a variable sand-granule matrix and is dominantly matrix-supported, with rare clast-supported domains. The matrix is heterogeneous and varies between beds, and can be dominated by fine to medium sand with a mud framework, or it can be pumice pebble rich and granular. It is poorly to moderately sorted, with rounded and angular, fine to medium pumice, scoria pebbles, and vesicular or black porphyritic fragments. Chunks of wood and mollusc shells also occur. This lithofacies is modified by bioturbation, with burrow networks, feeding, dwelling and escape structures that can be restricted to certain horizons and concentrated in wood-rich intervals. A horizon of crustacean occurs (*Callianassa*) and abundant burrow networks occurs 2 m below the pillow lava at site 3. Worm castings are in clusters, with concentrations of gastropod (*torrido*) burrows on woody layers. Other fossil types include bivalves (*Annedontia*, *thycryria* and *Lornia*) and limpets.



Figure 4.16. *The bioturbated pebbly sandstone lithofacies, (a) soured interval, (b) detail of pebble components, (c) heavily bioturbated layer, of crustacean trace fossils, (d) weak coarse pumice pebble bed (hammer and hand lens for scale).*

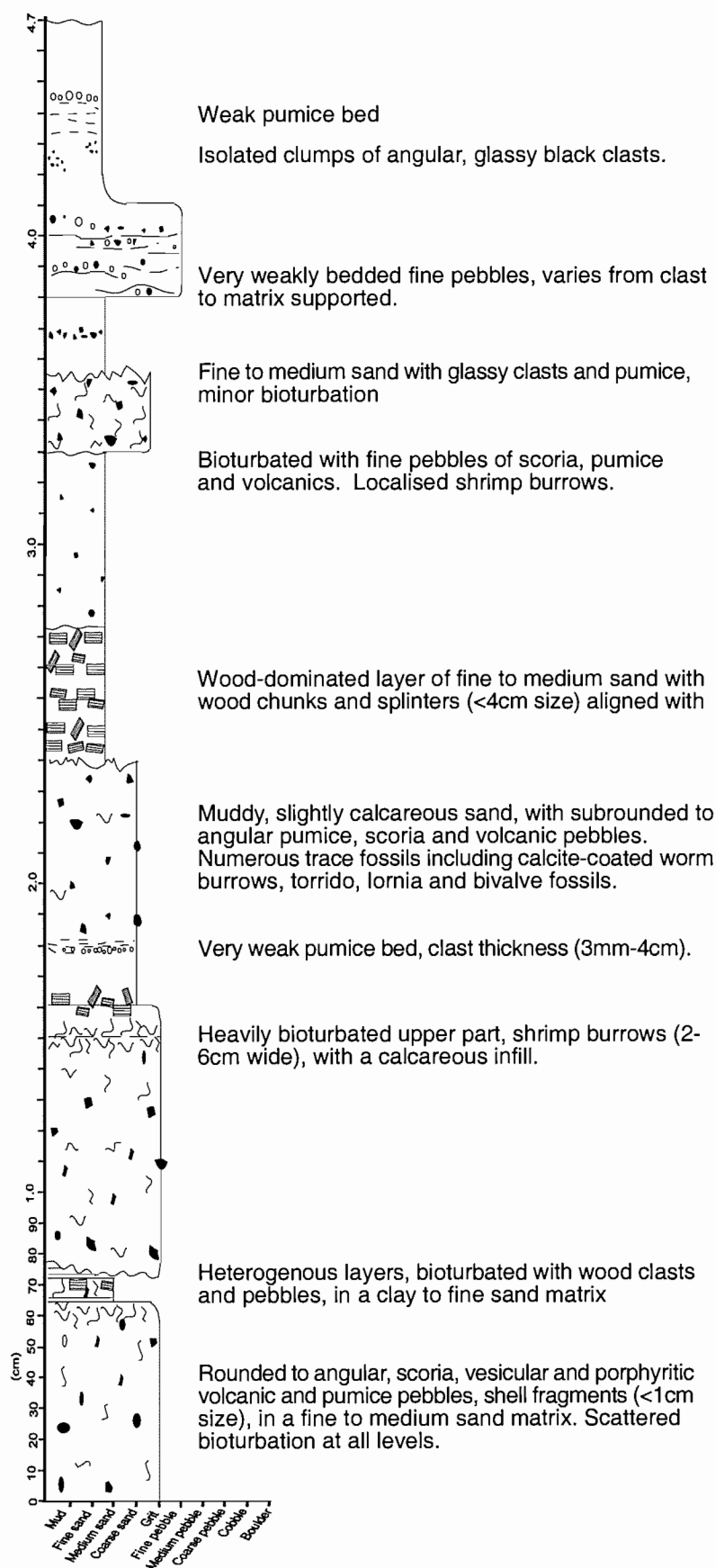


Figure 4.17. Detailed log of the bioturbated pebbly sandstone lithofacies, at site 3.

4.7.3 Transport and deposition

The bioturbated pebbly sandstone lithofacies is poorly sorted, with a range of clast types and is disorganised. The poor sorting involving mud and pebbles, and massive thick nature of the beds suggest that deposition was from a cohesive debris flow. Debris flows comprise a high sediment, low water concentration mixture, and moves down slope with a slow, slurry-like movement (Stow, 1994). Flow movement is supported by buoyancy, frictional strength, matrix strength and elevated, and dispersive pore pressures (Stow, 1994). This sediment mixture could have been sourced from subaerial or submarine sector collapse, initiated by destabilisation or over-saturation of semi-consolidated sediments.

4.8 Polymictic Breccia facies

4.8.1 Occurrence

The polymictic breccia lithofacies is limited in vertical and lateral extent and occurs only within a single interval at site 2. This facies overlies the pillow lava mound at its western extent. Its upper extent comprises coarse granule sandstone.

4.8.2 Description

The polymictic breccia facies is characterised by domains of variable clast size, shape and type, and it has chaotic bed-forms (**Figure 4.18**). It is distinguished by distinct angular, equant and blocky, fine to medium, pebbles, and some cobbles. The matrix is variable, with matrix-dominated domains of angular, black fine-grained porphyritic pebbles, with an altered white rim (**Appendix 4**), or of granules, and clast-supported domains of high concentrations of fragments of pillow lava and of both pillow lava and intraclasts. Overall, grains vary from sand to boulder size, with a framework of medium sand, a matrix of angular, pebbles, and coarse pebbles and cobbles. The coarse pebbles and cobbles comprise porphyritic and vesicular pillow lava clasts, several of which have a well-defined and glassy rim. The lava clasts are angular or curved in shape, with some comprising blobby and irregular forms that have gradational contacts with the sand framework. Individual lava clasts contain varying amounts of irregular and spherical vesicles, with localised vesicle alignments. The sandstone intraclasts are elongate and subrounded to wispy, and range in length from cm-scale to ~ 2 m. The intraclasts comprise thinly bedded, medium sand, which contain contorted and wavy laminations, and variable amounts of red scoria in each layer. In some areas, the wispy intraclasts disseminate into the matrix, forming the framework grains. Bedding is poorly defined, chaotic, laterally variable and discontinuous, with an undulating character that is locally wavy and displays a convex up-ward profile. The



Figure 4.18. *The polymictic breccia facies, (a) chaotic outcrop expression where it abuts the pillow lava mound (2.5 m scale), (b) clast-supported domain of fine and medium pebbles, (c) matrix supported domain of granules and fine pebbles, (d) globular and irregular, porphyritic lava clast in a fine grained matrix, (e) sand intraclast, with lava and angular pebbles (hand lens for scale).*

vague stratification is marked by variable crude grading, inclined elongate intraclasts, and domains of fine or coarse pebbles. The pebble beds contain sand intraclasts, inclined at a high angle to bedding. In contrast, the upper coarse granule sandstone interval is planar and laterally continuous, with an irregular base.

4.8.3 Transport and deposition

The angular clast shapes that comprise this facies are indicative of short distance transport and resedimentation. The occurrence of blocky and angular clasts with polyhedral to cubic forms suggests non-explosive fracturing and jointing was the mechanism involved in their formation (McPhie et al, 1993). The fine-grained matrix clasts comprise glassy margins, characteristic of quench fragmentation of lava surfaces that produces hyaloclastite. The angular to curvy pillow lava fragments suggest a proximal source, such as the adjacent pillow lava and sheet flow facies. The occurrence of large bulbous to angular lava clasts suggests they may have been derived from rock fall talus and spalled lava blocks. Conversely, the blobby and irregular lava clasts suggest magma-sediment mixing indicative of intrusion of magma into wet sediment that leads to peperite formation. The crude grading and the occurrence of sand intraclasts suggest that these clasts have been resedimented in a flow that retained high internal strength, like a debris flow (Ballance and Gregory, 1991). It was probably slow moving, creeping flow that maintained the cohesive strength during flowage, allowing it to rip-up pieces of substrate (intraclasts). The proximal occurrence of a pillow lava mound suggests the emplacement of this facies and the pillow lava and sheet flow facies are associated. The emplacement of the polymict breccia facies may have formed at the front of an advancing lava flow, contemporaneous with lava emplacement.

4.9 Coherent Lithofacies Group

4.9.1 Occurrence

The coherent lithofacies group occurs at sites 2, 3, 4 and 5. This lithofacies group ranges from thin cross-cutting dykes, to pillow lava mounds 5-15 m in height.

4.9.2 General description

Two facies occur within the coherent lithofacies group and are distinguished by different forms and contact relationships. In general, this lithofacies group is comprised of coherent bodies, which are concordant and discordant to bedding. The pillow lava and sheet flow facies have mound morphologies, which vary in thicknesses over its lateral extent. The cross-cutting dyke and mega-pillow facies are linear cross-cutting bodies, which have a mega-pillow form at their

highest point. The lavas are fine grained to glassy, with abundant phenocrysts in an altered [glassy] groundmass with microphenocrysts and vesicles. Phenocrysts comprise predominantly plagioclase, clinopyroxene and orthopyroxene, with lesser olivine and iron-titanium oxides (**Appendix 4**). Vesicles are irregular to subrounded in shape and occur in varying concentrations, with aligned vesicles in some areas. Geochemical analysis indicates basalt to basaltic andesite compositions for the coherent lithofacies group (**Chapter 5**).

4.9.3 Pillow lava and sheet flow facies

The pillow lava and sheet flow facies comprises 2-15 m thick, concordant piles of closely packed pillow lobes, with small, medium and mega-pillows with spherical and entail-like shapes. Pillow lobes are larger towards the base of the pile and gradually decrease in size with height (**Figure 4.19**). The thickest pile (site 2) has a broad, steep form that tapers abruptly to single pillows in the northwest. It is characterised in its centre by several mega-pillows (15 m height), surrounded by numerous smaller pillows. Piles of smaller pillows (site 3) have a broad wave-like form (5-8 m height), with relatively consistent pillow lobe sizes. The pillow piles have an irregular base, which slightly erode into the underlying sediments. The pillow lobes are characteristically tightly packed within the pile, and are sub-rounded to bulbous in cross section, from 1-10 m diameter or elongate in longitudinal section. Pillow lobes display radial jointing patterns, and at their base, high concentrations of flattened, horizontally aligned vesicles occur at 1-2 cm spacings. Radial jointing is delicate to indistinct within the smaller pillows, which generally have a glassy, locally cracked and concentrically layered rind. Fine-grained sediments occur in interstices in between pillows. Tabular, vertically jointed sheet flows occur at the top and base of the pillow lava piles. Sheet flows are limited in vertical and lateral extent, at < 1 m height and < 20 m long. The northern extent of the pillow mound at site 2, comprises vertical and bent cooling columns, with polygonal cross sections.

4.9.4 Cross-cutting dyke and mega-pillow facies

The cross-cutting dyke and mega-pillow facies comprises discordant bodies, with a mega-pillow bud at its highest point (**Figure 4.20**). The dykes cross-cut horizontally bedded sediments and are 10-15 m in vertical extent, and 30 cm to 3 m thick. The dykes occur separately from the pillow mounds and have a linear, elongate form, and are dissected by joint fractures perpendicular to the margins. In general, the margins are heavily brecciated, characterised by a carapace of regularly spaced breccia blocks, which also occur within the surrounding sediments. The mega-pillows mark the vertical extent of the dyke, which display radial jointing typical of pillow lobes and in this case, comprise linear or bent and overlapping columns. Mega-pillows are 5-10 m in diameter.

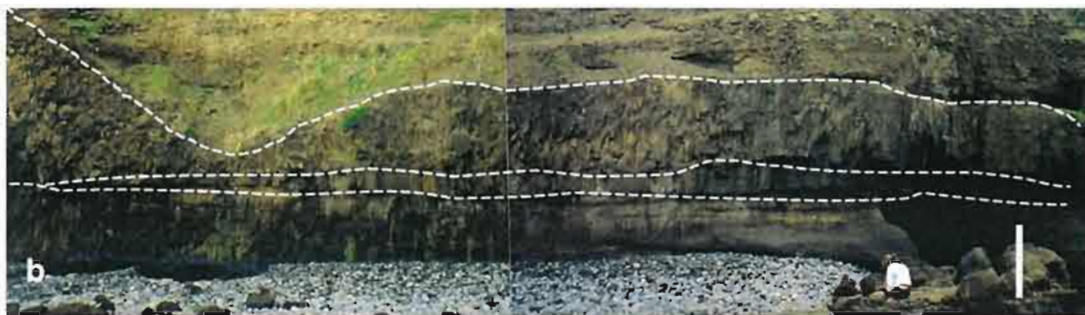


Figure 4.19. The pillow lava and sheet flow facies, (a) thick pillow lava mound at site 2 (5 m scale), (b) thin pillow lava mound at site 3, with basal sheet flow (2.5 m scale), (c) radially jointed pillow lobes with larger lobes towards the base of the pile, and a sheet flow towards the top (5 m scale), (d) detail of basal pillow lobe with rind (30 cm scale).



Figure 4.20. *The feeder dyke and mega-pillow facies, (a) feeder dyke with pillow lobe bud, (b) brecciated part, with joint fractures outlined (hand lens for scale), (c) radial jointing in mega-pillow (2.5 m scale).*

4.9.5 Emplacement

Facies of the coherent lithofacies group intrude and overly bedded sediments. Pillow lavas, and the quenched glassy rims of many examples are diagnostic of the subaqueous emplacement of basaltic lava (McPhie et al, 1993). The various pillow lobe diameters are believed to result from different magma discharge rates, with mega-pillow lobes indicating higher discharge rates than the smaller lobes (Hayward, 1979a). The cross-cutting dykes are interpreted to be intrusive feeders, from which the upper pillow lobe, which mark the vertical extent of the dyke, increased in size. The pillow mounds and feeder dykes contain interstitial sediment in crevices between lobes, and have intruded the clastic sediments, which indicates their formation from extrusion and flowage over the sediment surface, and in the case of mega-pillow atop feeder dykes, form from intrusion into sediment [that may have been water-saturated] (McPhie et al, 1993). This lava emplacement probably took place during the final stages of, or once sedimentation had ceased.

4.10 Discussion

Lithofacies types are a product of a unique set of physical conditions in the depositional environment, and provide a record of transport and deposition processes, rate of material release, bathymetry and the physical nature of the source materials (Cas and Wright, 1987). In this case, constraints can be placed on the eruptive history of the stratovolcano, nature of the depositional environment and the submarine processes that existed on the submerged volcano flanks. Each lithofacies of the Muriwai volcanic succession was derived from a particular set of conditions and thus represents the processes involved in their formation. In volcanic settings, these processes are induced by volcanism, or non-volcanic events such as resedimentation, which initiate sediment transport mechanisms. Volcanic settings characteristically generate high volumes of detritus, which leads to rapid sedimentation rates in the surrounding marine environment, and initiates submarine volcanoclastic transport. Initially volcanoclastic deposits form on the upper flanks, and later become remobilised into other parts of the basin. Resedimentation processes characterise the medial submarine depositional environment, in basins flanking the volcanic centre.

The thinly bedded fine sandstone lithofacies group, and bioturbated pebbly sandstone facies represent background sedimentation. The basal fine-grained and well-bedded sandstone facies record slow accumulation and possibly a period of volcanic quiescence. These sands represent sediments that accumulated before wholesale nearby volcanic activity commenced. The graded character of the sandstone suggests transport by turbidity currents, during which deposition was disturbed with the onset of volcanic activity and volcanoclastic sedimentation. The pebbly sandstones occur immediately underlying the coherent facies and represent rapid sediment

deposition, in debris flows that may be unrelated to volcanic activity or initiated by volcanic-related events such as an earthquake or sector collapse.

The scoriaceous and pumiceous lithofacies represent reworked volcanic debris, derived from one or more explosive eruptions. Volcanic material was initially deposited closer to source, and then later redeposited and transported away from their eruptive source. These facies record submarine resedimentation of volcanoclastics in a series of high particle-concentration turbidity currents. The thickly bedded granule sandstone lithofacies group enclosed in the pumiceous and scoriaceous facies, records transport of material in large volume turbidity currents. The coarse sand and granules and scarceness of large volcanic clasts indicate a change in the source material and in the sediments stored on the upper slopes.

The volcanic conglomerate lithofacies represent resedimentation of lava pebbles, which may be unrelated to eruptive activity. They comprise both well-rounded and angular basalt / andesite pebbles that were initially eroded, reworked and deposited closer to source, and then later remobilised and redeposited. The rounded pebbles probably originated from the displacement of pebble beds. The more angular pebbles underwent less reworking prior to transport. Pebbles and cobbles were resedimented in high-density sediment gravity flows. Volcanic clasts record earlier volcanic eruptions and derivation from a stratovolcano, probably a subaerial volcanic edifice.

The pumice and crystal rich facies contain ragged and angular clasts, which originated from distal pyroclastic fallout. These facies record hydraulic sorting of pyroclasts that occurred during water-settling of recently erupted, crystals and waterlogged pumice. These facies record primary pyroclastic eruptions and fallout from distal explosive volcanism. The coherent lithofacies of pillow lavas and dykes are an indication of primary volcanic activity in an area dominated by volcanoclastic deposition. The coherent facies intrude and overly the clastic sediments, which suggests that lava effusion and intrusion occurred during the final stages of sedimentation. Lava emplacement is locally associated with pillow fragments and hyaloclastite formation. The polymictic breccia facies contains angular pillow fragments and fine-grained glassy clasts derived from a proximal source. The polymictic breccia facies provides evidence of coeval lava emplacement in the quenching and spalling of material from the lava carapace that accumulated at the toe of the advancing lava flow.

Collectively, the lithofacies types of the Muriwai volcanic succession represent a part of a submarine volcanoclastic apron. The distribution of each lithofacies is a reflection of the flank bathymetry, the range of source materials and transport processes in action (Chapter 6).

Chapter 5: The physical properties of coherent and clastic volcanic components

5.1 Introduction

The Muriwai volcanic succession contains major volcanic components including dense basalt / andesite, fine-grained hyaloclastite, and vesicular scoria and pumice clasts. In addition, numerous free crystals occur. The volcanic clasts are a product of a specific set of eruptive conditions. An insight into the eruptive history of these volcanic components, from initial magmatic processes, to eruption and distribution can be evaluated from their physical properties. In this chapter, the physical properties of the four major volcanic clast types are determined from density, modal point counting, XRF analysis (bulk rock geochemistry) and short-wave infra-red (SWIR) spectroscopy. Clast vesicularity can constrain the timing of vesiculation and fragmentation, and magma compositions control eruption styles and volcanic products. In addition, infra-red spectra constrains the alteration and diagenetic history of the volcanic components and enclosing matrix.

The lava and vesicular volcanic clast samples were collected from the coherent lithofacies group, the pumiceous and scoriaceous lithofacies group, the bioturbated pebbly sandstone facies and the polymictic breccia facies. Data is limited due to weathering and alteration. This chapter aims to provide a general impression of the physical properties of representative lava and volcanic clast samples, which are described individually and in table 5.

5.2 Lava

Six lava clasts were analysed, and include six thin sections of coherent lava and lava clasts; geochemical analysis of two coherent lavas; and one used for density testing. Lava clasts make up between 5-75 % of the components of the clastic units. These clasts are porphyritic, with a micro-crystalline or glassy and phenocryst poor groundmass, which is variably altered. Plagioclase phenocrysts are abundant, with fewer pyroxene phenocrysts and iron-oxides (Appendix 5).

TABLE 5. The principle physical properties of the four major volcanic clasts.

| Type (sample no.) | Vesicularity Vol % ¹ | Feldspar modal % ² | Pyroxene modal % ² | Fe-Ti Oxides modal % ² | Composition: wt% SiO ₂ ³ |
|----------------------|------------------------------------|----------------------------------|----------------------------------|--------------------------------------|---|
| Lava coherent (5) | [4]-9 % | 22.2% | 7% | 1.6% | 50.82 |
| Lava (1/7) | - | 35.2% | 9% | 1.2% | - |
| Lava (3/2) | - | 23.2% | 2% | 1.2% | 53.82 |
| Lava clast (1/7A) | - | 15% | 1% | 1% | - |
| Lava clast (1/7B) | - | 49% | 8% | 3% | - |
| Lava clast (1/7C) | - | 20% | 18% | 3% | - |
| Hyaloclastite (1/7E) | - | 16% | 1.2% | 2.2% | 58.76 |
| Hyaloclastite (3/1) | - | - | - | - | 60.09 |
| Pumice (0/1A) | - | 42.8% | 10.2% | 2.8% | 55.74 |
| Pumice (0/1B) | [33]-45 % | 25.4% | 13.2% | 6% | 55.06 |
| Pumice (0/1C) | 13-[24] % | 26% | {5.2%} | 4.4% | - |
| Pumice (3/3C) | - | 18% | 7% | 7% | - |
| Pumice (3/3P) | - | 14% | 1% | 5% | - |
| Scoria (3/3A) | [33]-35 % | 4% | 0.2% | - | 59.61 |
| Scoria (3/2) | [43]-51 % | 5.4% | 0.2% | 1.2% | 59.36 |

1. Determined by method of Houghton and Wilson (1989), Appendix 7.
[] Vesicularity determined using water displacement method.
2. Point counting data, Appendix 5.
- { } May require more points to accurately reflect the pyroxene content.
3. XRF, Appendix 6

Plagioclase phenocrysts range from 15-49 modal %, and are sieve textured, zoned laths or aggregates. Plagioclase compositions fall in the range of andesine (An 42-47) (**Appendix 4**). Pyroxene phenocrysts are relatively sparse (1-18 modal %) and are either ortho- or clino-pyroxene. Lava samples are generally non- to incipiently vesicular (4-9 vol. % vesicles, table 5). Vesicle size is bimodal and unimodal (< 10-50 μm). These vesicles are encrusted with clay minerals (**Appendix 7**). Bulk rock SiO_2 abundances indicate basalt and basaltic andesite compositions (50.83 wt% to 53.82 wt%, Table 5) (**Appendix 6.1**). The range in phenocryst type and abundance in the individual lava clasts suggests a polymict origin.

5.3 Hyaloclastite

Two hyaloclastite clasts were analysed, and include a single thin section, and two geochemical analyses. Angular glassy hyaloclastite clasts occur in the polymictic breccia facies and the bioturbated pebbly sandstone facies. A distinct 2-5 mm thick, white rim comprised of altered phenocrysts, characterises the outer surface of these clasts. The groundmass is fine-grained, micro-crystalline, and glassy with sparse phenocrysts. Phenocrysts comprise feldspar laths (16 modal %) and sparse pyroxene phenocrysts (1.2 modal %) (**Table 1**) (**Appendix 5**). Plagioclase compositions fall in the range of labradorite (An 62) (**Appendix 4**). Bulk rock SiO_2 abundances indicate andesitic compositions (58.76 to 60.09 wt% SiO_2 , Table 5). The fine-grained nature of these clasts suggests they formed by quenching during lava effusion.

5.4 Pumice

Five pumice clasts were analysed, and include five thin sections of both free and cemented clasts, with two clasts used for geochemical analysis for density testing. Pumice clasts comprise between 1-80 % of the clastic units. Pumice occurs in cream and grey, or mingled cream and grey forms, and have variable vesicularity and phenocryst abundances. In general, pumice clasts contain euhedral and broken crystals of plagioclase (Andesine: An 44-54), ortho- and clino-pyroxene, and iron-titanium oxide. Quartz phenocrysts are rare. The grey pumice clasts have streaky domains and / or phenocryst cumulates (**Appendix 4**). Pumice clasts range in vesicularity from incipient to moderate (13-45 vol.% vesicles, Table 5). Vesicles have sub-rounded, irregular and coalesced morphologies, and have irregular shapes where they contact crystals (**Appendix 5.2**). Individual pumice clasts comprise variable or consistent vesicle sizes that range in size from <10 μm to 20 μm (**Appendix 4**). The pumice clasts have variable densities, which reflect vesicle abundance, although finer vesicles have been infilled by secondary mineral causing lower vesicularities (**Appendix 6**). Composition determined by bulk rock SiO_2 , indicate basaltic andesite compositions for the pumice (55.06 and 55.74 wt% SiO_2 , table 5). Although the major element abundances do not reflect the compositions typical of pumice, vesicle size and shape

reflect the properties of a viscous melt. Low SiO₂ contents presumably reflect relatively abundant ferromagnesian crystal phases, such as pyroxene and oxides.

5.5 Scoria

Two scoria clasts were analysed, and include two thin sections of free clasts, geochemical analyses and density determinations. Scoria makes up between < 1-10 % of the clastic components. Scoria clasts are red or black, crystal-poor, and contain high vesicle abundances. In general, the scoria clasts contain euhedral and broken crystals of plagioclase and pyroxene. Phenocrysts are dominated by feldspar (4-5.4 modal %), with plagioclase compositions in the range of labradorite (An 52-62). Scoria clasts vary in vesicularity from poor to moderate (33-51 vol. % vesicles, table 5). Vesicles have well rounded to sub-rounded morphologies and range in size from < 10 µm to 20 µm (**Appendix 4**) (**Appendix 5.2**). Composition determined by bulk rock SiO₂ abundances indicate andesitic compositions for the scoria (16.01 and 16.20 wt% SiO₂, table 5). A minor difference in wt% K₂O may be caused by the depletion of K₂O by surface weathering in NZM3/2. Scoria vesicle shape and abundance are typical scoria derived from basalt / andesite magmas.

5.6 Free Crystals

Free crystals comprise between 5-70 % of the clastic components (**Appendix 4**). Crystals include plagioclase, clino- and ortho- pyroxene, olivine, hornblende, titanomagnetite and quartz. In general, plagioclase and pyroxene crystals are the most abundant, with rare hornblende and olivine. Crystals shapes are euhedral and subhedral, or angular and broken. Euhedral free crystals suggest that they are juvenile fragments, released during explosive eruptions. Broken free crystals suggest they have been weathered from pyroclastic deposits, porphyritic lavas and volcanic clasts.

5.7 Comparison of vesicular clasts

Pumice and scoria clasts conventionally display distinct compositional differences. Pumice is typically understood to comprise silicic compositions, and be derived from a felsic melt. Scoria typically comprises mafic compositions, derived from a low viscosity, basic melt. The term pumice is used for clasts which show coalesced or stretched vesicle morphologies, whereas scoria is used for clasts that have rounded or subrounded vesicle shapes. Differences in vesicle morphology are related to different magma viscosities. However, bulk rock pumice compositions do not reflect the composition of a pumiceous melt due to the abundance of plagioclase, pyroxene and iron-titanium oxide phenocrysts. Minor occurrences of quartz phenocrysts suggest crystallization from a melt that did contain a quantity of silicic magma. The close compositional

difference between the scoria and pumice has implications for eruption and magmatic processes (Chapter 6).

5.8 Diagenesis

The groundmass of individual volcanic clasts and the enclosing matrix, contains hydrated silicate minerals indicative of secondary alteration. Short wave infra-red (SWIR) spectrometry of the clasts and matrix show similar mineralogical features, with major peaks at 1410, 1430, 1910 and 2300 nm (OH, H₂O and FeO wavelengths) (**Appendix 8.1**). These secondary minerals comprise an assemblage or selection of Natrolite, Mordenite, Stilbite, Mesolite, Warikite of the zeolite group, and Saponite, Sauconite, Nontronite, Montmorillonite of the smectite group (**Appendix 8.2**). Minerals such as Nontronite, Natrolite, Mordenite and Montmorillonite can be derived from basaltic glass, and original weathering from a mafic to ultra-mafic protolith (Deer et al, 1992). A potential source for these minerals could have initially been palagonite, an alteration product of basaltic glass (Fisher and Schmincke, 1984). This smectite-zeolite mineralogy is indicative of low temperature diagenesis, away from the influence of high temperature hydrothermal fluids (C. Gifkins, pers. comm. 2003).

5.9 Discussion

Lava and pumice clasts are the dominant volcanic components in the Muriwai volcanic succession, with many free feldspar and pyroxene crystals. Vesicular volcanic components comprise a significant amount of all clastic components and are clear evidence of a history of explosive eruptive activity. The vesicular volcanic clasts are highly heterogenous in crystal content, vesicularity and density. The magma mixing and geochemical complexity known to exist in the subvolcanic magma chambers of stratovolcanoes, is clearly visible in the streaky pumice clasts. However both mafic scoria and felsic pumice can be generated in a single eruption. For example, pumice fragments at Unimak Island, Alaska, contained both rhyodacite and basaltic andesite scoria compositions, indicating the interaction between magmas of different compositions prior to their eruption (Carson, 1998). In addition banded pumice clasts indicate magma mixing, and from its occurrence in Hokkaido, Japan, is known to be a transitional product between pumice and scoria ejection (Iwanaga, 1968).

Coherent lavas and clasts represent a period of effusive eruptive activity. The lavas clasts contain a range of phenocryst abundances. Finely- and coarsely- crystalline clasts suggest multiple eruptive phases, and / or multiple source vents. In addition, large plagioclase phenocrysts in a

groundmass of smaller laths, suggests mixing between two crystal phases. The range of lava types may have been sourced from separate magma chamber storage levels. The subvolcanic magma chambers of stratovolcanoes, receive influxes of variably evolved magmas (Waight et al, 1999). Together, the compositional range of the lavas and volcanic clasts suggest a complex plumbing network existed beneath the stratovolcano.

Particular volcanic settings show distinctive major element abundances (Wilson, 1989). In the Muriwai volcanic succession there is a compositional range from basalt to andesite. Bulk rock geochemistry indicates that the Muriwai volcanic succession represent a medium-K, calc-alkaline magma series for island arc volcanic suites. In addition, each clast type represents a particular compositional field. Lavas are basalt and basaltic-andesite, pumice clasts are basaltic-andesite, and the scoria and hyaloclastite are andesite. Petrological and geochemical work by Wright and Black (1981) on the Waitakere Group, show that basalt to basaltic andesites are the most abundant rock types with local occurrences of dacite. Plagioclase phenocrysts are abundant throughout the Waitakere Group, and are commonly sieve textured, which are typical of calc-alkaline magmatism (Wright and Black, 1981). Discrimination analysis of major elements and relative Nb, Y, Zr and Sr values, reveals that the basalts comprising the Waitakere Group are similar to basalts found in other calc-alkaline suites (Wright and Black, 1981). In addition, the Manukau subgroup shows slight K₂O depletions, relative to the Waipoua and Hukatere subgroups.

The PIMA data reflects the fact that many of the volcanic clasts are not pristine or fresh, with clay and zeolites in the enclosing clastic matrix and infilling vesicles in volcanic clasts. Zeolites are common in volcanoclastic rocks, and together with smectites indicate in situ formation in marine sediments (Fisher and Schmincke, 1984). Low overall matrix clay contents indicate that secondary weathering is negligible (W. Hermann, pers. comm., 2003). The PIMA data shows that coherent and clastic components are chemically related and were derived from a related source. In general, volcanic glass is a prominent component of volcanoclastic sequences and its thermodynamic instability produces specific minerals. Secondary minerals in the clasts and matrix of the Muriwai volcanic succession indicate a predominance of basaltic glass, with a minor component of silicic glass. A major source of the enclosing matrix may have originated from the weathering of altered basalt glass, which produces palagonite, probably from nearby pillow lava mounds on the seafloor. According to Gifkins (2003), this mineralogy reflects low-medium temperatures and moderate to low burial.

Chapter 6: Discussion

6.1 Introduction

Six stratigraphic sections that comprise the Muriwai volcanic succession were studied using a multidisciplinary approach, which included stratigraphic, sedimentological, facies analysis, bulk rock geochemistry, petrography, vesicularity, and short wave infra-red spectra analysis. This well-exposed succession permitted detailed observations of a submarine volcanoclastic deposit, and provides insights into the eruptive and sedimentary processes involved in their formation.

This chapter will synthesise and integrate the information presented in chapters 3, 4 and 5, on the stratigraphy, lithofacies and components of the Muriwai volcanic succession by interpreting the depositional environment, edifice morphology and vent proximity. In addition, interpretations of eruption styles, and a reconstruction of the volcanic architecture including the relationship of the study sites to other volcanic centres in the Waitakere Group.

6.2 The Muriwai volcanic succession

The exposed Muriwai volcanic succession is the eastern flank of a stratovolcano, and comprises a variety of coherent and clastic lithofacies with abrupt vertical and lateral facies changes. The facies are typical of submarine volcanoclastic deposits (Fisher and Schmincke, 1994), and include massive and bedded pumiceous and scoriaceous units, volcanic conglomerates, and coarse granule sandstones. The stratigraphy records the evolution of the source volcano: its eruptive history, growth and destruction, and the interaction of normal marine sedimentary processes.

The basal fine-grained sandstones are evidence of background sedimentation prior to the onset of volcanism, and during periods of quiescence, when the supply of volcanic detritus from the nearby volcanic centre waned. The thick, overlying volcanoclastic sequence records volcanic activity, which contrasts with the quiet marine environment represented by the basal well-bedded sandstones. Pyroclastic fallout layers are evidence of distal volcanism. The marine sediments represent submarine canyons, and possess a u-shaped, eroded relief. The coherent and clastic lithofacies represent canyon fill.

Nearby eruptive activity and down slope resedimentation are recorded by the thick sequence of volcanoclastic sediments and pillow lavas. Frequent small volume, or episodic large volume debris flows, may disperse volcanic detritus in all directions, from the upper, to the lower volcano flanks and basin (Dolozi and Ayres, 1991; Fiske et al, 1998). Domains of bioturbation indicate that regular but intermittent sediment influxes caused sediment instability, and turbulence on the sea floor (Hayward, 1976d). Rapid coarse sedimentation of volcanic detritus and strong currents, inhibited surface grazing biota (Hayward, 1976d).

6.3 Regional Setting

Subduction along the Indian-Pacific plate boundary, gave rise to submarine and island arc volcanic centres, and an adjacent marine basin (Hayward, 1979b). Submarine deposition and island arc volcanism are recorded by the facies at Muriwai. Contemporaneous obduction of the Northland allochthon formed a nearby landmass (Hayward, 1993). Along the length of the Miocene arc, the adjacent marine basin would have received influxes of volcanoclastic detritus, related to eruptive episodes. Eruptive activity from submerged and emergent volcanic centres dotted along the volcanic arc front, led to the growth and progradation of a series of volcanoclastic aprons. A thick volcanic succession of coherent and clastic rocks formed a shelf that bordered the Waitemata basin (**Figure 6.1**) (Hayward, 1977c).

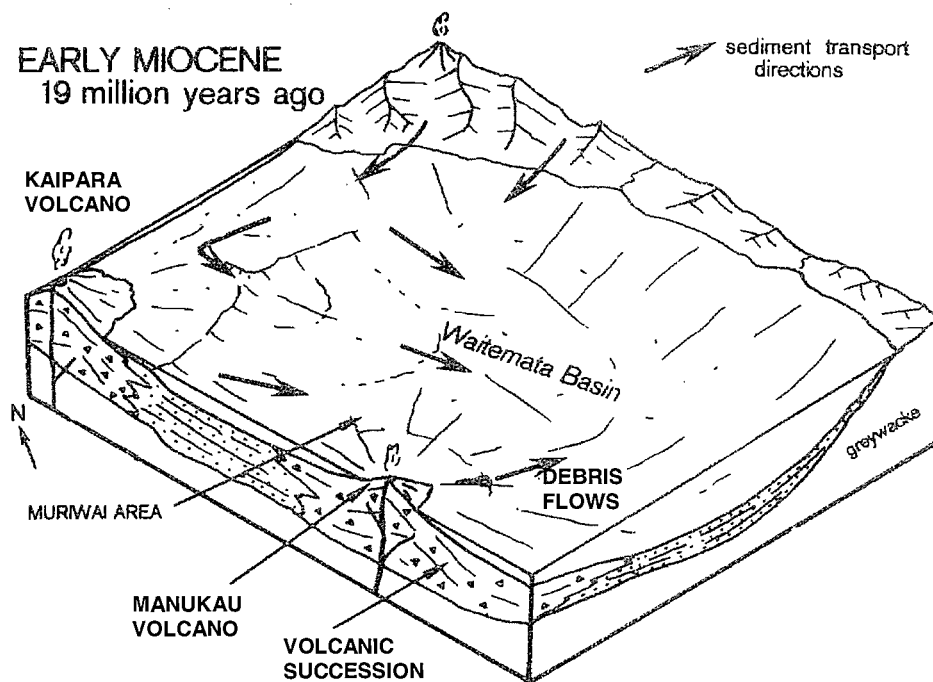


Figure 6.1: *The Manukau and Kaipara volcanic centres, shedding volcanic detritus into the surrounding marine basin (from Hayward, 1979a).*

Submarine canyons and channels flanking the source volcanic edifice, would have acted as dispersal networks for detritus (Gamberi, 2001). Major submarine channels probably separated individual volcanic centres along the arc. For example, in water depths of 3.5-4.5 km, in the Mariana arc, 2 km-wide and 60 km-long submarine channels, separate individual volcanic centres (Hargrove et al, 2001). These sediment pathways, combined with different submarine arc slopes, and prevailing current and wind directions would influence sediment dispersal patterns (Sigurdsson et al, 1980). The adjacent marine basin may have sourced eruptive products from multiple volcanic centres, due to sediment exchange between basins.

6.4 Depositional environment

Pillow lavas, fine-grained marine sediments such as mud-rich and calcareous sandstones, fossils, and bioturbation, constrain a subaqueous depositional setting. Faunal assemblages in the basal thinly bedded and bioturbated pebbly sandstone facies types, suggest a lower to mid bathyal environment, with likely water depths between 1000-3000 m (Hayward, 1976d).

The submarine volcanic succession comprise a range of laterally variable fine- and coarse-grained clastic lithofacies, including thin- and thick- bedded sandstones, conglomerates, pumiceous and scoriaceous units, thin-bedded muddy sandstones, and coherent pillow lavas and intrusions, similar to those observed in other areas (Mueller et al, 1994; Fyffe et al, 1999; Mueller et al, 2000). The bed thickness, and the combination of primary and reworked volcanic facies (eg. pumiceous and scoriaceous facies, and volcanic conglomerate facies) suggest deposition in a medial environment within the volcanoclastic apron. A volcanoclastic apron provides one of the most complete records of volcanic activity (Fisher and Schmincke, 1984). This medial environment differs from the vent facies and distal facies (Lafrance, et al, 2000). The abundance and thickness of volcanoclastic facies, a dominance of resedimented volcanic products, lack of high-temperature hydrothermal alteration and scarcity of coherent facies, which proliferate in vent proximal areas, are typical of medial depositional environments (Cas and Wright, 1987).

Primary pillow lavas and feeder dykes occur at several stratigraphic levels in the Muriwai volcanic succession. The location of the original source vent(s) can be approximated from offshore geophysical anomalies (Davey, 1974). Satellite vents generally occur within 15-18 km from the central vent (Hackett and Houghton, 1989). These relationships suggest that the pillow lavas at Muriwai are associated with the original Manukau volcanic centre, which is located to the west, and are nearby to the Kaipara centre, which occurs to the north west of Muriwai (**Figure 6.1**). Dominant transport directions, inferred from the dip of cross-bedded intervals, indicate that

transport from a western source is likely. In addition, larger and denser clasts, are deposited near source, with sand, granules and pebbles, and vesicular clasts the dominant components at Muriwai. The thickness of the succession, and abundance of clastic components imply that the site formed part of the volcanoclastic apron of one or more stratovolcanoes.

6.5 Source

Stratovolcanoes generally form high-relief cones, so it is likely that the source edifice was emerged above sea level. Subaerial volcanic centres are also inferred to have existed further north (Hayward, 1993). The non-volcanic particles that contributed to the Muriwai volcanic succession such as wood and coral fragments suggest nearby subaerial and shelf environments, with the possibility that the source volcanic edifice was emergent at the time of deposition. Coral colonization indicates water depths of no greater than 90 m (Hayward, 1977b), indicating a shallow water edifice. Wood particles suggest part of the edifice were vegetated, possibly due to a prolonged period of eruptive quiescence. Well-rounded basalt / andesite pebbles suggest fluvial reworking. Localised occurrences of well-rounded, black pebbles suggest derivation from a continental source, and the presence of a nearby landmass (Hayward, 1993).

In addition, the vertical and lateral lithological variability of the Muriwai volcanic succession implies that the upper parts of the edifice consisted of a heterogeneous arrangement of lava flows, and, unconsolidated pyroclastic and autoclastic detritus. Streams may have dissected the steep slopes and sector collapse structures. Clastic deposits are dominantly derived from the reworking of material sourced from proximal areas on the cone. The steep slopes of volcanic cones are inherently unstable and prone to sector collapse events, which may be triggered by subsidence or weakening of the cone structure through hydrothermal activity (van Wyk de Vries et al, 2000), dome growth, explosive eruptions or oversupply of detritus (Gardeweg et al, 1998). The Muriwai volcanic succession records a series of resedimentation events that were probably initiated by mass wasting processes, such as slope failure and slumping on the upper flanks.

The submerged foundations of the volcano would have a different morphology due to the interaction of volcanic and marine processes. The morphology of the submerged parts of the edifice may have consisted of a random arrangement of lavas, epiclastic deposits and pelagic sediments, similar to those occurring on Rumble IV in the Kermadec arc (Wright, 1996). Volcanoclastic deposits are a major part of the edifice construction (Mueller et al, 1994). The thick succession of volcanic sediments at Muriwai indicates that resedimented detritus comprises a significant component of the submerged volcano morphology, this is typical of long-lived edifices (Cas and Wright, 1987). Pillow lava mounds and intrusions provide evidence of satellite

vent eruptions, which may have been scattered on the submerged flanks of the volcano. The arrangement of submarine volcanoclastic deposits created a complex submarine environment around the volcano. The bathymetry may have been comparable to those offshore from Lipari and Vulcano in the Aeolian Arc (Gamberi, 2001), and Myojinsho cone, Japan (Fiske et al, 1998), which comprises a series of radial submarine canyons and channels, separated by depositional highs and levees that extend to the lower flanks and far reaches of the apron.

6.6 Eruption processes

Basaltic andesite pumice and andesitic scoria suggest several phases of nearby explosive eruptions. These volcanic clasts could be the product of strombolian, vulcanian, subplinian or plinian eruption, which commonly occur on stratovolcanoes. The thin pumice- and crystal- rich facies represent distal pyroclastic fallout, probably from a plinian eruption plume. The grey and white pumice, black and red scoria, and crystals collected at Muriwai indicate explosive eruptions. Such pyroclastic eruptions are common in subaerial environments, but have been increasingly recognised in moderate water depths (< 900 m) (Fiske et al, 2001). However the volcanic clasts collected do not have quenched margins and internal jointing observed on subaqueously-erupted clasts (Allen and McPhie, 2000). Episodic eruptions over time, would have produced abundant volcanoclastic detritus, a portion of which is preserved in the Muriwai volcanic succession. Lava flows and hyaloclastite represent effusive eruptive stages. Pillow lava and hyaloclastite form in subaqueous environments. Evidence for older subaerial lavas is apparent in the well-rounded basalt / andesite conglomerate clasts. The lavas are the products of relatively small-scale eruptions, whereas explosive eruptions, were probably on a much larger scale, and generated an abundance of detritus. Contact relationships suggest that volcanoclastic sedimentation and lava eruption were coeval, and probably closely associated with explosive activity. The stratigraphy and facies of the Muriwai volcanic succession record several late stage eruptive phases, including explosive eruptions, which generated abundant volcanoclastic detritus and were punctuated by effusive eruptions.

6.7 Petrogenesis

The lavas and intrusions in the Muriwai volcanic succession are basalts and basaltic andesites, and are typical volcanic products found in the Waitakere Group. They have calc-alkaline affinities, which is characteristic of rocks generated during plate subduction. The basalts represent the most mafic products within the succession at Muriwai. Andesitic scoria clasts have the most evolved compositions. Together these volcanic products represent a fractionation trend,

with the least fractionated products generated by effusive eruptions or intrusions and most fractionated by explosive eruptions. High pumice densities, variable vesicle abundances, zoned plagioclase phenocrysts, and high crystal contents in the pumice clasts, may be related to a complex history of magma petrogenesis, typical of arc volcanoes (eg. Defant et al, 2001). Zoned and sieve-textured plagioclase phenocrysts, in the coherent and clastic volcanic facies, may indicate mixing between old and new magma batches, in which crystals were entrained from an earlier eruptive event (Gamble et al, 1999). Grey basaltic andesite pumice, banded pumice, and black andesitic scoria also suggest complex magma mixing processes. It is possible for magma compositions from arc volcanoes to fluctuate over short time intervals due to crystal fractionation and magma mixing processes (Gamble et al, 1999), therefore data from the Muriwai volcanic succession represents a small part of the history of one or several volcanoes in the Miocene arc.

A range from primitive basalt to andesite compositions, together with clastic and coherent products suggests several eruptive phases. However these different products and compositional types are not necessarily restricted to separate eruptions. It is possible for the simultaneous eruption of basaltic andesite, andesite and dacite (eg. Me-akan volcano, Hokkaido: Wada, 1995). Therefore, these two separate eruptive types may have occurred in close temporal association.

6.8 Transport and deposition

The volcanoclastic facies at Muriwai were deposited from water-settled pyroclastic fallout, and water-supported sediment gravity flows and current-induced processes. Erosion, transport and deposition in the marine environment surrounding stratovolcanoes, is complex due to the interaction of volcanic and non-volcanic processes. Volcanic clasts are sub-angular or rounded, which indicates that they underwent reworking after eruption. Rounded lava pebbles indicate fluvial reworking over a long time period. The dominance of vesiculated scoria and pumice clasts, together with a crystal-rich matrix at Muriwai, suggests resedimentation from unconsolidated and unstable pyroclastic deposits on the upper flanks (Schneider et al, 2001). Gravity-induced rather than primary volcanic processes control resedimentation of volcanoclastic sediments at medial distances from the volcanic centre (Fiske et al, 1998). Transport and deposition of this detritus could have occurred synchronous with, or post-dated eruption. Scattered lava boulders and rip-up clasts indicate the shear strength of separate flow events. Volcanic-related processes control resedimentation of clastic detritus surrounding the arc, with abundant volcanic debris shed into the adjacent Waitemata Basin. There is no evidence of hot state of emplacement of the clasts, such as welding, eutaxitic texture, or plastic deformation, as produced in pyroclastic flows (Sparks et al, 1999).

Common bioturbation and mud in the basal fine-grained, bedded sandstones suggest deposition occurred in a normally quiet marine environment. Thin, well-sorted layers, of ragged pumice and euhedral and broken crystals, suggest distal primary pyroclastic fallout and settling in the water column. These explosive eruptions may have resulted in the accumulation of primary pyroclastic deposits on the sea floor, which were later resedimented. Resedimentation may have been initiated by intermittent rock falls, slumps and sector collapse of volcanic detritus, from around the source vent (Dolozi and Ayres, 1991). The thick volcanoclastic deposits, pillow lavas, and overlying thinly bedded marine sands, indicate that the influx of large volumes of volcanic detritus into the basin, interrupted background sedimentation and the slow accumulation of fines. Stratification suggests volcanic material was shed in pulses from the source. Catastrophic influxes of pyroclastic detritus may have induced mass wasting processes (c.f. Mueller and Corcoran, 1998). Stacking of thick, normally graded granule-sand beds, suggest deposition by successive turbidity currents. Deposition from normal current-induced processes was rare, however a mega-ripple suggests localised current activity occurred (c.f. Stanley and Taylor, 1977).

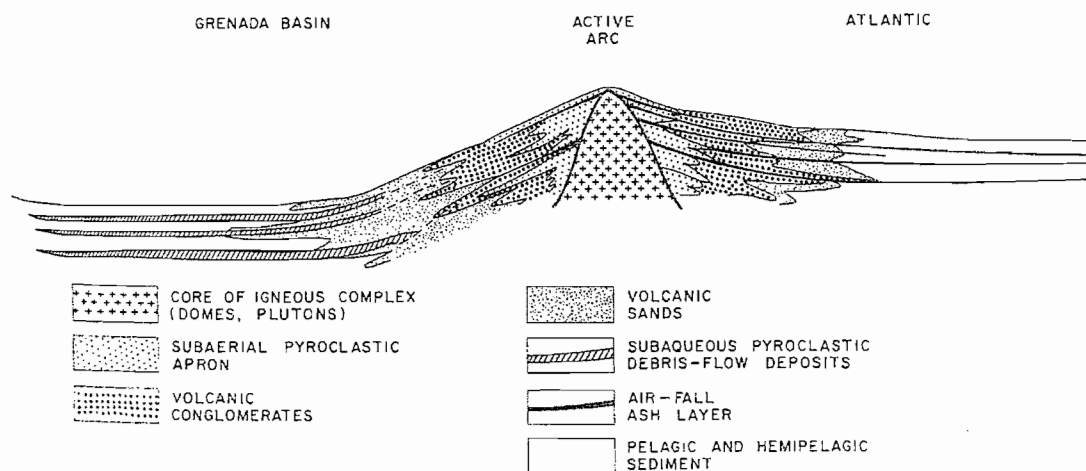


Figure 6.2. Cross section of the Lesser Antilles volcanic arc, with the flanking apron and organisation of volcanic detritus (from Sigurdsson et al, 1980).

The transport of volcanoclastic detritus into the submarine environment produces a constructional feature (apron) at the foot of, and encircling the volcanic edifice or flanking the arc (e.g. the Lesser Antilles volcanic arc: **Figure 6.2**). Arc apron geometry offshore from modern volcanic islands is extensive, producing major depocentres in 500-3600 m water depths (Ollier et al, 1998). Normal deep sea fans are large-scale features that develop seaward of a major sediment source, and are characterised by one or more feeder channels, levees, slump scars and debris flow

deposits (Stow, 1985). Volcaniclastic aprons can receive sediment from multiple sources including sediment related to volcanic activity, whereas submarine fans receive sediment from a single source (Stow, 1985). The volcaniclastic apron preserves rapid vertical and lateral facies changes, which are not comparable to typical submarine fans (Carey and Sigurdsson, 1984), with an intricate arrangement of primary volcanic, resedimented and volcanogenic facies, (Gamberi, 2001). However the resedimentation processes that operate on deep sea fans also operate on the clastic apron of marine stratovolcanoes, where volcaniclastic detritus is remobilised and deposited by normal marine sedimentary processes.

6.9 Facies architecture

The Muriwai volcanic succession once formed part of a dynamic island arc / basin setting. The facies architecture records the eastern part of a volcaniclastic apron, which is now exposed at Muriwai. The island arc was characterised by several large stratovolcanoes, and a single shield volcano, with smaller scattered vents. The facies architecture reflects compositionally variable effusive and explosive volcanism, which episodically generated lavas and volcanic clasts. The facies architecture reflects the effusion of sea floor pillow lavas, and resedimentation of volcanic detritus on the submarine flanks of the edifice. Clastic detritus was remobilised down the flanks into the basin, and accumulated on a volcaniclastic apron as a result of volcanic, and non-volcanic processes. The volcaniclastic apron formed as a result of eruptions, stages of edifice growth, and erosion. Erosion of the edifice may reflect sector collapse or slumping of un-consolidated volcanic detritus (Deplus et al, 2001). The apron probably developed as several overlapping and coalescing lobes. Volcaniclastic canyon-fill in the basal parts of the succession, records apron progradation, which probably occurred during the later stages of the volcano's history, with peripheral lava eruptions. Satellite vent eruptions probably occurred at a late stage in the volcanic history. This effusive eruptive activity was coeval with volcanic sedimentation. Coeval volcanism and sedimentation is a common feature of island arcs (Mueller et al, 2000).

The Muriwai volcanic succession is likely to be associated with a nearby volcanic centre, either the Manukau centre to the west and south west, or the Kaipara centre. Dates from Maori Bay pillow lavas (16.7-17.9 Ma) are within the period of eruptive activity that has been determined for the Manukau (23-15.5 Ma), and Kaipara centres (23-16 Ma) (Hayward et al, 2001). Satellite vent eruptions could have happened from either vent, although the location of the Manukau centre is more proximal (Hackett and Houghton, 1989). During the course of the eruptive history, these two volcanoes would generate large volumes of volcaniclastic detritus. Detritus from the Manukau and Kaipara stratovolcanoes would be deposited in extensive submarine volcaniclastic aprons. The deposit facies architecture at Muriwai suggests the source volcano was characterised

by explosive eruptions, with peripheral lava effusion on the flanks. The volcano edifice was eroded and degraded. The physical appearance of the Manukau centre many have been comparable to Lipari and Vulcano in the Aeolian Arc, or Stromboli, with a crest exposed above sea level and an extensive submarine clastic apron (c.f. Kokelaar and Romagnoli, 1995).

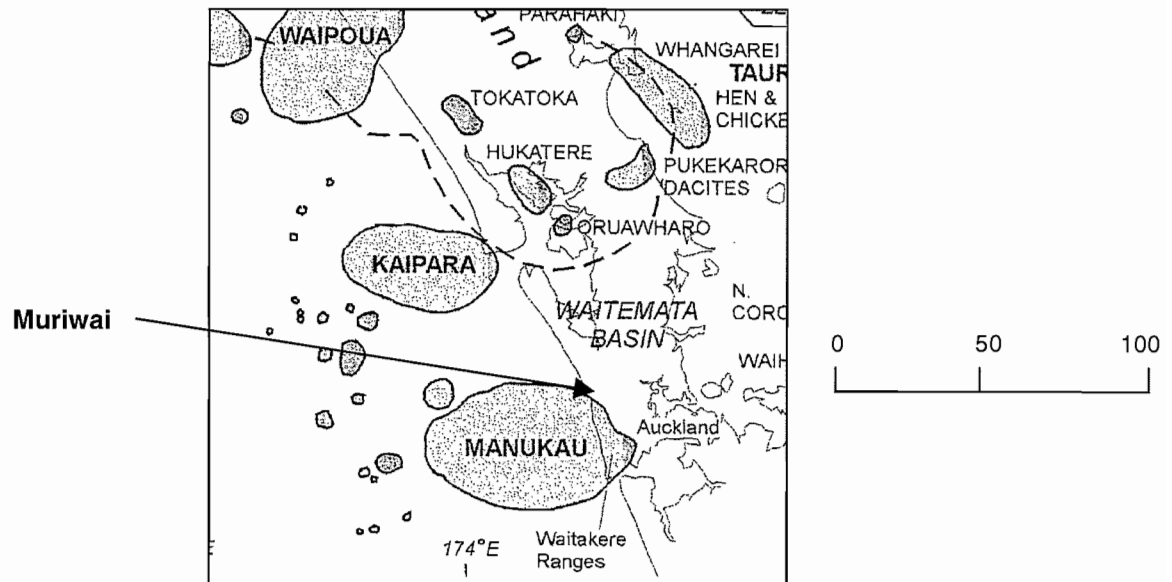


Figure 6.3. *The location of the Manukau and Kaipara centres in relation to Muriwai (from Hayward et al, 2001).*

Stratovolcanoes are typically characterised by several eruptive stages (Gomez-Tuena and Carrasco-Nunez, 2000). The evolution of the Muriwai volcanic centre is similar to that represented by a submarine volcano-sedimentary sequence, in the Kermadec group (Raoul Island), which initially formed a stratovolcano, with reef colonization, followed by flank collapse and satellite vent eruptions, then cessation of volcanism and subsidence (Brook, 1998). If the Manukau and Kaipara volcanoes initially formed in the subaqueous environment, the resulting edifice grew and eventually emerged above sea level. Thus a complex evolutionary history is implied for the Miocene source volcanoes at Muriwai. As the edifice grew to shallower depths (from 1500-1000 m: Pressure Compensation Level, Fisher 1984) decreasing pressure would have increased the explosivity of eruptions. During the final subaerial stages, the dimensions of the clastic apron increased, due to the abundance of pyroclastic detritus (Fisher and Schmincke, 1984).

Chapter 7: Summary

7.1 Conclusions

The Muriwai volcanic succession represents the eastern volcanoclastic apron of the offshore / island stratovolcanoes in the Miocene Northland volcanic Arc. The most likely source is the Manukau volcano, with components from the Kaipara volcano immediately to the north also likely. It records the submarine medial facies of largely resedimented pyroclastic deposits, as well as primary pyroclastic fallout and in situ lavas from satellite vents. Stratigraphic relationships, lithofacies analysis and componentry studies of the clastic and coherent components of the succession, can be used to reconstruct the volcanic setting and eruptive history.

Six major lithofacies were identified in the Muriwai volcanic succession. The first, thinly bedded fine sandstone lithofacies group comprise the basal part of the succession, and represent background sedimentation from turbidity currents presumably sourced from the Northland Allochthon prior to the major onset of volcanism. Thin pumice and crystal rich facies are interbedded with the thinly bedded fine sandstone lithofacies and the pumiceous and scoriaceous lithofacies group, and record water-settled fallout from explosive eruptions that interrupted background sedimentation. A thick volcanoclastic sequence comprise either pumiceous and scoriaceous lithofacies group, volcanic conglomerate lithofacies group or thickly bedded granule sandstone lithofacies group. The coherent lithofacies group (pillow lavas and dykes) occur at various intervals within the volcanoclastic facies. A polymictic breccia facies of angular glassy clasts, occurs at the toe of the Maori Bay pillow lava mound, and is interpreted to be hyaloclastite and pillow lava talus.

The volcanoclastic facies record resedimentation in sediment gravity flows of more proximal volcanoclastic deposits. Sand, granules and pebbles dominate the clastic components, and coarser material was presumably deposited closer to source. Submarine canyons have eroded into basal bedded sandstone, which have been filled by the volcanoclastic and coherent facies. Hence the volcanoclastic facies represent canyon fill and overbank facies, probably associated with stages of

voluminous pyroclastic eruptions and edifice destruction. The growth of these constructional aprons by way of resedimentation processes, are analogous to the sediment transport processes that operate on deep sea fans. The interlayering of volcanoclastic sediments with pillow lavas, and crosscutting dykes, indicates that volcanism and sedimentation were coeval.

Stratovolcanoes generate abundant volcanoclastic detritus, derived from explosive eruptions and erosion. Scoria, pumice and free crystals were derived from explosive eruptions. Rounded lava clasts suggest reworking in a fluvial setting. In situ pillow lavas and intrusions are direct evidence of effusive eruption stages. Bulk rock geochemistry defines the volcanic succession as a medium-K, calc-alkaline suite, characteristic of arc volcanism. Representative sampling suggests each clast represents a distinct composition. Lavas are basalt to basaltic andesite, pumice is andesite, and hyaloclastite and scoria are andesitic. These chemical variations suggest multiple eruptive events and varying degrees of fractionation.

Well-rounded conglomerate pebbles, wood particles, and coral fragments suggest that the source edifice was largely subaerial, with a bordering coral reef. The change in stratigraphy between redeposition of pyroclastic deposits and rounded lava clasts suggest that volcanism was interspersed with periods of eruptive quiescence, edifice degradation and subsidence, and that volcanism from the source volcano changed from dominantly effusive to explosive, with minor effusions from satellite vents.

The Muriwai volcanic succession provides an excellent example of a submarine medial volcanoclastic apron. The results of this thesis have established a stratigraphic framework to interpret the deposits and physical processes in the submarine environment of stratovolcanoes. In addition, knowledge of submarine processes gained from this work has relevance to the submarine setting of other marine volcanoes, such as seamounts or shield volcanoes.

7.2 Recommendations for further work

- K-Ar dating, to provide a chronostratigraphy of volcanic clasts in the Muriwai volcanic succession, would better characterise the eruptive history and constrain the eruptive sequence and timing of sedimentation events.
- Characterise the crystal components to constrain whether the free crystals show a compositional evolutionary trend, in relation to explosive eruptive activity.
- Detailed pyroclastic and compositional studies on 30-50 pumice and scoria clasts, including vesicularity and XRF, to compare with the properties of other vesicular volcanic clasts.
- Characterise the properties of the grey and white pumice, using back-scatter imaging of vesicle morphologies, for comparison with pumice generated from other stratovolcanoes, to enhance understandings of the fractionation and vesiculation processes at island arcs.
- Micro-probe work on the groundmass of the lavas, to better understand melt compositions.
- Research into magma petrogenesis of the source volcanoes, through detailed petrographic and mineralogical analysis, including trace element analysis and inclusions, to form a dataset of arc petrogenesis, and how that relates to separate eruptive phases of lava and pyroclasts.
- Relate the Muriwai volcanic succession to nearby volcanic deposits, such as the Piha Formation, to constrain the broad stratigraphy and lithofacies comprising the eastern flank of the Miocene apron and compare with similar deposits elsewhere.

- Cas, R. A. F. and J. Wright (1987). Volcanic Successions, Modern and Ancient. London, Allen and Unwin Ltd.
- Cole, J. W. (1986). Distribution and tectonic setting of Late Cenozoic volcanism in New Zealand. Late Cenozoic volcanism in New Zealand. I. E. M. Smith, The Royal Society of New Zealand. **23**: 7-20.
- Davey, F. J. (1974). "Magnetic anomalies off the west coast of Northland, New Zealand." Journal of the Royal Society of New Zealand **4**: 203-216.
- Defant, M. J., S. Sherman, R. C. Maury, H. Bellon, J. de Boer, J. Davidson, P. Kapezhinskis. (2001). "The geology, petrology and petrogenesis of Saba Island, Lesser Antilles." Journal of Volcanology and Geothermal Research **107**(1-3): 87-111.
- Deplus, C., A. Le Friant, G. Boudon, J. C. Komorowski, B. Villemant, C. Harford, J. Segoufin, J. L. Cheminee. (2001). "Submarine evidence for large-scale debris avalanches in the Lesser Antilles Arc." Earth and Planetary Science Letters **192**(2): 145-157.
- Dolozzi, M. B. and L. D. Ayers (1991). "Early Proterozoic, basaltic andesite tuff-breccia: downslope, subaqueous mass transport of phreatomagmatically-generated tephra." Bulletin of Volcanology **53**: 477-495.
- Fisher, R. V. (1984). Submarine volcanoclastic rocks. Marginal Basin Geology, Volcanic and associated sedimentary and tectonic processes in modern and ancient marginal basins. B. P. Kokelaar and M. F. Howells. Oxford-London-Edinburgh-Boston-Palo Alto-Melbourne, Blackwell Scientific Publications: 5-27.
- Fisher, R. V. and H. U. Schmincke (1984). Pyroclastic Rocks. Berlin-Heidelberg-New York-Tokyo, Springer-Verlag.
- Fisher, R. V. and H. U. Schmincke (1994). Volcanoclastic Sediment Transport and Deposition. Sediment transport and Depositional Processes. K. Pye. Cambridge, Blackwell Scientific Publications: 351-388.
- Fiske, R. S. and T. Matsuda (1964). "Submarine Equivalents of Ash Flows in the Tokiwa Formation, Japan." American Journal of Science **262**(1-5): 76-106.
- Fiske, R. S., K. V. Cashman, A. Shibata, K. Watanabe. (1998). "Tephra dispersal from Myojinsho, Japan, during its shallow submarine eruption of 1952-1953." Bulletin of Volcanology **59**: 262-275.
- Fiske, R. S., J. Naka, K. Iizasa, M. Yuasa, A. Klaus, (2001). "Submarine silicic caldera at the front of the Izu-Bonin Arc, Japan; voluminous seafloor eruptions of rhyolite pumice." Geological Society of America Bulletin **113**(7): 813-824.
- Fyffe, L. R., R. K. Pickerill, P. Stringer,. (1999). "Stratigraphy, sedimentology and structure of the Oak Bay and Waweig formations, Mascarene Basin; implications for the paleotectonic evolution of southwestern New Brunswick." Atlantic Geology **35**(1): 59-84.
- Gamberi, F. (2001). "Volcanic facies associations in a modern volcanoclastic apron (Lipari and Vulcano offshore, Aeolian Island Arc)." Bulletin of Volcanology **63**(4): 264-273.

- Gamble, J. A., C. P. Wood, R. C. Price, I. E. M. Smith, R. B. Stewart, T. Waight. (1999). "A fifty year perspective of magmatic evolution on Ruapehu Volcano, New Zealand: verification of open system behaviour in an arc volcano." Earth and Planetary Science Letters **170**(3): 301-314.
- Gardeweg, M. C., R. S. J. Sparks, S. J. Matthews. (1998). "Evolution of Lascar Volcano, northern Chile." Journal of the Geological Society of London **155**(1): 89-104.
- Gifkins, C. C. (2001). Submarine volcanism and alteration in the Cambrian, northern Central Volcanic Complex, western Tasmania. Australia, University of Tasmania.
- Gomez-Tuena, A. and G. Carrasco-Nunez (2000). "Cerro Grande Volcano; the evolution of a Miocene stratocone in the early Trans-Mexican volcanic belt." Tectonophysics **318**(1-4): 249-280.
- Gorsline, D. S. (1984). A review of fine-grained sediment origins, characteristics, transport and deposition. Fine-grained sediments. D. A. V. Stow and D. J. W. Piper. Oxford, Blackwell: 17-34.
- Hackett, W. R. and B. F. Houghton (1989). "A facies model for a Quaternary andesitic composite volcano: Ruapehu, New Zealand." Bulletin of Volcanology **51**: 51-68.
- Hargrove, U. S., R. J. Stern, S. Bloomer, M. I. Leybourne, M. Edwards, N. Becker. (2001). "Results of new high-resolution bathymetric and back-scatter sonar imaging and dredging of the Mariana arc and back-arc system." Abstracts with Programs - Geological Society of America **33**(6): 398.
- Hayward, B. W. (1975). Lower Miocene geology of the Waitakere Hills, West Auckland, with emphasis on the paleontology. New Zealand, University of Auckland.
- Hayward, B. W. (1976a). "Lower Miocene Geology and Sedimentary History of the Muriwai - Te Wāhoroa Coastline, North Auckland, New Zealand." N.Z. Journal of Geology and Geophysics **19**(5): 639-662.
- Hayward, B. W. (1976b). "Lower Miocene Stratigraphy and Structure of the Waitakere Ranges and The Waitakere Group (new)." N.Z. Journal of Geology and Geophysics **19**(6): 871-895.
- Hayward, B. W. (1976c). "Macropaleontology and Paleocology of the Waitakere Group, (lower Miocene) Waitakere Hills, Auckland." Tane (Auckland University Field Club, Journal), Auckland, New Zealand. **22**: 177-206.
- Hayward, B. W. (1976d). "Lower Miocene bathyal and submarine canyon ichnocoenoses from Northland, New Zealand." Lethaia **9**: 149-161.
- Hayward, B. W. (1977a). "Lower Miocene Polychaetes from the Waitakere Ranges, North Auckland, New Zealand." Journal of the Royal Society of New Zealand **7**(1): 5-16.
- Hayward, B. W. (1977b). "Lower Miocene Corals from the Waitakere Ranges, North Auckland, New Zealand." Journal of the Royal Society of New Zealand **7**(1): 99-111.
- Hayward, B. W. (1977c). "Miocene Volcanic Centres of the Waitakere Ranges, North Auckland, New Zealand." Journal of the Royal Society of New Zealand **7**(2): 123-141.
- Hayward, B. W. (1979a). Ancient undersea volcanoes: a guide to the geological formations at Muriwai, West Auckland, The Geological Society of New Zealand.

- Hayward, B. W. (1979b). "Eruptive History of the Early to Mid Miocene Waitakere Volcanic Arc, and Palaeogeography of the Waitemata Basin, Northern New Zealand." Journal of the Royal Society of New Zealand **9**(3): 297-320.
- Hayward, B. W. (1979c). "An Altonian, deep-water, fossil fauna from the eastern Waitakere Ranges, Auckland." Tane (Auckland University Field Club, Journal). Auckland, New Zealand. **25**: 209-217.
- Hayward, B. W. (1983). Sheet Q11 Waitakere. Geological map of New Zealand 1:50 000. Wellington, New Zealand Department of Scientific and Industrial Research.
- Hayward, B. W. (1993). The Tempestuous 10 Million Year Life of a Double Arc and Intra-arc Basin - New Zealand's Northland Basin in the Early Miocene. South Pacific Sedimentary Basins. P. F. Ballance. Amsterdam-London-New York-Tokyo, Elsevier. **2**: 113-142.
- Hayward, B. W. and M. A. Buzas (1979). "Taxonomy and Paleoecology of Early Miocene Benthic Foraminifera of Northern New Zealand and the North Tasman Sea." Smithsonian Contributions to Paleobiology **36**: 1-33.
- Hayward, B. W., P. M. Black, I. E. M. Smith, P. F. Ballance, T. Itaya, M. Doi, M. Takagi, S. Bergman, C. J. Adams, R. H. Herzer, D. J. Robertson. (2001). "K-Ar ages of early Miocene arc-type volcanoes in northern New Zealand." New Zealand Journal of Geology and Geophysics **44**: 285-311.
- Hochstetter, F. v. (1864). "Geologie von Neu-Seeland. Beitrage zur Geologie der Provinzen Auckland und Nelson." Novara-Expedition, Geologie Theil **1**(1): 274 p.
- Houghton, B. F. and C. J. N. Wilson (1989). "A vesicularity index for pyroclastic rocks." Bulletin of Volcanology **51**(6): 451-462.
- Hutton, F. W. (1870). "On the geology of the North Head of the Manukau Harbour." Transactions of the New Zealand Institute **2**: 161.
- Iwagana, M. (1968). "Petrogenesis of banded pumices from some volcanoes in Hokkaido, Japan." Journal of the Japanese Association of Mineralogists, Petrologists and Economic Geologists **59**(4): 125-142.
- Kamp, P. J. J. (1984). "Neogene and Quaternary extension and geometry of the subducted Pacific plate beneath North Island, N. Z.: implications for Kaikoura tectonics." Tectonophysics **108**: 241-266.
- Kear, D. (1994). "A "least complex" dynamic model for late Cenozoic volcanism in the North Island, New Zealand." New Zealand Journal of Geology and Geophysics **37**: 223-236.
- Kokelaar, P. and C. Romagnoli (1995). "Sector Collapse, Sedimentation and Clast Population Evolution at an Active Island-Arc Volcano - Stromboli, Italy." Bulletin of Volcanology **57**(4): 240-262.
- Lafrance, B., W. Mueller, Daigneault, R, Dupras, N. (2000). "Evolution of a submerged composite arc volcano; volcanology and geochemistry of the Noronnetal volcanic complex, Abitibi greenstone belt, Quebec, Canada." Precambrian Research **101**(2-4): 277-311.
- Lowe, D. R. (1982). "Sediment Gravity Flows: II. Depositional Models with special reference to the deposits of high density turbidity currents." Journal of Sedimentary Petrology **52**(1): 279-297.

- McBirney, A. R. (1973). "Factors Governing the Intensity of Explosive Andesitic Eruptions." Bulletin Volcanologique 37: 443-453.
- McPhie, J., R. L. Allen, M. Doyle. (1993). Volcanic Textures. University of Tasmania, Hobart, Centre for Ore Deposit and Exploration Studies.
- Mueller, W., E. H. Chown, R. Potvin,. (1994). "Substorm wave base hydroclastic deposits in the Archean Lac des Vents volcanic complex, Abitibi Belt, Canada." Journal of Volcanology and Geothermal Research 60(3-4): 273-300.
- Mueller, W. and P. L. Corcoran (1998). "Late-orogenic basins in the Archaean Superior Province, Canada; characteristics and interferences." Sedimentary Geology 120(1-4): 177-203.
- Mueller, W., A. A. Garde, H. Stendal. (2000). "Shallow-water eruption-fed, mafic pyroclastic deposits along a Paleoproterozoic coastline; Kangerluluk volcano-sedimentary sequence, Southeast Greenland." Precambrian Research 101(2-4): 163-192.
- Ollier, G., P. Cochonat, J. F. Lenat, P. Labazuy. (1998). "Deep-sea volcanoclastic sedimentary systems: an example from La Fournaise volcano, Reunion Island, Indian Ocean." Sedimentology 45: 293-330.
- Powell, A. W. (1935). "Tertiary Mollusca from Motutara, West Coast, Auckland." Rec. Auck. Mus. i: 327-340.
- Schneider, J. L., A. Le Ruyet, F. Chanier, C. Buret, J. Ferriere, J. N. Proust, J. B. Rosseel,. (2001). "Primary or secondary distalvolcanoclastic turbidites: how to make the distinction? An example from the Miocene of New Zealand (Mahia Peninsula, North Island)." Sedimentary Geology 145(1-2): 1-22.
- Searle, E. J. (1944). "Geology of the southern Waitakere Hills Region, West of Auckland City." Transactions of the Royal Society of New Zealand 74(1): 49-70.
- Sigurdsson, H., R. S. J. Sparks, S. N Carey, T. C. Huang. (1980). "Volcanogenic sedimentation in the Lesser Antilles Arc." Journal of Geology 88: 523-540.
- Smith, S. P. (1881). "On some Indications of Changes of Level of the Coastline in the Northern Part of the North Island." Transactions of the New Zealand Institute xiii: 398-410.
- Smith, I. E. M., Ed. (1986). Late Cenozoic Volcanism in New Zealand, The Royal Society of New Zealand.
- Smith, G. A. and R. D. Smith (1985). "Specific Gravity Characteristics of Recent Volcanoclastic Sediment: Implications for Sorting and Grain Size Analysis." Journal of Geology 93(5): 619-622.
- Sparks, R. S. J., S. R. Tait, Y. Yanev, (1999). "Dense welding caused by volatile resorption." Journal of the Geological Society of London 156(2): 217-225.
- Stanley, D. J. and P. T. Taylor (1977). "Sediment Transport down a seamount flank by a combined current and gravity process." Marine Geology 23: 77-88.
- Stow, D. A. V. (1985). Deep-sea clastics: where are we and where are we going? Sedimentology: recent developments and applied aspects. P. J. Brenchley and B. P. J. Williams. Oxford, Blackwell. 18.

- Stow, D. A. V. (1994). Deep sea processes of sediment transport and deposition. Sediment Transport and Deposition. K. Pye. Cambridge, Blackwell Scientific Publications: 257-291.
- Taylor, N. H. (1927). "Pumiceous Silts in the Waitakere Ranges, Auckland." N. Z. Journ. Sc. and Techn. ix: 166-167.
- van Wyk de Vries, B., N. Kerle, D. Petley,. (2000). "Sector collapse forming at Casita Volcano, Nicaragua." Geology 28(2): 167-170.
- Wada, K. (1995). "Fractal structure of heterogeneous ejecta from the Me-akan Volcano, eastern Hokkaido, Japan; implications for mixing mechanism in a volcanic conduit." Journal of Volcanology and Geothermal Research 66(1-4): 69-79.
- Waight, T. E., R. C. Price, R. B. Stewart, I. E. M. Smith, J. Gamble. (1999). "Stratigraphy and geochemistry of the Turoa area, with implications for andesite petrogenesis at Mt Ruapehu, Taupo Volcanic Zone, New Zealand." New Zealand Journal of Geology and Geophysics 42(4): 513-532.
- Walker, G. P. L. (1975). "Generalized facies models for resedimented conglomerates of turbidite association." Geological Society of America Bulletin 86: 737-748.
- Wison, M. (1989). Igneous Petrogenesis. London, Unwin Hyman.
- Wright, A. C. and P. M. Black (1981). "Petrology and geochemistry of the Waitakere Group, North Auckland, New Zealand." New Zealand Journal of Geology and Geophysics 24: 155-165.
- Wright, I. C. (1996). "Volcaniclastic processes on modern submarine arc stratovolcanoes: Sidescan and photographic evidence from the Rumble IV and V volcanoes, southern Kermadec Arc (SW Pacific)." Marine Geology 136(1-2): 21-39.
- Yamagishi, H. (1985). "Growth of pillow lobes - Evidence from pillow lavas of Hokkaido, Japan, and North Island, New Zealand." Geology 13: 499-502.

APPENDIX 1

Literature Review

**Submarine volcanic deposits derived from stratovolcanoes:
clast-forming processes, transport mechanisms,
and facies architecture.**

Emma Mathews (BSc)

A literature review submitted in partial fulfilment of the requirements of the Degree
of Bachelor of Science with Honours



University of Tasmania



Centre for Ore Deposit Research
(CODES)

School of Earth Sciences

ABSTRACT

The submarine deposits of submerged to emergent stratovolcano edifices have distinctive vertical and lateral facies distributions. Primary pillow lavas and volcanoclastic debris are interbedded with fossiliferous marine sediments. Characteristically, large volumes of clastic detritus are generated by stratovolcanoes, which are deposited on a submerged volcanoclastic apron flanking the volcanic arc. Eruption style and fragmentation, edifice growth and destruction, and transport and deposition mechanisms control volcano morphology and lithofacies types. Explosive submarine volcanism is poorly understood due to inaccessibility, but fragmentation and eruption styles are modified by hydrostatic pressure. Changes in dominantly effusive to dominantly explosive eruptions as edifice height increases, effects the clastic to coherent ratio of ensuing deposits. Primary volcanic transport and sedimentary resedimentation mechanisms disperse detritus away from the source vent. The facies architecture and distribution of primary pyroclastic, resedimented volcanoclastic and volcanogenic sedimentary facies types provides a record of the transportation and depositional processes, and eruption environment. Seafloor exploration of modern stratovolcanoes combined with facies analysis of well exposed ancient successions are necessary to better understand the processes and products of submarine stratovolcanoes. Current understanding of the processes, deposits and facies architecture of submarine to subaerial arc stratovolcanoes are reviewed in this work.

CONTENTS:

| | |
|--|--------|
| Abstract | i |
| Contents..... | ii |
| Tables and Figures | iii |
| INTRODUCTION | 1 |
| CHAPTER 1: THE SETTING OF SUBMARINE STRATOVOLCANOES | 3 |
| Tectonic Setting..... | 3 |
| Basin Environment and Sedimentation..... | 4 |
| Arc-Stratovolcano Morphology | 5 |
| Submarine Deposits and Lithofacies types | 7 |
| CHAPTER 2: CLAST-FORMING PROCESSES AND PRODUCTS | 10 |
| Explosive Fragmentation..... | 10 |
| Non-explosive Fragmentation | 14 |
| Volcanic Products | 15 |
| CHAPTER 3: TRANSPORT AND DEPOSITION MECHANISMS | 17 |
| Resedimentation mechanisms | 19 |
| Primary volcanic transport mechanisms | 23 |
| CHAPTER 4: THE FACIES ARCHITECTURE OF MODERN AND ANCIENT DEPOSITS | 27 |
| Modern environments | 28 |
| Ancient Successions | 29 |
| DISCUSSION | 32 |
| REFERENCES | 33 |

TABLES AND FIGURES:

pages

| | | |
|--------------------|---|----|
| Table 1: | Facies associations and deposit types | 6 |
| Figure 1.1: | Tectonic landforms at a convergent plate margin | 3 |
| Figure 1.2: | The production and transport of sediments from a subaerial arc..... | 4 |
| Figure 1.3: | The production and transport of sediments from a submerged arc..... | 5 |
| Figure 1.4: | Proximal, medial and distal facies | 7 |
| Figure 1.5: | Growth stages of an island volcano | 8 |
| Figure 2.1: | Major clast-forming processes in relation to water depth..... | 11 |
| Figure 2.2: | Classification of subaerial eruption styles | 12 |
| Figure 3.1: | Transport and deposition on a submarine stratovolcano | 17 |
| Figure 3.2: | Classification of background resedimentation..... | 19 |
| Figure 3.3: | Sediment gravity flow classification | 20 |
| Figure 3.4: | Fallout from a deep submarine eruption | 24 |
| Figure 3.5: | Subaqueous pyroclastic flows..... | 25 |
| Figure 4.1: | Facies model of a marine stratovolcano | 27 |
| Figure 4.2: | The Nayoka and Dokonavato cross-sections..... | 31 |

INTRODUCTION

Volcanism at stratovolcanoes is a characteristic of island arc settings. The edifices of oceanic arc stratovolcanoes vary from submarine to emergent. The influx of volcanic detritus from submarine and subaerial eruptions has a strong influence on the marine environment and normal sedimentary processes. Eruption style and ambient sedimentary and eruption-generated transport processes, control the nature and geometry of submarine volcanic successions (McPhie and Allen, 1992).

Studies of the processes and products in modern volcanic terrains provide a framework for understanding the formation of ancient successions, which may be an incomplete record of events at outcrop scale (Cas and Wright, 1987). Modern submarine stratovolcanoes exist in the Lesser Antilles Arc (Sigurdsson et al, 1980), the Kermadec Arc (Wright, 1996), and the Aeolian Arc (Gamberi, 2001). Stratovolcano deposits and island arc stratigraphies are dominated by enormous quantities of volcanoclastic detritus (Larue et al, 1991) formed from the fragmentation of volcanic rocks (Carey, 2001).

Clastic products dominate the submarine deposits of stratovolcanoes. Fragmentation styles, eruption style and submarine transport and deposition mechanisms produce complex facies architectures. These mechanisms, and the interplay between submarine volcanic and non-volcanic processes in this setting, are fundamental to the formation of volcano-sedimentary deposits, and provide insights into island arc evolution (Carey and Sigurdsson, 1984).

Submarine volcanic processes have a critical role in deposit formation, but have not been the focus of extensive research. The inaccessibility of modern environments, has led to very few studies of submarine stratovolcano facies architectures. This review provides a comparison of facies associations typically found in ancient submarine stratovolcano successions in Northland New Zealand (Hayward, 1976a; 1976b; 1979a; 1979b; 1993), and New Hebrides (Mitchell, 1970). Facies transitions of an ancient seamount from Fiji (McPhie et al, 1995) have also been adopted for their resemblance to the foundations of a submarine stratovolcano edifice.

The understanding of subaqueous transport and deposition mechanisms at island arc settings, requires a review of both volcanic and sedimentary processes. Publications of deep-sea sediment transport from Stow et al (1996), and Pickering et al (1988), are central to current understandings in deep-sea environments and basins. The influence of volcanism in submarine environments has been thoroughly documented by Carey and Sigurdsson (1984). Work by Fisher (1984) and Fisher and Schmincke (1984; 1994) provide detailed investigations of submarine volcanoclastic rocks, pyroclastic rocks and volcanoclastic transport and deposition, respectively. General publications on the processes and products in volcanic environments are provided by Cas and Wright (1987), McPhie et al (1993), and Orton (1996). Understandings of the unusual hydrodynamic properties of volcanic particles in water (Smith and Smith, 1985; Cashman and Fiske, 1991; Manville et al, 2002), is important in consideration of submarine pyroclastic transport.

This work will synthesise current understanding of volcanic and non-volcanic processes in the submarine environment surrounding a stratovolcano, focusing in particular on clast forming processes, clast transport mechanisms, and the influence of these processes in creating submarine deposits. The general processes and products particular to stratovolcanoes in the submarine environment are reviewed, as they relate to deposition and emplacement of submarine deposits.

CHAPTER 1: THE SETTING OF SUBMARINE TO EMERGENT STRATOVOLCANOES

TECTONIC SETTING AND ISLAND ARCS

Convergent plate margins are characterised by complex tectonic belts, sedimentation and magmatic arc activity (Pickering et al, 1988). Active volcanism at convergent plate margins is a product of subduction, and is characteristically highly explosive, due to the high water and volatile content of the magma (Walker, 2001). Magma compositions vary from calc-alkaline to tholeiitic, and commonly andesitic. Basaltic to rhyolitic compositions also occur in arc settings (Wilson, 1989). Arc-volcanoes are typically polygenetic stratovolcanoes, built on a basement of older deformed volcanics, and either oceanic or continental crust. Submarine and subaerial edifices define linear to arcuate volcanic chains, 200-300 km wide, and 1000's of km long, (Cas and Wright, 1987). Long-lived explosive and effusive eruptions characteristically generate high volumes of coherent and volcanoclastic detritus (Einsele, 2000; Cas and Wright, 1987, Davidson and De Silva, 2001), which progrades from the arc platform into adjacent marine basins (Carey and Sigurdsson, 1984).

Elongate tectonic-basins of variable depth and size form adjacent to volcanic arcs and relative to plate boundaries (Orton, 1996; Pickering et al, 1988). These environments are known as trench, fore-arc (Dickinson, 1995), marginal / back-arc (Marsaglia, 1995) and intra-arc basins (Smith and Landis, 1995) (**Figure 1.1**).

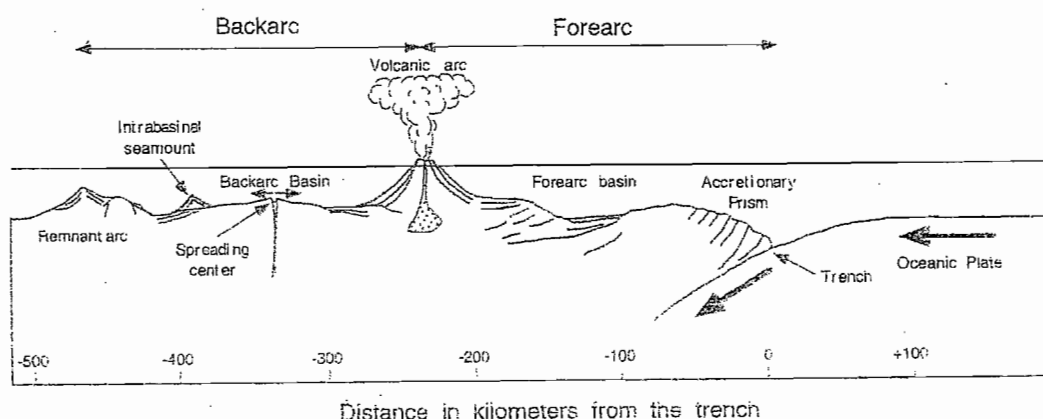


Figure 1.1: The arrangement of tectonic landforms that comprise a convergent plate margin, with the volcanic arc and adjacent marine basins in relation to the trench (from Carey, 2001).

BASIN ENVIRONMENT AND SEDIMENTATION

Marine basins forming adjacent to the island arc are dynamic environments, and their location can migrate with the arc axis over time (Orton, 1996). Sedimentation patterns are complex, controlled by sediment supply and volcanism (Stow et al, 1996), tectonic uplift, basin extension and arc-splitting (Carey and Sigurdsson, 1984; Ingersoll and Busby, 1995). Sediments are generally sourced from subaerial and / or submerged volcanic centres (**Figures 1.2 and 1.3**).

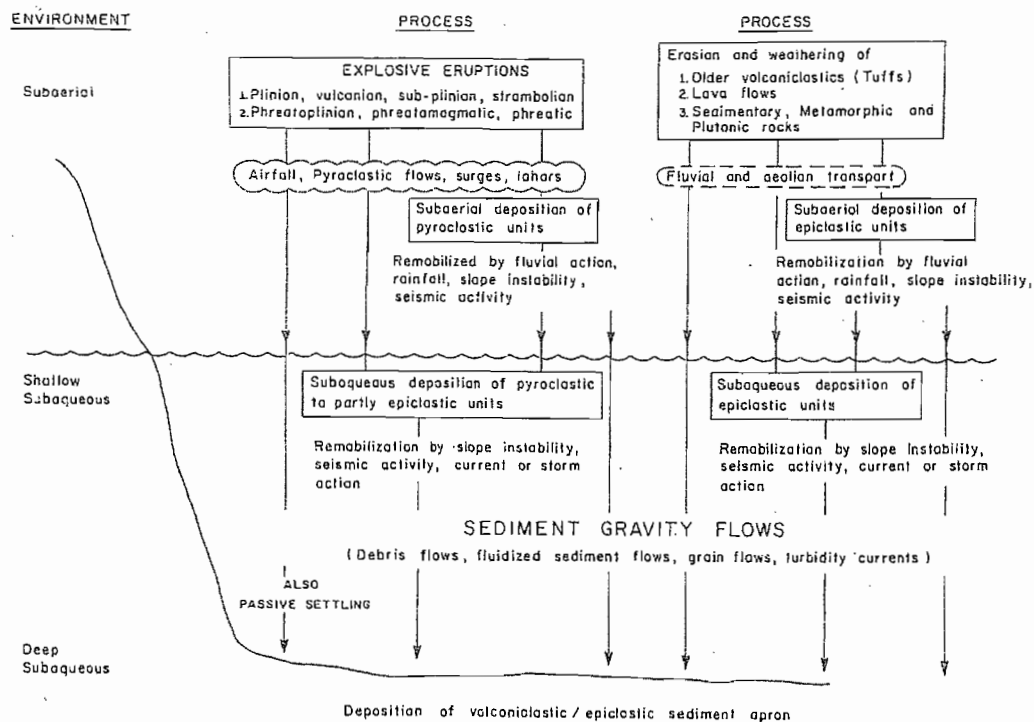


Figure 1.2: The production and transport of sedimentary particles from a subaerial arc volcano, and submarine deposition (from Carey and Sigurdsson, 1984).

Arc-related sedimentation has the same controls as other deep marine environments (Pickering et al 1988), where clastic deposition typically occurs on submarine fans, ramps, aprons, and basin plains (refer to Pickering et al, 1986 for classification, and Stow et al, 1996, for discussion). Thick, prograding volcanoclastic sequences occur at convergent margins (Pickering et al, 1988). The influxes of overlapping volcanic detritus, forms an asymmetrical apron that extends from the arc flank, 1000's of km long (Carey and Sigurdsson, 1984; Orton, 1996), and intercalate with normal marine basin sediments. For example, volcanoclastic debris intercalate with clays weathered from mafic volcanic landforms, biogenic components, and distal wind-blown dust (Carey and

Sigurdsson, 1984) that accumulates during quiescent volcanism. The deposits of normal marine basins are generally thin, distal basin fill of multiple source materials (Karig and Moore, 1975; Orton, 1995). Marginal basin sedimentation reflects basin evolution and arc growth (Carey and Sigurdsson, 1984). Due to isolation from other forms of sedimentation (Karig and Moore, 1975), and minimal erosion, marginal basin sediments can provide a record of volcanism.

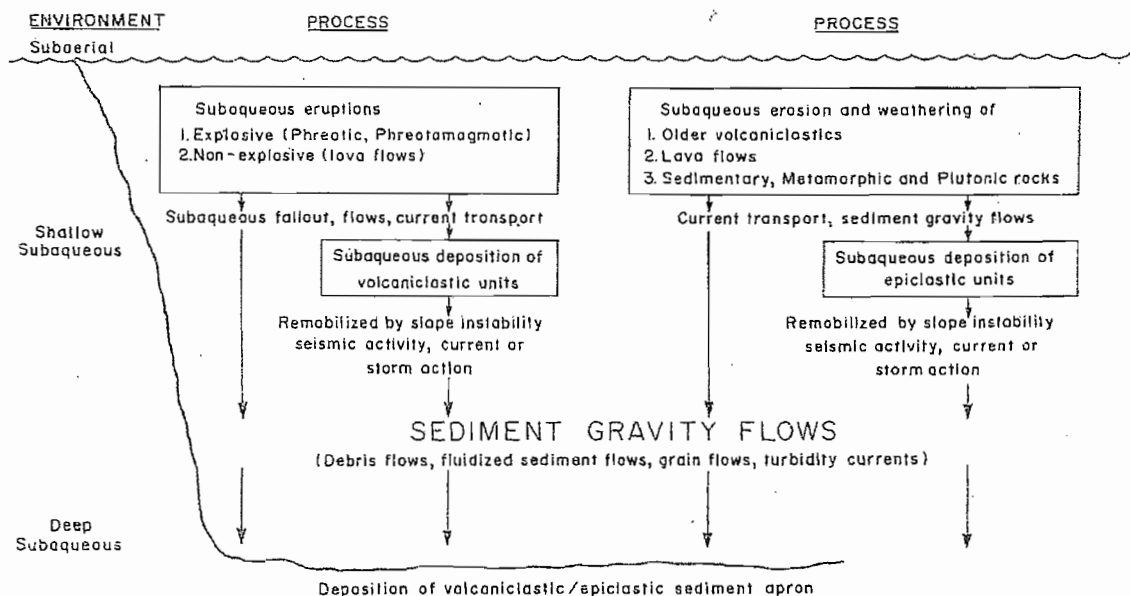


Figure 1.3: The production and transport of sedimentary particles from a submerged arc volcano (from Carey and Sigurdsson, 1984).

ARC STRATOVOLCANO MORPHOLOGY

Stratovolcanoes, or composite cones, are conical, steep sided landforms with sector collapse structures and satellite vents scattered on the flanks (Walker, 2001). Lava flows and large volumes of volcanoclastic detritus, derived from effusive and explosive eruptions over a long period, construct the crest, flank and apron elements of the morphology (Fisher and Smith, 1991). Arc stratovolcanoes may exhibit variable morphologies, due to differences in the dominant clast-forming processes that take place with edifice growth. These variations are indicated by litho-facies changes that form during the transition from a submarine to subaerial setting. Smith and Landis (1995) identify the central cone, apron (fan), and distal basin facies types for submarine edifices (Table 1), which approximate proximal, medial, distal facies distributions (Figure 1.4). Submarine deposition on the apron is where large amounts of volcanoclastic detritus accumulate.

| Facies Association | Deposit Type (Lithofacies) | Characteristics | Occurrence (geometry) |
|--|---|--|---|
| <p>Central Facies</p> <p>0 - ~10 km</p> <p>(proximal cone)</p> | <p>Pillow lava (cf. Jones, 1968; Yamagishi, 1985, Kano et al, 1993)</p> <p>Sheet lava (cf. Yamagishi, 1991; Batiza & White, 2001)</p> <p>Intrusions (dykes and sills) Kano et al, 1993;</p> <p>Hyaloclastite (cf. Yamagishi, 1991)</p> <p>Pyroclastic & hydroclastic breccias (Yamagishi, 1991; McPhie, 1995)</p> <p>Peperite (Mitchell, 1970; McPhie et al, 1993)</p> <p>Wave worked volcanoclastics (Fritz & Howells, 1991)</p> <p>Reef talus (Mitchell, 1970)</p> | <p>Internal radial jointing, entrail-like form, ropy surfaces</p> <p>Massive to columnar joints, smooth surface</p> <p>Finger-like, radial jointing, marginal brecciation</p> <p>Glassy clasts, monogenetic, angular or pillow fragment breccias</p> <p>Broken coherent fragments and juvenile clasts</p> <p>Clastic texture, blocky or globular</p> <p>Sandstone, ripples, x-stratification, plane beds, graded layers</p> <p>Angular - rounded pebble-sized blocks, poorly bedded, calcirudite</p> | <p>Steep mounds and piles</p> <p>Tabular</p> <p>Apophyseal or massive</p> <p>Blanketing carapace</p> <p>Flank deposit</p> <p>Intrusion contacts</p> <p>Bounding central facies</p> <p>Localised</p> |
| <p>Apron Facies</p> <p>~ 5 - ~35 km</p> <p>(medial fan)</p> | <p>Ignimbrites and pyroclastic flow deposits (Cas & Wright, 1991; Fisher, 1984)</p> <p>Pumiceous or ash flow deposits (Fiske & Matsuda, 1964)</p> <p>Debris flow deposits (Kano et al, 1993; Fisher, 1984)</p> <p>Coarse-grained volcanoclastic turbidites (Schneider et al, 2001)</p> <p>Volcanoclastic debris avalanche deposits (Ballance & Gregory, 1991)</p> <p>Fine / coarse-grained fall deposits (Fisher, 1984; Allen & Cas, 1998)</p> <p>Calc-arenite turbidites (if shallow water carbonates are present)</p> | <p>Non-welded or welded, massive to stratified</p> <p>Lapilli-tuff, doubly graded, mud interbeds</p> <p>Poor-no internal bedding, matrix supported, inverse grading</p> <p>Sand-siltstone, normally graded, with ripples & laminations</p> <p>Coarse-grained, richly volcanoclastic, with rip-up clasts.</p> <p>Well - poorly sorted beds, ash-rich or pumice-rich lapilli</p> | <p>Extensive sheets</p> <p>Massive to thin bedded</p> <p>Localized</p> <p>Marl interbeds</p> <p>Thick beds</p> <p>Thick, sheet-like</p> |
| <p>Distal Facies</p> <p>~20 - ~70 km</p> <p>(basin)</p> | <p>Fine-grained volcanoclastic turbidites (Walker, 1985)</p> <p>Pelagic / hemipelagic muds and oozes (Stow, 1994)</p> <p>Fine-grained fall deposits (Cashman & Fiske, 1991)</p> | <p>Normally graded</p> <p>Interbedded with volcanoclastics, fine grained, bioturbated</p> <p>Bimodal sorting of pumice and lithics</p> | <p>Channel fill</p> <p>Thin, blanketing</p> <p>Mantle bedding</p> |

Table 1. Facies associations and deposit types of submerged oceanic arcs (modified from Smith and Landis, 1995), with relevant references in brackets.

The major controls on submarine edifice morphology are eruption magnitude and frequency (Orton, 1996), magma composition and physical properties of the magma, sector collapse and mass wasting processes (Cas and Wright, 1987; Deplus, et al, 2001). These controls may produce similarities in the morphology of submarine and terrestrial edifices (Cas and Wright 1987).

The interplay between primary volcanic with ambient marine processes, changes in clast fragmentation processes and transport mechanisms, leads to variable stratovolcano morphologies. Rumble IV, a submarine stratovolcano in the modern Kermadec Arc is elongate, and composed of a complex arrangement of lava flows, with volcanoclastic and mass movement deposits that are overlain and interdigitate with pelagic-hemipelagic sediments (Wright, 1996). A stratified, heterogeneous submarine edifice (Wright, 1996), dominated by a clastic apron is produced due to increased erosion on submarine slopes (Fornari, 1986) along with variations in clast generation and transport processes.

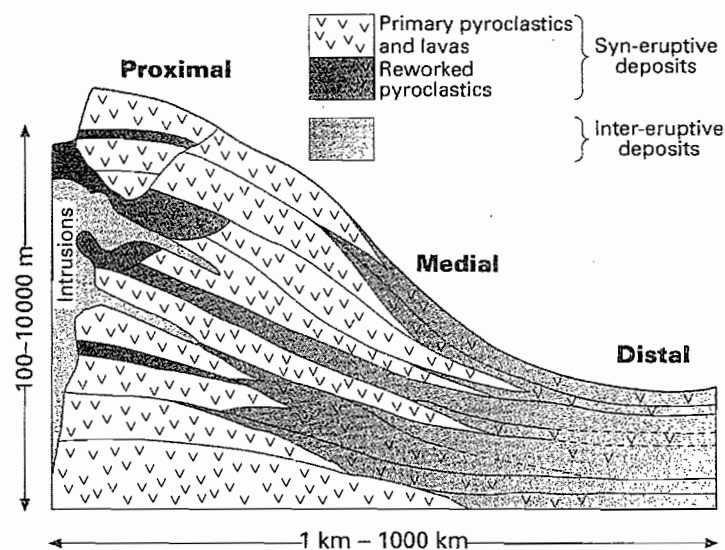


Figure 1.4: General proximal, medial and distal facies distributions relative to the source volcano (from Orton, 1996).

SUBMARINE DEPOSITS AND LITHOFACIES TYPES

The submarine deposits surrounding stratovolcanoes record eruptive activity and edifice construction from the sea floor, to a volcanic island. Complex sedimentation patterns occurring in basins adjacent to the arc produce diverse submarine volcanic deposits, with rapid vertical and lateral litho-facies changes and fine scale heterogeneities (Fisher and Schmincke, 1994). They are interbedded with non-volcanic, bioturbated, fossiliferous marine sediments. Proximal deposits may be incomplete (Hayward, 1976; Cas and

Wright, 1987) due to earthquakes, slope failure, faulting, uplift and subsidence. The most complete record of volcanism may be found in medial-distal deposits (Fisher and Schmincke, 1984). Due to limited erosion in submarine settings, submarine volcanic deposits are well preserved. A review of proximal, medial and distal deposits provides the best representation of an arc stratovolcano.

Volcano morphology influences the distribution of facies types. Changes in characteristic litho-facies of the lateral central, apron and distal facies types occur during the growth of an arc volcano from the sea floor to subaerial conditions (**Table 1**). Stratovolcano construction is comparable to the construction of other submerged volcanoes, regardless of magma composition and tectonic setting, and takes place in stages, from deep-water, to shallow and then emergent (Fisher, 1984) (**Figure 1.5**). Overall, there is a vertical increase in the lava-to-clastic ratio, which makes up a large proportion of all deposits related to stratovolcanoes. The Pressure Compensation Level (PCL), defined by Fisher (1984), is a broad depth interval, approximately between 1000-1500 m, where eruption styles change from predominately effusive to explosive. The deep-water interval, stage A, is where the foundations are dominated by coherent lava flows. Minor hyaloclastite and pillow lavas provide key evidence of a subaqueous eruption environment (Fisher, 1984). As construction progresses, stage B1 passes through the PCL where clastic materials increase in proportion to lava (Fisher, 1984). An emergent volcano, stage B2, sees an increase hydroclastics and pyroclastics and in the dimensions of the clastic apron. As particle abundances amplify so does the range of clast transport mechanisms, causing lateral deposit changes.

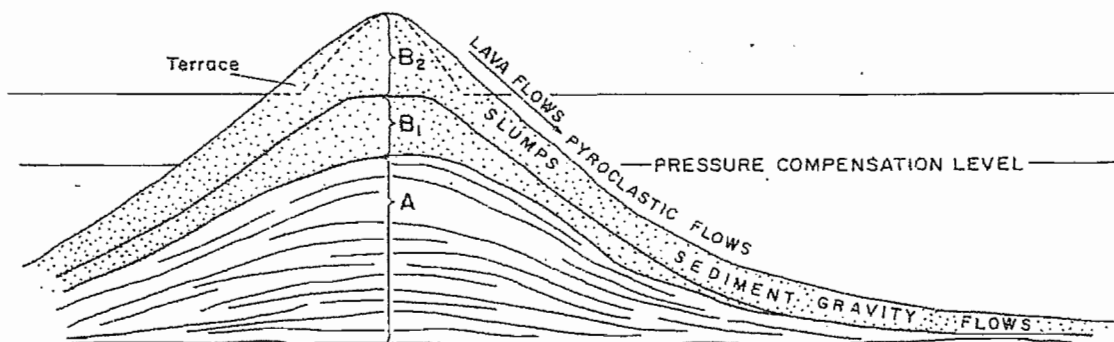


Figure 1.5: A stratified island volcano morphology of the dominant lithofacies type, which reflects growth stages, from deep water (A), through the PCL to shallow water (B1), and emergent (B2) (from Fisher, 1984).

The volcanoclastic apron is composed of primary and reworked pyroclastic detritus (Cashman and Fiske, 1991). Varying wind patterns, submarine slopes and ocean currents effect facies distributions (Orton, 1996), which may be asymmetrical (Sigurdsson et al, 1980). Eruption style, dispersal, eruption column height and fragmentation, influence the extent of deposition and ensuing deposit geometries.

Complex facies distributions, genetic associations and contact relationships occur. Hence stratigraphic interpretation and correlation of volcanic sequences requires that genetically related, contemporaneous facies associations are recognised (McPhie and Allen, 1992). Deposit types can also be categorised as primary volcanic, resedimented volcanoclastic and volcanogenic sedimentary facies types, depending on the dominant transport mechanism (McPhie et al, 1993).

CHAPTER 2: CLAST-FORMING PROCESSES AND PRODUCTS

Highly explosive eruptions from arc stratovolcanoes generate a range of fragmental ejecta and volcanic clasts. Changes in the dominant clast-forming processes, may occur with edifice construction from deep water, to emergent. Quiet lava effusions and violent explosive eruptions involve volcanic fragmentation and fracture processes in the subaerial and submarine conditions (**Figure 2.1a**). Juvenile or primary volcanic clasts may form from the erupting magma and release of magmatic volatiles, and by cooling and quenching from magma-water interactions. The characteristics, size and quantity of pyroclastic fragments reflect eruption style (Cas and Wright, 1987). Additionally, volcanic clasts can be generated by secondary weathering and fracturing of pre-existing volcanic deposits. Primary clast-forming processes are: cooling-contraction granulation, contact-surface steam explosivity, bulk interaction steam-explosivity, and magmatic explosivity (Kokelaar, 1986; Heiken and Wohletz, 1991) (**Figure 2.1b**). These processes commonly occur simultaneously and are influenced by water depth (Kokelaar, 1986) (**Figure 2.1**). The type of clast-formation process can also affect clast transport and deposition (Heiken and Wohletz, 1991).

EXPLOSIVE FRAGMENTATION PROCESSES

The physical properties of the magma, the presence or absence of external water and the ambient pressure, control whether an explosive or effusive eruption takes place (Cas, 1992). Explosive magmatic, phreatomagmatic and phreatic explosive eruptions generate pyroclastic material (**Figure 1.2**). Fragmentation occurs simultaneously with magma ejection during explosive volcanic eruptions (McPhie et al, 1993). Andesitic magma is disrupted into particles during the rise and vesiculation of the erupting magma (McBirney, 1973). Further fragmentation occurs during the explosive release of volatiles, generating magmatic (pyroclastic), phreatic and phreatomagmatic (hydroclastic) ejecta (McPhie et al, 1993). A high degree of explosivity at andesitic stratovolcanoes is due to high concentrations of magmatic volatiles, a high water content of andesitic magmas, and is not only caused by hydro volcanic explosions (Fisher and Schmincke, 1984). Hydrostatic pressure suppresses steam expansion and volatile-driven explosions in deep water, and governs the intensity of phreatomagmatic and phreatic

activity (Kokelaar, 1986). Significant fragmentation is restricted to depths shallower than ~3 km in seawater (Head and Wilson, 2003).

The fragmentation processes of subaqueous basaltic volcanism examined by Kokelaar (1986) at Surtsey can be used to characterise the types of clast formation processes involved during eruptions at stratovolcanoes.

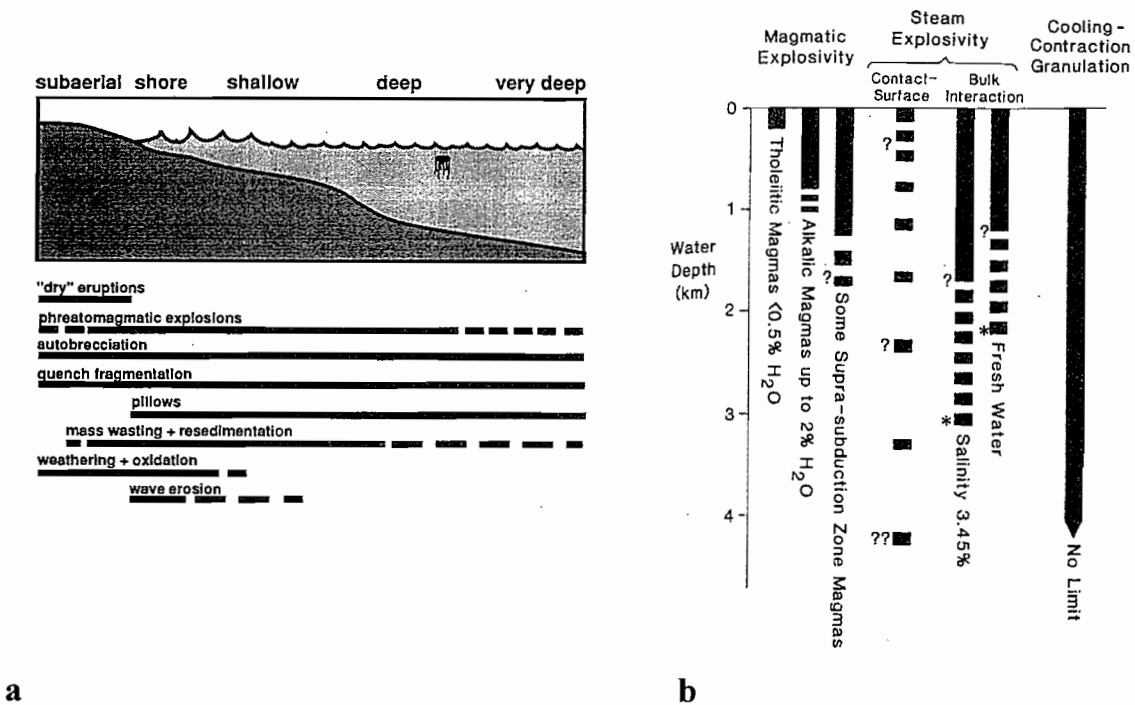


Figure 2.1: **a)** Changes in eruption and clast forming processes in relation to water depth (from McPhie, 1995). **b)** The water depths at which clast-forming processes can occur (from Kokelaar, 1986).

Subaerial eruptions

Shallow to emergent explosive magmatic eruptions exhibit characteristic eruption styles. Magmatic explosivity is a “dry” eruption mechanism, generating large volumes of juvenile pyroclasts. They are recognized as dry, because external water is a minor component (McPhie et al, 1993). The exsolution and expansion of magmatic volatiles, decompression and vesicle growth results in the explosive release of magma (Heiken and Wohletz, 1991). At high pressures, gas exsolution is greatly reduced and magmatic fragmentation is restricted (Head and Wilson, 2003). The depth at which magmatic explosivity takes place is determined by the juvenile volatile content of the magma (Kokelaar, 1986). Volatile exsolution and expansion is uninhibited at low hydrostatic pressures (Kokelaar, 1986).

Magma composition, viscosity, temperature, density, and vent geometry, control the character of explosive magmatic eruptions (McPhie et al, 1993). Eruptions from stratovolcanoes include vulcanian, strombolian, subplinian and plinian. Vulcanian eruptions produce discrete, short-lived explosions that create a series of small eruption columns, and widely dispersed ejecta (Cas and Wright, 1987). In this case, the rapid release of degassed, congealed lava from a blocked conduit leads to explosive activity, and vertical ejection of gas and pyroclasts (McPhie et al, 1993). This is thought to be triggered by alternating magmatic and phreatomagmatic processes (Heiken and Wohletz, 1991). Subplinian and plinian eruptions produce steady high-energy explosions. Continuous gas blasts that rapidly accelerate through the conduit produce large volume eruptions that disperse pyroclastic ejecta $>500 \text{ km}^2$ from the vent (Cas and Wright, 1987). Alternatively, Hawaiian and Strombolian eruption styles from high viscosity basaltic magmas (Walker, 1973) are mildly explosive and inefficient fragmentation mechanisms (McPhie et al, 1993).

A classification scheme underpinned by the area of dispersal and degree of fragmentation has been developed for subaerial explosive eruptions (Walker, 1973). In the subaerial case, the size of the eruption column reflects the degree of fragmentation and dispersal (**Figure 2.2**). According to Walker's (1973) classification, clastic-dominated eruptions that have a wide dispersal are known as sheet-forming, and lava spatter eruptions have a limited dispersal area and are cone-building.

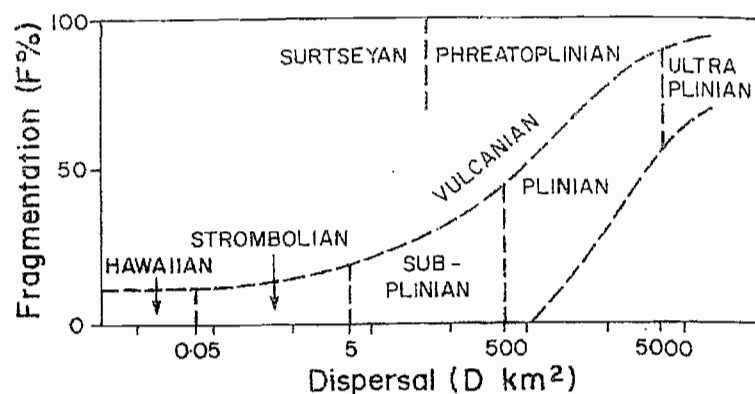


Figure 2.2: Fragmentation (F) and dispersal (D) characteristics of different eruption styles (Walker, 1973).

Submarine eruptions

Explosive eruptions are constrained by water depth and hydrostatic pressure. The PCL delimits a transition from dominantly explosive to dominantly effusive eruptions. Explosive basaltic eruptions are estimated to occur around 200-500 m water depth. Alkali basalt and andesitic eruptions are estimated to occur around 500-1000 m (McBirney, 1963). The depth of fragmentation may vary due to changes in the physical properties of the magma, and different magma-water interactions (Kokelaar, 1986).

Submerged or shallow water vents in arc settings, produce “wet” explosive eruptions from magma-water interactions. Water depth and hydrostatic pressure suppress steam expansion and explosivity (Head and Wilson, 2003), which governs the intensity of phreatomagmatic and phreatic activity (Kokelaar, 1986). Direct magma-water interactions and phreatomagmatic activity initiates contact-surface steam explosivity processes, which is caused by magmatic explosivity (Head and Wilson, 2003). Two types of steam explosivity have been identified (**Figure 2.1a**). Contact-surface steam explosivity or the fuel-coolant interaction, involves the rapid vaporisation of superheated water (Kokelaar, 1986). Bulk interaction steam explosivity involves explosive steam expansion, controlled by the ambient pressure and rate of heat exchange between the magma and water (Kokelaar, 1986). In the first case, interaction of the magma surface with water, results in the formation of a thin unstable film of coalesced steam bubbles. Oscillatory collapses of the film cause fine magma fragmentation and turbulent mixing of the magma with water (Kokelaar, 1986). In the second case, water is trapped close to, or engulfed by magma, resulting in rootless explosions. Magma fragmentation and clasts formation results from the tearing of magma around explosively expanding steam and shattering of rigid magma by pressure waves (Kokelaar, 1986).

Theoretical modelling of submarine explosive eruptions along with observational data, indicate hydro volcanic explosions can occur at greater pressures than previously thought (Clague et al, 2000). Head and Wilson (2003) proposed significant pyroclastic explosions could occur at depths greater than 3000 m, although subaqueous eruption styles are yet to be defined as they are less readily observed. Changes to the eruption column, degree of fragmentation and dispersal would take place in the submarine environment, due to marine processes and the ambient pressure, hence modifying subaqueous eruption styles. The distribution of modern submarine volcanic deposits and juvenile ejecta found on the seafloor may provide clues to eruption styles and eruption

dynamics in marine settings. A classification scheme underpinned by juvenile ejecta distributions, along with further observational data would enhance understandings of submarine clast-forming processes.

NON-EXPLOSIVE FRAGMENTATION PROCESSES

Non-explosive fragmentation processes can take place in either submarine or subaerial conditions and are not restricted by water depth. Fragmentation occurs by rapid chilling of effusive volcanic products, and includes quenching, fracturing, spalling and granulation of lava. These processes are important in deep water where steam explosivity is suppressed (Kokelaar, 1986).

Effusive eruptions

Effusive eruptions are the result of degassing during magma emplacement, which produces low magma volatile contents, and effusive lava extrusion. Chilling and brittle fracturing of the outer lava surface during flowage can cause mechanical friction and fragmentation (McPhie et al, 1993). Autobrecciation occurs when flowage of a viscous, congealed lava or internal movement within the lava crust, produces deformation and stress fractures (Cas and Wright, 1987). Depending on viscosity and strain rate, plastic stretching or brittle fracturing generates slabs and blocks of fragmented lava on the outer lava surface. Autobrecciation is often accompanied by quench fragmentation in subaqueous settings.

Quench fragmentation and cooling contraction granulation processes, occur from the rapid cooling of the outer surface of lava flows and intrusions (McPhie et al, 1993). This process fractures and disintegrates chilled coherent bodies. Rapid cooling of pillow margins, lava flows, feeder dykes, or the exterior of lava fountain droplets initially results in contraction and intricate fracturing of the outer layer, producing a rigid shell. This is followed by contraction of the interior, which leads to granulation of the quenched rim (Kokelaar, 1986). Lava fragments are generated from a build up of thermal stress accrued during rapid cooling (McPhie et al, 1993).

Weathering and fracture-controlled fragmentation

Weathering, erosion and fracturing along joint planes of pre-existing volcanic material are secondary fragmentation processes (Cas and Wright, 1987) (**Figure 1.3**). The production of large volumes of volcanoclastic fragments is dependant on the surrounding environment, and proximity to the volcanic centre. Debris avalanches and landslides on the steep, unstable flanks of stratovolcanoes (Fisher and Smith, 1991), along with gravitational failure of fractured lava flows, generate rock fragment talus (McPhie et al, 1993). Weathering of deformed volcanic piles and semi-consolidated volcanoclastic deposits also generates volcanic particles (Cas and Wright, 1987). Fragments are produced through abrasion and collision during transport, and are redistributed along with primary fragments far from the source (Cas and Wright, 1987). This fragmentation mechanism can take place during or between eruption episodes.

PRODUCTS

Depending on the depth of clast-formation and fragmentation mechanism, different clasts are produced, and distinctive fragmental deposits are formed. The type, size and character of pyroclasts produced during a single eruption can vary due to changes in the amount of water within the magma, and also due to the influence of external water on eruption style (Kokelaar, 1986). Collectively, volcanic clasts formed by any fragmentation process may be termed volcanoclastic.

Non-explosive fragmental products are not restricted by water depth. Autobreccia fragments are blocky to irregularly shaped, and lack the glassy rims characteristic of hyaloclastite. Autobreccia blocks may fuse in-situ and form a carapace around the moving lava flow (McPhie et al, 1993). Loose dislodged blocks may form fragment breccias on the margins of pillow lava, block lava and massive feeder dykes. Lava chunks, sand-granule lava grains, glass splinters and hyaloclastite, are produced in-situ by quenching and granulation processes (Kokelaar, 1986). Individual fragments may be curvy-planar blocks or splinters and produce in-situ or resedimented deposits (McPhie et al, 1993). Epiclastic deposits may be a mixture of lava talus, eroded volcanic fragments, recycled pyroclasts, and freshly erupted particles (McPhie et al, 1993).

Explosive pyroclastic fragments restricted by water depth include phreatomagmatic clasts generated by steam explosivity, which produces irregular, bulbous, nearly spherical, blocky, pyramidal or splintery clast shapes (Kokelaar, 1986). Ash-sized pyroclasts are typically blocky to poorly vesicular, and admixed with accretionary lapilli (Heiken and Wohletz, 1991). Dry magmatic eruptions produce variable juvenile, crystal and lithic fragments (Cas and Wright, 1987), depending on eruption style. Explosive eruptions generally produce angular to ragged pumice, scoria, glass shards and bombs. In addition, the products of vulcanian eruptions contain non-juvenile components from the lava plug (Heiken and Wohletz, 1991). Strombolian ash contains spherical, droplet-shaped to filamentous achneliths and spatter of lava lumps (Walker and Croasdale, 1970). Pumice clasts have different hydrodynamic properties, depending on whether the vesicles are air or water-filled and hot or cold (Cashman and Fiske, 1991; Mandeville et al, 2002).

CHAPTER 3: TRANSPORT AND DEPOSITION

MECHANISMS

Volcaniclastic detritus derived from stratovolcanoes at island arcs undergo subaerial and submarine transport and then deposition, which also includes sedimentary particles. Transport may be associated with particles derived from volcanic eruptions, or the remobilisation of volcanic and sedimentary deposits (**Figure 3.1**). Normal submarine transport is an episodic process, dependant on sediment supply. Large influxes of volcaniclastic particles generated through volcanism, modifies normal submarine transport and deposition mechanisms. Transport of volcanic particles involving primary and syn-eruptive mechanisms is not well understood in subaqueous settings. Normal resedimentation mechanisms such as turbidity currents and debris flows are well understood, and may be used to better understand subaqueous volcanic transport.

The behaviour of some subaqueous sediment flows are understood from their occurrence on land (Stow, et al, 1996), and in laboratory experiments with flumes (McLeod et al, 1999). Sedimentary particles in water move in particulate form, by suspension, traction, flotation and solution, and in mass movement form, which includes mass flows, debris flows, slumps and debris avalanches (Cas and Wright, 1987). The behaviour of subaqueous sediment flows is driven by the interstitial medium, water (Cas and Wright, 1987), which also acts as the dominant sediment support agent. Sediment gravity flows, for example, are either grain or water supported (Lowe 1979). Secondary transport of volcaniclastic particles, have water as the dominant interstitial fluid. Alternatively, pyroclastic flows are gas or gas and water supported. Flow behaviour in subaqueous conditions is influenced by water ingestion. Particulate flows exhibit either turbulent or laminar flow behaviour. Clasts transported by mass flows move collectively as a mass and interact (McPhie et al, 1993).

Subaqueous pyroclastic flows exhibit stratified flow behaviour, similar to turbidity currents. The lower parts of pyroclastic flows exhibit laminar flow behaviour, overlain by an upper turbulent ash cloud that gradually becomes suspended into the water column (Yamazaki et al, 1973). The primary particle support agent may change from gas to water support during transport, modifying flow behaviour. Changes in dominant support agent, accompanied with a change from laminar to turbulent flow, or vice versa, produces

flow transformations (Fisher, 1984), which progressively develop with distance from source (Fisher and Schmincke, 1994).

Particle settling velocity underpins subaqueous transport and deposition mechanisms (Cas and Wright, 1987). There is a large variation in the physical properties of volcanoclastic particles (McPhie et al, 1993). As volcanic clasts have variable size and densities, models applicable to normal sediment transport may be difficult to apply to volcanic transportation processes. Pumice in particular is difficult to model, as there is often an inverse relationship between the specific gravity and grain size of pumice due to the vesicle content (Smith and Smith, 1985). Sorting of volcanoclastic sediments is a function of the hydraulic properties of each pyroclast type. This variability is due to diverse pyroclast composition, grain size and density (Smith and Smith, 1985; Manville et al, 2002).

The various forms of subaqueous sediment transport in the submarine environment surrounding arc stratovolcanoes are linked by flow transformations. This may suggest a relationship between primary pyroclastic flows, syn-eruptive transport and normal resedimentation, where volcanism creates major sedimentation events.

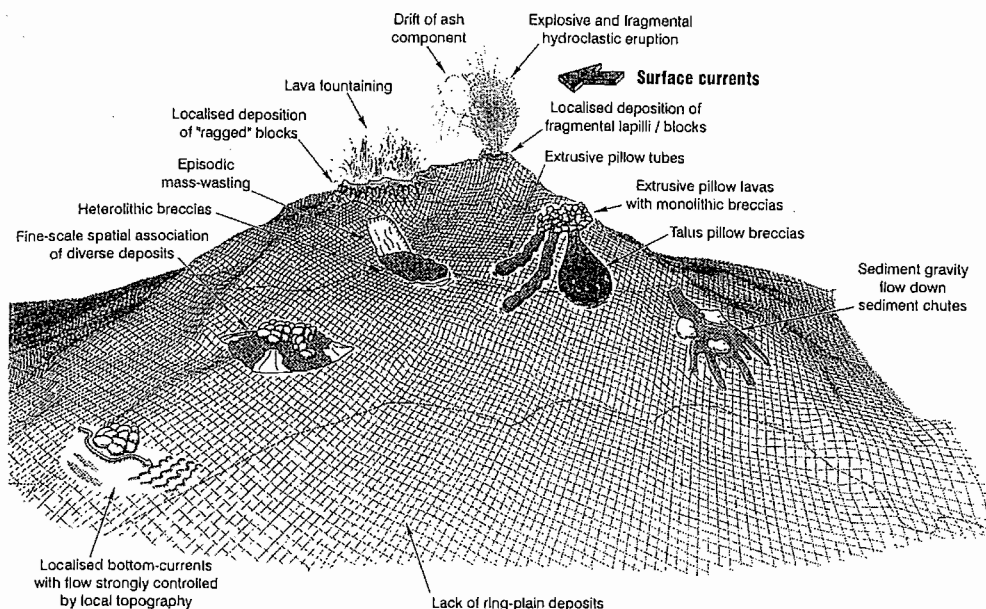


Figure 3.1: Transport and deposition processes on a submarine basalt-andesite stratovolcano (from Wright, 1996)

SUBMARINE RESEDIMENTATION MECHANISMS

Normal background resedimentation, along with bottom current processes are episodic subaqueous transport processes (**Figure 1.3**). Sedimentary particles and volcanoclastic detritus can be transported in the deep-sea, depending on sediment supply. Resedimentation mechanisms may dominate during quiescent volcanic activity, and efficiently resediment volcanic material days or years after an eruption. Resedimentation mechanisms are gravity-driven, subject to sediment supply. Large volumes of clastic material is transported from shallow to deep water (Stow, 1994; Stow, et al, 1996), and is efficiently transported long distances (Pickering et al, 1988) in mass movement form, as debris flows and sediment gravity flows (**Figure 3.2**). Bottom current transport processes are less efficient, and winnow, stir, entrain and slowly disperse fine particles (Stow, 1994, Wright, 1996). Submarine resedimentation involves water-supported transport.







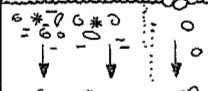
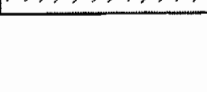
| PROCESSES: | CHARACTERISTICS: | DEPOSITS: |
|--|---|--|
| resedimentation | | |
| rockfall |  | talus deposit |
| slide/slump |  | debris avalanche deposit |
| debris flow |  | debris flow deposit |
| grain flow |  | { grain flow fluidised flow liquefied flow } deposit |
| fluidised flow | | |
| liquefied flow | | |
| turbidity current (high/low density) |  | turbidite |
| normal bottom currents | | |
| internal tides waves |  | normal current deposit |
| canyon currents |  | contourite |
| bottom (contour currents) | | |
| surface currents and pelagic settling | | |
| flocculation |  | pelagite, hemipelagite, water-settled fall deposit |
| pelletisation | | |
| flotation | | |

Figure 3.2: Classification of background resedimentation processes (from McPhie et al, 1993).

Sediment gravity flows

Sediment gravity flows are particle / water mixtures that move down-slope because the sediment mixture has a higher density relative to seawater (Pickering et al, 1988; Stow, 1994). Most flows are characterised by multiple support mechanisms (Stow et al, 1996). Lowe (1979) proposed a nomenclature for sediment gravity flows, based on flow rheology and particle support mechanisms (**Figure 3.3**). This classification has relevance to understandings of the behaviour of volcanoclastic transport, however further study is called for.

| FLOW BEHAVIOR | FLOW TYPE | | SEDIMENT SUPPORT MECHANISM |
|-------------------|--------------|---------------------------------|--|
| FLUID | FLUIDAL FLOW | TURBIDITY CURRENT | FLUID TURBULENCE |
| | | FLUIDIZED FLOW | ESCAPING PORE FLUID (FULL SUPPORT) |
| | | LIQUEFIED FLOW | ESCAPING PORE FLUID (PARTIAL SUPPORT) |
| PLASTIC (BINGHAM) | DEBRIS FLOW | GRAIN FLOW | DISPERSIVE PRESSURE { MATRIX STRENGTH MATRIX DENSITY |
| | | MUDFLOW OR COHESIVE DEBRIS FLOW | |

Figure 3.3: Sediment gravity flow classification proposed by Lowe (1979).

In volcanic settings, cold subaqueous gravity flows and density currents transport volcanoclastics in a water-supported medium (White, 2000). Subaqueous syn-eruptive mass flows and density currents involve water-supported transport of juvenile, eruption-fed detritus away from the site of eruption and flow generation (McPhie et al, 1993).

They can be initiated directly from primary eruptions and pyroclastic transport, from the transformation of a hot pyroclastic flow into a density current as it enters the sea (**Figure 3.5 C**), or from dense aqueous pyroclastic suspension, into a grain flow (White, 2000). Or indirectly, from the remobilisation of unmodified pyroclastics. Pyroclasts either rapidly cool and settled out of suspension, or flow from the vent as warm to cold clasts, and became incorporated into a density current (Fiske and Matsuda, 1964). Deposition occurs from a reduction in transport velocity and from changes in flow type due to changes in dominant particle support.

Turbidity Currents

Turbidity currents, are the main type of sediment-driven underflow in oceans and lakes, and compared to other types of sediment gravity flow (Lowe, 1979), can sustain dilute sediment suspensions by fluid turbulence (Stow, 1994). Turbidity currents are initiated by debris flows and the saturation of slumps, storms, or point-source delivery of suspended sediments into the sea (Stow, 1994; Wright, 1996). Turbidity currents comprise an anatomy of a head of coarse grains at the front, a body and a dilute thin tail (Stow, 1994). The flow can be sustained over distances of 4000-5000 km by generating a dynamic equilibrium, turbulence loop (autosuspension) (Stow, 1994). Turbidity current deposition is restricted by flow turbulence (suspension) of clay-sand sized particles, hindered settling of high concentration turbulent suspensions of coarse sand-gravel sized grains, and matrix buoyant lift and clast collisions between pebble-cobble sized clasts (Lowe, 1982). Sediment grains are deposited by gravitational segregation during flowage. Varying grain populations (clast size) of different turbidity currents produces high and low density currents. These differences also produce variations to flow behaviour and transport energy (McPhie et al, 1993).

Where large influxes of volcanoclastic detritus are introduced into surrounding basins, volcanoclastic turbidites efficiently transport and deposit volcanic detritus. Turbidity currents form from low-density, slow-settling ash out of suspension, or rapid settling coarse dense ash (Fiske and Matsuda, 1964). Based on a thick turbidite deposit on the east coast of New Zealand, Schneider et al (2001) has recognised that volcanoclastic turbidites originate directly (primary), or indirectly (secondary) from volcanism. Turbidites that are rich in primary volcanic particles, such as glass shards and hydroclastic fragments, originate contemporaneously with an eruption (Schneider et al, 2001). Volcanoclastic turbidites fed by one (monomagmatic), or multiple (multimagmatic) eruptions (Schneider et al, 2001) are referred to as syn-eruptive, or eruption-fed gravity flows. In this case, they may have originated either from flow transformation of pyroclastic flows, or reworking of stored volcanoclastic material (Schneider et al, 2001). Flow initiation and flow behaviour are determined by eruption characteristics, including eruption style and the interaction of the eruption column with the surrounding water (White, 2000). Water ingestion continually dilutes and modifies flow behaviour during the course of syn-eruptive transport (Kano, 1996).

Debris Avalanches and Rockfalls

Mass movements are rare on the gently sloping sea floor. Local, or large-scale collapse of over-steepened areas may be triggered by volcanic events or normal seafloor instabilities. Episodic failure of semi-consolidated, loose sediments may induce mass movements (**Figure 3.2**). Mass movements involve non-cohesive, momentum-driven transport of particles by bed-load particle movement, by traction and saltation, or laminar grain-flows of gravel and boulders (Stow, 1994). The steep slopes of stratovolcanoes, combined with earthquakes, sector collapse and eruptive events can trigger rock-falls, debris avalanches, slides and slumps (Stow, 1994). Mass flows and grain flows may also form from slabs and blocks shed from an advancing lava flow front, producing breccia deposits (Kano, 1996; White, 2000). The movement of debris avalanches and rockfalls is not dependant on an interstitial fluid (Cas and Wright, 1987) and can erode and incorporate the lower sediments into the flow, and make sediments available to other resedimentation processes (Kokelaar and Romagnoli, 1995). After a sector collapse event, coarse, fan-shaped and chaotic debris avalanche, or talus deposits are produced at the slope base (Kokelaar and Romagnoli, 1995). These events may disrupt particles and initiate turbidity current transport.

Debris Flows

Cohesive debris flows have high sediment, low water concentrations, and display plastic flow behaviour, producing a slow, slurry-like movement (Fisher, 1984; Stow, 1994). Large volumes of clay to boulder size clasts can be transported 10's to 100's of km by this mechanism. The flow is laminar to turbulent, supported by buoyancy, frictional strength, matrix strength, elevated pore pressure and dispersive pressure (Stow, 1994).

Subaqueous volcanoclastic debris flows that deposited the Parnell Grits (New Zealand) were interpreted by Ballance and Gregory (1991) to be the result of subaerial sector collapse and debris avalanches. Particle interaction, cohesive matrix strength, and buoyancy, controlled the behaviour of the flows in subaerial conditions. On entry to the sea, water and sediment ingestion at the flow head, lowered its cohesive strength, probably transforming it into a sediment gravity flow. Experimental simulations of particle-laden flows, indicates that on entry to the ocean, water is entrained, resulting in gravitational collapse and formation of a gravity current (McLeod et al, 1999). High pore pressures were sustained during submarine transport of the Parnell Grits, inferred from

the transportation of large clasts, and injections of grit into the substrate (Ballance and Gregory, 1991). These volcanoclastic debris flows involve initiation by proximal volcanic-related events, and may or may not result from syn-eruptive resedimentation.

PRIMARY VOLCANIC TRANSPORT MECHANISMS

Primary volcanic transport involves juvenile pyroclasts and lava generated by explosive and effusive eruptions (Fisher and Schmincke, 1984) (**Figure 1.2**). Dispersal of juvenile material is eruption-generated, initiated by energy provided during volcanic activity. Explosive eruptions are more efficient in the dispersal of pyroclasts than non-volcanic transport, with higher transport velocities and voluminous sedimentation events produced as a result. This form of subaqueous transport includes emplacement of coherent bodies, suspension particle transport and mass flow processes. These mechanisms involve a single event, with minimal time lapse between eruption, transport and deposition.

Subaqueous Lavas

The subaqueous emplacement of viscous, basaltic or andesitic lavas is characterised by pillow lava formation (Yamagishi, 1985; McPhie et al, 1993). Pillow formation involves the slow moving propagation and cooling of lava lobes. Individual pillow lobes advance through widening longitudinal spreading cracks, into a growing lobe (Yamagishi, 1985), resulting in lobe inflation. New breakouts through the crust and extension of transverse spreading cracks create new toes and the development of new solidified lava crusts (Yamagishi, 1985). Steep-sided pillow mounds occur on the sea floor proximal to the volcano. They are a chaotic array of interconnected elongate pillow lobes, fed by a 'mega-pillow' lobe above (Hayward, 1979). Vesicle size and abundance can indicate depth of emplacement, and longitudinal sections can help determine the direction of propagation (Hayward, 1979). The local relief produced by lava outcrops provides a topographic barrier to sediment dispersal (Gamberi, 2001).

Water-settled Fallout

Explosive volcanic eruptions from submerged or subaerial vents along the arc generate abundant pyroclasts. Pyroclastic material is subject to transport and deposition in the submarine environment by water-settled fallout from suspension, or by ocean currents (McPhie et al, 1993). The different shape and density of lithic clasts, crystals, scoria and

pumice, give them distinct settling velocities (or terminal velocity). Water-settled fallout is controlled by particle density, and the interstitial medium, which is admixed into the buoyant plume during ascent (Cashman and Fiske, 1991). In deep-water, the eruption column does not breach the water surface, and fallout occurs on the margins of the expanding column, where particles are transported laterally from the umbrella region by ocean currents, and then from suspension settling (Cashman and Fiske, 1991). When the settling velocity of a particle exceeds the vertical lift of the eruption column, they begin to fall out of suspension (**Figure 3.4**).

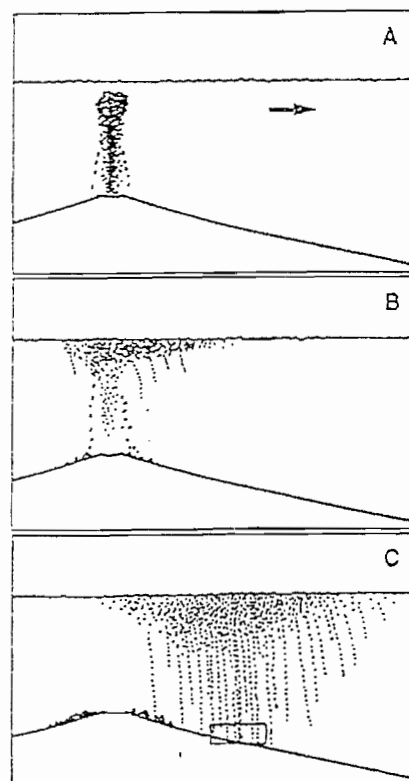


Figure 3.4: Fallout from a short-lived, deep submarine eruption, depicting particles with high settling velocities, falling out from the column margins (A), particles with lower settling velocities, falling from the base of the expanding umbrella (B), and extensive fallout from the laterally drifting umbrella (from Cashman and Fiske, 1991).

The large settling velocities of high-density particles leads to vent-proximal fallout, which also occurs if the water column becomes inundated with high pyroclast concentrations (Manville et al, 2002). The drifting umbrella region produces extensive fallout of lighter clasts, which may be made available to transport by other processes (White, 2000). Water-settled fallout is comparable to subaerial fallout, which are both well sorted according to density (Fisher and Schmincke, 1984 McPhie et al, 1993; Orton,

1996). In water the hydraulic properties of individual particles leads to better sorting, especially of coarse-grained submarine fallout. Hydraulically equivalent pumice and lithics fall out of suspension and are deposited simultaneously, producing a bimodal clast size distribution of 5 : 1 in the same layer (Cashman and Fiske, 1991).

Subaqueous pyroclastic flows

Pyroclastic flows are non-cohesive mass flows of hot pyroclasts, with high particle / gas concentrations. They are driven by gravity, eruption-driven momentum and efficient particle support (McPhie et al, 1993). Subaqueous pyroclastic flows can be generated from the explosive eruption of a submerged or subaerial vent (**Figure 3.5**).

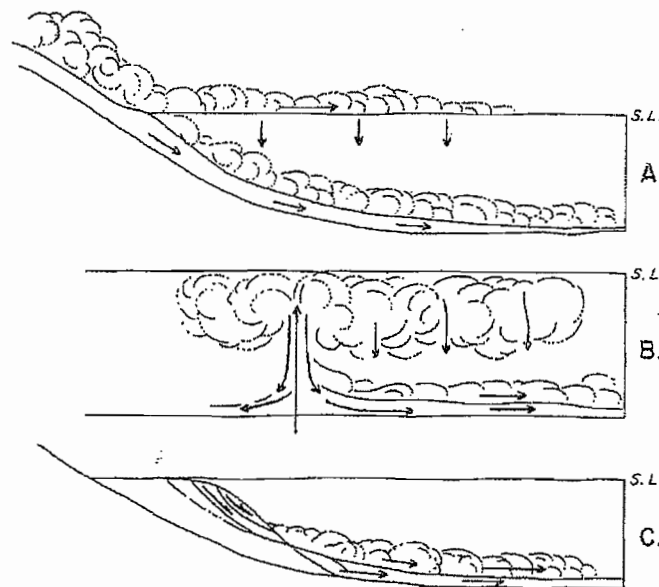


Figure 3.5: Subaerially-generated pyroclastic flows undergo density separation on entry to the sea, and continue to flow in water (A). Subaqueously-generated pyroclastic flows develop from column collapse (B). Pyroclastic density current, generated from a pyroclastic flow, or slumping of unstable pyroclastic debris (C) (from Fisher, 1984).

Pyroclastic flows occur in various forms, including scoria and ash flows generated from stratovolcanoes, pumice flows and block and ash flows (McPhie et al, 1993). In order for a true pyroclastic flow to be sustained during transport in submerged conditions, the integrity of the flow cannot be affected by water ingestion or explosive disruption, which converts primary particle support, from gas to water (Cas and Wright, 1991). Evidence of hot subaqueous emplacement includes thermoremanent magnetisation data (Yamazaki

et al, 1973), deep marine welding of an ash-flow (Kokelaar and Busby, 1992) and successful transport of pyroclastic flow into submarine environment from Krakatau (Mandeville et al, 1996). These indications support the idea that heat-retention and gas support can occur in subaqueous conditions, although there are opposing views on the subaqueous transport of pyroclastic flows (Fisher, 1984; Cas and Wright, 1991; Kokelaar and Busby, 1992; Mandeville et al, 1996).

Subaqueous pyroclastic flows comprise a lower dense avalanche portion, which does not intermingle with water, overlain by an upper turbulent ash cloud that becomes dispersed into the surrounding water column (Yamazaki et al, 1973). Transport into a subaqueous environment of a subaerially-generated pyroclastic flow, produces a high concentration basal portion, flow deflation and gravitational separation of the overriding turbulent flow. Low concentration pyroclastic density currents occur along the flow margins, where water is ingested and cooling of clasts has taken place in subaqueous conditions.

A cold subaqueous pyroclastic flow can develop from flow transformation of a pyroclastic flow. A subaqueous scoria-flow deposit on in the Shimane Peninsula, Japan, Kano et al (1994), was found to originate from a submerged stratovolcano. Due to dilution and water ingestion during submarine transport and flowage, it transformed into a pyroclastic gravity flow (Kano et al, 1994). In proximal areas, thermoremanent magnetization of pumice and lithic clasts pointed towards the scoria flow being initially a hot gas and water supported flow. As hot clasts were lost from the flow during transport, the scoria-flow transformed into a cold high-density turbidity current (Kano et al, 1994). It is thought that a high density of hot, steam buffered scoria clasts, gave the flow the capacity to retain heat in the initial stages (Kano et al, 1994). Changes produced during submarine transport of a pyroclastic flow resulted in the formation of a syn-eruptive gravity flow.

CHAPTER 4: FACIES ARCHITECTURE OF MODERN AND ANCIENT DEPOSITS

Facies models provide a framework for facies architecture reconstructions (McPhie and Allen, 1992). The facies model of a marine stratovolcano created by Cas and Wright (1987) (**Figure 4.1**), reveals the facies geometry and distribution common to submarine stratovolcanoes. It provides a framework from which genetically-related deposits can be identified and correlated. Facies distributions of modern and ancient deposits should define a straightforward pattern relative to the eruptive centre(s) (Smith and Landis, 1995) (**Table 1**). These relationships may be readily determined in modern successions, where in-situ deposits reside in their depositional environment, however, abrupt vertical and lateral facies changes lead to difficulties in interpreting ancient successions. Lateral facies architecture variations are outlined below and vertical heterogeneities described where possible.

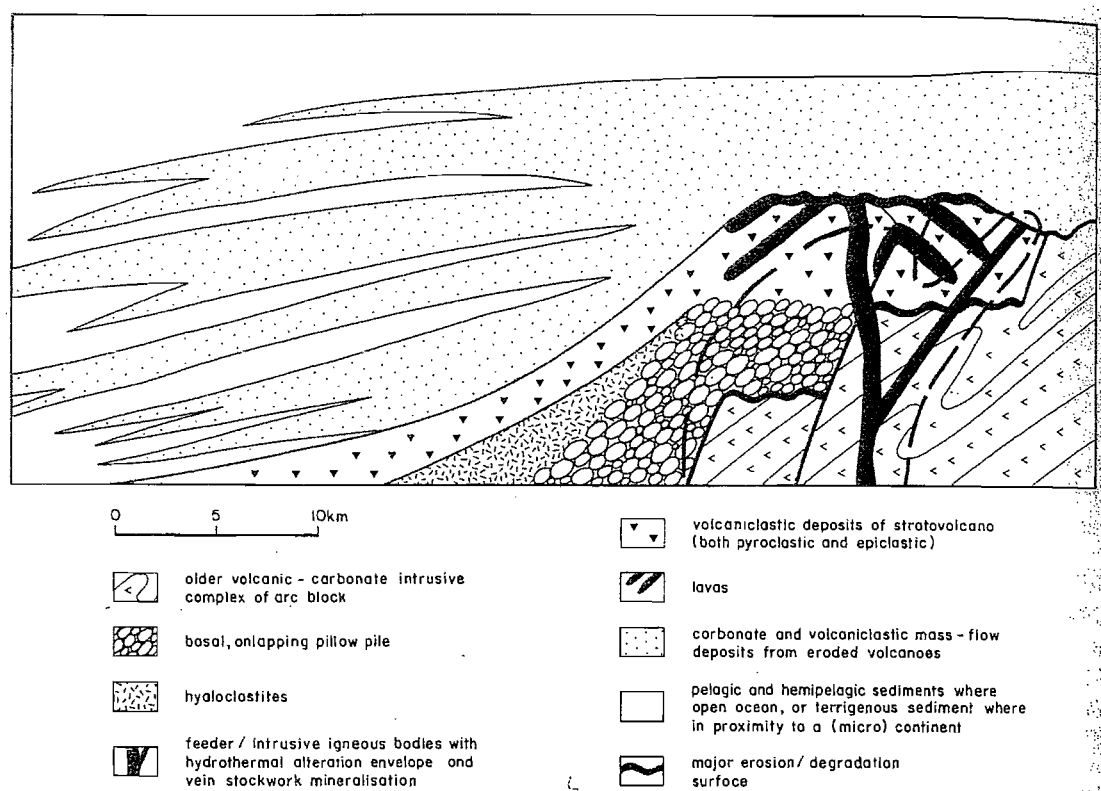


Figure 4.1: Facies model for marine stratovolcano (from Cas and Wright, 1987), with relevance to central, apron and basin facies distributions.

MODERN VOLCANIC ENVIRONMENTS

Bathymetry and reflectivity data, camera surveys, sonar imaging, gravity coring and seismic recording are methods used to better understand present day facies distributions. Using examples, the characteristics of the central, apron and basin facies associations are reviewed, as they define the facies architecture of a submarine stratovolcano deposit.

The arrangement of coherent and clastic deposits making up the central facies, reveal fine scale vertical variation at the scale of the volcano. The cone of two submarine stratovolcanoes, Rumble IV and Rumble V (Wright, 1996) consist of lobate and pillow lava vent complexes, 5-10 metre high, volcanoclastic breccias and sands, and pelagic sediments. The abundance of clastic deposits increases vertically, with fine-grained sediments decreasing towards the edifice crest (Fisher and Schmincke, 1984; Wright, 1996). Varying proportions of lava, breccia, volcanoclastics and pelagic sediments, have varying spatial distributions on the lower flanks (Wright, 1996). The cone area of the facies model shows a combination of coherent and clastic rocks, although fine spatial variations and details have not been identified.

The apron preserves complex, rapid vertical and lateral facies arrangements of dominantly clastic sediments (Carey and Sigurdsson, 1984) that are not comparable to a submarine fan (Carey and Sigurdsson, 1984). The arc apron geometry offshore from modern volcanic islands is extensive, with depocentres from 500 to 3600 metre water depths (Ollier et al, 1998). In proximal areas the apron is characterised by primary volcanic outcrop, slides, deltas, and debris avalanche deposits, while the coarse-grained turbidites and undifferentiated volcanic basement of the outer fan are overlain with fine sediment cover (Ollier et al, 1998). There is an intricate arrangement of primary volcanic, resedimented volcanoclastic, and volcanogenic sedimentary facies types on the arc-flanking apron, at the southern end of the Aeolian arc (Gamberi, 2001). Pyroclastic deposits are overlain by coarse volcanogenic sediment, which dominate the apron. Resedimented volcanoclastic facies (autobreccia and hyaloclastite) encircle pillow lava seamounts on the upper flanks (Gamberi, 2001). Broad erosional valleys dominate these fan deposits, with chutes and canyons separated by curved depositional swales and ridges (Gamberi, 2001; Ollier et al, 1998). Slide and slump structures may be a major feature of the facies architecture (Ollier et al, 1998; Kokelaar and Romagnoli, 1995). Deposits indicative of resedimentation processes dominate the apron, which notably change from

coarse proximal deposits to finer sediments at distal parts. These features are not included in the facies model.

Distal facies denoting broad-scale volcanoclastic deposition in the marine basins adjacent to modern arcs are thin and extensive. Apron volcanoclastics intercalate with deep marine grey-brown pelagic-hemipelagic basin sediments offshore from volcanic islands and arcs (Ollier et al, 1998). Fine-grained volcanogenic sediments contain small percentages of dispersed ash (Sigurdsson et al, 1980), other layers include fallout, pyroclastic debris flow, turbidites, and grain flows. Many deposits indicate sediment gravity flow deposition, and the spatial distribution of debris flows compared to fallout may be asymmetrical (Sigurdsson et al, 1980). The extent and particular characteristics of basin facies are not shown on the model, which would have benefited from a scale.

ANCIENT SUCCESSIONS

Geophysical, plate tectonics, and palaeontological methods, all contribute evidence to the reconstruction of ancient successions. The facies architecture of ancient arc-successions contain abrupt vertical and lateral facies changes (Mitchell, 1970; Houghton and Landis, 1989; McPhie, 1995). The apron and basin facies are the most likely to be preserved, although the central facies may be absent (Fisher and Schmincke, 1994).

Geophysical anomalies define two parallel Miocene arc belts offshore from the present day landmass on the North Island of New Zealand. Onshore outcrops of the arc-succession, reflect regional crustal evolution, including subsidence, compression, allochthon obduction, basin sedimentation, and island arc volcanism (Hayward, 1993). Primary volcanic, resedimented volcanoclastic, volcanogenic sedimentary and basin facies types have been linked with the lower flank, upper flank, crest and satellite vents of the Manukau stratovolcano (Hayward, 1993). Marine fossils have revealed that eruption and clastic deposition occurred at varying depths. Primary volcanic deposits are found within the coarse volcanoclastic slope and fine volcanoclastic base of slope facies associations. Boulder and cobble-bearing breccias and conglomerates of the coarse volcanoclastic slope facies are thought to be a proximal association that accumulated on the bathyal slopes (Hayward, 1993). These are interbedded with fine submarine channel and canyon-filling sediments that accumulated at mid bathyal depths, 1000-2000 m. Basinal facies include a submarine fan and basin floor deposits, of volcanogenic

sedimentary and volcanic poor turbidites and pelagic sediments (Hayward, 1993). Facies relationships are gradational, with coarse volcanoclastics interdigitating with the fine volcanoclastics, which in turn interfingers with basin sediments (Hayward, 1976b). The submarine sequence is complicated by terrestrial andesite flows that intrude and overlie the sequence, and folds and faults that separate outcrops into blocks (Hayward, 1976a). Central / proximal deposits undergo little transport compared with distal deposits, which are usually finer. This is reflected in the facies architecture.

A submerged basaltic seamount has similar characteristics with the subaqueous stage of a stratovolcano. A sequence of subaqueous lava flows, resedimented volcanoclastics and bedded volcanogenic sediments, from the Pliocene Ba Volcanic Group, Fiji, result from eruption and deposition on the submerged flanks of a basaltic seamount (McPhie, 1995). The controls on edifice morphology, and subaqueous sediment deposition may be likened to the initial growth stages of a submarine stratovolcano (Schmidt and Schmincke, 2001), producing rapid vertical and lateral facies changes and comparative facies architecture characteristics.

Cross-sections and a primary volcanic facies contour map produced by McPhie (1995) can be used to approximate the seamount facies architecture. The Nayoka and Dokonavato cross sections (**Figure 4.2**) have a roughly perpendicular orientation to the proposed volcanic centre, and were used as lineations to show a transition from primary massive basalt facies, to pillow fragment and monomict breccia, conglomerate and sandstone volcanogenic sedimentary facies. An increase in the proportion of resedimented volcanoclastics occurs away from the central facies, and intercalates with volcanogenic facies types. Monomict breccias and lapilli breccias become more abundant distally, and probably represent mass flow deposits. Distal deposits of massive basalt and pillow lava are probably associated with satellite vent facies on the flanks. Relationships were gradational between the breccias and coherent rocks, with bedded volcanogenic sediments blanketing them. This facies trend is consistent with the layout given by McPhie (1995), and with the facies architecture common to submarine stratovolcanoes.

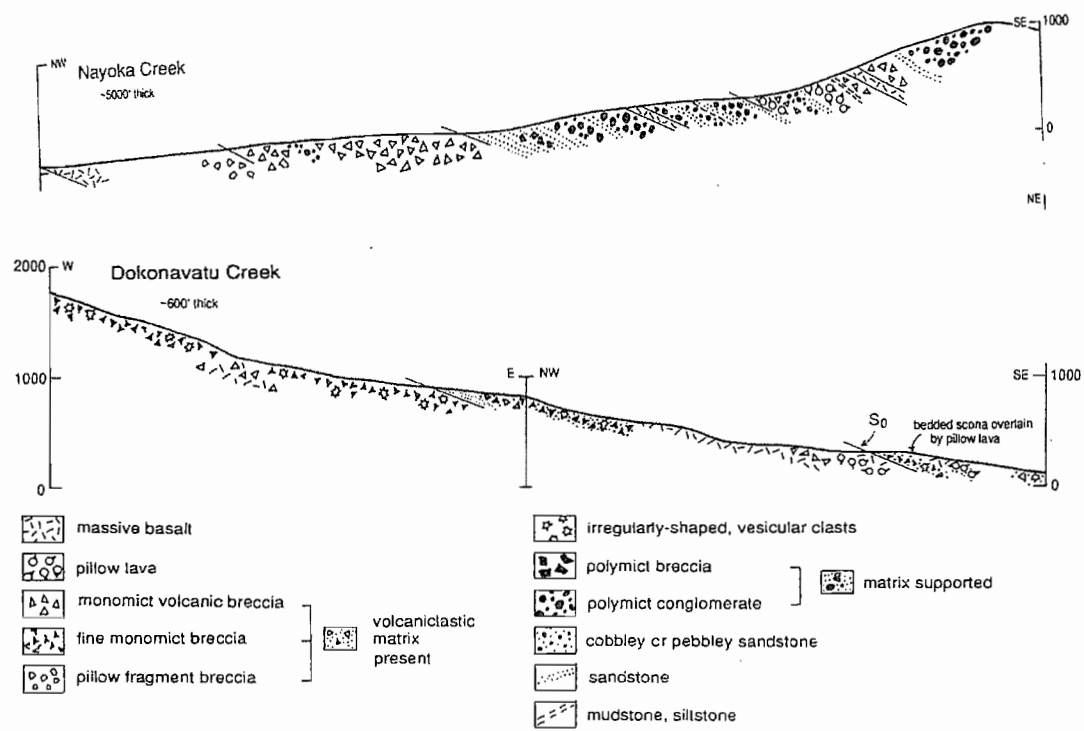


Figure 4.2: The Nayoka and Dokonavatu cross sections (from McPhie, 1995).

DISCUSSION

The submarine deposits of submerged and emergent stratovolcanoes can be better recognised and interpreted when the volcanic products and transportational and depositional processes influencing their formation are understood. Explosive and effusive volcanism has a major affect on normal background sedimentary and marine processes. Submarine volcanic deposits are well preserved and provide one of the best records of intrabasinal, and in many cases, extrabasinal volcanic activity. Submarine deposits result from the amalgamation of primary volcanic transport and marine resedimentation mechanisms. Submarine eruption-generated and syn-eruptive transport mechanisms dominate over normal resedimentation, where volcanoclastic influxes have been introduced by volcanic eruptions.

Features specific to submarine to emergent island arc edifices could be used to better identify the facies architecture and deposit features of submarine or island stratovolcanoes. A multidisciplinary approach that employs information from many areas is required to understand and interpret ancient stratovolcano and arc deposits. Although modern submarine volcanic environments are relatively inaccessible, modern settings are useful for comparison with ancient deposits. Submarine processes and facies architecture can be modelled on analogues such as seamounts and submarine shield volcanoes.

Submarine volcanic activity is important in the creation of submarine stratovolcano deposits. As pyroclastic material can exceed 95% of the total eruptive products derived from island arcs (McBirney, 1973), explosive eruptions in this setting are a significant mechanism of clast formation and transport. It would be beneficial to observe submarine eruption columns and explosive eruptions at depth. Further studies of the effects of hydrostatic pressure on fragmentation and submarine eruption styles are required, as they control volcano morphology and deposit types. This information would further develop current understanding of stratovolcanoes, the dynamics of submarine eruptions and the recognition of deposits. It could also benefit regional tectonics and arc and basin evolution reconstructions.

REFERENCES

- Ballance, P. F. and M. R. Gregory (1991). "Parnell Grits - Large subaqueous volcanoclastic gravity flows with multiple particle support mechanisms." Sedimentation in Volcanic Settings, SEPM Spec. Publ. **45**: 189-200.
- Batiza, R. and J. D. L. White (2001). Submarine Lavas and Hyaloclastite. Encyclopedia of Volcanoes. H. Sigurdsson. San Diego, Academic Press: 361-381.
- Carey, S. (2001). Volcanoclastic sedimentation around island arcs. Encyclopedia of Volcanoes. H. Sigurdsson. San Diego, Academic Press: 627-642.
- Carey, S. and H. Sigurdsson (1984). A Model of Volcanogenic Sedimentation in Marginal Basins, Marginal Basin Geology, Volcanic and associated sedimentary and tectonic processes in modern and ancient marginal basins, B. P. Kokelaar and M. F. Howells. Oxford, Blackwell Scientific Publications: 37-57.
- Cashman, K. V. and R. S. Fiske (1991). "Fallout of Pyroclastic Debris from Submarine Volcanic Eruptions." Science **253**: 275-280.
- Cas, R. A. F. and J. V. Wright (1987). Volcanic Successions, Modern and Ancient. London, Allen and Unwin Ltd.
- Cas, R. A. F. and J. V. Wright (1991). "Subaqueous pyroclastic flows and ignimbrites; an assessment." Bulletin of Volcanology **53**(5): 357-380.
- Cas, R. A. F. (1992). "Submarine Volcanism: Eruption Styles, Products, and Relevance to Understanding the Host-Rock Successions to Volcanic-Hosted Massive Sulfide Deposits." Economic Geology **87**: 511-541.
- Clague, D. A., A. S. Davis, Bishoff, J. L., Dixon, J. E., Geyer, R. (2000). "Lava bubble-wall fragments formed by submarine hydrovolcanic explosions on Lo'ihi Seamount and Kilauea Volcano." Bulletin of Volcanology **61**: 437-449.

Davidson, J. and S. De Silva (2001). Composite Volcanoes. Encyclopedia of Volcanoes. H. Sigurdsson. San Diego, Academic Press: 361-381.

Deplus, C., A. Le Friant, Boudon, G., Komorowski, J. C., Villemant, B., Harford, C., Segoufin, J., Cheminee, J. L. (2001). "Submarine evidence for large-scale debris avalanches in the Lesser Antilles Arc." Earth and Planetary Science Letters **192**(2): 145-157.

Dickinson, W. R. (1995). Forearc Basins. Tectonics of Sedimentary Basins. C. J. Busby and R. V. Ingersoll. Cambridge, Blackwell Science.

Einsele, G. (2000). Volcaniclastic sediments. Sedimentary Basins, evolution, facies, and sediment budget. G. Einsele. Berlin-Heidelberg-New York, Springer-Verlag: 64-74.

Fisher, R. V. (1984). Submarine volcaniclastic rocks. In: Marginal Basin Geology, Volcanic and associated sedimentary and tectonic processes in modern and ancient marginal basins, B. P. Kokelaar and M. F. Howells. Oxford-London-Edinburgh-Boston-Palo Alto-Melbourne, Blackwell Scientific Publications:

Fisher, R. V. and H. U. Schmincke (1984). Pyroclastic Rocks. Berlin-Heidelberg-New York-Tokyo, Springer-Verlag.

Fisher, R. V. and G. A. Smith (1991). "Volcanism, Tectonics and Sedimentation." Sedimentation in Volcanic Settings, SEPM Spec. Publ. **45**: 1-5.

Fisher, R. V. and H. U. Schmincke (1994). Volcaniclastic Sediment Transport and Deposition. Sediment transport and Depositional Processes. K. Pye. Oxford, Blackwell Scientific Publications: 351-388.

Fiske, R. S. and T. Matsuda (1964). "Submarine Equivalents of Ash Flows in the Tokiwa Formation, Japan." American Journal of Science **262**(1-5): 76-106.

Fornari, D. J. (1986). "Submarine lava tubes and channels." Bulletin of Volcanology **48**: 291-298.

Fritz, W. J. and M. F. Howells (1991). "A shallow marine volcanoclastic facies model: an example from sedimentary rocks bounding the subaqueously welded Ordovician Garth Tuff, North Wales, U.K." Sedimentary Geology **74**: 217-240.

Gamberi, F. (2001). "Volcanic facies associations in a modern volcanoclastic apron (Lipari and Vulcano offshore, Aeolian Island Arc)." Bulletin of Volcanology **63**(4): 264-273.

Gorsline, 1984

Hayward, B. W. (1976a). "Lower Miocene Stratigraphy and Structure of the Waitakere Ranges and The Waitakere Group (new)." N.Z. Journal of Geology and Geophysics **19**(6): 871-895.

Hayward, B. W. (1976b). "Lower Miocene Geology and Sedimentary History of the Muriwai - Te Waharoa Coastline, North Auckland, New Zealand." N.Z. Journal of Geology and Geophysics **19**(5): 639-662.

Hayward, B. W. (1979a). Ancient undersea volcanoes: a guide to the geological formations at Muriwai, West Auckland, The Geological Society of New Zealand.

Hayward, B. W. (1979b). "Eruptive History of the Early to Mid Miocene Waitakere Volcanic Arc, and Palaeogeography of the Waitemata Basin, Northern New Zealand. " Journal of the Royal Society of New Zealand **9** (3): 297-320.

Hayward, B. W. (1993). The Tempestuous 10 Million Year Life of a Double Arc and Intra-arc Basin - New Zealand's Northland Basin in the Early Miocene. South Pacific Sedimentary Basins. P. F. Ballance. Amsterdam-London-New York-Tokyo, Elsevier. **2**: 113-142.

Head, J. W., III and L. Wilson (2003). "Deep submarine pyroclastic eruptions; theory and predicted landforms and deposits." Journal of Volcanology and Geothermal Research **121**(3-4): 155-193.

Heiken, G. and K. Wohletz (1991). "Fragmentation Processes in Explosive Volcanic Eruptions." Sedimentation in Volcanic Settings, SEPM Spec. Publ. **45**: 19-26.

Houghton, B. F. and C. A. Landis (1989). "Sedimentation and volcanism in a Permian arc-related basin, southern New Zealand." Bulletin of Volcanology **51**: 433-450.

Ingersoll, R. V. and C. J. Busby (1995). Tectonics of Sedimentary Basins. Tectonics of Sedimentary Basins. C. J. Busby and R. V. Ingersoll. Cambridge, Blackwell Science: 1-51.

Jones, J. G. (1968). "Pillow Lava and Pahoehoe." The Journal of Geology **76**: 485-488.

Kano, K., T. Yamamoto, Takeuchi, K. (1993). "A Miocene island-arc volcanic seamount: the Takashibiyama Formation, Shimane Peninsula, SW Japan." Journal of Volcanology and Geothermal Research **59**(1-2): 101-119.

Kano, K. Orton, G. J. & Kano, T. (1994). A hot Miocene subaqueous scoria-flow deposit in the Shimane Peninsula, SW Japan. Journal of Volcanology and Geothermal Research **60**, 1-14.

Kano K. (1996). A Miocene coarse volcanoclastic mass-flow deposit in the Shimane Peninsula, SW Japan: product of a deep submarine eruption?, Bulletin of Volcanology **58**, 131-143

Karig, D. E. and G. F. Moore (1975). "Tectonically controlled sedimentation in marginal basins." Earth and Planetary Science Letters **26**: 233-238.

Kokelaar, P. (1986). "Magma-water interactions in subaqueous and emergent basaltic volcanism." Bulletin of Volcanology **48**: 275-289.

Kokelaar, P. and C. Busby (1992). "Subaqueous Explosive Eruptions and Welding of Pyroclastic Deposits." Science **257**: 196-201.

Kokelaar, P. and C. Romagnoli (1995). "Sector Collapse, Sedimentation and Clast Population Evolution at an Active Island-Arc Volcano - Stromboli, Italy." Bulletin of Volcanology **57**(4): 240-262.

Larue, D. K., A. L. Smith, et al. (1991). "Oceanic island stratigraphy in the Caribbean region: don't take it for granite." Sedimentary Geology **74**: 289-308.

Lowe D. R. (1979). Sediment Gravity Flows: Their classification and some problems of application to natural flows and deposits, SEPM Spec. Pub. **27**, 75-82

Lowe D. R. (1982). "Sediment Gravity Flows: II. Depositional Models with special reference to the deposits of high density turbidity currents." Journal of Sedimentary Petrology **52**(1): 279-297.

Mandeville, C. W., Carey S., and Sigurdsson, H. (1996). Sedimentology of the Krakatau 1883 Submarine pyroclastic deposits, Bulletin of Volcanology **57**, 512-529

Manville, V., Segschneider, B., and White, J. D. L. (2002). "Hydrodynamic behaviour of Taupo 1800a pumice: implications for the sedimentology of remobilized pyroclasts." Sedimentology **49**: 955-976.

Marsaglia, K. M. (1995). Interarc and Backarc Basins. Tectonics of Sedimentary Basins. C. J. Busby and R. V. Ingersoll. Cambridge, Blackwell Science.

McBirney, A. R. (1963). "Factor governing the nature of submarine volcanism." Bulletin Volcanologique **26**: 455-469.

McBirney, A. R. (1973). "Factors Governing the Intensity of Explosive Andesitic Eruptions." Bulletin Volcanologique **37**: 443-453.

McLeod, P., S. Carey, Sparks, R. S. J. (1999). "Behaviour of particle-laden flows into the ocean: experimental simulation and geological implications." Sedimentology **46**: 523-536.

McPhie, J. and R. L. Allen (1992). "Facies architecture of mineralised submarine volcanic sequences: Cambrian Mount Read Volcanics, Western Tasmania." Economic Geology **87**: 587-596.

McPhie, J., R. L. Allen, Doyle, M. (1993). Volcanic Textures. University of Tasmania, Hobart, Centre for Ore Deposit and Exploration Studies.

McPhie, J. (1995). "A Pliocene Shoaling Basaltic Seamount - Ba Volcanic Group at Rakiraki, Fiji." Journal of Volcanology and Geothermal Research **64**(3-4): 193-210.

Mitchell, A. H. G. (1970). "Facies of an Early Miocene Volcanic Arc, Malekula Island, New Hebrides." Sedimentology **14**: 201-243.

Ollier G., Cochonat P., Lenat J. F. & Labazuy P. (1998). Deep-sea volcanoclastic sedimentary Systems: an example from La Fournaise volcano, Reunion Island, Indian Ocean, Sedimentology **45**, 293-330.

Orton, G. J. (1996). Volcanic Environments. Sedimentary Environments: Processes, Facies and Stratigraphy. H. G. Reading. London, Blackwell Science: 485-566.

Pickering, K. T., D. A. V. Stow, et al. (1986). "Deep-water facies, processes and models: A review and classification scheme for modern and ancient sediments." Earth-Science Reviews **23**: 75-174.

Pickering, K. T., R. N. Hiscott, et al. (1988). Deep Marine Environments, Clastic Sedimentation and Tectonics. London, Unwin Hyman Ltd.

Schmidt, R., and Schmincke, H. (2001). Seamounts and island building. Encyclopedia of Volcanoes. San Diego, Academic Press: 383-402.

Schneider, J. L., A. Le Ruyet, et al. (2001). "Primary or secondary distal volcanoclastic turbidites: how to make the distinction? An example from the Miocene of New Zealand (Mahia Peninsula, North Island)." Sedimentary Geology **145**(1-2): 1-22.

Sigurdsson, H. Sparks R. S. J. Carey, S. N. & Huang, T. C. (1980). Volcanogenic Sedimentation in the Lesser Antilles Arc, Journal of Geology **88**: 523-540.

Smith, G. A. and R. D. Smith (1985). "Specific Gravity Characteristics of Recent Volcanoclastic Sediment: Implications for Sorting and Grain Size Analysis." Journal of Geology **93**(5): 619-622.

Smith, G. A. and C. A. Landis (1995). Intra-arc Basins. Tectonics of Sedimentary Basins. C. J. Busby-Spera and R. V. Ingersoll. Cambridge, Blackwell Science: 263-298.

Stow, D. A. V. and D. J. W. Piper (1984). Deep-water fine-grained sediments: facies models. Fine Grained Sediments. D. A. V. Stow and D. J. W. Piper. Oxford, Blackwell Scientific Publications. **15**: 611-646.

Stow, D. A. V. (1994). Deep sea processes of sediment transport and deposition. Sediment Transport and Deposition. K. Pye. Cambridge, Blackwell Scientific Publications: 257-291.

Stow, D. A. V., H. G. Reading, and Collinson, J. D. (1996). Deep Seas. Sedimentary Environments: Processes, Facies and Stratigraphy. H. G. Reading. Oxford, Blackwell Science: 395-453.

Walker, G. P. L. and R. Croasdale (1970). "Characteristics of Some Basaltic Pyroclastics." Bulletin Volcanologique **35**(2): 303-317.

Walker, G. P. L. (1973). "Explosive volcanic eruptions - a new classification scheme." Geol. Rundschau **62**: 431-446.

Walker 1975

Walker, G. P. L. (2001). Basaltic volcanoes and volcanic systems. Encyclopedia of Volcanoes. H. Sigurdsson. San Diego-San Francisco-New York-Boston-London-Sydney-Toronto, Academic Press. **1**: 283-289.

White, J. D. L. (2000). "Subaqueous eruption-fed density currents and their deposits." Precambrian Research **101**: 87-109.

Wilson, M. (1989). Igneous Petrogenesis. London, Unwin Hyman.

Wright, I. C. (1996). "Volcaniclastic processes on modern submarine arc stratovolcanoes: Sidescan and photographic evidence from the Rumble IV and V volcanoes, southern Kermadec Arc (SW Pacific)." Marine Geology **136**(1-2): 21-39.

Yamagishi, H. (1985). "Growth of pillow lobes - Evidence from pillow lavas of Hokkaido, Japan, and North Island, New Zealand." Geology **13**: 499-502.

Yamagishi, H. (1991). "Morphological and sedimentological characteristics of the Neogene submarine coherent lavas and hyaloclastites in Southwest Hokkaido, Japan." Sedimentary Geology **74**(1-4): 5-23.

Yamazaki, T. Kato, I. Muroi, I. and Abe, M. (1973). Textural Analysis and flow mechanism of The Donzurubo Subaqueous pyroclastic flow deposits, Bulletin Volcanologique **37**, 231-244

APPENDIX 2

Nomenclature

Terms used in the field

(from McPhie et al, 1993)

Sedimentary grainsize classification:

- Sand: <2 mm
- Granule: 2-4 mm
- Fine pebble: 4 mm-1.6 cm
- Medium pebble: 1.6-3.2 cm
- Coarse pebble: 3.2-6.4 cm
- Cobble: 6.4-25.6 cm
- Boulder: >25.6 cm

Pyroclast grainsize classification

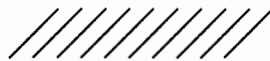
- Fine ash: <1/16 mm
- Coarse ash: 1/16-2 mm
- Lapilli tephra: 2-64 mm
- Bomb / block tephra >64 mm

Bedding thickness classification:

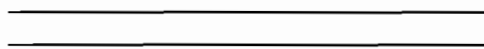
- Laminated: <1 cm
- Very thinly bedded: 1-3 cm
- Thinly bedded: 3-10 cm
- Medium: 10-30 cm
- Thick: 30-100 cm
- Very thick: >100 cm

Bedforms

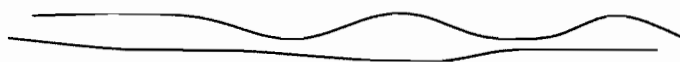
- Cross bedded



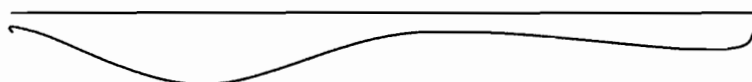
- Planar



- Pinch and swell



- Infilling

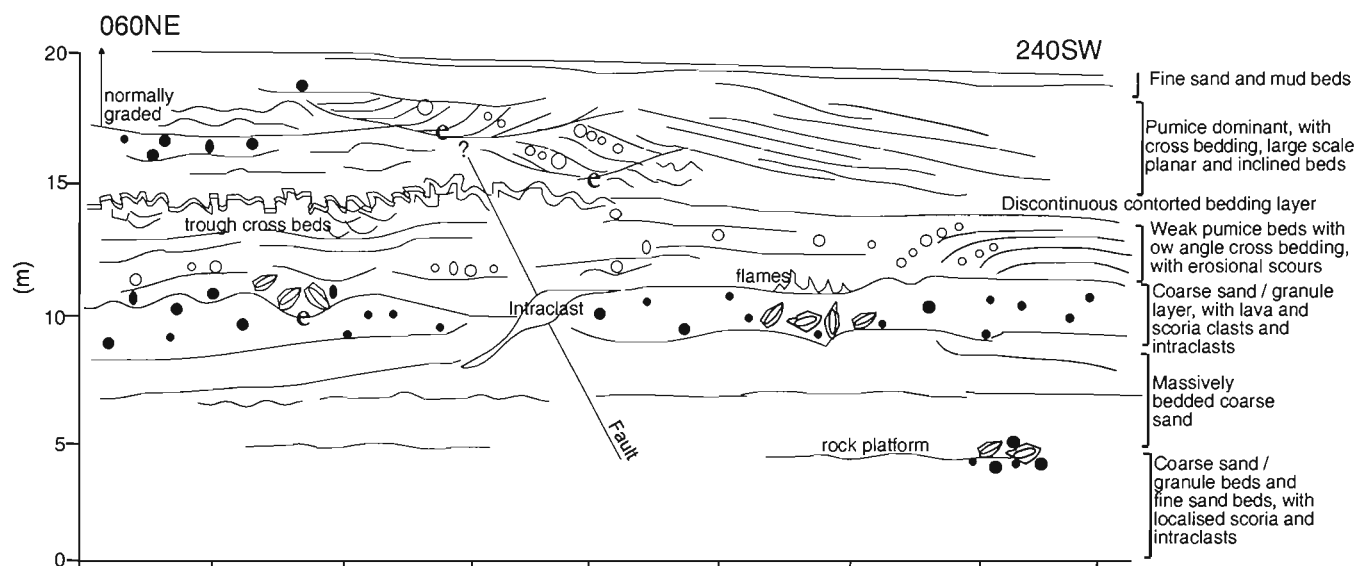


APPENDIX 3

Stratigraphic details of study sites

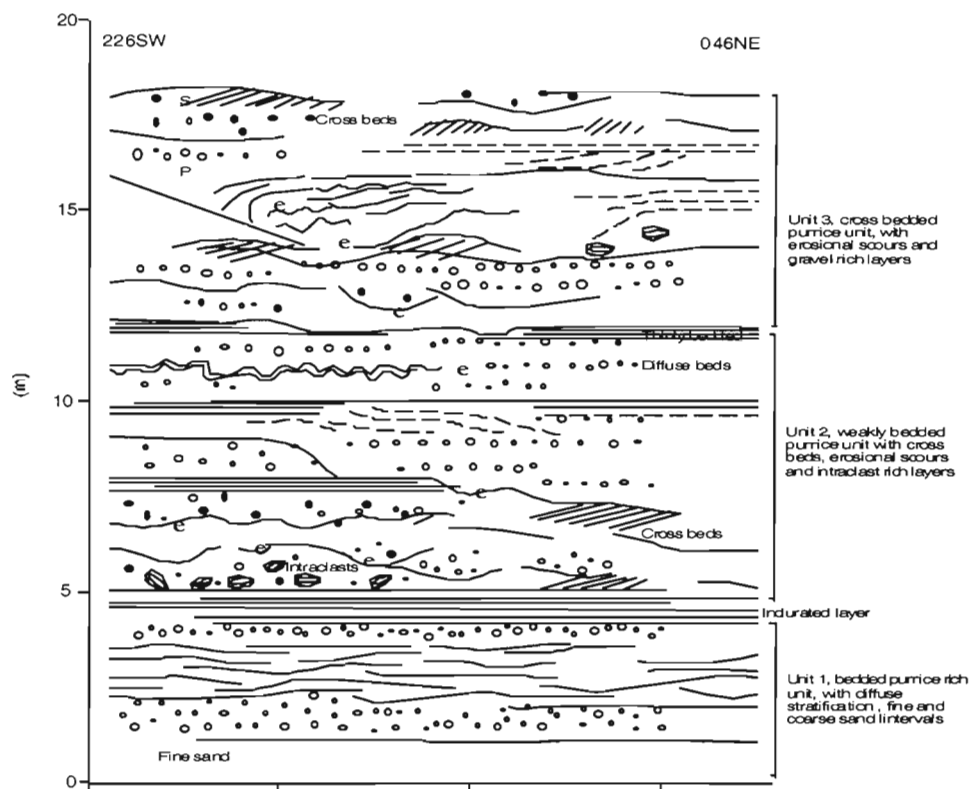
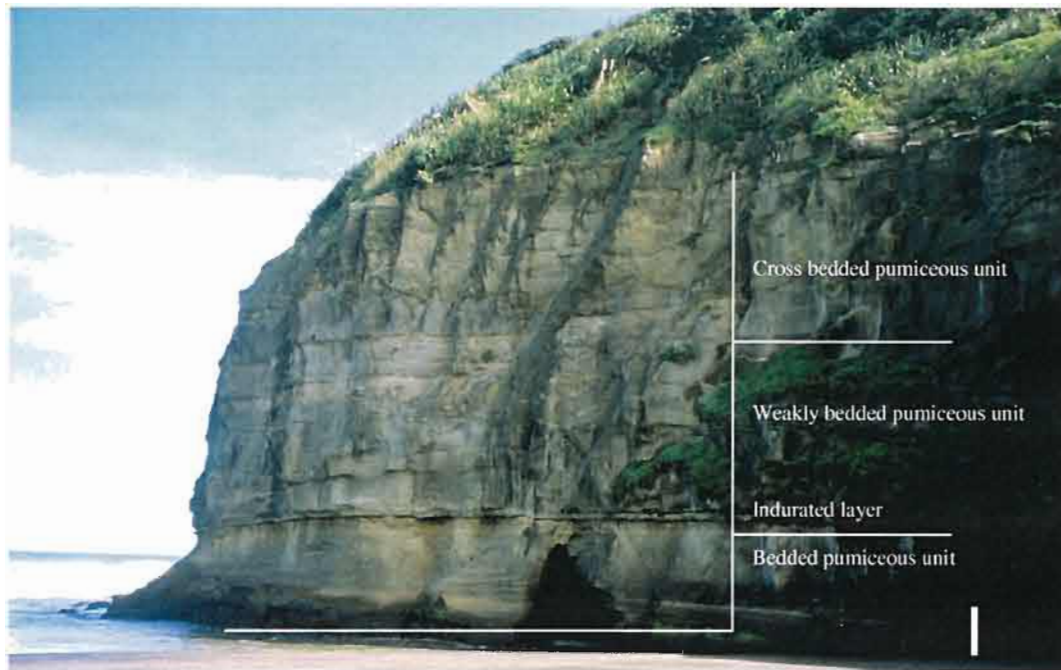
3A. Site 1, section A, photo and section sketch.

* See location of section sketch marked on the photo (3 m scale bar).



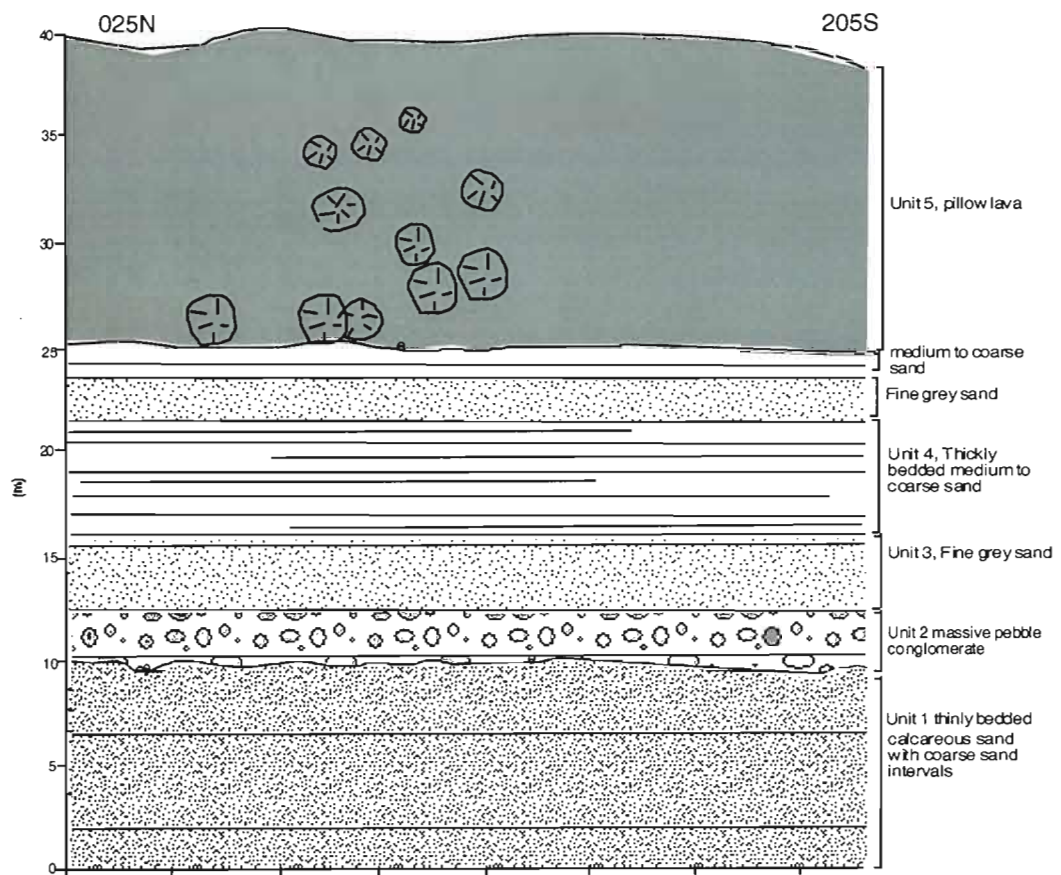
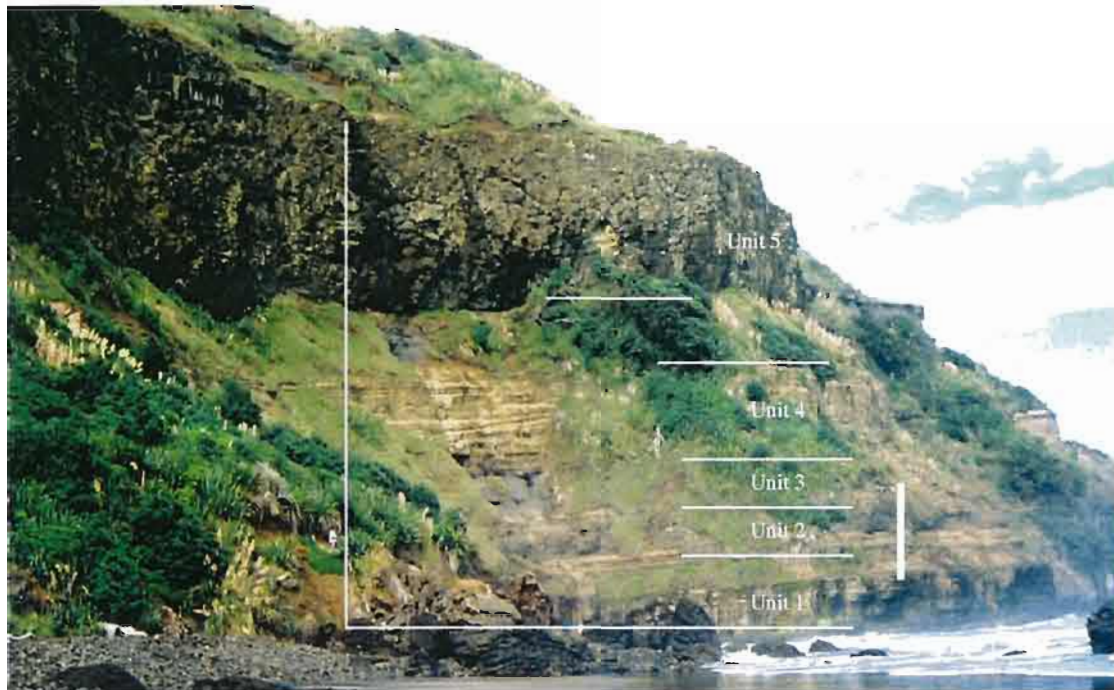
3B. Site 1, section B, photo and section sketch.

* See location of section sketch marked on the photo (2 m scale bar).



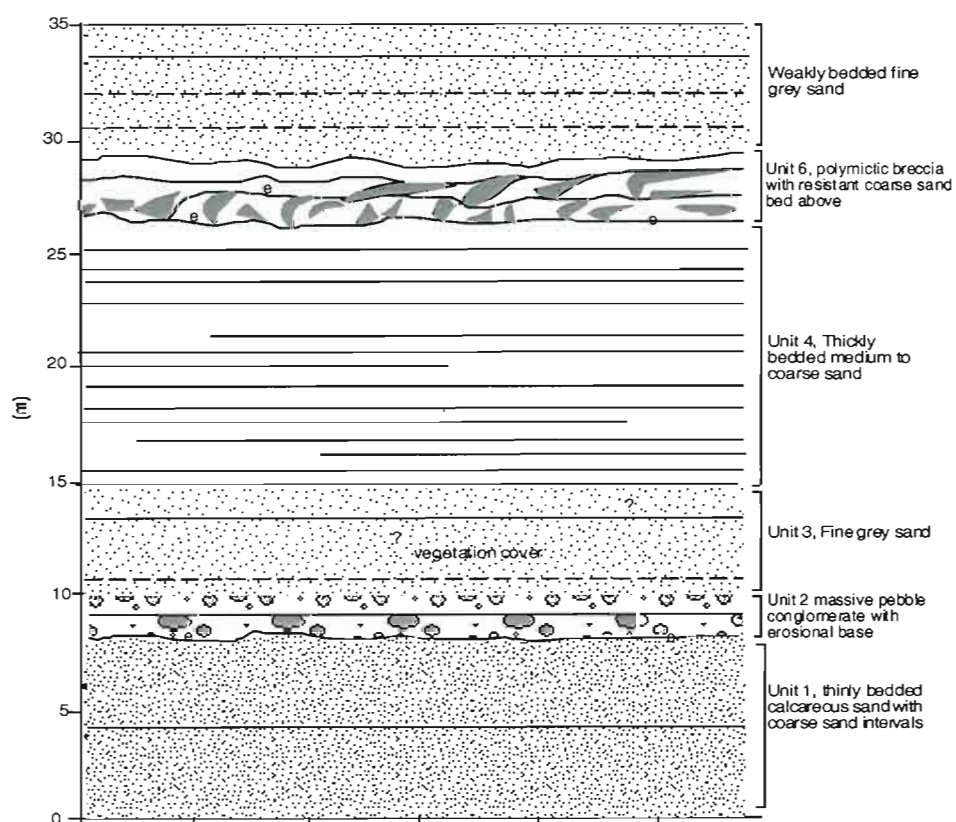
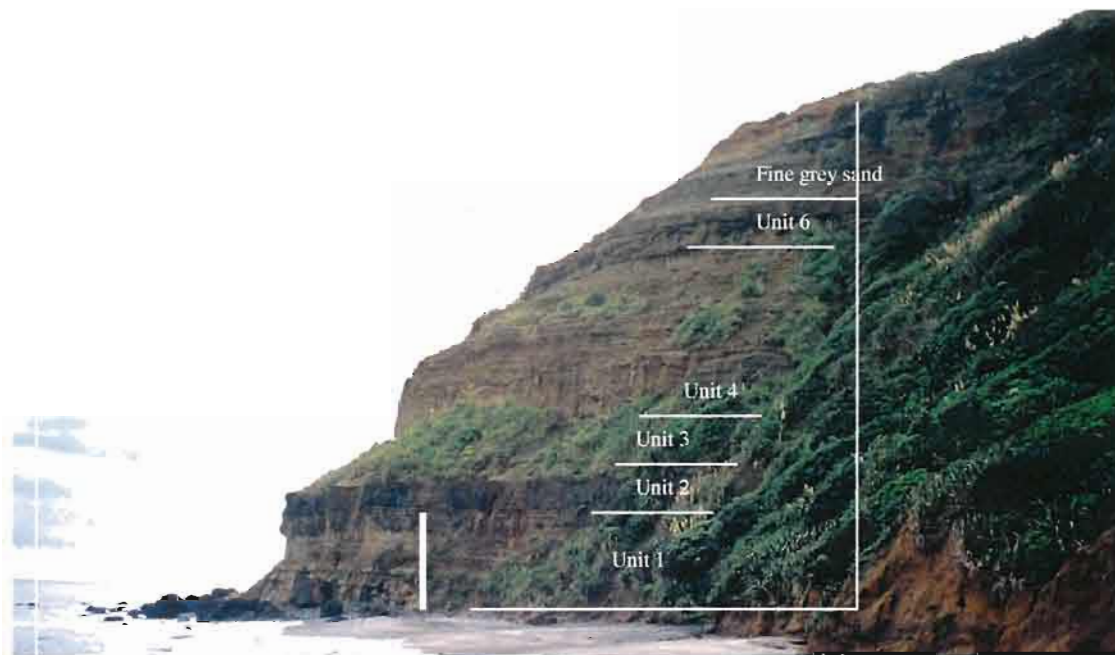
3C. Site 2, section A, photo and section sketch.

* See location of section sketch marked on the photo (10 m scale bar).



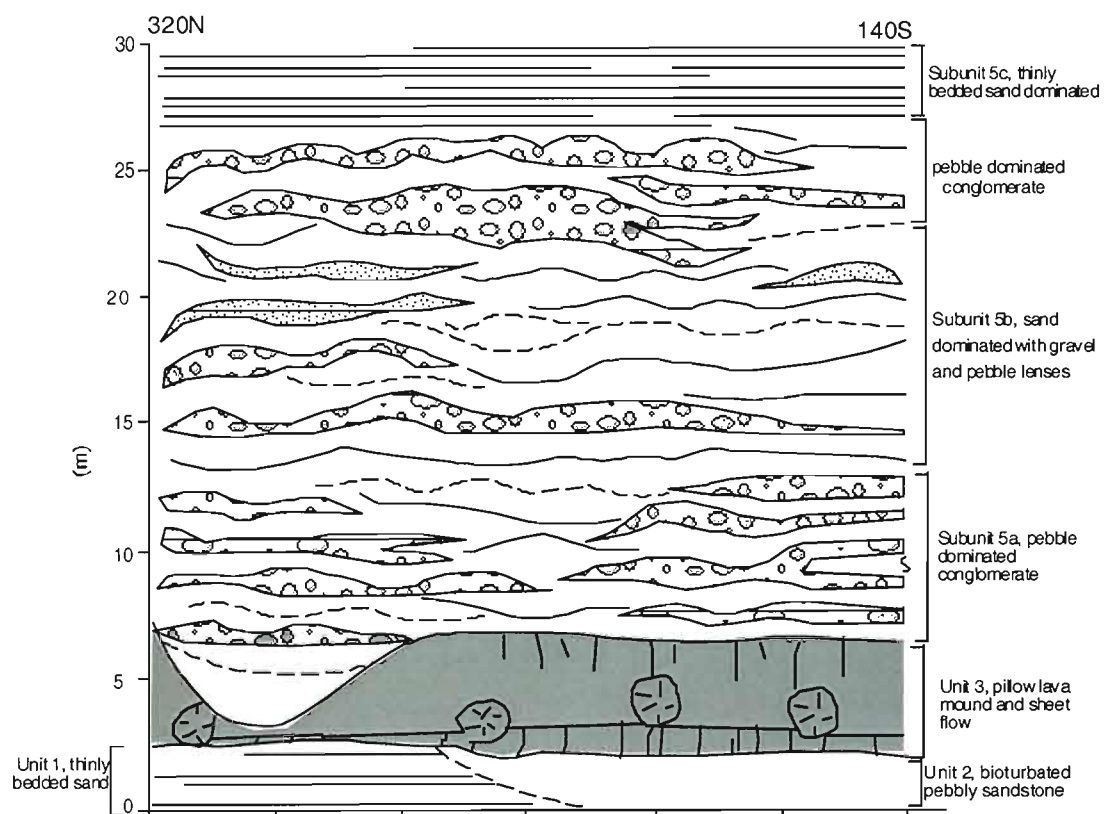
3D. Site 2 section C, photo and section sketch.

See location of section sketch marked on the photo (8 m scale bar).



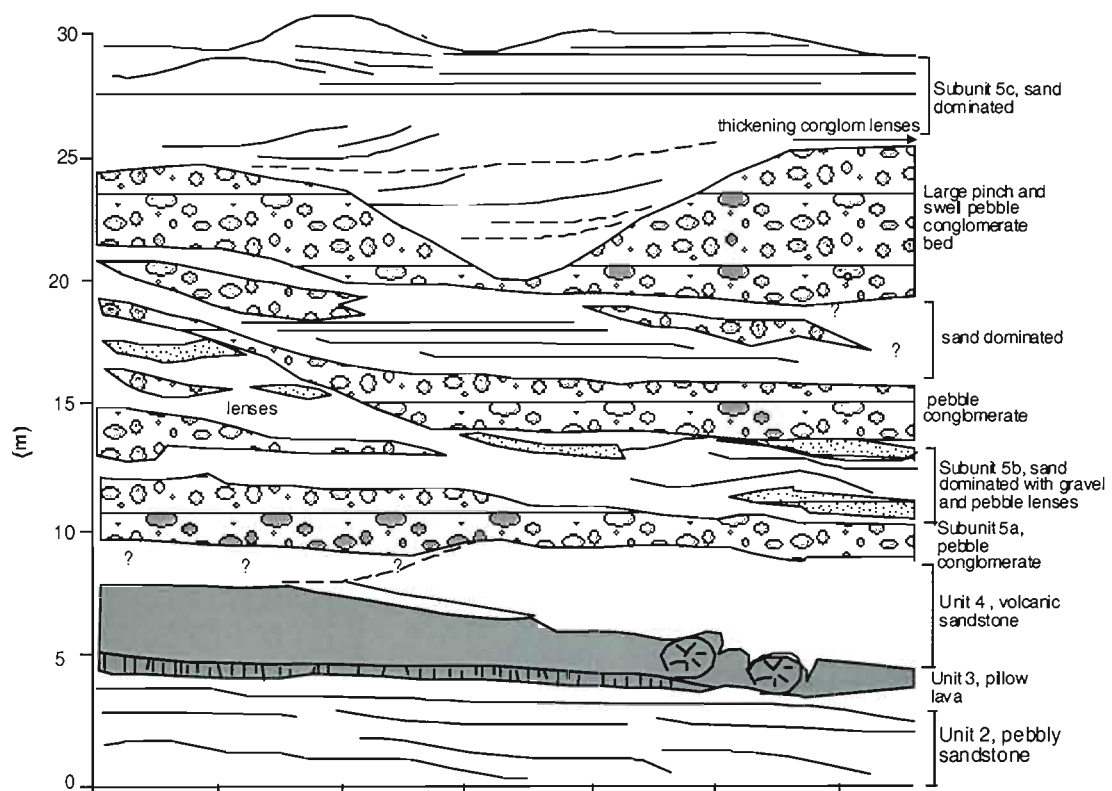
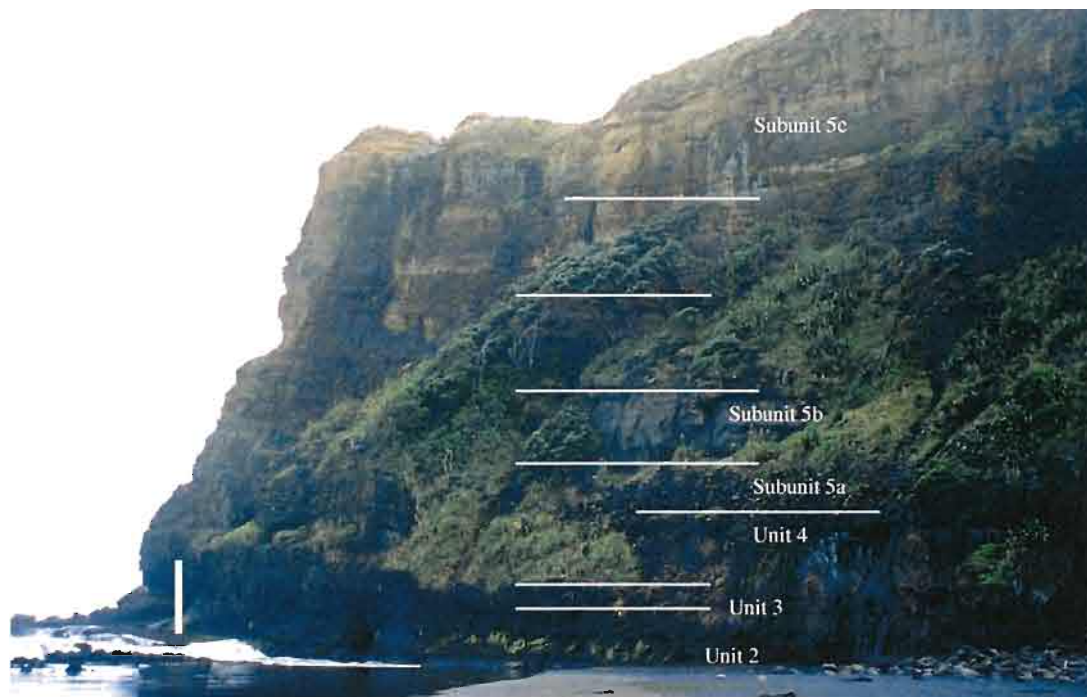
3E. Site 3, section B, photo and section sketch.

*See location of section sketch marked on the photo (2.5 m scale bar).



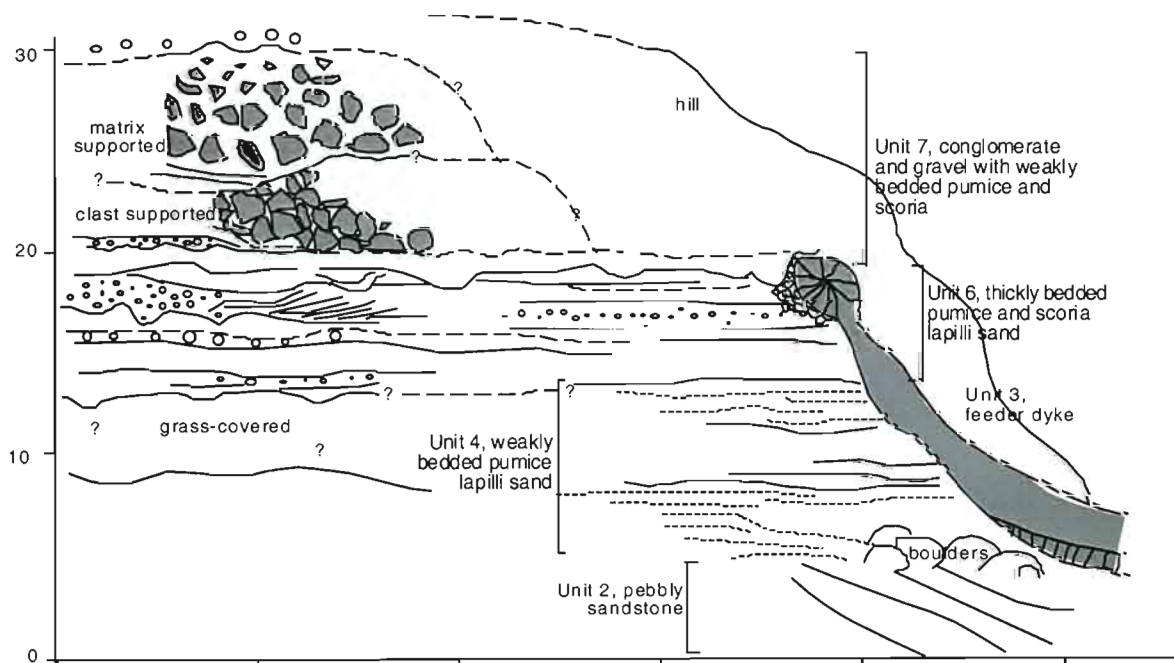
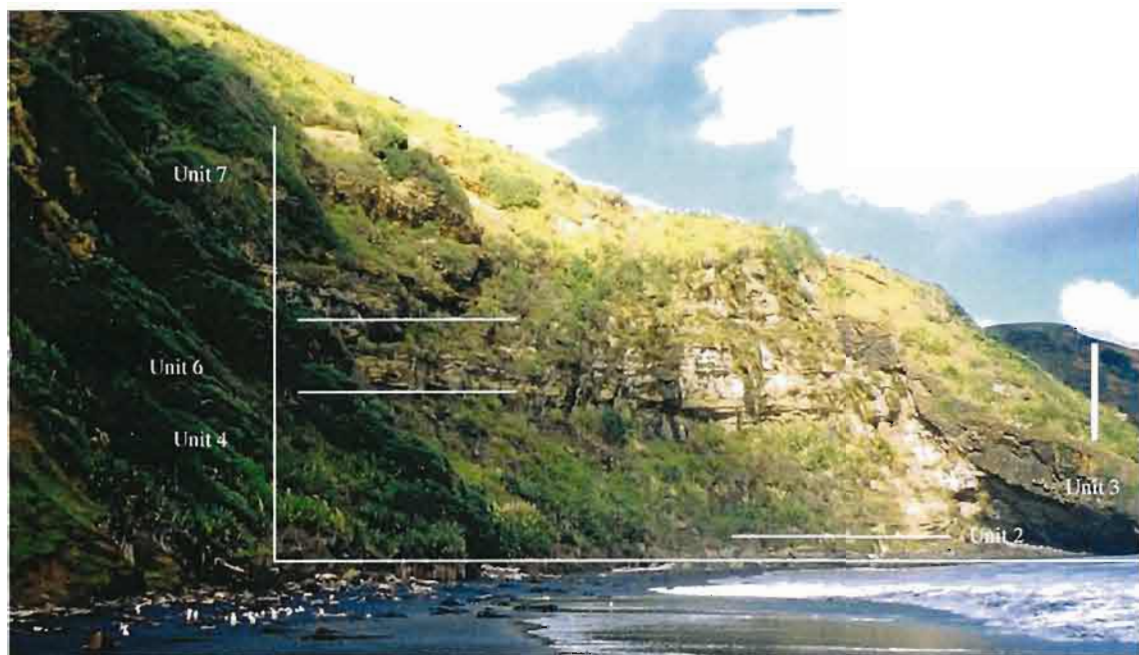
3F. Site 3, section C, photo and section sketch.

*See location of section sketch marked on the photo (5 m scale bar).



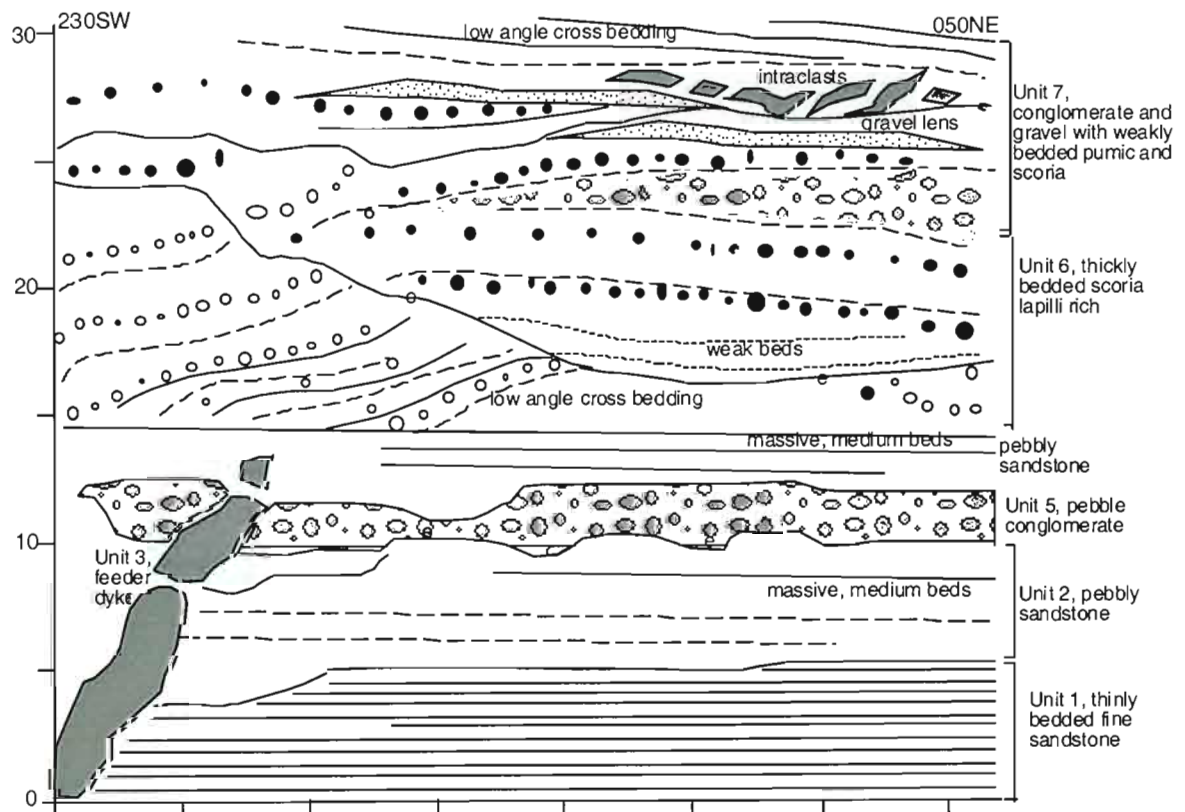
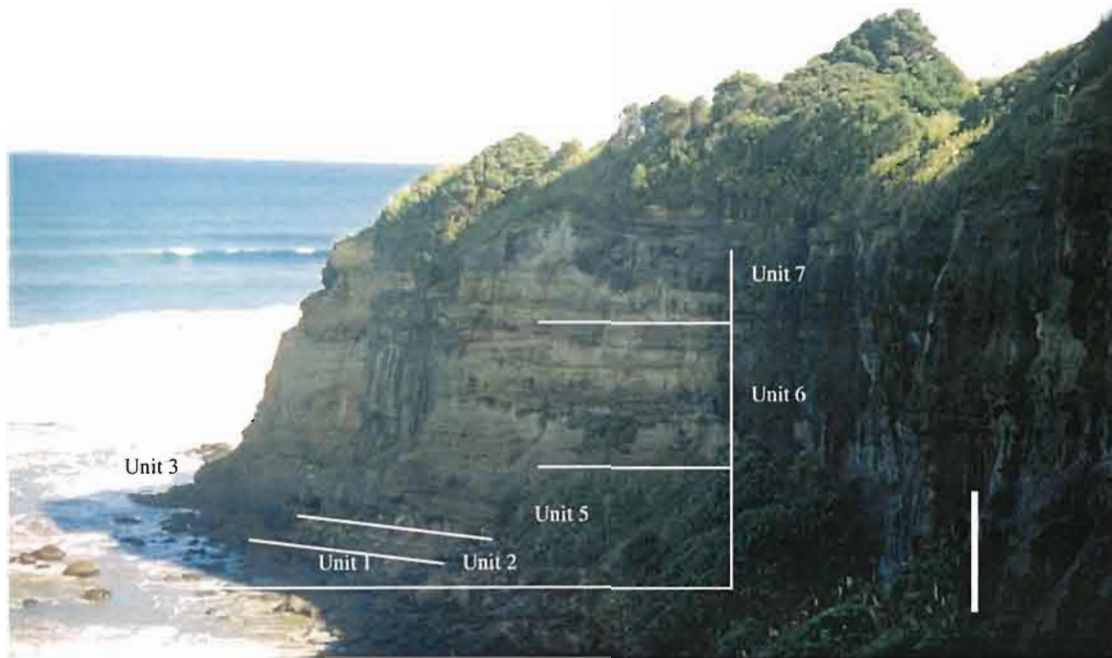
3G. Site 4, section A, photo and section sketch.

*See location of section sketch marked on the photo (10 m scale bar).



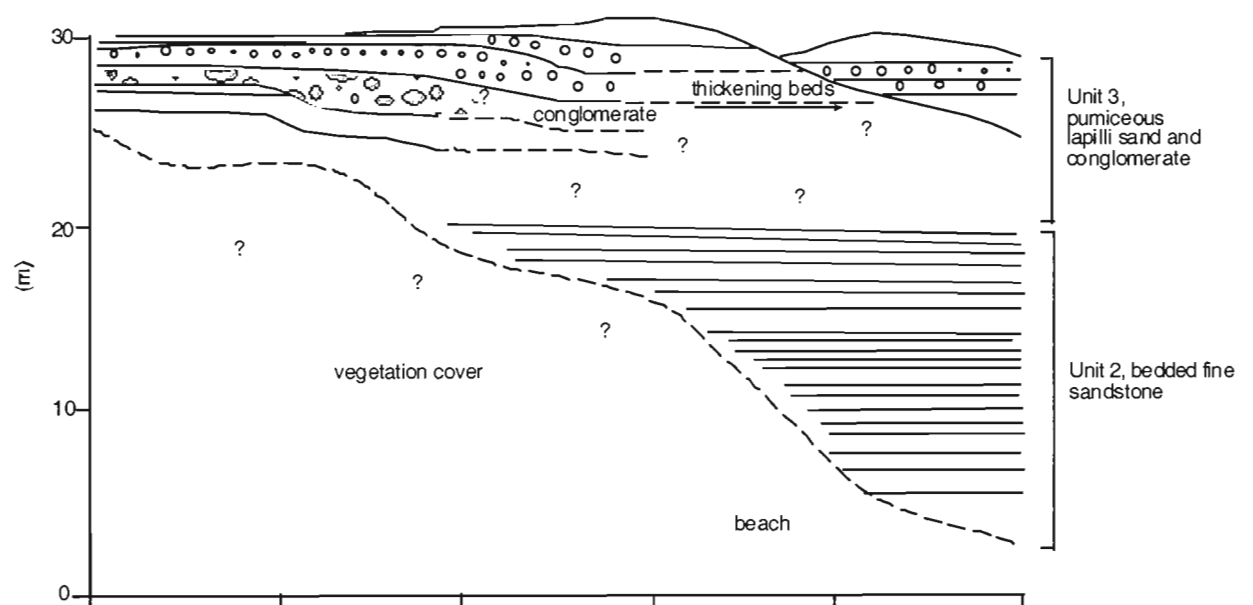
3H. Site 4, section B, photo and section sketch.

*See location of section sketch marked on the photo (10 m scale bar).



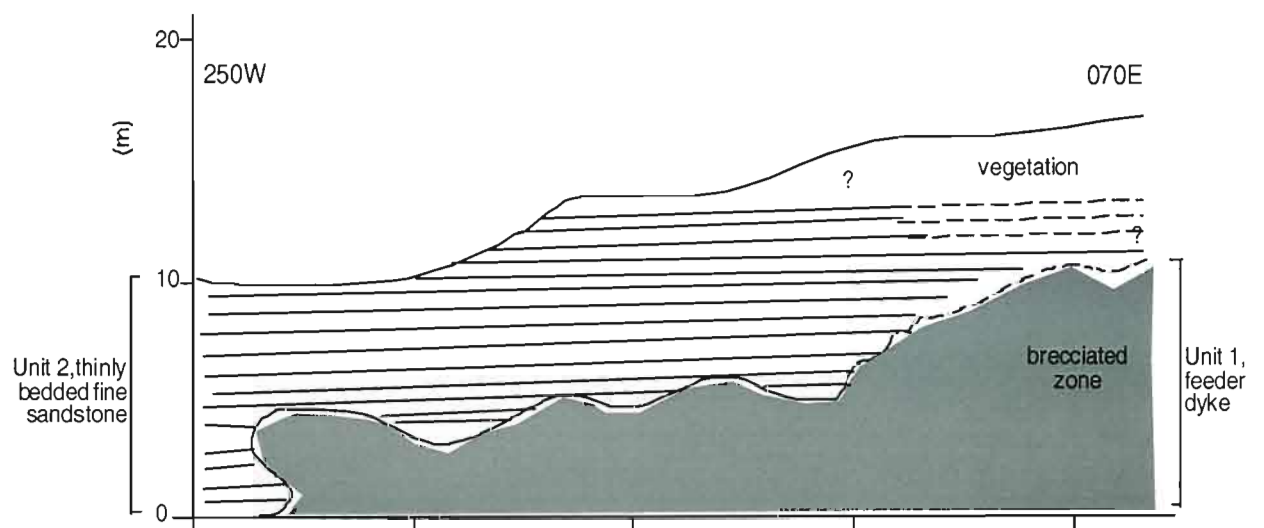
3I. Site 5, section A and B photo and section sketch.

*See location of section sketch marked on the photo (10 m scale bar).



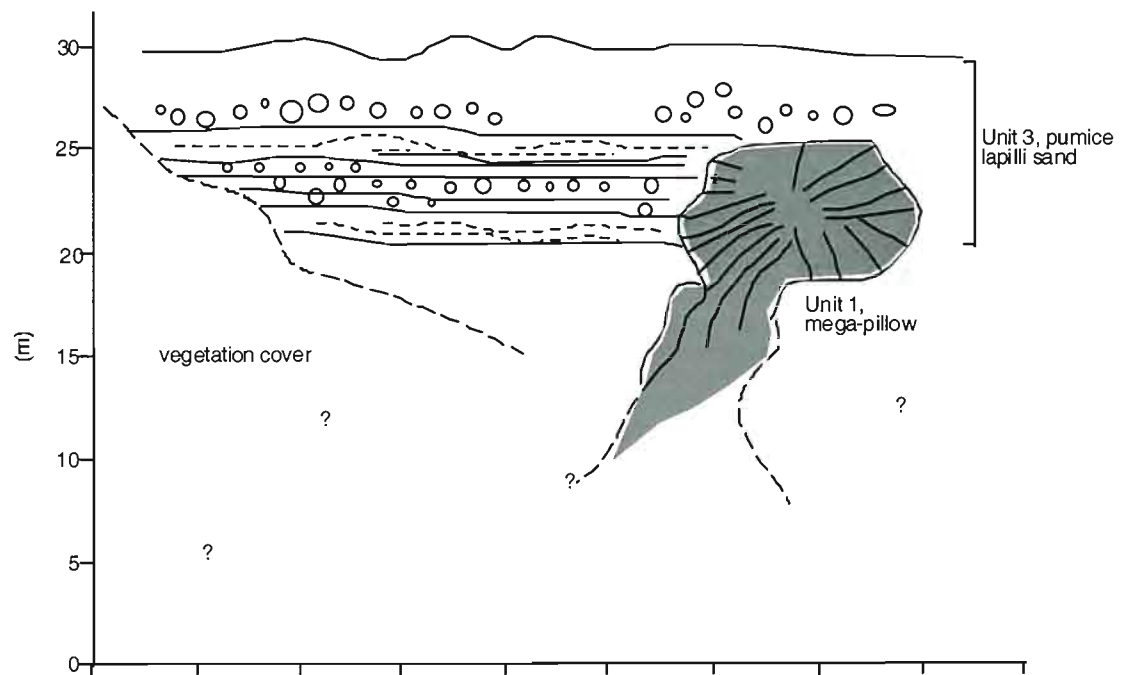
3J. Site 5, section C1, photo and section sketch.

*See location of section sketch marked on the photo (2 m scale bar).



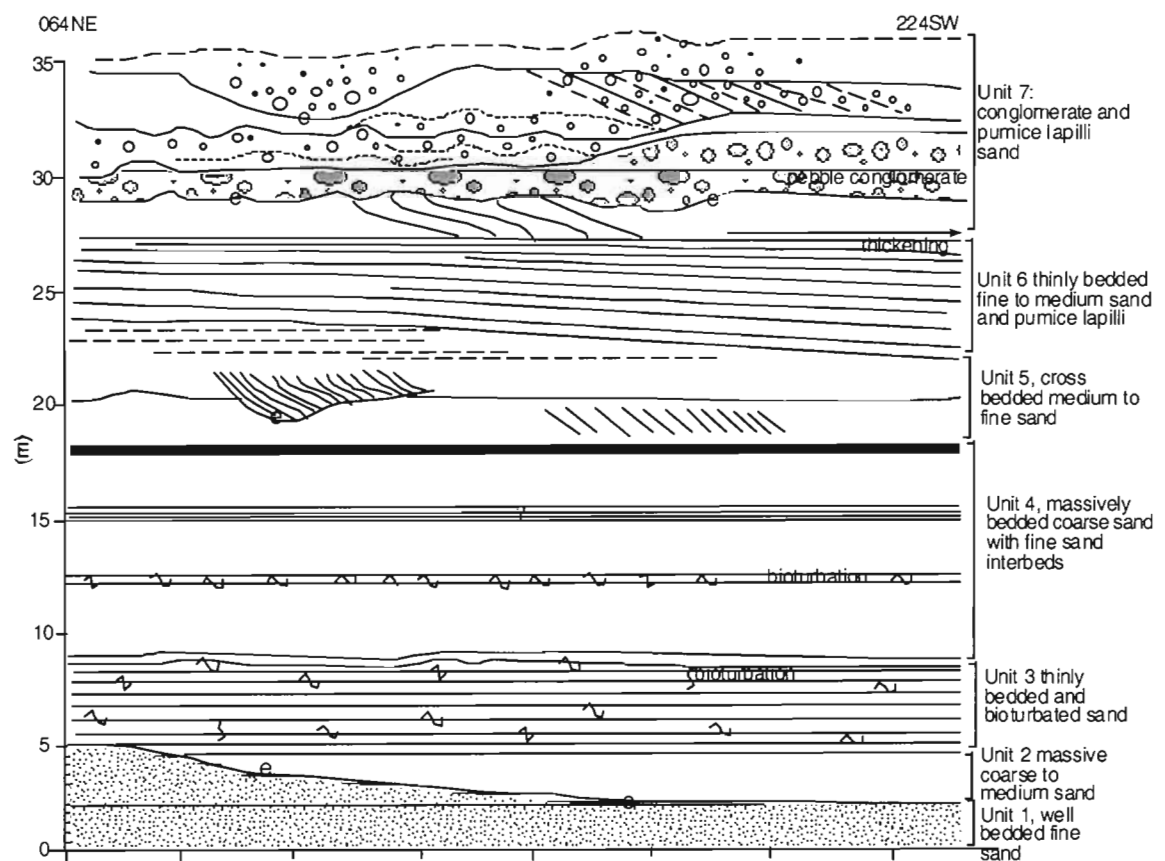
3K. Site 5, section C2 photo and section sketch.

*See location of section sketch marked on the photo (5 m scale bar).



3L. Site 6, section A, photo and section sketch.

*See location of section sketch marked on the photo (10 m scale bar).



APPENDIX 4

Thin Section Data

| PROPERTIES OF COHERENT VOLCANIC COMPONENTS | | | | | | | | | | |
|--|----------------------------|--|---------------------------|------------------------------------|---|-------------------------|--|--|--------------------------|---|
| | Sample No. | NZM 1/7 | NZM 3/2 | NZM 5 | NZM 3/2 | NZM 3/3A | NZM 1/7E | NZM 0/1A | NZM 0/1B | NZM 0/1C |
| | Type | Lava | Lava | Lava | Scoria | Scoria | Hyaloclastite | Pumice | Pumice | Pumice |
| Grainsize Estimations# % | <10 _{mm} | 10% | 70% | 20% | 25% | 18% | 90% | 15% | 17% | 28% |
| | 10-20 _{mm} | 80% | * | 50% | 60% (vesicles) | 80% | 10% | 85% | 80% | 60% |
| | 20-30 _{mm} | * | 25% | 20% | 15% | 2% | * | * | 2% | 10% |
| | 30-40 _{mm} | 10% | 5% | 10% | * | * | * | * | 1% | 2% |
| | 40-50 _{mm} | * | * | * | * | * | * | * | * | * |
| Vesicle size | | <10m-30m | Bimodal: <10, 40-50m | <10m-30m | <10m-20m | <10m-20m | * | 10m-20m | <10m | <10m |
| Components# % | Glass | 15% | 30% | 25% | 35% | 40% | 90% | 70% | 60% | 25% |
| | Phenocrysts | 80% Plag, Ol, Cpx, opx | 65% Plag, opx, cpx, qtz | 70% opx, cpx, plag, ol, opaq | 5% opx, plag, opaq, cpx, ol | 5% plag, cpx, opx, opaq | 10% plag, opx, opaq | 20% opx, cpx, plag, qtz, opaques | 25% opx, opaq, plag, cpx | 35% cpx, opaques, plag, opx |
| | Vesicles | 5% | 5% | 5% | 60% | 55% | * | 10% | 15% | 40% |
| Other Properties | Groundmass | Glassy | microphenocrysts, glassy | glassy, opaques | glassy | glass | glass, microphenocrysts | glass | glass, microphenocrysts | glass, microphenocrysts |
| | Phenocryst shape | Plag and opx megacrysts, laths of plag and cpx | plag cumulates, laths | Euhedral, plag cumulates | Euhedral-subhedral, minor disequilibrium textures | Euhed -subhedral | euhedral and broken | euhedral to broken | euhedral to broken | euhedral to broken |
| | Plagioclase compositions## | An42 | An47 | An44 | An62 | An52 | An62 | An48 | An54 | An44 |
| | Secondary Features | Clay alteration of gm and on vesicle bound | Clays on vesicle selveges | Pervasive clays in mx and vesicles | * | Clays on vesicle rims | Devitrification, zeolites, altered rim | * | * | * |
| | Notes | Plag sieve tx and disequilibrium tx on plag boundary | Plag sieve tx | * | accidental clast of porphyritic lava, minor sieve tx plag | Phenocryst cumulates | Sieve tx in plag | Accessory clast: plag, opx, opaq cumulate, with ol | Opx, opaq, plag cumulate | Plag and cpx cumulates. Accidental lithic |

Percentage grainsize and components are based on estimations

Plagioclase compositions were obtained using the Michelle Levy method.

Sample numbers relate to the Bays in which they were collected, from south Muriwai Beach in the north (0), to Maori Bay (1), Collins Bay (2), Pillow Lava Bay (3), Powell Bay (4), to Bartrum Bay in the south (5), followed by an approximate unit number (these numbers may or may not correlate with the existing site numbers).

| PROPERTIES OF CLASTIC UNITS | | | | | | | | | | |
|-----------------------------|--------------------------|----------------------------------|-----------------------------|---|---|---------------------------------------|--|--|--|---------------------------|
| | Sample No. | NZM 0/1 | NZM 1/1A | NZM 1/1B | NZM 1/2 | NZM 1/3 | NZM 1/7A | NZM 1/7B | NZM 1/7C | NZM 1/7D |
| Grainsize Estimations % | Type | pum bx sand | Calc sand | crystal sand | Conglom mx | sand | pillow Bx | pillow Bx | pillow Bx | pillow Bx |
| | <10 _μ m | 78% | 50% | 10% | 20% | 10% | 10% | 40% | 20% | 95% |
| | 10-20 _μ m | 20% | 50% | 80% | * | 90% | * | * | * | 5% |
| | 20-30 _μ m | 2% | * | 10% | * | * | 40% | * | 15% | * |
| | 30-40 _μ m | * | * | * | 70% | * | 40% | * | 10% | * |
| | 40-50 _μ m | * | * | * | 10% | * | 10% | 60% | 15% | * |
| Components % | Pumice | 10% | <2% | * | * | * | * | 1% | * | * |
| | Lava | 15% | 5% | 30% porphyritic | 60% vesicular & porphyritic | 20% porphyritic | 75% | 59% | 70% c and f pheno assem | 20% porphyritic |
| | Scoria | 10% | * | * | * | <1% | 3% | * | 2% | 1% |
| | Glass | (see matrix) | * | 20% clasts | * | * | * | * | * | 4% shards |
| | Lithics | * | 13% | 15% | 20% | * | 1% | * | * | * |
| | Crystals | 35% cpx, opx, plag, qtz, opa | 5% qtz, opa | 30% Ol, opa, qtz, plag, cpx, opx, hnbld | 10% cpx, qtz, plag | 68 % cpx, opx, plag, qtz, ol | 5% Ol, cpx, opx, hnbld, opa | plag, opx, cpx, opa | 15% plag, cpx, opx | 55% plag, cpx, opx, ol |
| | Fossils | * | 5% forams, gastropod, coral | 2% gastropod, forams | * | <1% coral | * | * | * | * |
| | Matrix | 30% glassy | 70% fine grained | 3% interstitial qtz and glass | 10% clay and glass | 10% | 16% interstitial qtz | 40% crystal rich | 13% crystal and glass | 20% |
| Other features | Clast shape | angular | subangular-subround | subround-subangular | round-subround | angular-subangular | subround pebs, ragged crystals | subr pebs, angular mx | subang-round | angular or euهدral |
| | Sorting Support | well clast | Well Matrix | Well clast | Moderate clast | well clast | poor-mod clast | poor clast | moderate clast | well clast |
| | Plagioclase compositions | An 41 | * | An 40 | * | An54 | * | An42 | * | An38 |
| | Secondary Features | * | Clacite replacement | * | weathered sample, zeolites, corroded clasts | Clay on clast rims; iddingsite | clays in plag and vesicles corroded crystals | clays in vesicles | * | Weathered and devit mx |
| | Notes | Very fine grained, vitric matrix | Clay and glass mx | Ragged crystals | Ragged crystals | crystal rich sandstone; sieve tx plag | Lava: c and f pheno assemblages | Lava: c and f pheno assem; Ol pheno within black peb | Lava: c and f pheno assem; 50% pebbles > 50 m size | Clays surround components |

| PROPERTIES OF CLASTIC UNITS | | | | | | | | | | |
|-----------------------------|--------------------------------|-----------------------------------|--|----------------------------------|--------------------------|------------------------------------|-----------------------------------|---|---|-------------------------|
| NZM 2/1(s) | NZM 2/4(F) | NZM 2/4C | NZM 3/1(N) | NZM 3/3(N) | NZM 3/3 | NZM 3/3B | NZM 3/3C | NZM 3/3D | NZM 3/3F | NZM 3/3(s) |
| | Sand | ? | Poorly sorted | Volc sand | sand | sand | | | fallout | |
| 90% | 75% | 35% | 5% | 20% | 43% | 88% | 25% | 68% | 15% | * |
| 10% | 20% | 20% | 40% | 75% | 40% | 10% | 10% | 25% | 10% | 7% |
| * | 5% | 40% | 5% | 5% | 15% | 2% | 5% | 5% | 10% | 8% |
| * | * | 3% | 10% | * | 2% | * | 20% | 2% | 20% | 10% |
| * | * | 2% | 10% | * | * | * | 40% > 50m g size | * | 45% | 15% |
| * | 2% | 15% | 2% | * | 19% | * | 70% | * | 80% | 75% |
| 10% | 25% | 20% porphyritic | 25% | 18% | 10% | 33% porphyritic | * | 10% porphyritic | 9% porphyritic | 8% |
| * | 1% | * | * | 1% | 1% | 5% | * | * | 1% | 2% |
| 4% clasts | 2% | * | 30% palagonite | 10% | * | * | 5% bubble wall frags | 20% | * | * |
| * | 5% | 4% | 10% | 15% f grained | * | 15% | * | 20% weathered aggregates | * | 5% |
| 70% plag, cpx, qtz | 50% plag, cpx, qtz, ol | 55% plag, qtz, opx, cpx, Ol, opaq | 25% opx, cpx, plag, ol | 35% plag, cpx, opx, ol, qtz | 65 % cpx, opx, plag, qtz | 45% cpx, opx, ol, plag, opaq | 10% qtz, plag, opaq, opx, cpx, ol | 50% cpx, opx, ol, plag | 5% plag, opaq, opx, cpx, qtz | 5% opx, plag, cpx, opaq |
| 1% forams | * | * | * | 1% | * | * | * | * | * | * |
| 15% clay and glass | 15% | 6% | 8% | 20% | 5% | 2% | 15% crystal rich, glassy (ash) | * | 5% | 5% devit ash |
| angular | round clasts, angular crystals | Angular-subang | pebs subround, crystals angular | angular to subround | subang to angular | subang - subround | broken crystals: ragged pumice | subround-subang | ragged pumice, euhedral crystals | subround - ragged |
| very well clast | well clast | moderate clast | Poorly matrix (?) | mod to poor clast | well clast | well clast | very well clast | mod- well clast | bimodal clast | well clast |
| An48 | An38 | An38 | * | An41 | An50 | An45 | An54 | An45 | An52 | * |
| Altered mx | clays and devit | Plag recryst; mx clays | minor clays and recryst plag in mx; altered plag | clay in mx and on rims of clasts | * | glassy alterat of some lava clasts | * | interstitial recryst, altered glassy lithics and lava | minor clays | * |
| Plag dominated | | Ragged and broken crystals | 30% pebbles are >50m | * | * | Broken crystals; angular | * | Rounded crystals | altered phenocrysts; accidental lithics | 60% pumice >50m |

| PROPERTIES OF CLASTIC UNITS | | | | | | | |
|-----------------------------|--|---|---|---|------------------------------------|--|-------------------------------|
| NZM 3/3 P | NZM 3/4A | NZM 4/1A | NZM 4/1B | NZM 4/3(N) | NZM 5/2A | NZM 5/2B | NZM 5/6 |
| pumiceous | | f sand | c crystal sand | | | | |
| 20% | 60% | 95% | * | 5% | 10% | 35% | 60% |
| 15% | 10% | * | 30% | 55% | 70% | 50% | 30% |
| 10% | * | * | 40% | 5% | 15% | 10% | 10% |
| 10% | 10% | 5% | 25% | 30% | 5% | 5% | * |
| 5% | 20% | * | 5% | 5% | * | * | * |
| 45% | 12% | * | * | 40% | 10% | 15% | 60% |
| 15% | 20% | * | 64% | 10% | 43% | 20% | 2% |
| 2% | 2% | * | 1% | 2% | 2% | 1% | * |
| * | 1% | 20% clast alteration | * | * | * | * | 3% |
| * | * | * | 10% | * | * | 4% f grained agg | * |
| 28% opaq, cpx, opx, plag | 60% opx, cpx, plag | 5% qtz, cpx, calcite, opx, opaq | 5% ol, qtz, cpx, opaq, calcite, | 33% cpx, opaq, opx, plag | 24% plag, opx, cpx, opaq | 15% ol, plag, cpx, opx | 35% qtz, cpx, opx, plag, opaq |
| * | * | 5% | * | * | 1% | * | * |
| 10% clay | 5% clay | 70% | 20% glass and Calcite | 15% glassy (ash) | 20% recryst plag? | 45% clays & recryst plag | * |
| angular to subrounded | angular-subangl | subang-subround | subr-subang | subround-angular pumice, euhed crystals | ang-subang | ang-subang | angular-subang |
| bimodal clast | mod-poor clast | well matrix | well clast | bimodal clast | well clast | well-mod clast | well-bimodal clast |
| * | An44 | * | * | * | An40 | * | An44 |
| corrosion of crystals | altered rims around clasts | Alteration of mafic crystals components | strongly altered, calcite recryst, minor chlorite of mafic clasts | minor clays | Secondary matrix, altered crystals | Very altered plag crystals, and recryst plag in mx | devit glass |
| 40% pumice >50m | zoned, included and sieve tx plag. 20-30m size | minor calcite replace | Blocky calcite cement in mx and complete replace of some clasts | Fallout layer? | Sieve tx and corroded plag | shrinkage cracks in clays, reaction rims in ol. | * |

Key

m = microns

* = no data

recryst = recrystallization

gm = groundmass

tx = texture

cpx = clinopyroxene

opx = orthopyroxene

ol = Olivine

Devit = Devitrification

Opaq = Opaques

hnblnd = Hornblende

Plag = plagioclase

c = coarse

f = fine

pheno = phenocryst

assem = assemblage

Bx = breccia

Peb = pebble

agg = aggregate

APPENDIX 5:

**Point counting data and thin section
descriptions of lava and volcanic clasts.**

| POINT COUNTING (500 points) | | | | | | | | | |
|-------------------------------|--------|--------|------|------------|---------|---------|---------|---------|--------|
| Sample No. | NZM1/7 | NZM3/2 | NZM5 | NZM1/7E | NZM0/1A | NZM0/1B | NZM0/1C | NZM3/3A | NZM3/2 |
| Type | lava | lava | lava | hyaloclast | pumice | pumice | pumice | scoria | scoria |
| Groundmass or glass | 218 | 272 | 292 | 402 | 215 | 230 | 43 | 215 | 222 |
| Feldspars | 176 | 116 | 111 | 80 | 214 | 127 | 130 | 20 | 27 |
| Pyroxenes | 45 | 10 | 35 | 6 | 51 | 66 | 26 | 1 | 1 |
| Vesicles | 55 | 96 | 54 | 1 | 6 | 47 | 279 ** | 264 | 249 |
| Other minerals (FeTi oxides) | 6 | 6 | 8 | 11 | 14 | 30 | 22 | * | 1 |

** High values due to vesicle morphology, and localised counting area.

| POINT COUNTING (100 points) | | | | | | |
|--------------------------------------|------------|------------|------------|--------------|--------------|--------------|
| Sample No. | NZM1/7A | NZM1/7B | NZM1/7C | NZM3/3C | NZM3/3(s) | NZM3/3P |
| Type | lava clast | lava clast | lava clast | pumice clast | pumice clast | pumice clast |
| Groundmass or glass | 76 | 39 | 59 | 48 | 30 | 44 |
| Feldspars | 15 | 49 | 20 | 18 | 18 | 14 |
| Pyroxenes | 1 | 8 | 18 | 7 | 5 | 1 |
| Vesicles | 7 | 1 | * | 20 | 44 | 36 |
| Other minerals (FeTi oxides, quartz) | 1 | 3 | 3 | 7 | 3 | 5 |

5-1. Raw point counting data: 500 points counted for major components, additional 100 point counting of extra clasts.

* = no data

5-2. Thin section descriptions of specific lava and volcanic clasts used for point counting, with microscope photos.

SAMPLE: NZM1/7 **TYPE:** lava **LOCATION:** Site 2, unit 5, section A, pillow lava and sheet flow facies. **DESCRIPTION:** Black – grey feldspar-phyric, incipient to poorly vesicular (basalt?) lava. Phenocrysts of plag and clino-pyroxene occur in clusters. Plagioclase phenocrysts have corroded rims and are zoned and sieve textured. Isolated euhedral ortho-pyroxene phenocrysts. Groundmass comprises euhedral and subhedral plagioclase laths, olivine and clino- and ortho-pyroxene phenocrysts, with clay alteration in between crystals. **PHOTO:** 5A & 5B (0.55mm scale bar).

SAMPLE: NZM3/2 **TYPE:** lava **LOCATION:** Site 3, unit 3, section C, pillow lava and sheet flow facies. **DESCRIPTION:** Grey, coarsely crystalline, poorly vesicular, feldspar-phyric basaltic andesite. Feldspar phenocrysts (40-50 μm) have pervasive sieve textures and occur in plagioclase phenocryst clusters. Groundmass is glassy with well-developed micro-phenocrysts of plagioclase, and poorly developed olivine and clino-pyroxene. Clays encrust vesicle selvages, with domains of corroded phenocrysts adjacent. Vesicles are ragged (~ 20 %). **PHOTO:** 5C (0.55mm scale bar).

SAMPLE: NZM5 **TYPE:** lava **LOCATION:** Site 5, unit 1, section C1, cross-cutting dyke and mega-pillow facies. **DESCRIPTION:** Black-grey feldspar-phyric, incipient to poorly vesicular basalt. Feldspar phenocrysts are euhedral with sieve textures. Phenocrysts of plagioclase, with rare ortho- and clino-pyroxene occur in clusters. Crystal boundaries are variably corroded. Groundmass consists of feldspar laths and subhedral ortho- and clino-pyroxene micro-phenocrysts, with small black clusters of titanomagnetite. It is variably altered, with clay selvages lining vesicles, and interstitial clay pervading inter-crystalline domains. **PHOTO:** 5D (0.55mm scale bar).

SAMPLE: NZM1/7A **TYPE:** lava clast **LOCATION:** Site 2, unit 2, section B, tabular conglomerate facies. **DESCRIPTION:** Grey, finely crystalline, poorly vesicular, subrounded lava clast. Groundmass contains micro-phenocrysts and feldspar laths, titanomagnetite and altered crystal forms similar to that of pyroxene, with internal quartz (and olivine?). Localised alignment of plagioclase laths. Vesicle morphologies are irregular and lined with clay. Note black alteration rim, compared to unaltered groundmass. **PHOTO:** 5E (0.55mm scale bar).

SAMPLE: NZM1/7B **TYPE:** lava clast **LOCATION:** Site 2, unit 6, section C, polymictic breccia facies. **DESCRIPTION:** Dark grey, coarsely crystalline, subrounded lava clast. Euhedral phenocrysts of plagioclase columns, and ortho-pyroxene, titanomagnetite and few clino-pyroxenes. Plagioclase phenocrysts are concentrically zoned with pervasive sieve texture of individual crystals. Clino-pyroxene phenocrysts contain titanomagnetite inclusions. Groundmass is micro-crystalline, with irregularly shaped vesicles, encrusted with yellow clays. **PHOTO:** 5F (0.55mm scale bar).

SAMPLE: NZM1/7C **TYPE:** lava clast **LOCATION:** Site 2, unit 6, section C, polymictic breccia facies. **DESCRIPTION:** Light grey, finely crystalline subangular lava clast. Phenocrysts of poorly-developed plagioclase laths, with heavily sieve-textured crystals, and altered ortho- and clino- pyroxenes. Individual crystals are completely replaced by secondary minerals (zeolite after olivine?). Groundmass is feldspar-phyric, with small subhedral pyroxene and abundant titanomagnetite. Rare vesicles are encrusted with clays. **PHOTO:** 5G (0.55mm scale bar).

SAMPLE: NZM1/7E **TYPE:** Hyaloclastite **LOCATION:** Site 2, unit 6, section C, polymictic breccia facies. **DESCRIPTION:** Dark brown, very finely crystalline, angular hyaloclastite clast, with altered rim. Subhedral phenocrysts of plagioclase, titanomagnetite, clino- and ortho- pyroxene (< 10-20 μ) with slightly corroded rims, and few olivines. Groundmass contains micro-phenocrysts in glass, sparsely vesicular. The clast rim is white, with an altered groundmass. **PHOTO:** 5H (0.275mm scale bar).

coarsely crystalline pumice. Subhedral and broken phenocrysts of plagioclase, titanomagnetite ortho- and clino- pyroxenes are abundant. Large plagioclase phenocrysts are sieve textured, and pyroxenes contain titanomagnetite inclusions. Groundmass is glassy and variably vesicular. Vesicles are elongate and irregularly shaped. A single internal phenocryst cumulate clast, of plagioclase columns, titanomagnetite and clino- and ortho- pyroxene, is ragged with crystals fracturing off into groundmass. **PHOTO:** 5I (0.55mm scale bar).

SAMPLE: NZM0/1B **TYPE:** Pumice clast **LOCATION:** Site 1, section A, pumiceous and scoriaceous lithofacies group. **DESCRIPTION:** Grey, finely vesicular and coarsely crystalline pumice clast. Abundant phenocrysts of plagioclase, ortho- and clino- pyroxene and titanomagnetite. Concentrically zoned plagioclase and sieve textured. Phenocrysts occur in clusters. Heterogenous groundmass, glassy with fine-grained domains and poorly vesicular domains. Vesicles have small and irregular to elongate morphologies. **PHOTO:** 5L (0.275mm scale bar)

SAMPLE: NZM0/1C **TYPE:** Pumice clast **LOCATION:** Site 1, section A, pumiceous and scoriaceous lithofacies group. **DESCRIPTION:** Grey, vesicular, coarsely crystalline pumice clast. Phenocrysts of plagioclase, ortho- pyroxene and titanomagnetite, are broken, euhedral or subhedral. Individual plagioclase phenocrysts are sieve textured and concentrically zoned. Isolated phenocryst clusters of ortho- pyroxene, titanomagnetite and plagioclase. Vesicles are abundant, with subrounded, elongate to irregular morphologies. The groundmass is micro-crystalline. **PHOTO:** 5J & 5K (0.55mm scale bar).

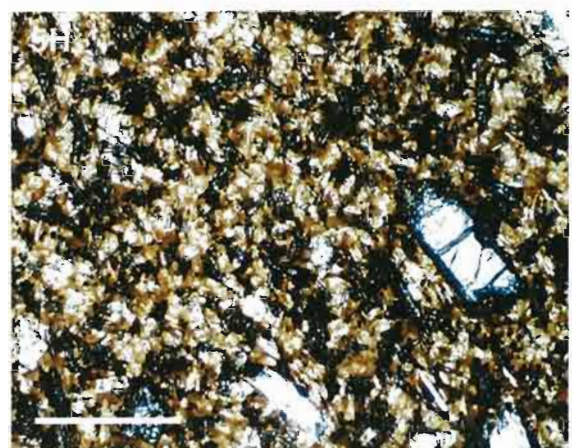
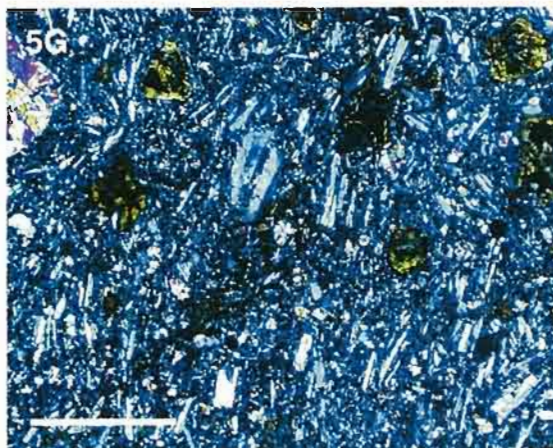
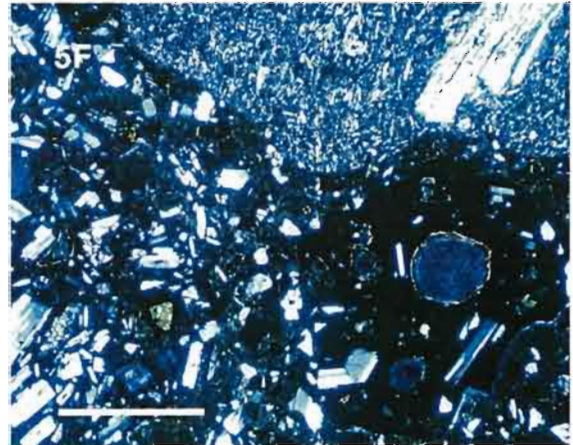
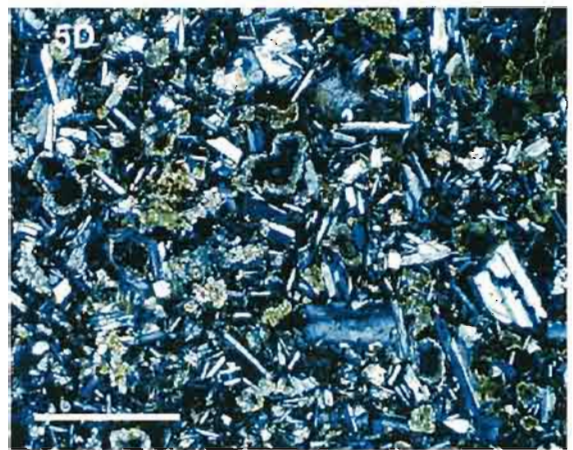
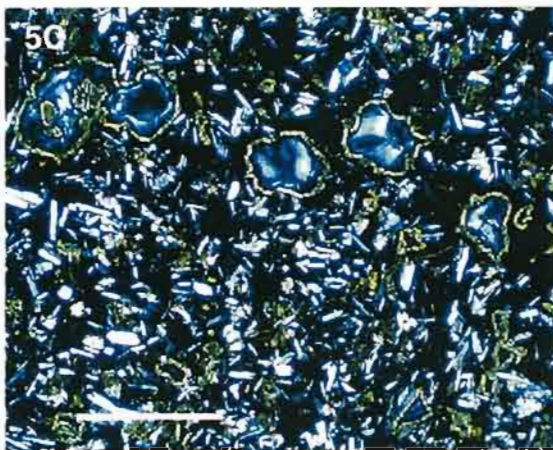
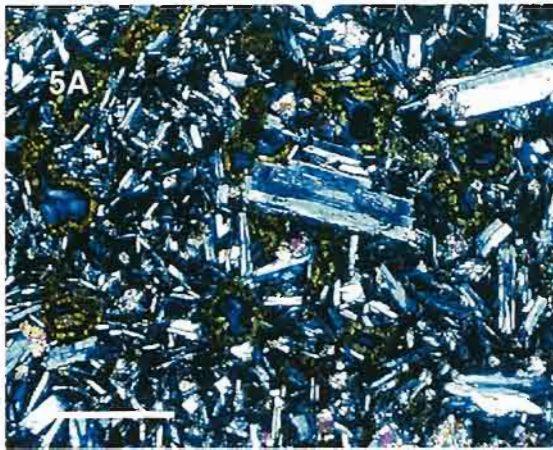
SAMPLE: NZM3/3C **TYPE:** Pumice clast **LOCATION:** Site 4, section A, pumiceous and scoriaceous lithofacies group. **DESCRIPTION:** Cream to white, fine-grained, vesicular, ragged pumice clast. Sparsely crystalline, with rounded to broken phenocrysts of plagioclase, titanomagnetite, quartz, and ortho- pyroxene. Vesicles vary from fine to coarse, with domains of subrounded to coalescing vesicles, adjoining much finely vesicular domains. Groundmass is glassy and contains plagioclase and ortho-pyroxene micro-phenocrysts. **PHOTO:** 5M (0.55mm scale bar)

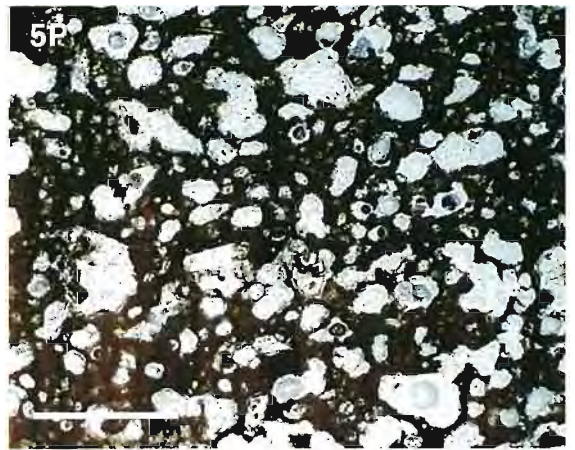
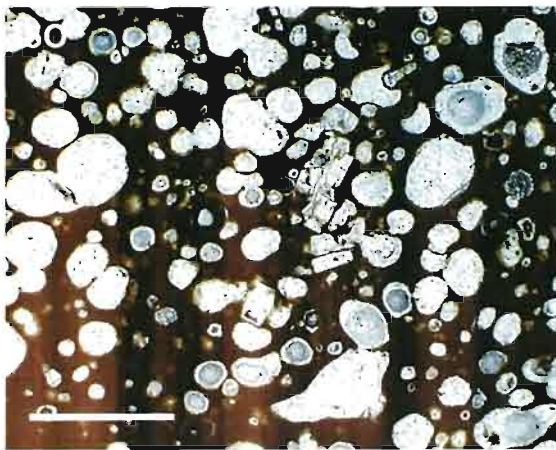
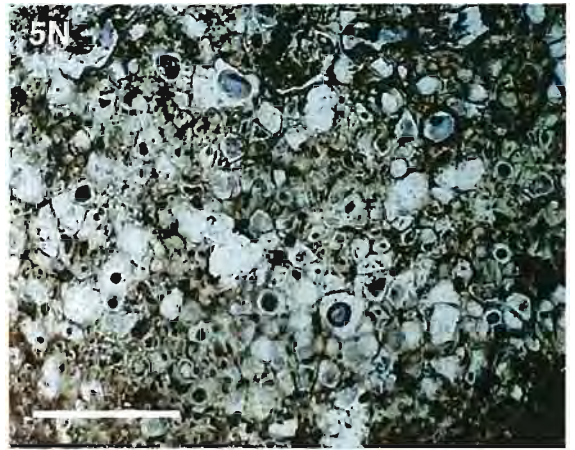
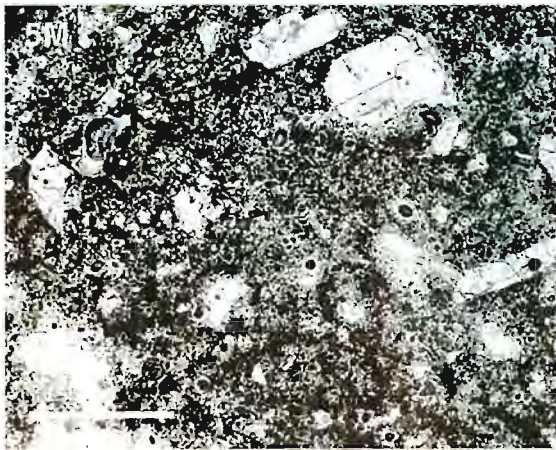
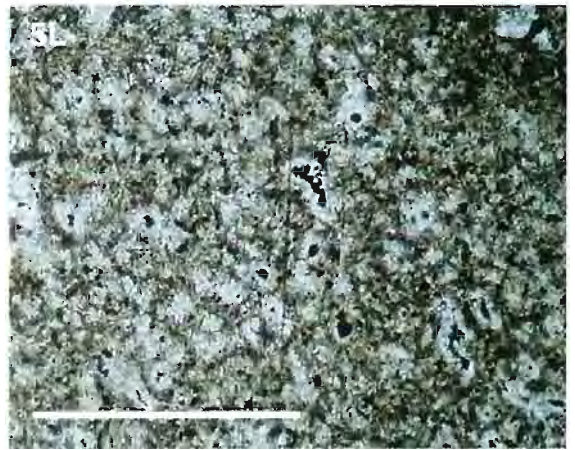
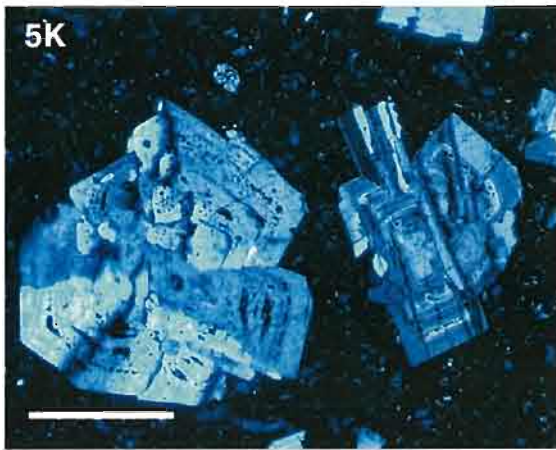
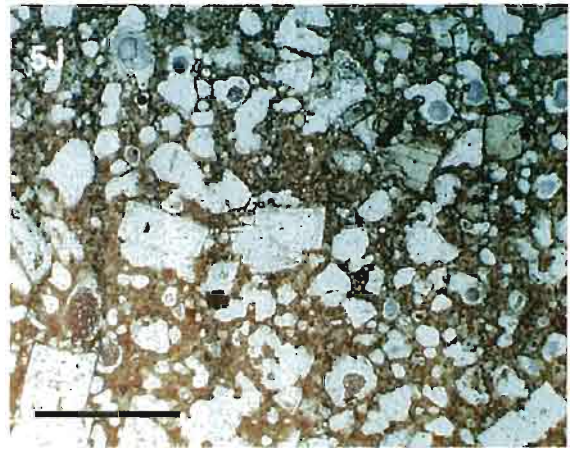
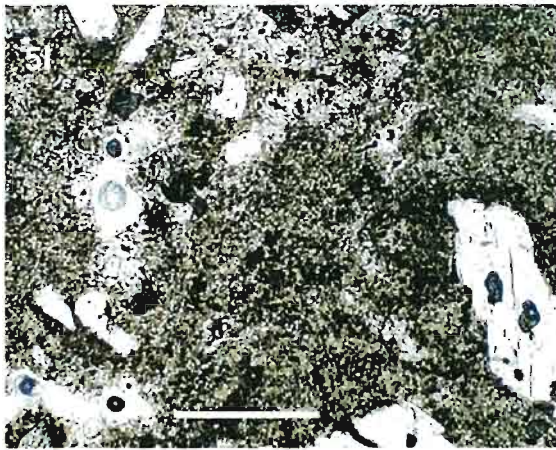
SAMPLE: NZM3/3(s) **TYPE:** Pumice clast **LOCATION:** Site 4, section A, pumiceous and scoriaceous lithofacies group. **DESCRIPTION:** White to cream, coarsely crystalline, vesicular and ragged pumice clast. Contains euhedral plagioclase, quartz, ortho- and clino- pyroxene, and titanomagnetite phenocrysts. Vesicles have smooth edges, and are rounded or coalescing, with coarse and finely vesicular domains. Groundmass is glassy with micro-phenocrysts. **PHOTO:** 5N (0.275mm scale bar)

SAMPLE: NZM3/3P **TYPE:** Pumice clast **LOCATION:** Site 4, section A, pumiceous and scoriaceous lithofacies group. **DESCRIPTION:** Cream to grey finely crystalline, vesicular, sub-rounded pumice clast. Contains sparse, euhedral to corroded phenocrysts of plagioclase, clino-pyroxene and titanomagnetite. Vesicles are subrounded to irregular and coalesced, with smooth edges. Groundmass is glassy with sparse micro-phenocrysts. Pervasive, fine-grained clay alteration.

SAMPLE: NZM3/3A **TYPE:** Scoria clast **LOCATION:** Site 4, section B, pumiceous and scoriaceous lithofacies group. **DESCRIPTION:** Black to dark red, fine-grained, vesicular scoria clast. Sparsely crystalline, with phenocrysts of euhedral plagioclase. Phenocryst clusters of titanomagnetite, plagioclase, clino- and ortho- pyroxene. Vesicles are rounded- subrounded, with smooth edges. Groundmass is heterogenous and contains scattered plagioclase laths. **PHOTO:** 5O (0.55mm scale bar)

SAMPLE: NZM3/2 **TYPE:** Scoria clast **LOCATION:** Site 4, section B, pumiceous and scoriaceous lithofacies group. **DESCRIPTION:** Dark brown to black, fine-grained scoria clast. Sparsely crystalline, with phenocrysts of plagioclase, titanomagnetite, ortho- and clino- pyroxene. Individual plagioclase laths heavily sieve textured. Clusters of coarse and finely crystalline phenocrysts (accidental clast?). Vesicles are irregular to sub-rounded and have rough edges.





APPENDIX 6

Bulk Rock Geochemistry

| XRF ANALYSES | | SES-CODES, University of Tasmania | | | | Analyst: Phil Robinson. Sample Preparation Katie McGoldrick | | | | | | | | |
|----------------|-----------|-----------------------------------|------------------|--------------------------------|--------------------------------|---|------|------|-------------------|------------------|-------------------------------|--------------|--------|-------|
| MAJORS program | | 7/09/1999 | | | | Rock Crushing by Emma Mathews using tungsten carbide mill | | | | | | | | |
| Sample No. | Rock type | SiO ₂ | TiO ₂ | Al ₂ O ₃ | Fe ₂ O ₃ | MnO | MgO | CaO | Na ₂ O | K ₂ O | P ₂ O ₅ | Loss inc. S- | Total | S |
| NZM 1/7E | Hyal | 57.38 | 1.23 | 15.69 | 9.07 | 0.15 | 2.60 | 5.84 | 4.02 | 1.40 | 0.26 | 2.05 | 99.70 | <0.01 |
| NZM 3/1 | Hyal | 59.14 | 1.05 | 16.21 | 8.03 | 0.17 | 2.05 | 5.33 | 4.11 | 2.04 | 0.30 | 1.62 | 100.05 | <0.01 |
| NZM 3/2 | Lava | 51.34 | 1.04 | 17.96 | 8.05 | 0.11 | 3.60 | 8.97 | 3.14 | 0.76 | 0.43 | 4.75 | 100.15 | 0.02 |
| NZM 5 | Lava | 47.41 | 1.12 | 16.65 | 10.49 | 0.12 | 5.11 | 8.71 | 2.86 | 0.54 | 0.29 | 6.46 | 99.76 | 0.02 |
| NZM 3/3A | scoria | 56.97 | 1.10 | 15.30 | 8.42 | 0.16 | 2.63 | 4.96 | 4.34 | 1.44 | 0.25 | 4.38 | 99.95 | 0.05 |
| NZM 3/2 | scoria | 55.52 | 1.13 | 15.16 | 8.11 | 0.14 | 3.08 | 4.76 | 4.05 | 1.38 | 0.20 | 6.31 | 99.85 | 0.06 |
| NZM 0/1 | pumice | 52.25 | 0.73 | 17.23 | 7.88 | 0.14 | 4.08 | 6.88 | 3.70 | 0.73 | 0.12 | 6.25 | 99.99 | 0.05 |
| NZM 0/1B | pumice | 51.89 | 0.76 | 16.97 | 8.54 | 0.16 | 4.42 | 7.23 | 3.42 | 0.74 | 0.12 | 6.19 | 100.43 | 0.05 |

METHOD:

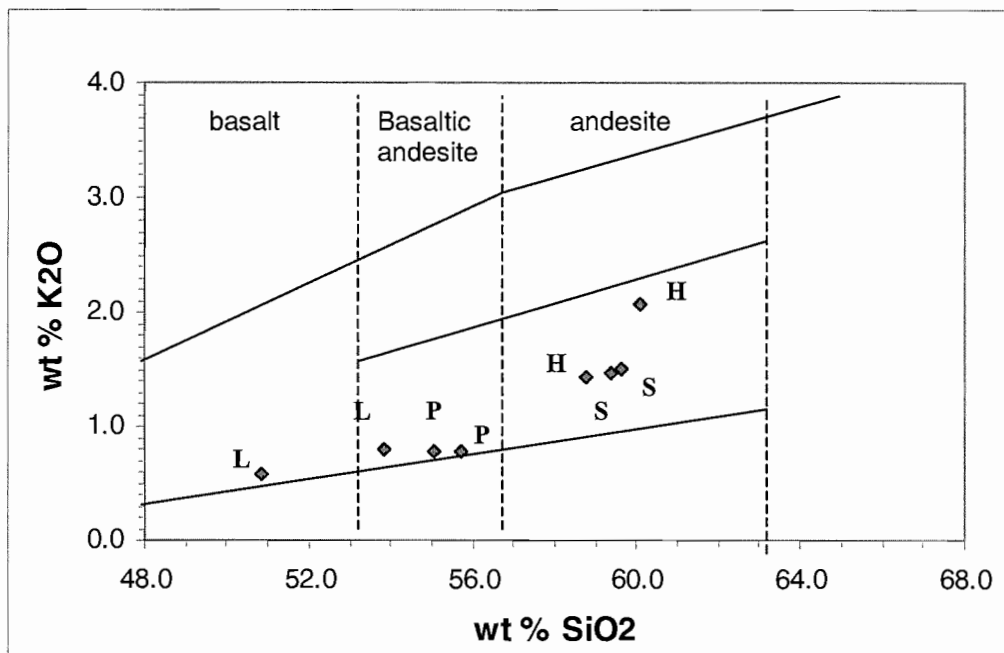
A limited number of clasts were analysed on account of the degree of weathering and secondary alteration of the components.

As a result, analysis of a few representative volcanic clasts endeavours to reflect the general composition of multiple volcanic components.

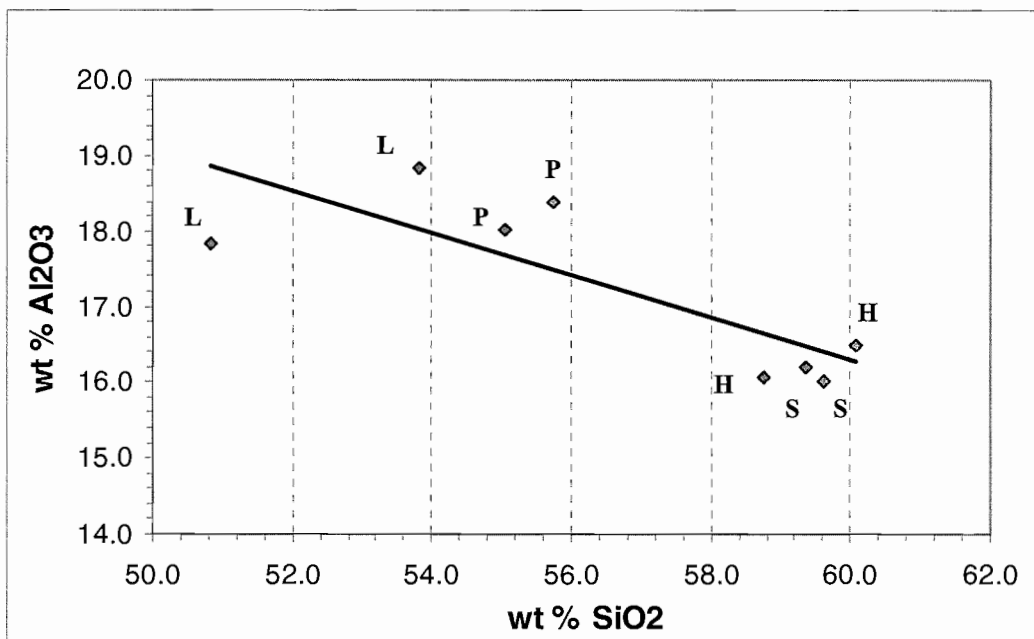
Major element analysis was determined from two samples apiece of lava (porphyritic), pumice (grey), scoria (black) and fine-grained, glassy clasts (hyaloclastite).

Plots of the total wt% of the major elements were constructed with LOI removed.

6.1. Wt % SiO₂ against wt% K₂O plot, showing composition of lava (L), pumice (P), scoria (S) and hyaloclastite (H) clasts, in relation to division for island arc rocks.

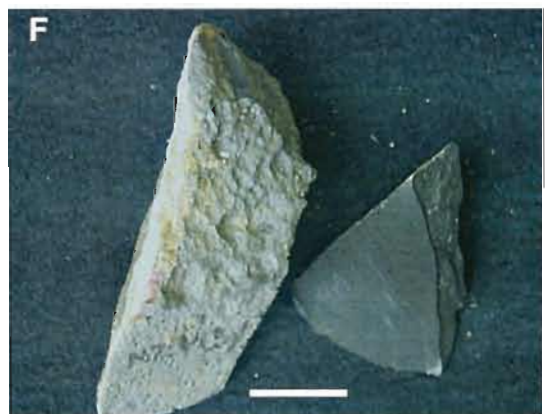


6.2. wt % SiO₂ against wt % Al₂O₃ plot, showing broad fractionation trend of lava, pumice, scoria and hyaloclastite.



Samples of lava and volcanic clasts used for bulk rock geochemistry:

- A. Scoria from pumiceous and scoriaceous interval at Pillow Lava Bay (NZM3/3A).
- B. Scoria from pumiceous and scoriaceous interval at Pillow Lava Bay (NZM3/2)
- C. Lava from thin pillow lava mound at Pillow Lava Bay (NZM3/2).
- D. Lava from brecciated part of feeder dyke at Bartrum Bay (NZM5).
- E. Hyaloclastite from polymict breccia interval at Maori Bay (NZM1/7E).
- F. Hyaloclastite from pebbly sandstone interval at Pillow Lava Bay (NZM3/1).
- G. Pumice clast from pumiceous and scoriaceous interval at Otokamiro Point (NZM0/1A).
- H. Pumice clast from pumiceous and scoriaceous interval at Otokamiro Point (NZM0/1B).



APPENDIX 7

Vesicularity Data

7.1. Vesicularity %

Representative volcanic clast samples were collected from the pumiceous and scoriaceous lithofacies group, at Otakamiro Point and Pillow Lava Bay. Representative lava samples were obtained from the pillow lava at Maori Bay and from the feeder dyke at Bartrum Bay. A lava clast was used for the dense rock equivalent (DRE).

Each clast was thoroughly washed and scrubbed to remove organic contaminants. Clasts were cut into cubes for analysis, then dried for 24 hours at 85°C, and their dry weights obtained. The volumes of the clasts were determined by measurement of each side with callipers.

Vesicularity % is determined by using the method of Houghton and Wilson (1989).

$$\text{Density} = \frac{\text{Dry Weight}}{\text{Clast volume}}$$

$$\text{Vesicularity} = \frac{100 (\text{DRE} - \text{Clast Density})}{\text{DRE Density}}$$

- Samples are limited due to the lack of pristine rocks.

7.2 Raw density data:

DRY WEIGHT OF VOLCANIC CLASTS: 24 HOURS @ 85 DEGREES C

| | Sample No. | Dry Weight (g) | Volume | Density (g/cm ³) | Vesicularity (from dry weights) | Vesicularity (from H ₂ O displacement method) ** | Vesicularity classification (from Houghton and Wilson) |
|--------|------------|----------------|-----------|------------------------------|---------------------------------|---|--|
| Pumice | NZM0/1B | 7.1 | 4.904313 | 1.4477053 | 44.8369151 | 32.889 | Poor - mod |
| Pumice | NZM0/1C | 11.7 | 5.12265 | 2.28397412 | 12.97179687 | 23.7296 | Incipient - poor |
| Scoria | NZM3/3A | 7.2 | 4.1990813 | 1.714660796 | 34.66468526 | 33.0592 | poorly |
| Scoria | NZM3/2 | 6.5 | 5.1030124 | 1.27375746 | 51.46509678 | 43.2849 | Moderate |
| Lava | NZM1/7 | 6.7 | 2.5529538 | 2.624411038 | DRE | * | * |
| Lava | NZM5 | 11 | 4.586922 | 2.398122314 | 8.622161 | 4.021098004 | non - incipient |

DRE = Dense Rock Equivalent

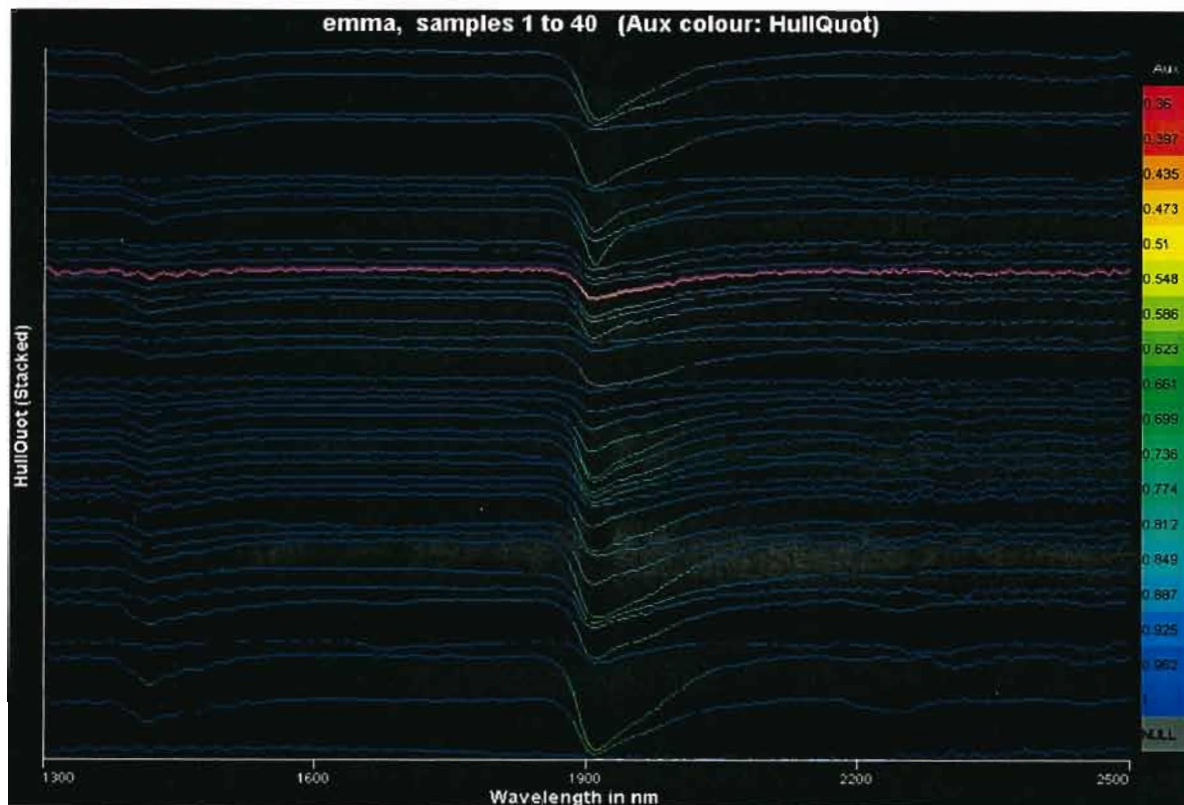
** Lower accuracy than dry weight method.

APPENDIX 8

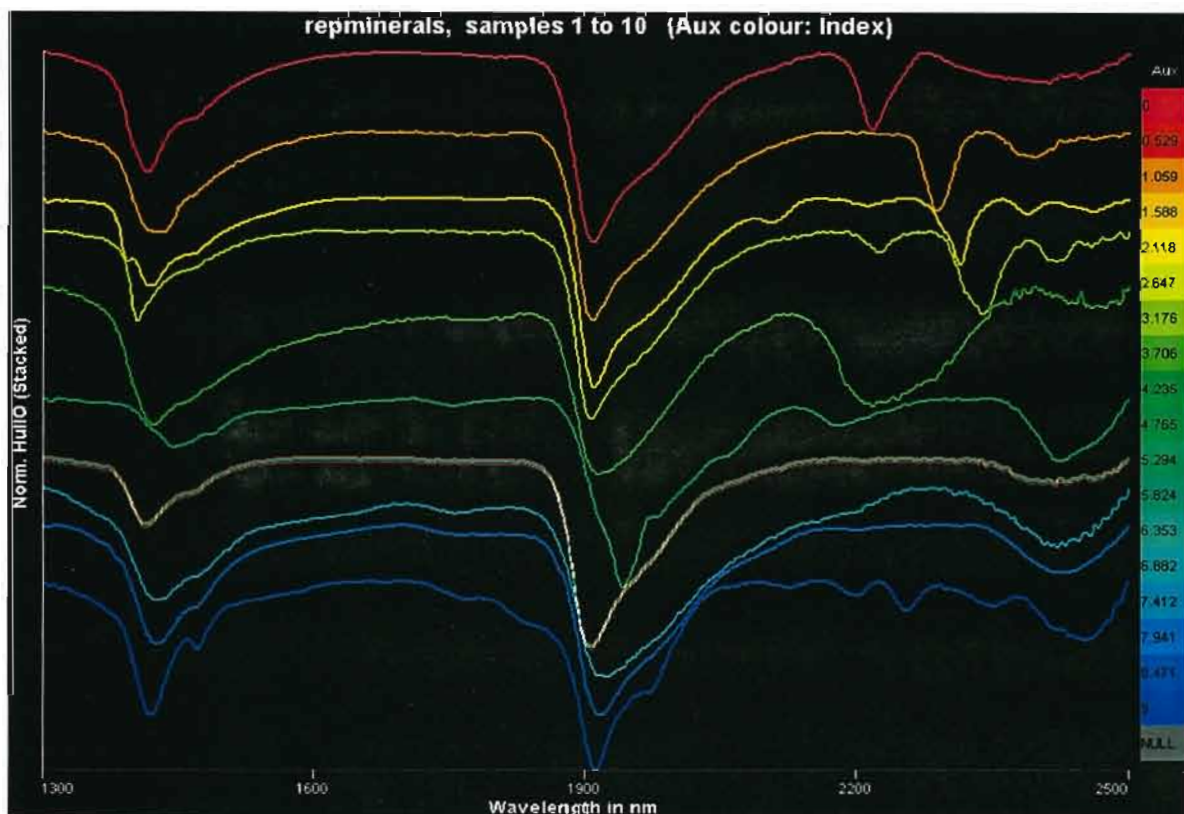
PIMA DATA

PIMA (Portable Infra-red Mineral Analyser) METHOD

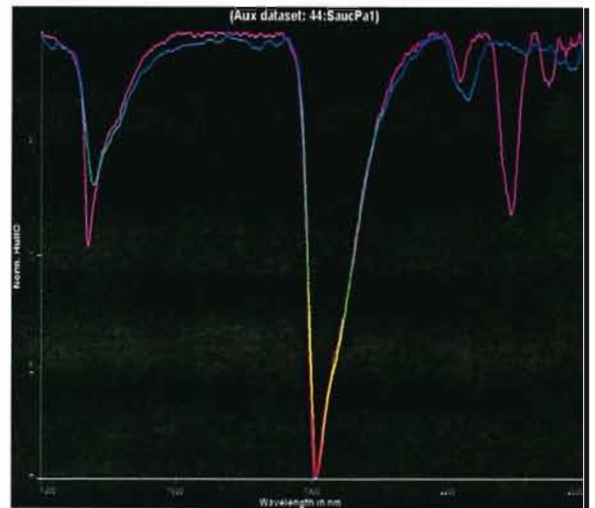
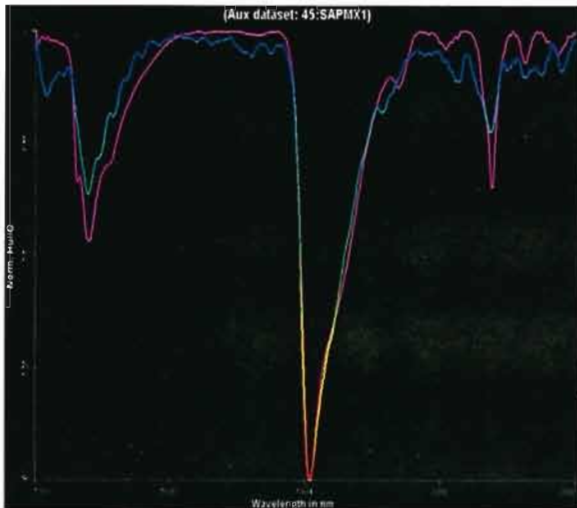
1. Analysis of the rock matrix within the Muriwai Volcanic succession is useful for determination of the source of weathered particles found in the matrix of the clastic rocks. Typical assemblages found on the seafloor where deposition of the Muriwai rocks took place, may be low temperature, contain zeolites and derived from related sources.
2. The SWIR spectra of individual rock samples were measured using a PIMA.
3. This data was converted from .FOS file into text files, which were then imported into *The Spectral Geologist* for interpretation.
4. The signatures of samples from the Muriwai succession were compared individually to recognised SWIR mineral spectra in *The Spectral Geologist* mineral library. Wally Hermann assisted to narrow down correlations of sample signatures with the major minerals (discovered very few clays at Muriwai).
5. This initial examination revealed a correlation with the Zeolite and Smectite mineral assemblages.
6. Then each signature of the minerals within the zeolite and smectite groups were compared individually to the major peaks of the Muriwai samples.



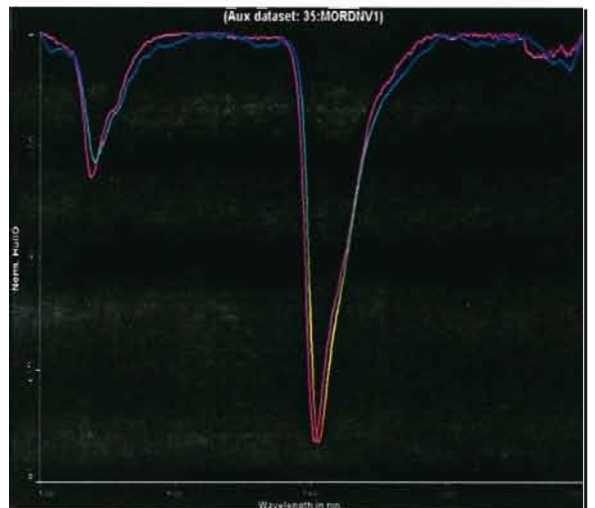
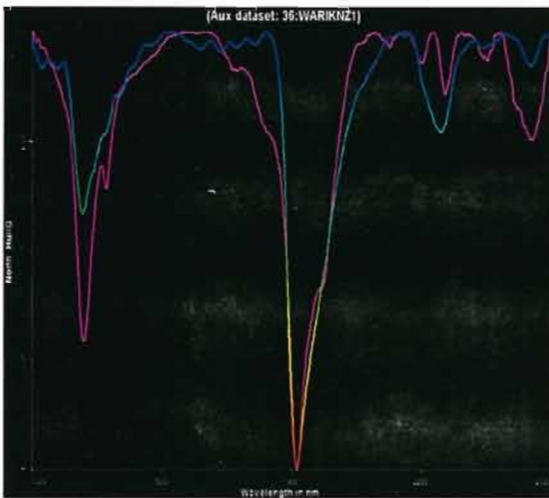
8.1. Stack of short wave infra-red signatures for samples.



8.2. 10 most commonly occurring minerals from samples, which include from top to bottom: Montmorillonite (red); Nontronite; Saponite; Sauconite; Opal: Mesolite; Mordenite; Natrolite; Stilbite; Wairakeite (blue). In normalised Hull Quotient.
Examples of match between mineral signatures and analysed samples.



8.3. Pink= analysed sample / blue= mineral library signature. Left: Hyaloclastite sample (NNM1/7), with saponite. Right: Pumiceous and scoriaceous lithofacies sand sample (NNM4/3), with sauconite.



8.4. Pink= analysed sample / blue = mineral library signature. Left: Pumice clast sample (3/3(s)) with Warikite. Right: Thickly bedded granule sand from sample (NNM5/2) with mordenite.